Universidade do Minho
Escola de Ciências

Rosana Maria Abreu Alves

Function and Regulation of *Candida albicans* and *C. glabrata* Carboxylic Acid Transporters and their Role in Biofilm Formation, Antifungal Drug Resistance and Phagocytosis

May 2020

Function and Regulation of *Candida albicans* and *C. glabrata* Carboxylic Acid Transporters and their Role in Biofilm Formation, Antifungal Drug Resistance and Phagocytosis

Rosana Maria Abreu Alves

UMinho | 2020


REPÚBLICA PORTUGUESA
CIÊNCIA, TECNOLOGIA E ENSINO SUPERIOR
FCT Fundação para a Ciência e a Tecnologia
NORTE2020
POCH
PORTUGAL 2020
UNIÃO EUROPEIA
Fundo Social Europeu

Universidade do Minho
Escola de Ciências

Rosana Maria Abreu Alves

Function and Regulation of *Candida albicans* and *C. glabrata* Carboxylic Acid Transporters and their Role in Biofilm Formation, Antifungal Drug Resistance and Phagocytosis

PhD Thesis
Doctoral Program in Molecular and Environmental Biology
Branch of Cellular Biology and Health

Work supervised by
Professora Doutora Sandra Paiva
Professora Doutora Margarida Casal
Professora Doutora Mariana Henriques

May 2020

ACKNOWLEDGMENTS

"Yes, I get by with a little help from my friends."

- The Beatles

First and foremost I am profoundly grateful in ways that would never be adequately expressed here to Prof Sandra Paiva. She provided me with the most appropriate and thoughtful guidance in each and every step of my PhD. I would like to express my profound gratitude for her exceptional availability, help and friendship. Thank you for pushing and helping me to reach my goals. I would also like to acknowledge my co-supervisors. Prof Margarida Casal has provided me invaluable mentorship and feedback along this journey. A word of thanks to Prof Mariana Henriques for being always available.

I am grateful to all my labmates for such a pleasant working atmosphere. To my dear Cláudia, who I cannot thank enough for providing me such support through these years. To Paulo and Humberto. And also to Maria, Joana, Mário, Pedro, Margarida and Rui.

I cannot stress enough how important my collaborators have been during the whole period of my PhD. I am grateful to Prof David Drubin for accepting me at his lab at UC Berkeley. My special thanks to Daphné, Itziar, Charlotte and Michelle. I am also extremely grateful to Prof Patrick Van Dijck for receiving me so well in his lab during my two visits at KU Leuven. My special thanks to everyone at MCB department for such warm hospitality.

I must add a special word of thanks to Prof Alistair Brown and Prof Björn Johansson and to both members of my Accompanying Thesis Committee, Prof Paula Sampaio and Prof Joaquin Ariño, for all the valuable suggestions during the whole period of my PhD.

I definitely feel very blessed for the love and care of so many people. I want to name my dear friends Marina Amorim, Ana Rego, José Sousa, Ona Rogiers, Justine Feyereisen, Michelle Holtappels, Gabriela Mol, Fábio Tamaki, Rodolfo Águas, Mário Sousa, Patrícia Rodrigues and Hugo Rangel for their genuine friendship throughout these years.

Last but not least, my final thank you must go to my Father, my Mother and my Sister for their unconditional love and support. They are and always will be my biggest inspiration. Thank you for bringing me up according to your high moral values, for all you have sacrificed for me and for giving me the opportunity and the freedom to pursue my own interests even when they seemed somewhat risky or incomprehensible.

STATEMENT OF INTEGRITY

I hereby declare having conducted this academic work with integrity. I confirm that I have not used plagiarism or any form of undue use of information or falsification of results along the process leading to its elaboration. I further declare that I have fully acknowledged the Code of Ethical Conduct of the University of Minho.

ABSTRACT

Function and regulation of *Candida albicans* and *C. glabrata* carboxylic acid transporters and their role in biofilm formation, antifungal drug resistance and phagocytosis

Candida species are the most frequent opportunistic fungal pathogens in humans and a common source of life-threatening infections in intensive care patients. The urgent need to find adequate therapeutic approaches to treat these infections has boosted the efforts to elucidate the genetic circuits governing immune evasion and host adaptation, but also antifungal resistance in *Candida* species.

This thesis displays a set of studies addressing the physiological impact of two non-fermentable carbon sources commonly found in the human host, namely lactate and acetate, in both *C. albicans* and *C. glabrata*. Under certain circumstances, these carboxylic acids represent the main carbon and energy sources that sustain the survival of these pathogens. The efficient uptake of these substrates by regulated plasma membrane transporters play a critical role in such conditions. Therefore, *Candida* carboxylate transporters were studied regarding their physiology and regulation, as well as their potential role in biofilm formation, antifungal drug resistance and immune recognition.

Growth of *C. albicans* in the presence of lactate was found to affect biofilm formation and morphology, as well as susceptibility to fluconazole. These phenotypes are dependent on Jen1 and Jen2 carboxylate transporters. Adaptation to lactate induces cell wall remodeling, a process that was found to be partially mediated by the Rlm1 transcription factor and to affect the interaction of *C. albicans* with immune cells.

In a second part of the work, global transcriptomic analyses in *C. glabrata* revealed that fluconazole treatment induces gene expression reprogramming in a carbon source and pH-dependent manner. The mitochondrial cochaperone Mge1 has emerged as a key regulator of fluconazole susceptibility during these conditions, by reducing the metabolic flux towards toxic sterol formation. Additionally, three putative carboxylate transporters of *C. glabrata*, that belong to the AceTr family, were also studied. These transporters were shown to play a critical role in acetate assimilation and contribute to the persistence of *C. glabrata* within the human host.

The systematic analysis of how host microenvironments influence the physiology of *Candida* species highlighted important mediators of host-pathogen interactions, such as carboxylate transporters. These proteins allow a rapid adaptation of *Candida* to the human host, contributing to their pathogenic potential.

Keywords: alternative carbon sources, biofilms, *C. albicans*, carboxylate transporters, *C. glabrata*

RESUMO

Função e regulação de transportadores de ácidos carboxílicos em *Candida albicans* e *C. glabrata* e o seu papel na formação de biofilmes, resistência a antifúngicos e fagocitose

As leveduras oportunistas mais frequentes em humanos pertencem ao género *Candida* e são uma fonte comum de infeções sistémicas em pacientes hospitalizados. A procura urgente de novas terapias para tratar estas infeções tem aumentado os esforços para elucidar, em *Candida*, os circuitos genéticos que governam a evasão imune, a adaptação ao hospedeiro, mas também a resistência a antifúngicos.

Esta tese apresenta um conjunto de estudos que abordam o impacto fisiológico de duas fontes de carbono não-fermentáveis, os ácidos láctico e acético, em *C. albicans* e *C. glabrata*. Em certos microambientes, estes substratos são as principais fontes de energia e carbono disponíveis e o seu transporte para o interior da célula, de um modo eficiente, é fundamental. Esta tese teve como principal objetivo compreender a fisiologia e a regulação de transportadores de ácidos carboxílicos em *Candida,* assim como o seu papel na formação de biofilmes, resistência a antifúngicos e reconhecimento imunológico. Numa primeira parte do trabalho, foi demonstrado que a presença de lactato afeta a formação e morfologia de biofilmes em *C. albicans*, bem como a sua suscetibilidade ao fluconazol. Estes fenótipos são dependentes dos transportadores de ácidos carboxílicos Jen1 e Jen2. Foi também revelado que a adaptação ao lactato induz a remodelação da parede celular, um processo que, em parte, é mediado pelo fator de transcrição Rlm1, e afeta a interação de *C. albicans* com as células do sistema imunitário. Numa segunda parte do trabalho, foi realizada uma análise transcriptómica em *C. glabrata*. Esta análise revelou que o tratamento com fluconazol induz uma reprogramação da expressão genética, de um modo dependente da fonte de carbono e do pH. Nessas condições, o cochaperone mitocondrial Mge1 apresenta-se como um regulador chave da suscetibilidade a este antifúngico, por reduzir o fluxo metabólico em direção à formação de esteróis tóxicos. Por fim, foi também demonstrado que três transportadores da família AceTr desempenham um papel crítico na assimilação de acetato, contribuindo para a persistência deste microrganismo no hospedeiro humano.

A análise sistemática da influência dos microambientes do hospedeiro na fisiologia das espécies de *Candida* revelou importantes mediadores, como os transportadores de ácidos carboxílicos, que permitem uma rápida adaptação destas espécies ao hospedeiro e contribuem para o seu potencial patogénico.

Palavras-chave: biofilmes, *C. albicans*, *C. glabrata*, fontes alternativas de carbono, transportadores de carboxilatos

LIST OF PUBLICATIONS

The work performed during this PhD resulted in the following peer-reviewed scientific publications:

1. Alves R, Barata-Antunes C, Casal M, Brown AJP, Van Dijck P, Paiva S. (2020) Adapting to survive: how *Candida* overcomes host-imposed constraints during human colonization. *Plos Pathogens*

2. Alves R, Sousa-Silva M, Vieira D, Soares P, Chebaro Y, Lorenz MC, Casal M, Soares-Silva I, Paiva S. (2020) Carboxylic acid transporters in *Candida* pathogenesis. *mBio*

3. Alves R, Kastora SL, Gonçalves A, Azevedo N, Rodrigues CF, Silva S, Demuyser L, Van Dijck P, Casal M, Brown AJP, Henriques M, Paiva S (2020) Transcriptional responses of *Candida glabrata* biofilm cells to fluconazole are modulated by the carbon source. *npj Biofilms and Microbiomes.*

4. Oliveira-Pacheco J*, Alves R*, Costa-Barbosa A, Cerqueira-Rodrigues B, Pereira-Silva, Paiva S, Silva S, Henriques M, Pais C, Sampaio P (2018) The role of *Candida albicans* transcription factor *RLM1* in response to carbon adaptation. *Frontiers in Microbiology*. (*both authors contributed equally)

5. Alves R, Mota S, Silva S, Rodrigues CF, Alistair JP, Henriques M, Casal M, Paiva S (2017) The carboxylic acid transporters Jen1 and Jen2 affect the architecture and fluconazole susceptibility of *Candida albicans* biofilm in the presence of lactate. *Biofouling.*

6. Mota S, Alves R, Carneiro C, Silva S, Brown AJ, Istel F, Kuchler K, Sampaio P, Casal M, Henriques M, Paiva S (2015) *Candida glabrata* susceptibility to antifungals and phagocytosis is modulated by acetate. *Frontiers in Microbiology.*

7. Alves R, Duarte C, Timmermans B, Van Ende M, Lewin S, Brunke S, Casal M, Van Dijck P, Paiva S. Acetate assimilation is an integral part of *Candida glabrata* persistence within the human host. (Manuscript in preparation)

Peer-reviewed scientific publications not included in this thesis:

1. Gómez-Varela AI, Stamov DR, Miranda A, Alves R, Barata-Antunes C, Dambournet D, Drubin DG, Paiva S, De Beule PAA (2020) Simultaneous co-localized super-resolution fluorescence microscopy and atomic force microscopy: combined SIM and AFM platform for the life sciences. *Scientific Reports*

Book chapters not included in this thesis:

1. Alves R*, Barata-Antunes C*, Talaia G, Paiva S. Metabolismo do intestino e sua regulação. In: Bioquímica Fisiológica: Integração do Metabolismo na Especialização dos Órgãos. Fardilha M, Oliveira P & Ferreira R (Ed). Edições Afrontamento. (2019). ISBN: 978-989-746-203-0. (*both authors contributed equally)

Oral presentations at International Conferences, Meetings and Workshops:

1. Alves R, Gonçalves A, Timmermans B, Van Ende M, Casal M, Van Dijck P, Paiva S. Acetate assimilation is an integral part of *Candida glabrata* survival in the human host. 37th SMYTE – Small Meeting on Yeast Transport and Energetics. September 11-15; 2019; Nové Hrady, Czech Republic.

2. Alves R, Timmermans B, Van Ende M, Casal M, Van Dijck P, Paiva S. Functional characterization of putative acetate transporters and channels in the human fungal pathogen *Candida glabrata*. XXIX International Conference on Yeast Genetics and Molecular Biology. August 18-22; 2019; Gothenburg, Sweden. **(ICYGMB Travel Grant)**

3. Alves R, Mota S, Carneiro C, Silva S, Brown AJ, Istel F, Kuchler K, Sampaio P, Casal M, Henriques M, Paiva S. Biofilm formation, antifungal drug susceptibility and phagocytosis in *Candida glabrata* are modulated by the carbon source. 33rd SMYTE - Small Meeting on Yeast and Transport Energetics, Lisbon, Portugal, July 21-24, 2015.

Poster presentations at International Conferences, Meetings and Workshops:

1. Alves R, Timmermans B, Van Ende M, Henriques M, Casal M, Van Dijck, Paiva S. Role of carboxylate transporters during carbon adaptation. HFP2019: Molecular Mechanisms of Host-Pathogen Interactions and Virulence in human fungal Pathogens. May 18-24; 2019; La Colle sur Loup, France. **(YFT Grant ALC19-038)**

2. Alves R, Kastora S, Casal M, Brown AJ, Henriques M, Paiva S. Adapting to survive: how *Candida glabrata* responds to environmental physiological constrains. 14th ASM Conference on *Candida* and Candidiasis. April 15-19, 2018; Providence, RI, USA. **(FLAD Travel Grant)**

3. Alves R, Kastora S, Pinho E, Rodrigues CF, Silva S, Casal M, Brown AJ, Henriques M, Paiva S. Global transcriptome characterization of *Candida glabrata* biofilms in response to acetate and fluconazole.

ImResFun - Final Meeting Marie Curie Initial Training Network: Molecular Mechanisms of Fungal Pathogen-Host Interaction, September 3-7, 2017; Innsbruck, Austria.

Oral presentations at National Conferences, Meetings and Workshops:

1. Alves R, Van Dijck P, Brown AJP, Henriques M, Casal M, Paiva S. Adapting to survive: how *Candida* spp. respond to environmental physiological constraints. IV Simpósio Programa Doutoral em Biologia Molecular e Ambiental. October 25, 2018; Braga, Portugal.

2. Oliveira-Pacheco J, Alves R, Costa AB, Cerqueira-Rodrigues B, Pereira-Silva P, Paiva S, Silva S, Henriques M, Pais C, Sampaio P. The role of *Candida albicans* transcription factor RLM1 in response to carbon adaptation. XXI Jornadas de Biologia de Leveduras: "Professor Nicolau van Uden". June 8-9, 2018; Braga, Portugal.

3. Alves R, Oliveira-Pacheco J, Cerqueira-Rodrigues B, Paiva S, Silva S, Henriques M, Sampaio P. The impact of carbon source in *Candida albicans* virulence: participation of *RLM1* in host pathogen interaction. XLI Jornadas Portuguesas da Genética, June 8-9, 2017; Aveiro, Portugal.

4. Alves R, Mota S, Silva S, Rodrigues CF, Brown AJ, Henriques M, Casal M, Paiva S. Lactic acid increases the susceptibility of *Candida albicans* to fluconazole. XIX Congresso Nacional de Bioquímica, December 8-10, 2016; Guimarães, Portugal. **(Best Oral Communication)**

5. Mota S, Alves R, Carneiro C, Silva S, Brown A J, Istel F, Kuchler K, Sampaio P, Casal M, Henriques M, Paiva S. *Candida glabrata* susceptibility to antifungals and phagocytosis is modulated by the carbon source. XXXIX Jornadas Portuguesas da Genética, May 25-27, 2015; Braga, Portugal.

Poster presentations at National Conferences, Meetings and Workshops:

1. Gonçalves A, Alves R, Casal M, Van Dijck P, Paiva S. *Candida glabrata* biofilm development on medical devices is modulated by the presence of alternative carbon sources. Microbiotec. December 7-9, 2017; Porto, Portugal.

2. Alves R, Oliveira-Pacheco J, Cerqueira-Rodrigues B, Paiva S, Silva S, Henriques M, Sampaio P. Metabolic plasticity as a strategy for virulence: participation of *Candida albicans* transcription factor RLM1 in host-pathogen interaction. I Simpósio de Bioquímica Aplicada, May 31, 2017; Braga, Portugal. **(Best Poster Presentation)**

3. Alves R, Kastora S, Pinho E, Rodrigues CF, Silva S, Casal M, Brown A J, Henriques M, Paiva S. Impact of alternative carbon sources and antifungal treatment on *Candida glabrata* biofilms' transcription profile. XIX Congresso Nacional de Bioquímica, December 8-10, 2016; Guimarães, Portugal.

4. Alves R, Mota S, Barata-Antunes C, Silva S, Rodrigues CF, Brown A J, Henriques M, Casal M, Paiva S. Carboxylic acid transportes Jen1 and Jen2 affect *Candida albicans* biofilms' formation and susceptibility to fluconazole. XL Jornadas Portuguesas da Genética, June 1-2, 2016; Coimbra, Portugal.

TABLE OF CONTENTS

CHAPTER 7 – CONCLUSIONS AND FUTURE PERSPECTIVES

LIST OF FIGURES

LIST OF TABLES

ACRONYMS

AAPs	Amino Acid Permeases
ABC	ATP-Binding Cassette
AceTr	Acetate uptake Transporter
Acetyl-coA	Acetyl-Coenzyme A
ATO	Acetate Transporter ortholog
ATP	Adenosine Triphosphate
BMDMs	Bone Marrow-derived Macrophages
cAMP-PKA	cyclic Adenosine Monophosphate dependent Protein Kinase A
cDNA	complementary Deoxyribonucleic Acid
CFUs	Colony Forming Units
ClonNAT	Nourseothricin
CRISPR	Clustered Regularly Interspaced Short Palindromic Repeats
CSM	Complete amino acid mixture
CV	Crystal Violet
CWI	Cell Wall Integrity
DcSAM	Decarboxylated S-adenosylmethionine
DMEM	Dulbecco's Modified Eagle's Medium
DNA	Deoxyribonucleic acid
ECM	Extracellular Matrix
EDTA	Ethylenediamine Tetraacetic Acid
ER	Endoplasmic reticulum
FACS	Fluorescence-activated cell sorting
FEG-SEM	Field Emission Gun Scanning Electron Microscopy
FRT	FLP recombinase recognition target
GlcNAc	N-acetylglucosamine
GPI	Glycosylphosphatidylinositol
GUT	Gastrointestinally induced Transition
H_2O_2	Hydrogen peroxide
HEPES	4-(2-hydroxyethyl)-1-piperazineethanesulfonic acid

HGTs	Hexose transporters
HPLC	High-pressure liquid chromatography
HSE	Heat Shock Element
HSPs	Heat shock proteins
HYG	Hygromycin B
IL-10	Interleukin 10
LB	Luria-Bertani broth medium
LDH	Lactate Dehydrogenase
MAPK	Mitogen activated protein kinase
MAPKK	MAPK kinase
MAPKKK	MAPKK kinase
MFC	Minimal Fungicidal Concentration
MFIs	Median Fluorescence Intensities
MFS	Major Facilitator Superfamily
MIC	Minimal Inhibitory Concentration
MOI	Multiplicity of infection
NEDA	N-(1-napthyl)ethylenediamine dihydrochloride
NETs	Neutrophil extracellular traps
NO	Nitric Oxide
NOS	Nitric Oxide Species
$O_2^{\bullet}$	Superoxide anion
$O_2^{\cdot\cdot}$	Superoxide
OD	Optical density
$^{\bullet}OH$	Hydroxyl radicle
OPTs	Oligopeptide transporters
OST	Oligosaccharyl Transferase Complex
PAMP	Pathogen-associated molecular pattern
PBS	Phosphate buffered saline
PCR	Polymerase chain reaction
PI	Propidium Iodide
PKC	Protein Kinase C
PMNs	Polymorphonuclear leukocytes

PMTs	Protein O-MannosylTransferases
PRRs	Pattern-recognition receptors
qRT-PCR	Quantitative real-time PCR
RNA	Ribonucleic acid
RNS	Reactive nitrogen species
ROS	Reactive oxygen species
RPMI	Roswell Park Memorial Institute
SAM	s-adenosylmethionine
SAM -	Sorting Assembly Machinery
SAPs	Secretory aspartyl proteinases
SC	Synthetic complete
SD	Synthetic defined
SDA	Sabouraud dextrose agar
SDB	Sabouraud dextrose broth
SDS	Sodium dodecyl sulphate
SEM	Scanning Electron Microscopy
SHS	Sialate:H^+ symporter
Sod	Superoxide dismutase
Sp2DC	Sp2 decarboxylase
SPS complex	Ssy1-Ptr3-Ssy5 complex
SQM	Sterol quantitation method
TCA	Tricarboxylic acid cycle
TMS	Transmembrane segments
TNF-α	Tumor necrosis factor alpha
UDP-GlcNAc	Uridine diphosphate N-acetylglucosamine
UG	Urogenital
WT	Wild type
XS genes	Oxidative stress genes
YFP	Yellow fluorescent protein
YNB	Yeast nitrogen base
YPD	Yeast extract-Peptone-Dextrose

in loving memory of my Grandmas

CHAPTER 1

GENERAL INTRODUCTION

Disclaimer

Part of this chapter contains work that has been previously published in *Plos Pathogens*.

-

Alves R, Barata-Antunes C, Casal M, Brown AJP, Van Dijck P, Paiva S. (2020) Adapting to survive: how *Candida* overcomes host-imposed constraints during human colonization. *Plos Pathogens*. doi: 10.1371/journal.ppat.1008478

-

THESIS OVERVIEW

Candida species are the most common fungal pathogens of humans and have emerged as a leading cause of human mortality among the immune-compromised population. The impact of *Candida* on human health is exacerbated by the fact that the available antifungals to eradicate these organisms are severely limited and often ineffective. The scientific challenge of finding novel therapeutic targets to treat these infections is highly limited by the close evolutionary relationship between these microbes and their mammalian hosts.

The rapid increase of *Candida* infections in the last decade has motivated researchers to explore the adaptation mechanisms of these pathogens to the human host. For years, research involving fungal microbes, and in particular *Candida* species, has been performed under historically standardized laboratory settings, and yet they often grow under different environmental conditions in the human host. This has hampered the discovery of important regulators, for cell adaptation and survival under different host niches, that can be potentially used as targets for antifungal development.

Considering the different niches in which *Candida* grows in the body, this thesis proposes to advance our knowledge on the interactions established between these pathogens and the human host. In particular, it covers a set of studies addressing the physiological impact of lactate and acetate, two nonfermentable carbon sources commonly found in the human host, in both *C. albicans* and *C. glabrata*. These nutrients and respective transporters were shown to impact biofilm formation, antifungal drug resistance and immune recognition, important aspects of *Candida* pathogenesis.

Chapter 1 defines the aims of this work and details each chapter of the thesis. It also provides an overview of the different strategies employed by *Candida* species to survive and proliferate within the human host, including sophisticated mechanisms to evade immune surveillance, to adapt to constantly changing host microenvironments and to resist antifungal therapy. A review on how these strategies directly affect *Candida* physiology and pathogenicity is also provided.

The ability to transport carboxylic acids represents an advantage for *Candida* when these nutrients are the main exogenous carbon sources available in the host. In **Chapter 2**, the two major fungal families of

carboxylate transporters are revisited as well as their contribution for *Candida* pathogenesis. A phylogenetic analysis of 101 putative carboxylate transporters, belonging to both Jen and AceTr families, is provided for 12 medically relevant *Candida* species. The designation of ATO, standing for Ammonia Transport Outward, is redefined as "Acetate Transport Ortholog" for all *Candida* members belonging to the AceTr family, to better reflect and describe their function as acetate transporters. A brief discussion correlating the expansion of some of these transporters in specific *Candida* species with their pathogenic potential is also provided.

Chapter 3 describes the impact of lactate on *C. albicans* biofilm formation and antifungal drug resistance. Both lactic acid-grown planktonic and biofilm cells were used to characterize *C. albicans* susceptibility to the most common used antifungal drug fluconazole. The involvement of both Jen1 and Jen2, two carboxylate transporters, was also assessed on these processes. Moreover, multiple components of the extracellular matrix were analyzed, including their impact on antifungal resistance. The results presented in this chapter contribute to our understanding on how acidic pH niches associated with the presence of lactate alter *C. albicans* biofilm formation, morphology and antifungal drug resistance.

Chapter 4 explores the impact of lactate on *C. albicans* immune recognition. Growth of *C. albicans* cells in the presence of lactate was shown to induce the secretion of tartaric acid, which has the potential to modulate the TCA cycle on the host cells and reduce cellular viability. In addition, adaptation to lactate reduced *C. albicans* internalization by immune cells and consequently the efficient elimination of these pathogens, which was correlated with a lower exposure of cell wall β-glucans. The transcription factor Rlm1 is proposed as a mediator of cell wall remodeling during carbon adaptation.

Chapter 5 presents a genome-wide transcriptome analysis of *C. glabrata* biofilm cells that have been exposed to different environmental settings in order to identify potential molecular players involved in fluconazole resistance. This study reveals how acetate modulates the transcriptional responses of *C. glabrata* biofilms to fluconazole, suggesting that the host microenvironment influences directly the physiology of *C. glabrata*, affecting how this pathogen responds to antifungal treatment. Additionally, *C. glabrata* Mge1, a cochaperone involved in iron metabolism and protein import into the mitochondria, is proposed as a key regulator of fluconazole susceptibility during carbon and pH adaptation, by reducing the formation of toxic sterols.

The metabolism of carboxylic acids has been demonstrated to play an important role in *Candida* pathogenesis. For instance, both Jen and Ato transporters have been consistently found upregulated in several genome-wide screenings, when *C. albicans* cells grow inside neutrophils or macrophages. Although *C. glabrata* has a remarkable ability to thrive inside immune cells, Jen transporters are absent and Ato transporters have not been characterized in this pathogen.

Chapter 6 comprises the identification and functional characterization of all members of the AceTr family in *C. glabrata*, as well as additional proteins potentially involved in the uptake of acetate. Single and multiple mutants in these transporters were constructed in *C. glabrata* and further analyzed by growth and transport assays. The proteins were also heterologously expressed and characterized in a *Saccharomyces cerevisiae* strain defective in acetate uptake. This chapter highlights the importance of acetate assimilation for *C. glabrata* persistence inside the human host.

Chapter 7 is a conclusion chapter that summarizes all the studies conducted in the scope of this thesis. This chapter consolidates the results and findings of the different studies, discusses the broader context of the research work performed, and proposes a direction and focus for future work.

INTRODUCTION

The human body is home to a large number of microbes that play essential roles in maintaining human health. However, under particular host-compromising conditions, they can shift from harmless commensals to opportunistic pathogens to cause inflammation and disease. Fungal communities, which can include *Candida* species, constitute an integral part of the human microbiota that, under normal conditions, asymptomatically colonize several niches, including the skin, oral cavity, gastrointestinal, and urogenital tracts [1–3]. The remarkable ability to alternate between local current microenvironments within internal host niches such as blood or tissues is often linked with their pathogenic potential. Therefore, environmental changes promoted either by alterations in host microbiota or the host immune system may allow these microorganisms to overgrow, cross the epithelial barriers, and cause severe, life-threatening infections [4].

Among the *Candida* species that trigger human disease, *Candida albicans*, *C. glabrata*, *C. parapsilosis*, *C. tropicallis* and *C. krusei* are the most common [4–6]. Yet, other emerging species, including *C. auris*, *C. guilliermondii*, *C. lusitaniae*, and *C. metapsilosis*, are of particular concern because they are rapidly spreading worldwide, with several reported outbreaks [5,7,8]. Moreover, *Candida* infections are difficult to diagnose, commonly resulting in delayed antifungal treatments that have been associated with hospital mortality [9]. The antifungal drugs available to eradicate these fungal pathogens are also limited and often ineffective, mainly because of the intrinsic multidrug resistance of certain *Candida* species and their ability to form biofilms on implanted medical devices [10–12]. Considering that each species presents its own distinctive features in relation to invasive potential, morphogenesis, antifungal susceptibility, and biofilm formation, studies focusing on the adaptation to different host and environmental factors have the potential to reveal novel molecular players of virulence pathways.

Here, we provide an overview of established and emerging strategies used by *Candida* to adapt to common environmental challenges faced by these fungi during immune evasion and human colonization (Figure 1.1). As we review major host-imposed constraints, we highlight the central regulatory circuits required for fungal adaptation to these challenges. We also discuss the impact of such physiological reprogramming on key aspects of *Candida* pathogenicity, with a particular emphasis on immune evasion, biofilm formation, and antifungal drug resistance. We propose that the genetic circuits governing *Candida*

adaptation to human niches can be exploited in search of new antifungal targets and diagnosis improvement.

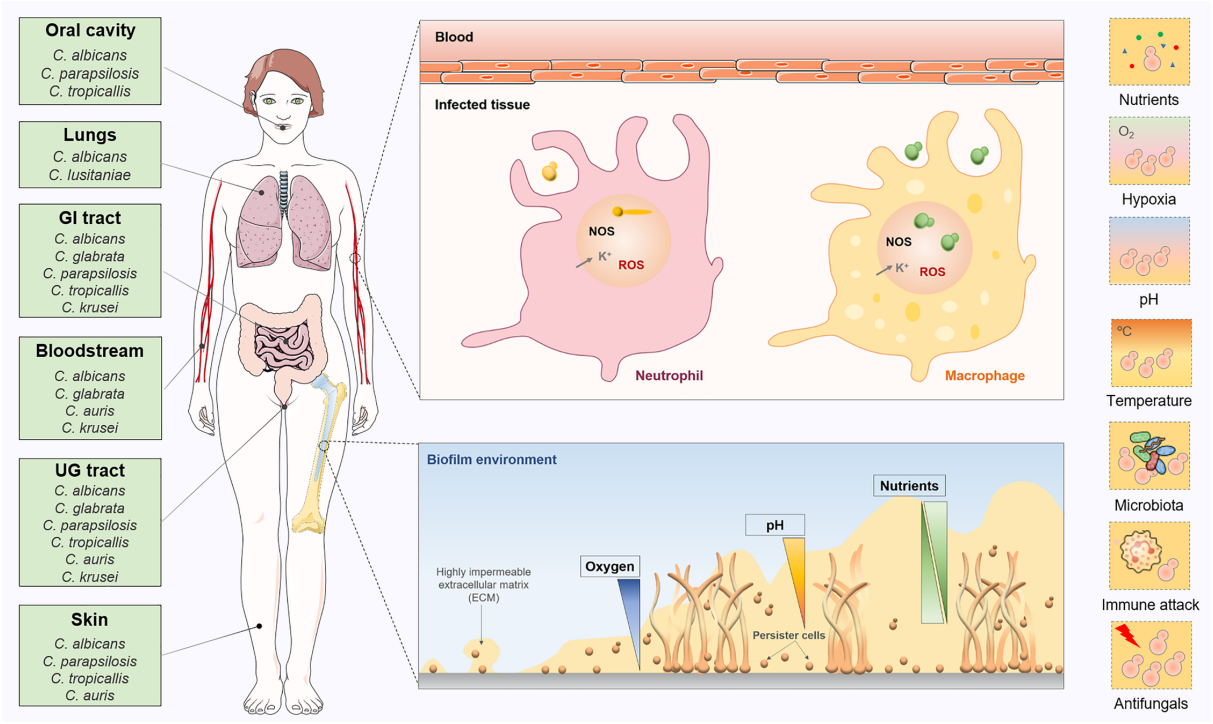

Figure 1.1. *Candida* biogeography and the different host-imposed constraints during human colonization. The most frequently isolated *Candida* species are listed according to their principal habitat in the human body (oral cavity, lungs, gastrointestinal tract, bloodstream, urogenital tract, and skin). The different host-imposed constraints are highlighted for several microenvironments where *Candida* thrives in the human body, including inside phagocytic cells or biofilms. Key references: *C. albicans* [2,3], *C. glabrata* [3], *C. parapsilosis* [2], *C. tropicalis* [2], *C. lusitaniae* [13], and *C. krusei* [6]. ECM, extracellular matrix; NOS, nitric oxide species; ROS, reactive oxygen species; UG, urogenital.

1.1 *Candida* within the human host

The human host contains a variety of environmental niches in which *Candida* species can thrive. Adaptation to these sites requires rapid and coordinated changes in *Candida* metabolism and physiology in order to avoid or escape immune surveillance and to counteract several host-imposed constraints (for example, nutrient limitation, oxygen deprivation, pH fluctuations, changes in temperature, or oxidative, nitrosative, and cationic stresses). Moreover, *Candida* species interact with other microbial residents, establishing either cooperative or antagonistic relationships, which may affect their growth and influence the outcome of an infection.

Depending on the local environmental cues, some *Candida* species may exhibit different cellular morphologies. These include budding forms, which have been associated with commensalism, and the filamentous forms hyphae and pseudohyphae, often related with invasive and disseminated disease [14,15]. However, these cell types were found in infected tissues, suggesting they all promote pathogenicity. *C. albicans* has also the ability to switch into more functionally and genotypically distinct cell types, which may present improved fitness in specific host niches [15]. In particular, "white" yeast cells can switch to mating specialized "opaque" cells, and a subset of these can also transit into a third, "gray" morphology [16]. An additional distinctive group of cells, known as GUT (gastrointestinally induced transition), seems to display enhanced fitness in the gastrointestinal tract when compared with other cell types [17]. The morphogenic transitions depend on a highly dynamic cell wall that acts as an environmental barrier, and it is essential for host–pathogen interactions. The core skeleton of the cell wall is composed of the polysaccharide β-1,3-glucan, covalently linked to β-1,6-glucan and chitin. The outer layer contains glycosylated mannoproteins cross-linked to β-1,6-glucans. The relative amount of each component fluctuates between morphologies and in response to external challenges, impacting immune responses [18,19].

1.1.1 Nutrient availability and *Candida* metabolic flexibility

Of the many challenges pathogens face in the human host, possibly none is more important than nutrient availability because cells must assimilate nutrients in order to thrive. These might include sugars, carboxylic acids, peptides, amino acids, lipids, or phospholipids. The assimilation of glucose, lactose and galactose is mediated via hexose transporters (HGTs), providing major sources of energy and carbon (Figure 1.2a). The well-studied yeast model *Saccharomyces cerevisiae*, which is relatively closely related

to some *Candida* species, uses glucose as a preferred carbon source and only switches to nonfermentable nutrients when glucose becomes depleted [20]. This hierarchical utilization requires highly evolved networks integrating several signaling pathways in order to repress the assimilation of alternative carbon sources [21–24]. This is partly achieved by the ubiquitination of key gluconeogenic and glyoxylate cycle enzymes following the exposure to glucose [25]. Notably, these enzymes appear to lack ubiquitination sites in *C. albicans*, *C. glabrata*, *C. parapsilosis*, and *C. tropicalis*, and consequently, they are not subjected to glucose-induced degradation [26,27]. The evolutionary rewiring of key metabolic ubiquitination targets has been suggested to increase the ability of *C. albicans* to colonize and cause infection in the mammalian host because, unlike *S. cerevisiae,* this yeast is able to assimilate sugars and alternative carbon sources simultaneously [26–28]. The availability of glucose is thought to enhance *C. albicans* virulence, owing to the fact that this sugar has been reported to induce hyphal morphogenesis at low physiological concentrations [29-31] and promotes antifungal resistance [32,33]. Moreover, rapid glucose metabolism by *C. albicans* seems to be important during infection because immune cells, specifically macrophages, rely on glucose for survival [34]. This limitation is exploited by *C. albicans*, which elicits rapid macrophage death by depleting the available glucose [34].

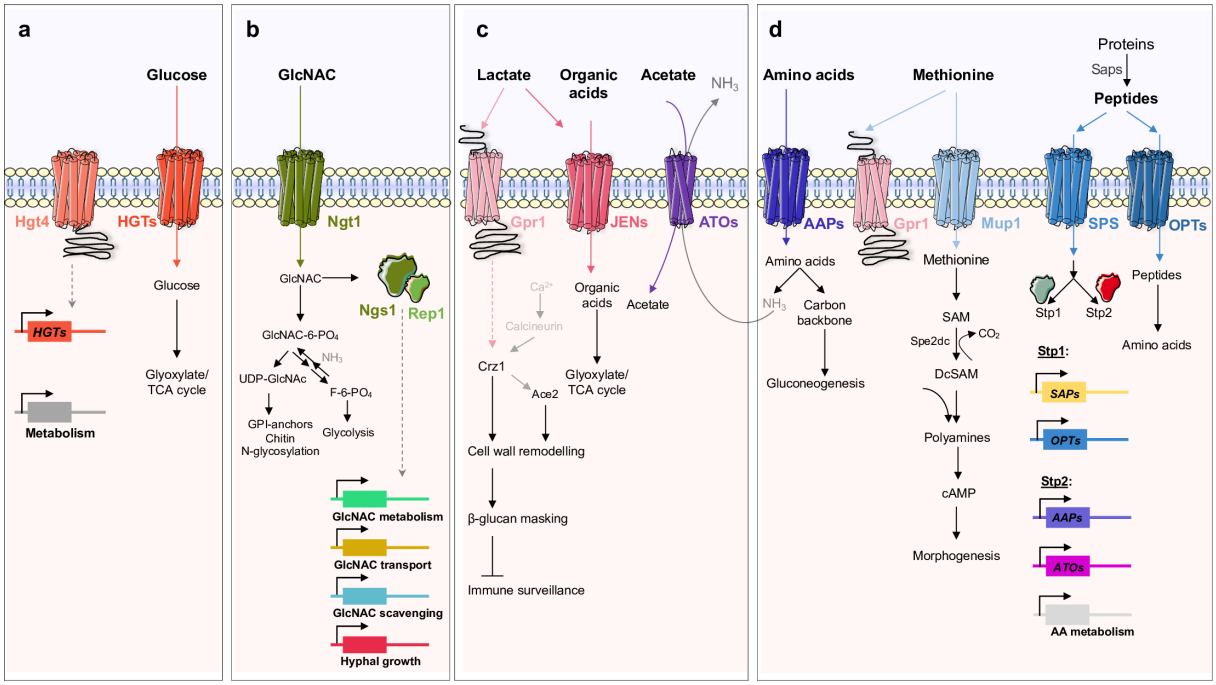

Figure 1.2. Schematic representation of the main sensing, transport, and transduction systems for the utilization of different host nutrients in *Candida* species. (a) In *C. albicans*, glucose is sensed by Hgt4, generating an intracellular signal that induces the expression of HGTs and other metabolic genes. **(b)** In *C. albicans* and *C. tropicalis*, the uptake of GlcNAc occurs through the Ngt1 transporter. **(c)** The uptake

of carboxylic acids is facilitated by the JEN (in *C. albicans*) and ATO transporters (in *C. albicans* and *C. glabrata*). In *C. albicans*, Gpr1 is reported to be a lactate and methionine sensor. In the presence of lactate, Gpr1 is thought to activate Crz1 in a calcineurin-independent manner and, together with Ace2, regulates a polygenic response that leads to β-glucan masking. **(d)** Peptides and amino acids are sensed by the SPS complex, which induces the expression of OPTs, AAPs, and ATO transporters, as well as SAPs and amino acid catabolic genes. Intracellular ammonia resulting from the catabolism of GlcNAc or amino acids is exported via Ato transporters. In the presence of methionine, and in low glucose conditions, the methionine-induced morphogenesis is activated via Gpr1 sensor and Mup1 transporter. AA, amino acid; AAP; amino acid permease; ATP, adenosine triphosphate; cAMP, cyclic adenosine monophosphate; DcSAM, decarboxylated S-adenosylmethionine; GlcNAc, N-acetylglucosamine; GPI, glycosylphosphatidylinositol; HGT, hexose transporter; OPT, oligopeptide transporter; SAM, S-adenosylmethionine; SAP, secretory aspartyl proteinase; SPS, Ssy1-Ptr3-Ssy5; Sp2DC, Sp2 decarboxylase; TCA, tricarboxylic acid cycle; UDP, urine diphosphate.

In glucose-limiting conditions, other alternative carbon sources, such as N-acetylglucosamine (GlcNAc) and carboxylic acids, are thought to play a critical role to sustain *Candida* growth. When infecting tissues and organs, *Candida* up-regulates several pathways involved in the utilization of alternative carbon sources, such as gluconeogenesis, the glyoxylate cycle, and fatty acid β-oxidation, suggesting that glucose levels may not be sufficient to satisfy the energetic requirements of the cells [28,35–37]. In *C. albicans* and *C. tropicalis*, GlcNAc, a monosaccharide produced mainly by bacteria in the gastrointestinal tract, enters the cell through the Ngt1 transporter, and is then sensed by the transcription factors, Ngs1 and Rep1, which control the expression of genes involved in the uptake and catabolism of GlcNAc [38–40] (Figure 1.2b). Depending on the metabolic state of the cells, GlcNAc can either be converted to uridine diphosphate-N-acetylglucosamine (UDP-GlcNAc) or to fructose-6-phosphate, which then enters the glycolytic pathway (Figure 1.2b). In *C. albicans*, GlcNAc can also be used as a signal to induce the expression of several virulence genes involved in white-opaque switching [41], hyphal morphogenesis [38–40,42], and cell death [43]. Additionally, GlcNAc metabolism seems to sustain *Candida* survival when growing inside phagocytic cells. The export of intracellular ammonia, derived from GlcNAc catabolism, has been reported to promote the alkalization of the phagosome, enabling cells to survive and escape from the acidic environment of the phagolysosome [44]. This mechanism is dependent on the transport of GlcNAc and subsequent catabolism through Hxk1, Nag1, and Dac1 enzymes [44]. Hence, mutants lacking the Ngt1 transporter or GlcNAc catabolic enzymes are defective in neutralizing the

phagosome [44]. The ability to manipulate ambient pH is reported for all species of the CTG clade, a phylogenetic group that translates the CUG codon into serine instead of leucine [45]. This is in contrast to what is found for the distantly related *C. glabrata*, whose genome does not appear to encode homologs of GlcNAc transporters or catabolic enzymes [44].

C. albicans can also raise the extracellular pH by metabolizing carboxylic acids [46]. This phenomenon is physiologically and genetically distinct from the GlcNAc-driven mechanism, as the metabolism of carboxylic acids, when used as the sole carbon source, does not generate ammonia or promote hyphal morphogenesis [44,46]. Physiologically relevant carboxylic acids such as lactate, acetate, succinate, butyrate, and propionate are produced either by host cells or host microbiota [47–49]. Lactate and acetate are particularly abundant in the gut and in vaginal secretions [47,50], but also inside phagocytic cells [51,52]. In *C. albicans*, the uptake of lactate is mediated by JEN transporters [51,53], while ATO transporters are potentially involved in the transport of acetate in both *C. albicans* and *C. glabrata* [52,54] (Figure 1.2c). These two transporter families are strongly induced after phagocytosis [51,52], and they modulate biofilm formation and resistance to antifungal drugs in both *C. albicans* and *C. glabrata* [54-56]. In particular, exposure to lactate has been shown to trigger the masking of β-glucan, a major pathogen-associated molecular pattern (PAMP), in several *Candida* species [57]. This affects the visibility of these pathogens to host immune defenses, which correlates well with the observed decrease in *C. albicans* uptake by macrophages and reduced phagocytic recruitment [57,58]. The β-glucan masking phenotype has been proposed to be dependent on Gpr1 and the transcription factor Crz1 [57]. These proteins control the expression of genes associated with the organization of the cell wall, ultimately contributing to the masking effect [57,59]. Therefore, the concomitant exposure of *Candida* cells to different carboxylic acids potentiates immune evasion and consequently *Candida* persistence.

The uptake of nitrogen is also critical for *Candida* survival. Different *in vivo* studies have demonstrated that genes involved in amino acid uptake and catabolism are strongly up-regulated in *C. albicans*, especially when phagocytosed by neutrophils and macrophages [36,60–62]. Indeed, several *C. albicans* and *C. glabrata* amino acid auxotrophic strains retain full virulence in mice, suggesting that these nutrients are readily available during infection [63–65]. Proteolytic enzymes, namely secretory aspartyl proteinases (SAPs), are of particular importance because they allow *Candida* to efficiently degrade the complement proteins and host connective tissues [66]. Once available, extracellular amino acids are then sensed by the SPS complex (composed of Ssy1, Ptr3, and Ssy5), which in turn activates the transcription factors,

Stp1 and Stp2 (Figure 1.2d). While Stp1 controls the expression of extracellular proteases and peptide transporters, Stp2 regulates amino acid permeases, Ato transporters, and catabolic enzymes [67,68] (Figure 1.2d). Along with GlcNAc and carboxylic acids, the catabolism of amino acids represents a third independent mechanism by which *Candida* rapidly neutralizes acidic microenvironments [52,69]. Previous studies reported that *C. albicans* mutants lacking *STP2* or *ATO* genes release less ammonia than wild type controls, failing to efficiently neutralize the acidic phagosome and undergo hyphal morphogenesis, which consequently affects their ability to escape phagocytic cells [52,70]. Recent data, however, suggest that the phagosomal membrane is highly permeable to ammonia, and the observed alkalization is rather a direct consequence of proton leakage induced by hyphal growth [71,72]. The transport of methionine via the high-affinity permease Mup1 and its subsequent metabolism have been also shown to induce morphogenesis in a process that is dependent on Gpr1 and the cAMP-PKA (cyclic Adenosine Monophosphate-Protein Kinase A) signaling cascade [73,74]. This methionine-induced morphogenesis pathway triggers the activation of adenylate cyclase by the production of increased levels of polyamines such as spermine and spermidine. These compounds are generated by the intracellular conversion of methionine into S-adenosylmethionine (SAM) and its decarboxylation by Spe2, which donates aminopropyl groups for polyamine synthesis [73] (Figure 1.2d).

1.1.2 Environmental pH fluctuations shape *Candida* physiology and pathogenicity

Changes in ambient pH represent an additional stress that *Candida* and other pathogens face in the human host. While the pH of human blood and tissues is slightly alkaline (pH 7.4), the pH of the oral cavity and the gastrointestinal and genitourinary tracts is acidic ($2 < pH < 6$). Adaptation to differing ambient pHs is critical for survival and growth in these niches. In fungi, including *Candida* species, pH signaling is mediated by the Rim pathway [75]. In *C. albicans*, the external pH is sensed by Rim21/Dfg16, Rim9, and an arrestin-like protein Rim8. Under alkaline pH, Rim8 is hyperphosphorylated, a signal that triggers the endocytosis of the plasma membrane complex and the recruitment of the signaling protease Rim13. This protease then cleaves the C-terminal inhibitory domain of Rim101, resulting in its activation. The activation of Rim101 promotes the expression of target genes involved in morphogenesis [76–79], growth [80], cell-wall remodeling [80], iron metabolism [81,82], adhesion [80], biofilm formation, and antifungal tolerance [75,83,84] (Figure 1.3).

On the other hand, the adaptation of *C. albicans* to acidic environments drives cell-wall remodeling by enhancing the exposure of two key fungal PAMPs (chitin and β-glucan) at the cell surface [85]. While pH-

dependent β-glucan exposure is regulated by a noncanonical signaling pathway, the remodeling of chitin is coordinated by several transcription factors, including Rim101, Bcr1, and Efg1 (Figure 1.3) [85,86]. The exposure of β-glucan at the cell surface hyperactivates the immune system largely through the recognition of the immunostimulatory β-glucan by Dectin-1, which enhances the recruitment of neutrophils and macrophages to the site of the infection [85]. This pH-dependent β-glucan exposure was also observed in *C. dubliniensis* and *C. tropicalis,* but not in *C. auris* or *C. glabrata* [85,86]. Surprisingly, adaptation to acidic environments induces β-glucan masking in *C. krusei*, suggesting that the outputs of pH-dependent signal transduction differ between these *Candida* species [85]. Additionally, the pH-dependent reorganization of the cell wall fluctuates over time in *C. albicans*, with β-glucan and chitin being masked after an initial period of exposure [86]. While the subsequent β-glucan masking is mediated by farnesol, this quorum-sensing molecule does not trigger the chitin cloaking [86]. These temporal fluctuations suggest dynamic cell-wall responses to environmental pH. Moreover, the early PAMP exposure appears to govern the outcome of the infection because subsequent remasking on the cell wall does not compensate for the initial induction of strong proinflammatory responses [86].

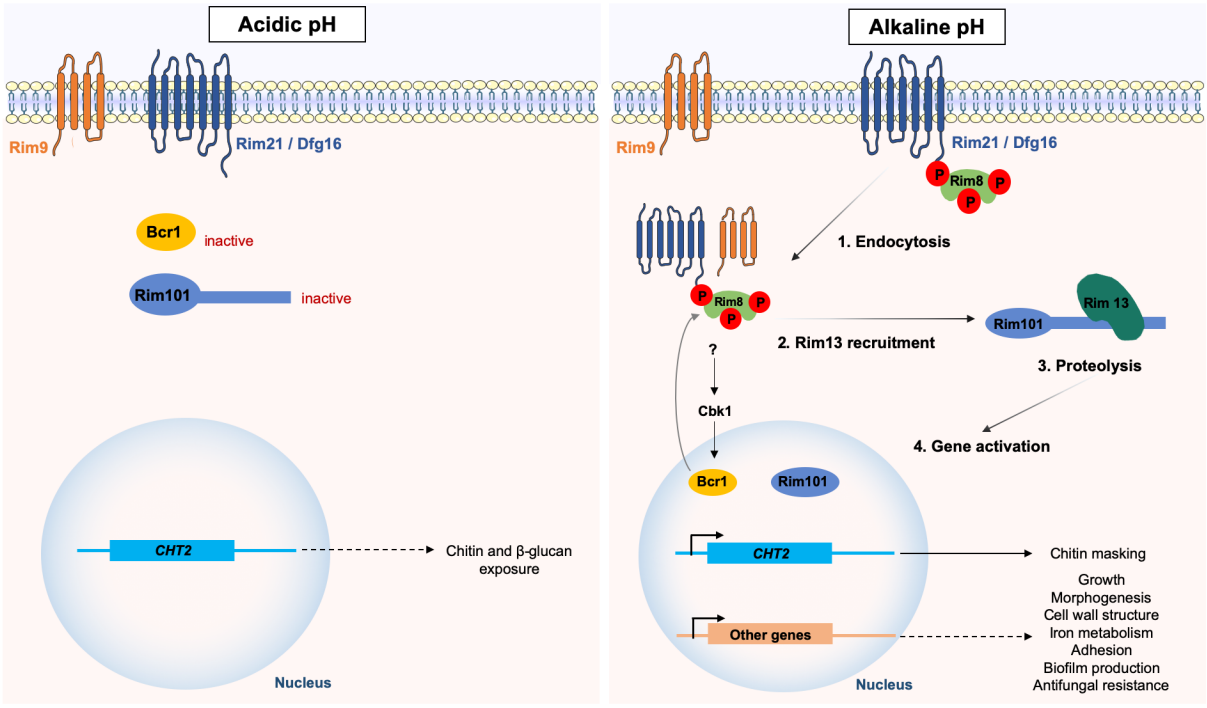

Figure 1.3. *Candida* adaptation to pH fluctuations. In *Candida* species, pH adaptation is mediated by the Rim pathway. Under acidic pH, the exposure of both chitin and β-glucan is enhanced and facilitates their recognition by the host innate immune system. Chitin exposure is promoted by the repression of both Rim101 and Bcr1, resulting in reduced expression of *CHT2*. β-glucan exposure is regulated by a noncanonical signaling pathway. Under alkaline pH, Rim8 is hyperphosphorylated, a signal that induces

the endocytosis of the Rim complex and the recruitment of Rim13. The C-terminal proteolysis of Rim101 by Rim13 activates it and promotes the expression of target genes, including *CHT2*.

1.1.3 Adaptation to oxygen-limiting niches is critical for *Candida* virulence

Oxygen levels inside the human host can vary greatly. While some niches are rich in oxygen, such as exposed skin or oral mucosa, others are anoxic or hypoxic, including the gastrointestinal tract [87]. Consequently, *Candida* cells must adapt to low-oxygen environments, particularly when colonizing the human gut, developing lesions or growing in biofilms [87,88]. Analyses of gene expression profiles of *C. albicans* cells shifted from normoxia to hypoxic growth conditions revealed the induction of several pathways, including glycolytic gene expression via Tye7 [89–91], fatty acid metabolism [92,93], heme biosynthesis and iron metabolism [89,92,94], cell-wall structure [89,92,94], and sterol biosynthesis via Upc2 [95,96]. In contrast, genes involved in the oxidative respiration were repressed [89,92,94]. Additionally, the Sit4 phosphatase, the Ccr4 mRNA deacetylase, and the Sko1 transcription factor have been identified as potential regulators of an early hypoxic response (10-20 min) [91,94].

Besides affecting the cellular metabolism and energy homeostasis, adaptation to hypoxia induces hyphal growth in *C. albicans* [94] and promotes immune evasion by triggering β-glucan masking at the cell surface [97]. β-glucan masking leads to reduced phagocytosis and attenuates local immune responses [97]. In contrast to lactate-induced β-glucan masking, hypoxia-induced masking does not depend on Gpr1 and Crz1. Instead, hypoxia-induced masking is mediated by mitochondrial and cAMP-PKA signaling [57,97]. Hypoxia induces the generation of mitochondrial superoxide [98,99], which is rapidly converted into diffusible hydrogen peroxide by superoxide dismutase 1 (Figure 1.4). Hydrogen peroxide has been proposed to somehow activate the cAMP-PKA pathway, which, in turn, triggers cell-wall remodeling and β-glucan masking [97]. However, the mechanism by which β-glucan masking is achieved at the cell surface remains unclear.

Hypoxia-induced β-glucan masking has been observed for some other pathogenic *Candida* species, namely *C. tropicalis* and *C. krusei*, but not in *C. glabrata*, *C. guilliermondi* or *C. parapsilosis* [97]. Therefore, during their evolution, hypoxic signaling has become integrated with PAMP masking only in some *Candida* pathogens. The adaptation to hypoxic environments enhances the ability of these *Candida* species to colonize the host. For example, it was shown that the recruitment of polymorphonuclear leukocytes (PMNs) to sites of *C. albicans* infection in mice was the main cause of hypoxia [88] (Figure

1.4). However, because of the hypoxia-induced β-glucan masking by *C. albicans* cells, these PMNs are not able to efficiently phagocytose the fungus, generate reactive oxygen species (ROS), or release extracellular DNA traps, allowing *C. albicans* to survive. Continued exposure to hypoxia leads to accumulation of lactate, prolonging the masking effect. Additionally, it was also observed that the antifungal activity of fluconazole is considerably reduced under hypoxic conditions. We speculate that the molecular mechanism behind this observation might include Upc2, considering its dual role in activating hypoxia-induced β-glucan masking [97] and conferring azole antifungal resistance [100]. In contrast to *C. albicans*, *C. tropicalis* is not able to induce β-glucan masking in response to hypoxia, and this species is more susceptible to PMN attack [88]. This is in agreement with the fact that *C. tropicalis* mainly infects neutropenic patients [101]. The molecular mechanisms allowing hypoxic adaptation are not completely defined. Nevertheless, it is clear that some *Candida* species take advantage of low-oxygen environments, either generated during infection or imposed by the specific host niche, to thrive by avoiding immune surveillance and escaping from antifungal therapy.

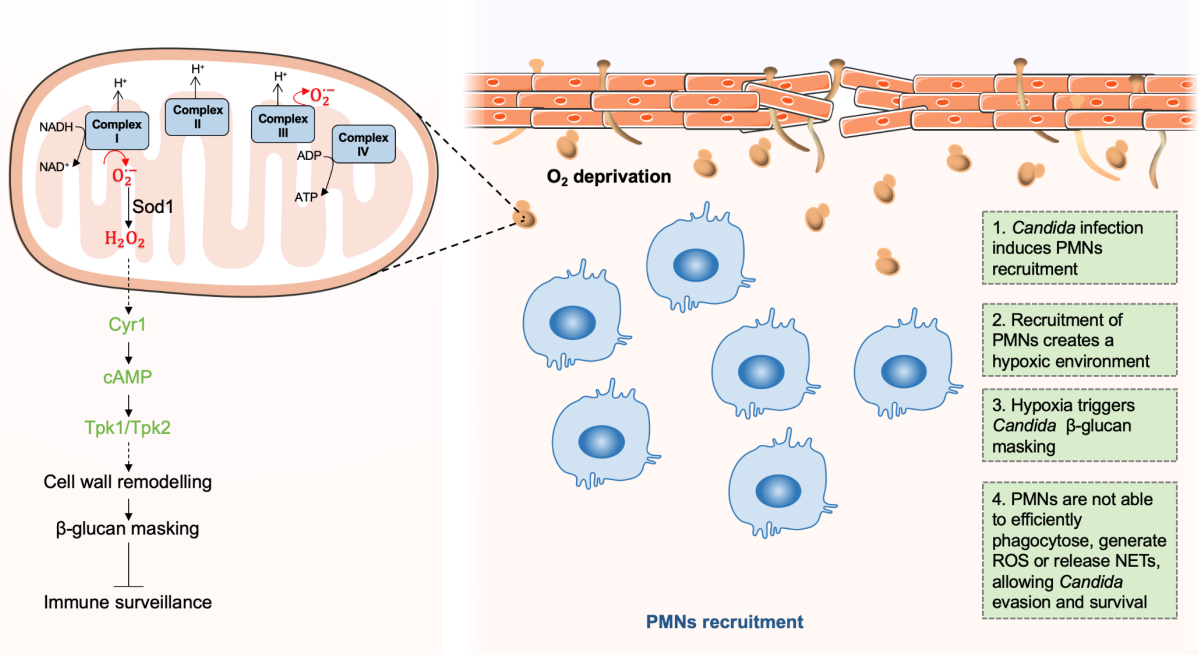

Figure 1.4. *Candida* adaptation to hypoxic host niches. During *C. albicans* infections, the recruitment of PMNs creates an hypoxic environment [88]. In the fungus, this oxygen limitation triggers increased formation of ROS, such as superoxide ($O_2^{\cdot-}$), from the electron transport chain [98,99]. Superoxide is then converted into diffusible hydrogen peroxide (H_2O_2) by the action of Sod1. H_2O_2 has been proposed to activate adenylyl cyclase (Cyr1) and cAMP-PKA (Tpk1/2) signaling, which in turn triggers cell-wall remodeling and β-glucan masking [97]. This β-glucan masking allows the fungus to evade phagocytosis

by the PMNs [88]. cAMP, cyclic adenosine monophosphate; NET, neutrophil extracellular trap; PKA, Protein Kinase A; PMN, polymorphonuclear leukocyte; ROS, reactive oxygen species.

1.1.4 *Candida* adaptation to temperature shifts is essential for full virulence

The human body temperature is considered to be a potent nonspecific defense against fungal infection, especially in febrile patients, because high temperatures considerably restrict fungal growth [102,103]. The human host presents fever as one of the first responses against a *Candida* infection, thereby exposing the fungal cells to temperatures ranging from 37 °C to 42 °C. These temperature fluctuations profoundly influence many physiological aspects of *C. albicans*, including morphology, mating, phenotypic switching, and drug resistance [104].

Changes in ambient temperature are sensed by a broad diversity of mechanisms. One of the most studied pathways is the evolutionarily conserved heat shock response, which mediates thermal homeostasis by controlling the levels of heat shock proteins (HSPs) [105]. HSPs are molecular chaperones sequestered in response to heat shock, rescuing proteins from unfolding or targeting damaged proteins for degradation. In *C. albicans*, the expression of HSP genes is activated by the heat shock transcription factor 1 (Hsf1), which becomes phosphorylated in response to temperature elevations, including thermal transitions that mimic fever [106,107]. After adaptation to the exposed temperature, Hsf1 phosphorylation returns to basal levels and several lines of evidence have suggested the existence of a negative feedback loop, in which Hsp90 negatively regulates Hsf1 [107–109]. Besides Hsf1, Hsp90 also controls the activation of other regulators that mediate long-term thermal adaptation (Figure 1.5). These include several mitogen-activated protein kinase (MAPK) signaling pathways, particularly the Hog1, Mkc1, and Cek1 pathways, which are intimately associated with cell-wall remodeling [110,111]. Other small HSPs such as Hsp12 and Hsp21 have also been identified as crucial for *C. albicans* to resist thermal stress [112,113]. HSPs and their associated signaling pathways have been widely implicated in antifungal resistance, emerging as potential antifungal targets to treat *Candida* infections [114]. Moreover, the activation of the Hsf1 transcriptional program in *C. albicans* has been associated with increased host cell adhesion, damage, and virulence, reinforcing the importance of this regulon in thermal homeostasis [115,116].

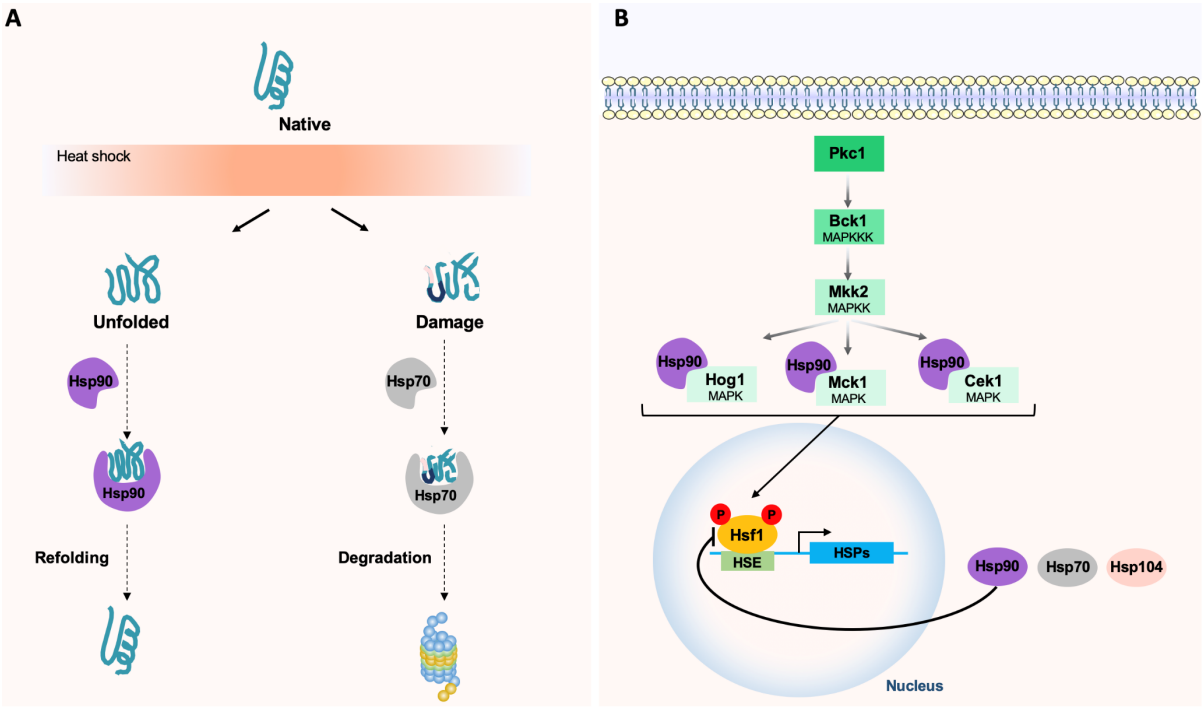

Figure 1.5. Molecular circuits required for thermal adaptation in *C. albicans*. (a) HSPs rescue proteins from unfolding or target damaged proteins for degradation. **(b)** In response to temperature upshifts, Hsf1 becomes phosphorylated, inducing the expression of HSP genes. After thermal adaptation, Hsf1 returns to basal levels through a negative feedback loop dependent on Hsp90. Long-term adaptation is controlled by Hsp90 through Hog1, Mkc1, and Cek1. HSE, heat shock element; HSP, heat shock protein; MAPK, mitogen-activated protein kinase; MAPKK/MAPKKK, MAPK kinase/ MAPKK kinase.

1.1.5 *Candida* and host microbiota: avoiding antagonistic interactions in health and disease

The structure of human microbiota is dynamic, often defined by host and environmental factors and also by physical and metabolic interactions between species. While some of these interactions are cooperative, others are antagonistic, and the latter may represent a major obstacle for *Candida*. This concept gained experimental support through studies involving the depletion of commensal microbiota by continued use of broad-spectrum antibiotics, which resulted in *Candida* overgrowth [117,118]. This suggests that some commensal microbial colonizers antagonize *Candida* spp. (and other exogenous pathogens) in order to maintain a homeostatic balance in the host. Some of these interactions are driven by metabolic competition, while others are mediated by quorum-sensing molecules that influence fungal cell behavior and regulate important virulence traits. Although quorum-sensing systems have been explored in great detail for pathogenic bacteria, they are relatively poorly understood in fungi [119]. The *C. albicans* molecule farnesol was the first quorum-sensing compound to be identified in an eukaryote [120] and has been the object of intense research. Yet, its precise mode of action remains unclear.

Lactobacillus species and *C. albicans* are a well-documented example of infectious antagonism [121–123]. *Lactobacilli* are a dominant species of the microbiota of the gastrointestinal and urogenital tracts, and they actively reduce the amount of fungal microbes by producing many fungicidal compounds [121–123]. Other commensal bacteria such as *Bacteroides thetaiotamicron* or *Blautia producta* can antagonize *C. albicans* by stimulating intestinal cells to produce antimicrobial peptides [124]. The pathogenic bacterium *Acinetobacter baumanii* has been also reported to interact antagonistically with *C. albicans* by biding to hyphae to promote apoptosis [125]. The elucidation of these types of interaction is of particular interest in the quest for novel targets for antifungal therapy, as the inhibitory secreted factors produced by these antagonists appear to have high fungicidal activity.

The disruption of commensal interactions through alterations in immune competence, by changes in environmental host conditions, or via antibiotic therapy may favor the outgrowth and overrepresentation of pathogenic microbes, with these growing at the expense of those organisms that fail to adapt. While antagonist interactions might lower the risk of infection, synergistic interactions during dysbiotic states are associated with increased pathogenesis because microbes can also interact to enhance colonization and persistence. An illustrative example is the infectious synergism established between several *Candida* species (including *C. albicans*, *C. dubliniensis*, *C. tropicalis*, and *C. krusei*) and the gram-positive bacterium *Staphylococcus aureus* [126,127]. *Candida* not only provides a substratum for the attachment and colonization of *S. aureus*, but also facilitates its invasion across mucosal barriers, thereby promoting persistence and systemic infection [128].

1.1.6 Host immune defenses: how *Candida* species counteract the immune response

Microbial pathogens are constantly surveyed by the innate immune system. Phagocytic cells such as dendritic cells, macrophages, monocytes, and neutrophils play important roles in clearing fungal pathogens from the bloodstream and tissues. Loss of innate immune cells or defects in their antifungal activities have major implications for the host. *Candida* cells are recognized through key PAMPs, some of which are located in the cell wall; for example, β-glucans, chitin, and mannans. These components are sensed by the multiple pattern-recognition receptors (PRRs) expressed by phagocytic cells, or secreted (for example, complement components). PPRs mediate binding of the pathogen to the phagocyte, and the PAMP-PRR interactions trigger intracellular signaling pathways within the immune cells that can induce phagocytosis and the production of proinflammatory cytokines and chemokines. In order to attenuate recognition and escape phagocytosis, *Candida* cells are able to actively mask cell-wall PAMPs

[129] and secrete specific proteases that target complement opsonization [130]. Alternatively, some *Candida* species can induce their phagocytic uptake into endothelial and epithelial cells and use these cells as "safe houses" by preventing maturation of the phagolysosome and subsequent killing [131]. If none of these strategies is employed, *Candida* cells are likely to be internalized and subjected to a combination of toxic oxidative and nonoxidative mechanisms that attempt to kill any intra- or extracellular yeast cell. These oxidative mechanisms include the production of reactive oxygen and nitrogen species (ROS and RNS, respectively), while nonoxidative killing mechanisms include the release of antimicrobial peptides and the induction of processes related to micronutrient restriction. Of note, while *C. albicans* is sensitive to the combinatorial stresses imposed by phagocytes [132], *C. glabrata* has adapted to survive within the inhospitable environment of the phagosome. This pathogen mounts robust stress responses against the ROS implemented by the phagocytic cell and neutralizes the phagocytic environment, thereby escaping phagocytosis [133].

1.1.6.1 Oxidative, nitrosative, and osmotic/cationic stresses

Phagocytic cells attempt to kill pathogens in part by employing toxic ROS and RNS, either intracellularly or extracellularly, as a major antimicrobial defense mechanism. ROS are produced by the NADPH oxidase complex, a process known as respiratory burst, and include chemicals such as the superoxide anion ($O_2^{\bullet}$), hydrogen peroxide (H_2O_2) and the hydroxyl radicle ($^{\bullet}OH$). Furthermore, ROS production in response to *C. albicans* infection has been shown to lead to the recruitment of additional phagocytes, creating a toxic oxidative environment for the fungus [134]. Inside phagocytes, ROS can interact with nitric oxide (NO), generating toxic products such as peroxynitrite [135]. These toxic chemicals cause irreversible damage to the pathogen by interacting with proteins, lipids, and nucleic acids.

Candida species attempt to counteract these stresses by activating cellular responses that include the activation of genes encoding proteins involved in stress detoxification and reparation. These include catalase, superoxide dismutases, glutathione peroxidases, and thioredoxins (Figure 1.6a) [136-138]. In *C. albicans* and *C. glabrata*, these stress pathways are regulated largely by the Hog1 stress-activated protein kinase [136,139], the transcription factor Cap1 [140–142], and the Rad53 DNA damage checkpoint kinase [143]. Together with the transcription factor Cta4, these signaling pathways play key roles in orchestrating the responses to osmotic, oxidative, and nitrosative stresses in these species [144]. In this way, these regulators promote the fitness of *C. albicans* during systemic infection. Indeed, mutants lacking these genes display attenuated virulence in mice, as well impaired tolerance to these stresses *in*

vitro and phagocytic survival [145,146]. Curiously, the oxidative stress response is delayed if the fungus is simultaneously exposed to cationic and oxidative stress [147]. This is tought to contribute to the ability of phagocytic cells to efficiently kill invading pathogens [117] (Figure 1.6a). Given the importance of these stress response pathways for *Candida* survival, key molecular players involved may represent attractive targets for antifungal development.

1.1.6.2 Host-enforced micronutrient restriction

The limitation of micronutrients, such as iron, copper, zinc, or manganese, is an effective way of controlling the outgrowth of invading microbes. These micronutrients are essential for the survival of both host and pathogen because they function as co-factors for enzymes, transcription factors, and other proteins that play crucial biochemical and cellular functions. However, our immune system attempts to restrict microbial access to these essential elements via a mechanism known as nutritional immunity [148].

Iron has well-studied implications for *Candida* pathogenesis, being a crucial micronutrient for *Candida* growth, survival and virulence [149]. During systemic candidiasis, the host restricts this metal by increasing the levels of iron-binding proteins, such as ferritin and hemoglobin alpha, and accumulating heme oxygenase (Figure 6b) [150,151]. Both *C. albicans* and *C. glabrata* have developed efficient iron-scavenging strategies that can overcome these host mechanisms. This contributes to their ability to survive phagocytosis and replicate inside macrophages by using their intracellular storages of iron [152,153]. *C. albicans* and *C. glabrata* cells exploit sophisticated iron-uptake systems to acquire either free iron [154,155] or iron from host iron-binding proteins, including hemoglobin [156], ferritin [82], and transferrin (Figure 6b). Additionally, the utilization of siderophores promotes resistance to macrophage killing: in *C. glabrata*, the Sit1 siderophore-iron transporter mediates iron acquisition, being critical for the survival of the yeast inside macrophages [152].

Copper is also involved in *Candida* virulence, both positively and negatively. The fungal reductive iron-uptake pathway includes multicopper oxidases, and hence, iron acquisition and mobilization depends on copper availability [157]. Interestingly, the host also uses copper as a defense mechanism against *Candida* by pumping excess quantities of this metal into *Candida*-containing phagosomes (Figure 1.6b) [158]. However, *C. albicans* adapts to this potential killing mechanism by differentially modulating the expression of copper- and manganese-dependent SODs (Sod1 and Sod3, respectively) [159]. Sod1 is

expressed when copper is in excess, but when copper levels decline, Sod3 is then expressed (Figure 1.6b) [159]. Thus, during infection, *C. albicans* is able to adjust copper uptake and management by using it as an enzymatic cofactor for SOD enzymes [159].

Zinc is an abundant micronutrient that has crucial roles in cellular functionality for both host and pathogen. The host attempts to limit zinc availability for the fungus by depleting extracellular zinc levels, mainly via calprotectin, an antimicrobial peptide expressed by neutrophils that binds zinc and manganese with high affinity (Figure 1.6b) [160]. Calprotectin promotes the antimicrobial activity of neutrophil extracellular traps (NETs), which are released by neutrophils after sensing large microbes such as *C. albicans* hyphae [161–163]. Zinc depletion also occurs inside immune cells as an antifungal mechanism to kill intracellular pathogens such as *C. albicans* and *C. glabrata* [164]. During infection, macrophages deplete intracellular zinc by pumping it into the Golgi apparatus via specific ZnT-type zinc transporters (Figure 1.6b) and increasing the expression of zinc-binding metallothioneins [165]. Additionally, macrophages up-regulate the zinc importer *ZIP2* to increase the intracellular levels of zinc (Figure 1.6b) [166]. This combination of strategies depletes zinc from the extracellular environment while dealing with the increased metabolic demands associated with microbial clearing [166]. To overcome zinc depletion, *C. albicans* overexpresses *ZRT1* and *ZRT2* genes, encoding zinc uptake transporter systems Zrt1 and Zrt2 (Figure 1.6b). Both transporters are regulated by the zinc finger transcription factor Zap1 (also known as Csr1) [167,168] and by pH [79]. Zinc transporters play important roles in *Candida* pathogenesis because overexpression of Zrt2 increases *C. albicans* virulence [169]. In addition to functioning as a zinc transporter, Zrt1 also serves as a receptor for the Pra1 zincophore [79,168], a secreted protein that binds and sequesters zinc from host cells during *C. albicans* invasion (Figure 1.6b) [170]. Similarly to copper, zinc has also been reported to be pumped in higher amounts into the phagosome to intoxicate internalized pathogens, constituting an important mechanism of killing (Figure 1.6b) [171].

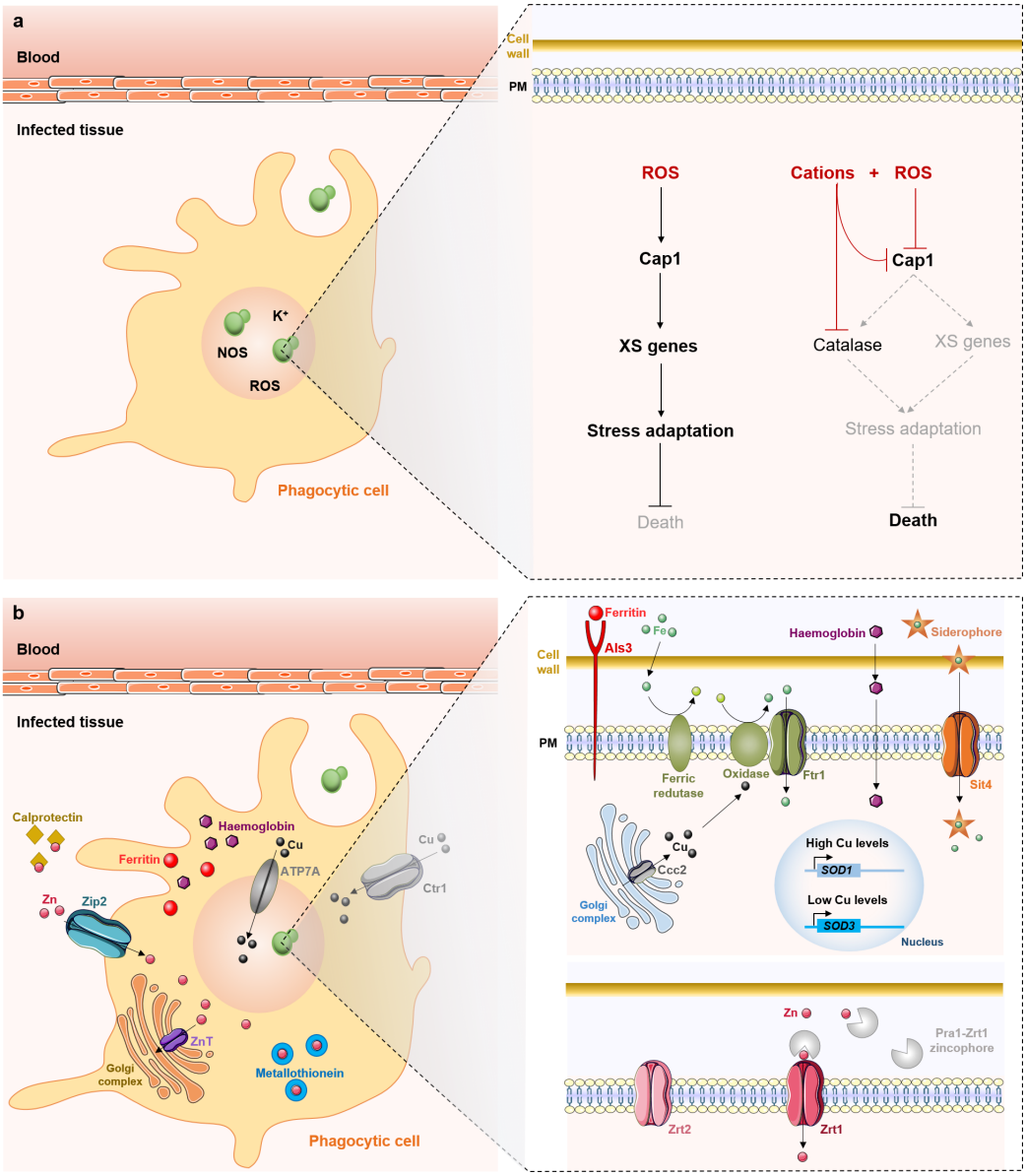

Figure 1.6. Host immune defenses and adaptation mechanisms displayed by *C. albicans* and *C. glabrata*. **(a)** Cap1 plays a key role in the activation of responses to ROS generated by phagocytic cells, leading to the induction of oxidative stress genes (XS genes), including catalase, superoxide dismutases, glutathione peroxidases, and thioredoxins, among others. However, cations inhibit catalase and Cap1, thereby delaying the induction of the oxidative stress response and leading to the death of *C. albicans* cells. **(b)** Host-enforced micronutrient restriction results in reduced iron, copper, and zinc availability, but *C. albicans* responds by up-regulating efficient metal-scavenging strategies. Host phagocytes also exploit the toxicity of copper and zinc by pumping these metals in excess into phagosomes to intoxicate internalized pathogens. NOS, nitric oxide species; PM, plasma membrane; ROS, reactive oxygen species; Sod, superoxide dismutase; XS, oxidative stress.

1.2 Environment-triggered biofilm formation and antifungal resistance

So far, we have described major molecular circuits required by *Candida* species to counteract several constraints they face in the human host. The ability of *Candida* to adapt to these stresses imparts the flexibility to colonize diverse host niches. The physiological capacity to respond efficiently to stress and survive hostile environments also endows the fungal cells with the advantage of being better prepared for future insults [172,173]. The generation of biofilms might represent another strategy to resist harsh conditions and persist in the human host.

The *Candida* species most frequently associated with the formation of biofilms, either in host tissues or implanted medical devices, are *C. albicans*, *C. glabrata*, *C. tropicalis*, and *C. parapsilosis* [174]. Biofilms represent three-dimensional communities of adherent cells, with distinct biological properties, that are embedded in a self-synthesizing extracellular matrix (ECM) composed predominantly of proteins, glycoproteins, carbohydrates, lipids, and nucleic acids [175]. The ECM helps to maintain the overall structural integrity of the biofilm, and it also acts as a physical barrier to drug penetration. Consequently, biofilm cells can survive drug concentrations more than a thousand times higher than those defined for planktonic cells [176]. This phenotype is partly associated with the sequestration of drugs by the biofilm ECM and partly with the occurrence of a subpopulation of so-called "persister cells". Persister cells exhibit a dormant-like physiology that has been demonstrated to make them highly resistant to antifungals [177]. These features contribute to the intrinsic resistance of *Candida* biofilms to conventional antifungal treatments, the host immune system, and other environmental perturbations, making biofilm-based infections a clinical challenge.

Genome-wide transcriptional profiling and proteomic approaches have identified hundreds of genes that are differentially expressed between *C. albicans* biofilm and planktonic cells. The up-regulation of glycolytic and sulfur amino acid genes, similar to what is observed when cells grow under hypoxia, suggests that *Candida* biofilms constitute a heterogeneous environment with hypoxic niches [178]. Moreover, more than 50 transcriptional regulators and 101 other genes have functionally validated roles in the formation of *Candida* biofilms [179–181]. Some of these play important roles in hyphal formation, adhesion, drug resistance, and matrix production (all intrinsic characteristics of biofilms), as well as in stress adaptation. It is not surprising, then, that adaptation to specific environmental niches modulates the ability of cells to form biofilms and, consequently, to resist antifungals [54,55,58,59,182–184].

1.3 REFERENCES

1. Kumamoto CA. Inflammation and gastrointestinal *Candida* colonization. Current Opinion in Microbiology. 2011;14(4): 386–391. doi:10.1016/j.mib.2011.07.015
2. Limon JJ, Skalski JH, Underhill DM. Commensal Fungi in Health and Disease. Cell Host Microbe. 2017;22: 156–165. doi:10.1016/j.chom.2017.07.002
3. Cauchie M, Desmet S, Lagrou K. *Candida* and its dual lifestyle as a commensal and a pathogen. Res Microbiol. 2017;168: 802–810. doi:10.1016/j.resmic.2017.02.005
4. Pappas PG, Lionakis MS, Arendrup MC, Ostrosky-Zeichner L, Kullberg BJ. Invasive candidiasis. Nat Rev Dis Prim. 2018;4: 18026. doi:10.1038/nrdp.2018.26
5. Tsai M-H, Hsu J-F, Yang L-Y, Pan Y-B, Lai M-Y, Chu S-M, et al. Candidemia due to uncommon *Candida* species in children: new threat and impacts on outcomes. Sci Rep. 2018;8: 15239. doi:10.1038/s41598-018-33662-x
6. Singh S, Sobel JD, Bhargava P, Boikov D, Vazquez JA. Vaginitis Due to *Candida krusei*: Epidemiology, Clinical Aspects, and Therapy. Clin Infect Dis. 2002;35(9): 1066–1070. doi:10.1086/343826
7. Bougnoux ME, Brun S, Zahar JR. Healthcare-associated fungal outbreaks: new and uncommon species, new molecular tools for investigation and prevention. Antimicrobial Resistance and Infection Control. 2018;7: 45. doi:10.1186/s13756-018-0338-9
8. Kohlenberg A, Struelens MJ, Monnet DL, Plachouras D, Apfalter P, Lass-Flörl C, et al. *Candida auris*: Epidemiological situation, laboratory capacity and preparedness in European Union and European economic area countries, 2013 to 2017. Eurosurveillance. 2018;23(13): 18-00136. doi:10.2807/1560-7917.ES.2018.23.13.18-00136
9. Morrell M, Fraser VJ, Kollef MH. Delaying the empiric treatment of *Candida* bloodstream infection until positive blood culture results are obtained: a potential risk factor for hospital mortality. Antimicrob Agents Chemother. 2005;49(9): 3640–3645. doi:10.1128/AAC.49.9.3640-3645.2005
10. Perlin DS, Rautemaa-Richardson R, Alastruey-Izquierdo A. The global problem of antifungal resistance: prevalence, mechanisms, and management. The Lancet Infectious Diseases. 2017;17(12): e383–e392. doi:10.1016/S1473-3099(17)30316-X

11. Pfaller MA, Diekema DJ, Turnidge JD, Castanheira M, Jones RN. Twenty years of the SENTRY Antifungal Surveillance Program: Results for *Candida* species from 1997-2016. Open Forum Infect Dis. 2019;6(Suppl. 1): S79–S94. doi:10.1093/ofid/ofy358
12. Nobile CJ, Johnson AD. *Candida albicans* Biofilms and Human Disease. Annu Rev Microbiol. 2015;69: 71–92. doi:10.1146/annurev-micro-091014-104330
13. Demers EG, Biermann AR, Masonjones S, Crocker AW, Ashare A, Stajich JE, et al. Evolution of drug resistance in an antifungal-naive chronic *Candida lusitaniae* infection. Proc Natl Acad Sci U S A. 2018;115(47): 12040–12045. doi:10.1073/pnas.1807698115
14. Thompson DS, Carlisle PL, Kadosh D. Coevolution of morphology and virulence in *Candida species*. Eukaryotic Cell. 2011;10(9): 1173–1182. doi:10.1128/EC.05085-11
15. Noble SM, Gianetti BA, Witchley JN. *Candida albicans* cell-type switching and functional plasticity in the mammalian host. Nature Reviews Microbiology. 2017;15(2): 96–108. doi:10.1038/nrmicro.2016.157
16. Tao L, Du H, Guan G, Dai Y, Nobile CJ, Liang W, et al. Discovery of a "White-Gray-Opaque" Tristable Phenotypic Switching System in *Candida albicans*: Roles of Non-genetic Diversity in Host Adaptation. PLoS Biol. 2014;12(4): e1001830. doi:10.1371/journal.pbio.1001830
17. Pande K, Chen C, Noble SM. Passage through the mammalian gut triggers a phenotypic switch that promotes *Candida albicans* commensalism. Nat Genet. 2013;45(9): 1088–1091. doi:10.1038/ng.2710
18. Hopke A, Brown AJP, Hall RA, Wheeler RT. Dynamic Fungal Cell Wall Architecture in Stress Adaptation and Immune Evasion. Trends in Microbiology. 2018;26(4): 284–295. doi:10.1016/j.tim.2018.01.007
19. Garcia-Rubio R, de Oliveira HC, Rivera J, Trevijano-Contador N. The Fungal Cell Wall: *Candida*, *Cryptococcus*, and *Aspergillus* Species. Frontiers in Microbiology. 2020;10: 2993. doi:10.3389/fmicb.2019.02993
20. Johnston M. Feasting, fasting and fermenting: Glucose sensing in yeast and other cells. Trends in Genetics. 1999;15(1): 29–33. doi:10.1016/S0168-9525(98)01637-0
21. Ene IV., Brunke S, Brown AJP, Hube B. Metabolism in fungal pathogenesis. Cold Spring Harb Perspect Med. 2014;4(12): a019695. doi:10.1101/cshperspect.a019695
22. Carlson M. Glucose repression in yeast. Curr Opin Microbiol. 1999;2(2): 202–207. doi:10.1016/S1369-5274(99)80035-6

23. Yin Z, Smith RJ, Brown AJP. Multiple signalling pathways trigger the exquisite sensitivity of yeast gluconeogenic mRNAs to glucose. Mol Microbiol. 1996;20(4): 751–764. doi:10.1111/j.1365-2958.1996.tb02514.x

24. López-Boado YS, Herrero P, Gascón S, Moreno F. Catabolite inactivation of isocitrate lyase from *Saccharomyces cerevisiae*. Arch Microbiol. 1987;147(3): 231–234. doi:10.1007/BF00463480

25. Holzer H. Proteolytic catabolite inactivation in *Saccharomyces cerevisiae*. Revisiones sobre biologia celular: RBC. 1989;21: 305–319.

26. Sandai D, Yin Z, Selway L, Stead D, Walker J, Leach MD, et al. The evolutionary rewiring of ubiquitination targets has reprogrammed the regulation of carbon assimilation in the pathogenic yeast *Candida albicans*. mBio. 2012;3(6): e00495-12. doi:10.1128/mBio.00495-12

27. Childers DS, Raziunaite I, Mol Avelar G, Mackie J, Budge S, Stead D, et al. The Rewiring of Ubiquitination Targets in a Pathogenic Yeast Promotes Metabolic Flexibility, Host Colonization and Virulence. PLoS Pathog. 2016;12(4): e1005566. doi:10.1371/journal.ppat.1005566

28. Barelle CJ, Priest CL, MacCallum DM, Gow NAR, Odds FC, Brown AJP. Niche-specific regulation of central metabolic pathways in a fungal pathogen. Cell Microbiol. 2006;8: 961–971. doi:10.1111/j.1462-5822.2005.00676.x

29. Hudson DA, Sciascia QL, Sanders RJ, Norris GE, Edwards PJB, Sullivan PA, et al. Identification of the dialysable serum inducer of germ-tube formation in *Candida albicans*. Microbiology. 2004;150(Pt 9): 3041–3049. doi:10.1099/mic.0.27121-0

30. Buu LM, Chen YC. Impact of glucose levels on expression of hypha-associated secreted aspartyl proteinases in *Candida albicans*. J Biomed Sci. 2014;21: 22. doi:10.1186/1423-0127-21-22

31. Maidan MM, Thevelein JM, Van Dijck P. Carbon source induced yeast-to-hypha transition in *Candida albicans* is dependent on the presence of amino acids and on the G-protein-coupled receptor Gpr1. Biochemical Society Transactions. 2005;33(Pt 1): 291–293. doi:10.1042/BST0330291

32. Mandal SM, Mahata D, Migliolo L, Parekh A, Addy PS, Mandal M, et al. Glucose directly promotes antifungal resistance in the fungal pathogen, *Candida* spp. J Biol Chem. 2014;289(37): 25468–25473. doi:10.1074/jbc.C114.571778

33. Rodaki A, Bohovych IM, Enjalbert B, Young T, Odds FC, Gow NAR, et al. Glucose promotes stress resistance in the fungal pathogen *Candida albicans*. Mol Biol Cell. 2009;20(22): 4845–4855. doi:10.1091/mbc.E09-01-0002

34. Tucey TM, Verma J, Harrison PF, Snelgrove SL, Lo TL, Scherer AK, et al. Glucose Homeostasis Is Important for Immune Cell Viability during *Candida* Challenge and Host Survival of Systemic Fungal Infection. Cell Metab. 2018;27(5): 988–1006.e7. doi:10.1016/j.cmet.2018.03.019

35. Fradin C, Kretschmar M, Nichterlein T, Gaillardin C, D'Enfert C, Hube B. Stage-specific gene expression of *Candida albicans* in human blood. Mol Microbiol. 2003;47(6): 1523–1543. doi:10.1046/j.1365-2958.2003.03396.x

36. Fradin C, De Groot P, MacCallum D, Schaller M, Klis F, Odds FC, et al. Granulocytes govern the transcriptional response, morphology and proliferation of *Candida albicans* in human blood. Mol Microbiol. 2005;56(2): 397–415. doi:10.1111/j.1365-2958.2005.04557.x

37. Lorenz MC, Fink GR. The glyoxylate cycle is required for fungal virulence. Nature. 2001;412: 83–86. doi:10.1038/35083594

38. Naseem S, Min K, Spitzer D, Gardin J, Konopka JB. Regulation of hyphal growth and N-acetylglucosamine catabolism by two transcription factors in *Candida albicans*. Genetics. 2017;206(1): 299–314. doi:10.1534/genetics.117.201491

39. Su C, Lu Y, Liu H. N-acetylglucosamine sensing by a GCN5-related N-acetyltransferase induces transcription via chromatin histone acetylation in fungi. Nat Commun. 2016;7: 12916. doi:10.1038/ncomms12916

40. Alvarez FJ, Konopka JB. Identification of an N-acetylglucosamine transporter that mediates hyphal induction in *Candida albicans*. Mol Biol Cell. 2007;18(3):965–975. Epub 27 Dec 2006. doi:10.1091/mbc.E06-10-0931

41. Huang G, Yi S, Sahni N, Daniels KJ, Srikantha T, Soll DR. N-acetylglucosamine induces white to opaque switching, a mating prerequisite in *Candida albicans*. PLoS Pathog. 2010;6(3): e1000806. doi:10.1371/journal.ppat.1000806

42. Simonetti N, Strippoli V, Cassone A. Yeast-mycelial conversion induced by N-acetyl-D-glucosamine in *Candida albicans*. Nature. 1974;250(464): 344–346. doi:10.1038/250344a0

43. Du H, Guan G, Li X, Gulati M, Tao L, Cao C, et al. N-Acetylglucosamine-induced cell death in *Candida albicans* and its implications for adaptive mechanisms of nutrient sensing in yeasts. MBio. 2015;6(5): e01376-15. doi:10.1128/mBio.01376-15

44. Vesely EM, Williams RB, Konopka JB, Lorenz MC. N-Acetylglucosamine Metabolism Promotes Survival of *Candida albicans* in the Phagosome. mSphere. 2017;2(5): e00357-17. doi:10.1128/msphere.00357-17

45. Butler G, Rasmussen MD, Lin MF, Santos MAS, Sakthikumar S, Munro CA, et al. Evolution of pathogenicity and sexual reproduction in eight *Candida* genomes. Nature. 2009;459(7247): 657–662. doi:10.1038/nature08064

46. Danhof HA, Vylkova S, Vesely EM, Ford AE, Gonzalez-Garay M, Lorenz MC. Robust Extracellular pH Modulation by *Candida albicans* during Growth in Carboxylic Acids. mBio. 2016;7(6): e01646-16. doi:10.1128/mbio.01646-16

47. Rowland I, Gibson G, Heinken A, Scott K, Swann J, Thiele I, et al. Gut microbiota functions: metabolism of nutrients and other food components. European Journal of Nutrition. 2018;57(1): 1–24. Epub 9 Apr 2017. doi:10.1007/s00394-017-1445-8

48. Morrison DJ, Preston T. Formation of short chain fatty acids by the gut microbiota and their impact on human metabolism. Gut Microbes. 2016;7(3): 189–200. doi:10.1080/19490976.2015.1134082

49. Valdes AM, Walter J, Segal E, Spector TD. Role of the gut microbiota in nutrition and health. BMJ. 2018;361: k2179. doi:10.1136/bmj.k2179

50. Owen DH, Katz DF. A vaginal fluid simulant. Contraception. 1999;59: 91–95. doi:10.1016/S0010-7824(99)00010-4

51. Vieira N, Casal M, Johansson B, MacCallum DM, Brown AJP, Paiva S. Functional specialization and differential regulation of short-chain carboxylic acid transporters in the pathogen *Candida albicans*. Mol Microbiol. 2010;75: 1337–1354. doi:10.1111/j.1365-2958.2009.07003.x

52. Danhof HA, Lorenz MC. The *Candida albicans* ATO Gene Family Promotes Neutralization of the Macrophage Phagolysosome. Infect Immun. 2015;83(11): 4416–4426. doi:10.1128/iai.00984-15

53. Soares-Silva I, Paiva S, Kötter P, Entian K-D, Casal M. The disruption of JEN1 from *Candida albicans* impairs the transport of lactate. Mol Membr Biol. 2004;21: 403–411. doi:10.1080/09687860400011373

54. Mota S, Alves R, Carneiro C, Silva S, Brown AJ, Istel F, et al. *Candida glabrata* susceptibility to antifungals and phagocytosis is modulated by acetate. Front Microbiol. 2015;6: 919. doi:10.3389/fmicb.2015.00919

55. Alves R, Mota S, Silva S, F. Rodrigues C, Alistair AJ, Henriques M, et al. The carboxylic acid transporters Jen1 and Jen2 affect the architecture and fluconazole susceptibility of *Candida albicans* biofilm in the presence of lactate. Biofouling. 2017;33: 943–954. doi:10.1080/08927014.2017.1392514

56. Alves R, Kastora SL, Gomes-Gonçalves A, Azevedo N, Rodrigues CF, Silva S, et al. Transcriptional responses of *Candida glabrata* biofilm cells to fluconazole are modulated by the carbon source. NPJ Biofilms Microbiomes. 2020;6: 4. doi:10.1038/s41522-020-0114-5

57. Ballou ER, Avelar GM, Childers DS, Mackie J, Bain JM, Wagener J, et al. Lactate signalling regulates fungal β-glucan masking and immune evasion. Nat Microbiol. 2016;2: 16238. doi:10.1038/nmicrobiol.2016.238

58. Ene I V., Adya AK, Wehmeier S, Brand AC, Maccallum DM, Gow NAR, et al. Host carbon sources modulate cell wall architecture, drug resistance and virulence in a fungal pathogen. Cell Microbiol. 2012;14: 1319–1335. doi:10.1111/j.1462-5822.2012.01813.x

59. Ene I V., Heilmann CJ, Sorgo AG, Walker LA, De Koster CG, Munro CA, et al. Carbon source-induced reprogramming of the cell wall proteome and secretome modulates the adherence and drug resistance of the fungal pathogen *Candida albicans*. Proteomics. 2012;12: 3164–3179. doi:10.1002/pmic.201200228

60. Zakikhany K, Naglik JR, Schmidt-westhausen A, Holland G, Schaller M, Hube B. In vivo transcript profiling of *Candida albicans* identifies a gene essential for interepithelial dissemination. Cell Microbiol. 2007;9(12): 2938–2954. doi:10.1111/j.1462-5822.2007.01009.x

61. Lorenz MC, Bender JA, Fink GR. Transcriptional response of *Candida albicans* upon internalization by macrophages. Eukaryot Cell. 2004;3: 1076–1087. doi:10.1128/EC.3.5.1076-1087.2004

62. Rubin-Bejerano I, Fraser I, Grisafi P, Fink GR. Phagocytosis by neutrophils induces an amino acid deprivation response in *Saccharomyces cerevisiae* and *Candida albicans*. Proc Natl Acad Sci U S A. 2003. doi:10.1073/pnas.1834481100

63. Jacobsen ID, Brunke S, Seider K, Schwarzmüller T, Firon A, D'Enfért C, et al. *Candida glabrata* persistence in mice does not depend on host immunosuppression and is unaffected by fungal amino acid auxotrophy. Infect Immun. 2010;78(3): 1066–1077. doi:10.1128/IAI.01244-09

64. Kirsch DR, Whitney RR. Pathogenicity of *Candida albicans* auxotrophic mutants in experimental infections. Infect Immun. 1991;59(9): 3297–3300.

65. Alonso-Monge R, Navarro-García F, Molero G, Diez-Orejas R, Gustin M, Pla J, et al. Role of the mitogen-activated protein kinase hog1p in morphogenesis and virulence of *Candida albicans*. J Bacteriol. 1999;181(10): 3058–3068.

66. Gropp K, Schild L, Schindler S, Hube B, Zipfel PF, Skerka C. The yeast *Candida albicans* evades human complement attack by secretion of aspartic proteases. Mol Immunol. 2009;47(2–3): 465–475. doi:10.1016/j.molimm.2009.08.019

67. Martínez P, Ljungdahl PO. An ER packaging chaperone determines the amino acid uptake capacity and virulence of *Candida albicans*. Mol Microbiol. 2004;51(2): 371–384. doi:10.1046/j.1365-2958.2003.03845.x

68. Martinez P, Ljungdahl PO. Divergence of Stp1 and Stp2 Transcription Factors in *Candida albicans* Places Virulence Factors Required for Proper Nutrient Acquisition under Amino Acid Control. Mol Cell Biol. 2005;25(21): 9435–9446. doi:10.1128/mcb.25.21.9435-9446.2005

69. Vylkova S, Lorenz MC. Modulation of Phagosomal pH by *Candida albicans* Promotes Hyphal Morphogenesis and Requires Stp2p, a Regulator of Amino Acid Transport. PLoS Pathog. 2014;10(3): e1003995. doi:10.1371/journal.ppat.1003995

70. Vylkova S, Carman AJ, Danhof HA, Collette JR, Zhou H, Lorenz MC. The fungal pathogen *Candida albicans* autoinduces hyphal morphogenesis by raising extracellular pH. mBio. 2011;2(3): e00055-11. doi:10.1128/mBio.00055-11

71. Westman J, Moran G, Mogavero S, Hube B, Grinstein S. *Candida albicans* hyphal expansion causes phagosomal membrane damage and luminal alkalinization. mBio. 2018;9(5): e01226-18. doi:10.1128/mBio.01226-18

72. May RC, Casadevall A. In Fungal Intracellular Pathogenesis, Form Determines Fate. mBio. 2018;9(5): e02092-18. doi:10.1128/mBio.02092-18

73. Schrevens S, Van Zeebroeck G, Riedelberger M, Tournu H, Kuchler K, Van Dijck P. Methionine is required for cAMP-PKA-mediated morphogenesis and virulence of *Candida albicans*. Mol Microbiol;108(3): 258–275. 2018. doi:10.1111/mmi.13933

74. Miwa T, Takagi Y, Shinozaki M, Yun CW, Schell WA, Perfect JR, et al. Gpr1, a putative G-protein-coupled receptor, regulates morphogenesis and hypha formation in the pathogenic fungus *Candida albicans*. Eukaryot Cell. 2004;3(4): 919–931. doi:10.1128/EC.3.4.919-931.2004

75. Cornet M, Gaillardin C. pH signaling in human fungal pathogens: A new target for antifungal strategies. Eukaryotic Cell. 2014;13(3): 342–352. doi:10.1128/EC.00313-13

76. Ramon AM, Porta A, Fonzi WA. Effect of environmental pH on morphological development of *Candida albicans* is mediated via the PacC-related transcription factor encoded by PRR2. J Bacteriol. 1999;181(24): 7524–7530.

77. Porta A, Ramon AM, Fonzi WA. PRR1, a homolog of *Aspergillus nidulans* palF, controls pH-dependent gene expression and filamentation in *Candida albicans*. J Bacteriol. 1999;181(24): 7516–7523.

78. Davis D, Wilson RB, Mitchell AP. RIM101-Dependent and -Independent Pathways Govern pH Responses in *Candida albicans*. Mol Cell Biol. 2000;20(3): 971–978. doi:10.1128/mcb.20.3.971-978.2000

79. Bensen ES, Martin SJ, Li M, Berman J, Davis DA. Transcriptional profiling in *Candida albicans* reveals new adaptive responses to extracellular pH and functions for Rim101p. Mol Microbiol. 2004;54(5): 1335–1351. doi:10.1111/j.1365-2958.2004.04350.x

80. Nobile CJ, Solis N, Myers CL, Fay AJ, Deneault JS, Nantel A, et al. *Candida albicans* transcription factor Rim101 mediates pathogenic interactions through cell wall functions. Cell Microbiol. 2008;10(11): 2180–2196. doi:10.1111/j.1462-5822.2008.01198.x

81. Baek YU, Li M, Davis DA. *Candida albicans* ferric reductases are differentially regulated in response to distinct forms of iron limitation by the Rim101 and CBF transcription factors. Eukaryot Cell. 2008;7(7): 1168–1179. doi:10.1128/EC.00108-08

82. Almeida RS, Brunke S, Albrecht A, Thewes S, Laue M, Edwards JE, et al. The hyphal-associated adhesin and invasin Als3 of *Candida albicans* mediates iron acquisition from host ferritin. PLoS Pathog. 2008;4(11): e1000217. doi:10.1371/journal.ppat.1000217

83. Garnaud C, García-Oliver E, Wang Y, Maubon D, Bailly S, Despinasse Q, et al. The rim pathway mediates antifungal tolerance in *Candida albicans* through newly identified Rim 101 transcriptional targets, including Hsp90 and Ipt1. Antimicrob Agents Chemother. 2018;62(3): e01785-17. doi:10.1128/AAC.01785-17

84. Marr KA, Rustad TR, John H R, White TC. The trailing end point phenotype in antifungal susceptibility testing is pH dependent. Antimicrob Agents Chemother. 1999;43(6):1383–1386. doi:10.1128/aac.43.6.1383

85. Sherrington SL, Sorsby E, Mahtey N, Kumwenda P, Lenardon MD, Brown I, et al. Adaptation of *Candida albicans* to environmental pH induces cell wall remodelling and enhances innate immune recognition. PLoS Pathog. 2017;13(5): e1006403. doi:10.1371/journal.ppat.1006403

86. Cottier F, Sherrington S, Cockerill S, del Olmo Toledo V, Kissane S, Tournu H, et al. Remasking of *Candida albicans* β-Glucan in Response to Environmental pH Is Regulated by Quorum Sensing. Alspaugh JA, editor. mBio. 2019;10: e02347-19. doi:10.1128/mBio.02347-19

87. Taylor CT. Hypoxia in the Gut. Cell Mol. Gasteroenterol. Hepatol. 2018;5(1): 61–62. doi:10.1016/j.jcmgh.2017.09.005

88. Lopes JP, Stylianou M, Backman E, Holmberg S, Jass J, Claesson R, et al. Evasion of Immune Surveillance in Low Oxygen Environments Enhances *Candida albicans* Virulence. mBio. 2018;9(6): e02120-18. doi:10.1128/mBio.02120-18

89. Askew C, Sellam A, Epp E, Hogues H, Mullick A, Nantel A, et al. Transcriptional regulation of carbohydrate metabolism in the human pathogen *Candida albicans*. PLoS Pathog. 2009;5(10): e1000612. doi:10.1371/journal.ppat.1000612

90. Bonhomme J, Chauvel M, Goyard S, Roux P, Rossignol T, D'Enfert C. Contribution of the glycolytic flux and hypoxia adaptation to efficient biofilm formation by *Candida albicans*. Mol Microbiol. 2011;80(4): 995–1013. doi:10.1111/j.1365-2958.2011.07626.x

91. Sellam A, van het Hoog M, Tebbji F, Beaurepaire C, Whiteway M, Nantelc A. Modeling the transcriptional regulatory network that controls the early hypoxic response in *Candida albicans*. Eukaryot Cell. 2014;13(5): 675–690. doi:10.1128/EC.00292-13

92. Setiadi ER, Doedt T, Cottier F, Noffz C, Ernst JF. Transcriptional Response of *Candida albicans* to Hypoxia: Linkage of Oxygen Sensing and Efg1p-regulatory Networks. J Mol Biol. 2006;361(3): 399–411. doi:10.1016/j.jmb.2006.06.040

93. Stichternoth C, Ernst JF. Hypoxic adaptation by Efg1 regulates biofilm formation by *Candida albicans*. Appl Environ Microbiol. 2009;75(11): 3663–3672. doi:10.1128/AEM.00098-09

94. Synnott JM, Guida A, Mulhern-Haughey S, Higgins DG, Butler G. Regulation of the Hypoxic Response in *Candida albicans*. Eukaryot Cell. 2010;9(11): 1734–1746. doi:10.1128/ec.00159-10

95. MacPherson S, Akache B, Weber S, De Deken X, Raymond M, Turcotte B. *Candida albicans* zinc cluster protein Upc2p confers resistance to antifungal drugs and is an activator of ergosterol biosynthetic genes. Antimicrob Agents Chemother. 2005;49(5): 1745–1752. doi:10.1128/AAC.49.5.1745-1752.2005

96. Znaidi S, Weber S, Al-Abdin OZ, Bomme P, Saidane S, Drouin S, et al. Genomewide location analysis of *Candida albicans* Upc2p, a regulator of sterol metabolism and azole drug resistance. Eukaryot Cell. 2008;7(5): 836–847. doi:10.1128/EC.00070-08

97. Pradhan A, Avelar GM, Bain JM, Childers DS, Larcombe DE, Netea MG, et al. Hypoxia Promotes Immune Evasion by Triggering β-Glucan Masking on the *Candida albicans* Cell Surface via Mitochondrial and cAMP-Protein Kinase A Signaling. mBio. 2018;9(6): e01318-18. doi:10.1128/mBio.01318-18

98. Hamanaka RB, Chandel NS. Mitochondrial reactive oxygen species regulate hypoxic signaling. Current Opinion in Cell Biology. 2009;21(6): 894–899. doi:10.1016/j.ceb.2009.08.005

99. Waypa GB, Smith KA, Schumacker PT. O2 sensing, mitochondria and ROS signaling: The fog is lifting. Molecular Aspects of Medicine. 2016;47–48: 76–89. doi:10.1016/j.mam.2016.01.002

100. Vasicek EM, Berkow EL, Flowers SA, Barker KS, Rogers PD. UPC2 is Universally Essential for Azole Antifungal Resistance in *Candida albicans*. Eukaryot Cell. 2014;13(7):933–946. doi:10.1128/EC.00221-13

101. Kontoyiannis DP, Vaziri I, Hanna HA, Boktour M, Thornby J, Hachem R, et al. Risk Factors for *Candida tropicalis* Fungemia in Patients with Cancer. Clin Infect Dis. 2001;33(10): 1676–1681. doi:10.1086/323812

102. Robert VA, Casadevall A. Vertebrate Endothermy Restricts Most Fungi as Potential Pathogens. J Infect Dis. 2009;200(10): 1623–1626. doi:10.1086/644642

103. Casadevall A. Thermal Restriction as an Antimicrobial Function of Fever. PLoS Pathogens. 2016;12(5): e1005577. doi:10.1371/journal.ppat.1005577

104. Shapiro RS, Robbins N, Cowen LE. Regulatory Circuitry Governing Fungal Development, Drug Resistance, and Disease. Microbiol Mol Biol Rev. 2011;75(2): 213–267. doi:10.1128/mmbr.00045-10

105. Lindquist S. Heat-shock proteins and stress tolerance in microorganisms. Curr Opin Genet Dev. 1992;2(5): 748–755. doi:10.1016/S0959-437X(05)80135-2

106. Nicholls S, Leach MD, Priest CL, Brown AJP. Role of the heat shock transcription factor, Hsf1, in a major fungal pathogen that is obligately associated with warm-blooded animals. Mol Microbiol. 2009;74(4): 844–861. doi:10.1111/j.1365-2958.2009.06883.x

107. Leach MD, Tyc KM, Brown AJP, Klipp E. Modelling the regulation of thermal adaptation in *Candida albicans*, a major fungal pathogen of humans. PLoS ONE. 2012;7(3): e32467. doi:10.1371/journal.pone.0032467

108. Duina AA, Kalton HM, Gaber RF. Requirement for Hsp90 and a CyP-40-type cyclophilin in negative regulation of the heat shock response. J Biol Chem. 1998;273(30): 18974–18978. doi:10.1074/jbc.273.30.18974

109. Zou J, Guo Y, Guettouche T, Smith DF, Voellmy R. Repression of heat shock transcription factor HSF1 activation by HSP90 (HSP90 complex) that forms a stress-sensitive complex with HSF1. Cell. 1998;94(4): 471–480. doi:10.1016/S0092-8674(00)81588-3

110. Leach MD, Budge S, Walker L, Munro C, Cowen LE, Brown AJP. Hsp90 Orchestrates Transcriptional Regulation by Hsf1 and Cell Wall Remodelling by MAPK Signalling during Thermal Adaptation in a Pathogenic Yeast. PLoS Pathog. 2012;8(12): e1003069. doi:10.1371/journal.ppat.1003069

111. Ene I V., Walker LA, Schiavone M, Lee KK, Martin-Yken H, Dague E, et al. Cell wall remodeling enzymes modulate fungal cell wall elasticity and osmotic stress resistance. mBio. 2015;6(4): e00986. doi:10.1128/mBio.00986-15

112. Mayer FL, Wilson D, Jacobsen ID, Miramón P, Slesiona S, Bohovych IM, et al. Small but crucial: The novel small heat shock protein Hsp21 mediates stress adaptation and virulence in *Candida albicans*. PLoS ONE. 2012;7(6); e38584. doi:10.1371/journal.pone.0038584

113. Fu MS, de Sordi L, Mühlschlegel FA. Functional characterization of the small heat shock protein Hsp12p from *Candida albicans*. PLoS ONE. 2012;7(8); e42894. doi:10.1371/journal.pone.0042894

114. Gong Y, Li T, Yu C, Sun S. *Candida albicans* Heat Shock Proteins and Hsps-Associated Signaling Pathways as Potential Antifungal Targets. Front Cell Infect Microbiol. 2017;7: 520. doi:10.3389/fcimb.2017.00520

115. Leach MD, Farrer RA, Tan K, Miao Z, Walker LA, Cuomo CA, et al. Hsf1 and Hsp90 orchestrate temperature-dependent global transcriptional remodelling and chromatin architecture in *Candida albicans*. Nat Commun. 2016;7: 11704. doi:10.1038/ncomms11704

116. Nicholls S, MacCallum DM, Kaffarnik FAR, Selway L, Peck SC, Brown AJP. Activation of the heat shock transcription factor Hsf1 is essential for the full virulence of the fungal pathogen *Candida albicans*. Fungal Genet Biol. 2011;48(3): 297–305. Epub 9 Sep 2010. doi:10.1016/j.fgb.2010.08.010

117. Mason KL, Downward JRE, Falkowski NR, Young VB, Kao JY, Huffnagle GB. Interplay between the gastric bacterial microbiota and *Candida albicans* during postantibiotic recolonization and gastritis. Infect Immun. 2012;80(1): 150–158. Epub 10 Oct 2011. doi:10.1128/IAI.05162-11

118. Mason KL, Downward JRE, Mason KD, Falkowski NR, Eaton KA, Kao JY, et al. Candida albicans and bacterial microbiota interactions in the cecum during recolonization following broad-spectrum antibiotic therapy. Infect Immun. 2012;80(10): 3371–3380. doi:10.1128/IAI.00449-12

119. Polke M, Jacobsen ID. Quorum sensing by farnesol revisited. Current Genetics. 2017;63(5): 791–797. doi:10.1007/s00294-017-0683-x

120. Hornby JM, Jensen EC, Lisec AD, Tasto JJ, Jahnke B, Shoemaker R, et al. Quorum Sensing in the Dimorphic Fungus *Candida albicans* Is Mediated by Farnesol. Appl Environ Microbiol. 2001;67(7): 2982–2992. doi:10.1128/AEM.67.7.2982-2992.2001

121. Jang SJ, Lee K, Kwon B, You HJ, Ko GP. Vaginal lactobacilli inhibit growth and hyphae formation of *Candida albicans*. Sci Rep. 2019;9(1): 8121. doi:10.1038/s41598-019-44579-4

122. Itapary dos Santos C, Ramos França Y, Duarte Lima Campos C, Quaresma Bomfim MR, Oliveira Melo B, Assunção Holanda R, et al. Antifungal and Antivirulence Activity of Vaginal *Lactobacillus* Spp. Products against *Candida* Vaginal Isolates. Pathogens. 2019;8(3): E150. doi:10.3390/pathogens8030150

123. Graf K, Last A, Gratz R, Allert S, Linde S, Westermann M, et al. Keeping *Candida* commensal: How lactobacilli antagonize pathogenicity of *Candida albicans* in an in vitro gut model. DMM Dis Model Mech. 2019;12(9): dmm039719. doi:10.1242/dmm.039719

124. Fan D, Coughlin LA, Neubauer MM, Kim J, Kim MS, Zhan X, et al. Activation of HIF-1α and LL-37 by commensal bacteria inhibits *Candida albicans* colonization. Nature Medicine. 2015;21(7): 808–814. doi:10.1038/nm.3871

125. Gaddy JA, Tomaras AP, Actis LA. The *Acinetobacter baumannii* 19606 OmpA protein plays a role in biofilm formation on abiotic surfaces and in the interaction of this pathogen with eukaryotic cells. Infect Immun. 2009;77(8): 3150–3160. doi:10.1128/IAI.00096-09

126. Nash EE, Peters BM, Fidel PL, Noverr MC. Morphology-independent virulence of *Candida* species during polymicrobial intra-abdominal infections with *Staphylococcus aureus*. Infect Immun. 2015;84(1): 90–98. doi:10.1128/IAI.01059-15

127. Todd OA, Fidel PL, Harro JM, Hilliard JJ, Tkaczyk C, Sellman BR, et al. *Candida albicans* augments *Staphylococcus aureus* virulence by engaging the staphylococcal agr quorum sensing system. mBio. 2019;10(3): e00910-19. doi:10.1128/mBio.00910-19

128. Schlecht LM, Peters BM, Krom BP, Freiberg JA, Hänsch GM, Filler SG, et al. Systemic *Staphylococcus aureus* infection mediated by *Candida albicans* hyphal invasion of mucosal tissue. Microbiol (United Kingdom). 2015;161(Pt 1): 168–181. doi:10.1099/mic.0.083485-0

129. Childers DS, Avelar GM, Bain JM, Larcombe DE, Pradhan A, Budge S, et al. Impact of the Environment upon the *Candida albicans* Cell Wall and Resultant Effects upon Immune Surveillance. Curr Top Microbiol Immunol Springer, Berlin, Heidelb. 2019. doi:https://doi.org/10.1007/82_2019_182

130. Speth C, Rambach G, Würzner R, Lass-Flörl C. Complement and fungal pathogens: An update. Mycoses. 2008;51(6): 477–496. doi:10.1111/j.1439-0507.2008.01597.x

131. Filler SG, Sheppard DC. Fungal invasion of normally non-phagocytic host cells. PLoS Pathog. 2006;2(12): e129. doi:10.1371/journal.ppat.0020129

132. Kaloriti D, Jacobsen M, Yin Z, Patterson M, Tillmann A, Smith DA, et al. Mechanisms underlying the exquisite sensitivity of *Candida albicans* to combinatorial cationic and oxidative stress that enhances the potent fungicidal activity of phagocytes. mBio. 2014;5(4): e01334-14. doi:10.1128/mBio.01334-14

133. Seider K, Brunke S, Schild L, Jablonowski N, Wilson D, Majer O, et al. The Facultative Intracellular Pathogen *Candida glabrata* Subverts Macrophage Cytokine Production and Phagolysosome Maturation. J Immunol. 2011;187(6): 3072–3086. doi:10.4049/jimmunol.1003730

134. Brothers KM, Gratacap RL, Barker SE, Newman ZR, Norum A, Wheeler RT. NADPH Oxidase-Driven Phagocyte Recruitment Controls *Candida albicans* Filamentous Growth and Prevents Mortality. PLoS Pathog. 2013;9(10): e1003634. doi:10.1371/journal.ppat.1003634

135. Prolo C, Álvarez MN, Radi R. Peroxynitrite, a potent macrophage-derived oxidizing cytotoxin to combat invading pathogens. BioFactors. 2014;40(2): 215–225. Epub 26 Nov 2013. doi:10.1002/biof.1150

136. Enjalbert B, Smith DA, Cornell MJ, Alam I, Nicholls S, Brown AJP, et al. Role of the Hog1 stress-activated protein kinase in the global transcriptional response to stress in the fungal pathogen *Candida albicans*. Mol Biol Cell. 2006;17(2): 1018–1032. Epub 7 Dec 2005. doi:10.1091/mbc.E05-06-0501

137. Enjalbert B, MacCallum DM, Odds FC, Brown AJP. Niche-specific activation of the oxidative stress response by the pathogenic fungus *Candida albicans*. Infect Immun. 2007;75(5): 2143–2151. doi:10.1128/IAI.01680-06

138. Pradhan A, Herrero-de-Dios C, Belmonte R, Budge S, Lopez Garcia A, Kolmogorova A, et al. Elevated catalase expression in a fungal pathogen is a double-edged sword of iron. PLoS Pathog. 2017;13(5): e1006405. doi:10.1371/journal.ppat.1006405

139. Smith DA, Nicholls S, Morgan BA, Brown AJP, Quinn J. A conserved stress-activated protein kinase regulates a core stress response in the human pathogen *Candida albicans*. Mol Biol Cell. 2004;15(9): 4179–4190. doi:10.1091/mbc.E04-03-0181

140. Alarco AM, Raymond M. The bZip transcription factor Cap1p is involved in multidrug resistance and oxidative stress response in *Candida albicans*. J Bacteriol. 1999;181(3): 700–708.

141. Znaidi S, Barker KS, Weber S, Alarco AM, Liu TT, Boucher G, et al. Identification of the *Candida albicans* Cap1p regulon. Eukaryot Cell. 2009;8(6): 806–820. doi:10.1128/EC.00002-09

142. Zhang X, De Micheli M, Coleman ST, Sanglard D, Moye-Rowley WS. Analysis of the oxidative stress regulation of the *Candida albicans* transcription factor, Cap1p. Mol Microbiol. 2000;36(3):618–629. doi:10.1046/j.1365-2958.2000.01877.x

143. da Silva Dantas A, Patterson MJ, Smith DA, MacCallum DM, Erwig LP, Morgan BA, et al. Thioredoxin Regulates Multiple Hydrogen Peroxide-Induced Signaling Pathways in *Candida albicans*. Mol Cell Biol. 2010;30(19): 4550–4563. doi:10.1128/mcb.00313-10

144. Chiranand W, McLeod I, Zhou H, Lynn JJ, Vega LA, Myers H, et al. CTA4 transcription factor mediates induction of nitrosative stress response in *Candida albicans*. Eukaryot Cell. 2008;7(2): 268–278. Epub 14 Dec 2007. doi:10.1128/EC.00240-07

145. Chaves GM, Bates S, MacCallum DM, Odds FC. *Candida albicans* GRX2, encoding a putative glutaredoxin, is required for virulence in a murine model. Genetics and Molecular Research. 2007;6(4): 1051–1063.

146. Hwang CS, Rhie GE, Oh JH, Huh WK, Yim HS, Kang SO. Copper- and zinc-containing superoxide dismutase (Cu/ZnSOD) is required for the protection of *Candida albicans* against oxidative stresses and the expression of its full virulence. Microbiology. 2002;148(Pt 11): 3705–3713. doi:10.1099/00221287-148-11-3705

147. Kos I, Patterson MJ, Znaidi S, Kaloriti D, da Silva Dantas A, Herrero-de-Dios CM, et al. Mechanisms underlying the delayed activation of the cap1 transcription factor in *Candida albicans* following combinatorial oxidative and cationic stress important for phagocytic potency. mBio. 2016;7(2): e00331. doi:10.1128/mBio.00331-16

148. Hood MI, Skaar EP. Nutritional immunity: Transition metals at the pathogen-host interface. Nature Reviews Microbiology. 2012;10(8): 525–537. doi:10.1038/nrmicro2836

149. Ramanan N, Wang Y. A high-affinity iron permease essential for *Candida albicans* virulence. Science. 2000;288(5468): 1062–1064. doi:10.1126/science.288.5468.1062

150. Potrykus J, Stead D, MacCallum DM, Urgast DS, Raab A, van Rooijen N, et al. Fungal Iron Availability during Deep Seated Candidiasis Is Defined by a Complex Interplay Involving Systemic and Local Events. PLoS Pathog. 2013;9(10): e1003676. doi:10.1371/journal.ppat.1003676

151. Potrykus J, Ballou ER, Childers DS, Brown AJP. Conflicting Interests in the Pathogen-Host Tug of War: Fungal Micronutrient Scavenging Versus Mammalian Nutritional Immunity. PLoS Pathog. 2014;10(3): e1003910. doi:10.1371/journal.ppat.1003910

152. Nevitt T, Thiele DJ. Host iron withholding demands siderophore utilization for *Candida glabrata* to survive macrophage killing. PLoS Pathog. 2011;7(3): e1001322. doi:10.1371/journal.ppat.1001322

153. Seider K, Gerwien F, Kasper L, Allert S, Brunke S, Jablonowski N, et al. Immune evasion, stress resistance, and efficient nutrient acquisition are crucial for intracellular survival of *Candida glabrata* within macrophages. Eukaryot Cell. 2014;13(1): 170–183. Epub 20 Dec 2013. doi:10.1128/EC.00262-13

154. Knight SAB, Lesuisse E, Stearman R, Klausner RD, Dancis A. Reductive iron uptake by *Candida albicans*: Role of copper, iron and the TUP1 regulator. Microbiology. 2002;148(Pt 1): 29–40. doi:10.1099/00221287-148-1-29

155. Knight SAB, Vilaire G, Lesuisse E, Dancis A. Iron acquisition from transferrin by *Candida albicans* depends on the reductive pathway. Infect Immun. 2005;73(9): 5482–5492. doi:10.1128/IAI.73.9.5482-5492.2005

156. Kuznets G, Vigonsky E, Weissman Z, Lalli D, Gildor T, Kauffman SJ, et al. A Relay Network of Extracellular Heme-Binding Proteins Drives *C. albicans* Iron Acquisition from Hemoglobin. PLoS Pathog. 2014;10(10): e1004407. doi:10.1371/journal.ppat.1004407

157. Mackie J, Szabo EK, Urgast DS, Ballou ER, Childers DS, MacCallum DM, et al. Host-imposed copper poisoning impacts fungal micronutrient acquisition during systemic *Candida albicans* infections. PLoS ONE. 2016;11(6): e0158683. doi:10.1371/journal.pone.0158683

158. Ballou ER, Wilson D. The roles of zinc and copper sensing in fungal pathogenesis. Current Opinion in Microbiology. 2016;32: 128–134. doi:10.1016/j.mib.2016.05.013

159. Li CX, Gleason JE, Zhang SX, Bruno VM, Cormack BP, Culotta VC. *Candida albicans* adapts to host copper during infection by swapping metal cofactors for superoxide dismutase. Proc Natl Acad Sci. 2015;112(38): E5336–E5342. doi:10.1073/pnas.1513447112

160. Edgeworth J, Gorman M, Bennett R, Freemont P, Hogg N. Identification of p8,14 as a highly abundant heterodimeric calcium binding protein complex of myeloid cells. J Biol Chem. 1991;266(12): 7706–7713.

161. Urban CF, Ermert D, Schmid M, Abu-Abed U, Goosmann C, Nacken W, et al. Neutrophil extracellular traps contain calprotectin, a cytosolic protein complex involved in host defense against *Candida albicans*. PLoS Pathog. 2009;5(10): e1000639. doi:10.1371/journal.ppat.1000639

162. Urban CF, Reichard U, Brinkmann V, Zychlinsky A. Neutrophil extracellular traps capture and kill *Candida albicans* and hyphal forms. Cell Microbiol. 2006;8(4): 668–676. doi:10.1111/j.1462-5822.2005.00659.x

163. Branzk N, Lubojemska A, Hardison SE, Wang Q, Gutierrez MG, Brown GD, et al. Neutrophils sense microbe size and selectively release neutrophil extracellular traps in response to large pathogens. Nat Immunol. 2014;15(11): 1017–1025. doi:10.1038/ni.2987

164. Miramón P, Kasper L, Hube B. Thriving within the host: *Candida* spp. interactions with phagocytic cells. Medical Microbiology and Immunology. 2013;202(3): 183–195. doi:10.1007/s00430-013-0288-z

165. Vignesh KS, Landero Figueroa JA, Porollo A, Caruso JA, Deepe GS. Zinc Sequestration: Arming Phagocyte Defense against Fungal Attack. PLoS Pathog. 2013;9(12): e1003815. doi:10.1371/journal.ppat.1003815

166. Subramanian Vignesh K, Landero Figueroa JA, Porollo A, Caruso JA, Deepe GS. Granulocyte macrophage-colony stimulating factor induced Zn sequestration enhances macrophage superoxide and limits intracellular pathogen survival. Immunity. 2013;39(4): 697–710. doi:10.1016/j.immuni.2013.09.006

167. Kim MJ, Kil M, Jung JH, Kim J. Roles of zinc-responsive transcription factor Csr1 in filamentous growth of the pathogenic yeast *Candida albicans*. J Microbiol Biotechnol. 2008;18(2): 242–247.

168. Nobile CJ, Nett JE, Hernday AD, Homann OR, Deneault JS, Nantel A, et al. Biofilm matrix regulation by *Candida albicans* Zap1. PLoS Biol. 2009;7(6): e1000133. doi:10.1371/journal.pbio.1000133

169. Xu W, Solis N V., Ehrlich RL, Woolford CA, Filler SG, Mitchell AP. Activation and Alliance of Regulatory Pathways in *C. albicans* during Mammalian Infection. PLoS Biol. 2015;13(2): e1002076. doi:10.1371/journal.pbio.1002076

170. Citiulo F, Jacobsen ID, Miramón P, Schild L, Brunke S, Zipfel P, et al. *Candida albicans* scavenges host zinc via Pra1 during endothelial invasion. PLoS Pathog. 2012;8(6): e1002777. doi:10.1371/journal.ppat.1002777

171. Sheldon JR, Skaar EP. Metals as phagocyte antimicrobial effectors. Current Opinion in Immunology. 2019;60: 1–9. doi:10.1016/j.coi.2019.04.002

172. Brown AJP, Budge S, Kaloriti D, Tillmann A, Jacobsen MD, Yin Z, et al. Stress adaptation in a pathogenic fungus. Journal of Experimental Biology. 2014;217(Pt 1): 144–155. doi:10.1242/jeb.088930

173. Brown AJP, Gow NAR, Warris A, Brown GD. Memory in Fungal Pathogens Promotes Immune Evasion, Colonisation, and Infection. Trends in Microbiology. 2019;27(3): 219–230. Epub 30 Nov 2018. doi:10.1016/j.tim.2018.11.001

174. Cavalheiro M, Teixeira MC. *Candida* Biofilms: Threats, Challenges, and Promising Strategies. Front Med. 2018;5: 28. doi:10.3389/fmed.2018.00028

175. Soll DR, Daniels KJ. Plasticity of *Candida albicans* Biofilms. Microbiol Mol Biol Rev. 2016;80(3): 565–595. doi:10.1128/mmbr.00068-15

176. Taff HT, Mitchell KF, Edward JA, Andes DR. Mechanisms of *Candida* biofilm drug resistance. Future Microbiology. 2013;8(10): 1325–1337. doi:10.2217/fmb.13.101

177. Wuyts J, Van Dijck P, Holtappels M. Fungal persister cells: The basis for recalcitrant infections? PLoS Pathog. 2018;14(10): e1007301. doi:10.1371/journal.ppat.1007301

178. Rossignol T, Ding C, Guida A, D'Enfert C, Higgins DG, Butler G. Correlation between biofilm formation and the hypoxic response in *Candida parapsilosis*. Eukaryot Cell. 2009;8(4): 550–559. doi:10.1128/EC.00350-08

179. Zarnowski R, Westler WM, Lacmbouh GA de, Marita JM, Bothe JR, Bernhardt J, et al. Novel entries in a fungal biofilm matrix encyclopedia. mBio. 2014;5: e01333-14. doi:10.1128/mBio.01333-14

180. Nobile CJ, Fox EP, Nett JE, Sorrells TR, Mitrovich QM, Hernday AD, et al. A recently evolved transcriptional network controls biofilm development in *Candida albicans*. Cell. 2012;148: 126–138. doi:10.1016/j.cell.2011.10.048

181. Martínez-Gomariz M, Perumal P, Mekala S, Nombela C, Chaffin WLJ, Gil C. Proteomic analysis of cytoplasmic and surface proteins from yeast cells, hyphae, and biofilms of *Candida albicans*. Proteomics. 2009;9(8): 2230–2252. doi:10.1002/pmic.20070059

182. Ene IV., Cheng SC, Netea MG, Brown AJP. Growth of *Candida albicans* cells on the physiologically relevant carbon source lactate affects their recognition and phagocytosis by immune cells. Infect Immun. 2013;81: 238–248. doi:10.1128/IAI.01092-12

183. Chew SY, Ho KL, Cheah YK, Ng TS, Sandai D, Brown AJP, et al. Glyoxylate cycle gene ICL1 is essential for the metabolic flexibility and virulence of *Candida glabrata*. Sci Rep. 2019;9(1): 2843. doi:10.1038/s41598-019-39117-1

184. Oliveira-Pacheco J, Alves R, Costa-Barbosa A, Cerqueira-Rodrigues B, Pereira-Silva P, Paiva S, et al. The role of *Candida albicans* transcription factor RLM1 in response to carbon adaptation. Front Microbiol. 2018;9: 1127. doi:10.3389/fmicb.2018.01127

CHAPTER 2

CARBOXYLIC ACID TRANSPORTERS IN *CANDIDA* PATHOGENESIS

Disclaimer

Part of this chapter contains work that has been previously published in *mBio.*

-

Alves R, Sousa-Silva M, Vieira D, Soares P, Chebaro Y, Lorenz M, Casal M, Soares-Silva I, Paiva S (2020) Carboxylic acid transporters in *Candida* pathogenesis. *mBio*.

doi: 10.1128/mBio.00156-20

-

ABSTRACT

Opportunistic pathogens such as *Candida* species can use carboxylic acids, like acetate and lactate, to survive and successfully thrive in different environmental niches. These nonfermentable substrates are frequently the major carbon sources present in certain human body sites, and their efficient uptake by regulated plasma membrane transporters plays a critical role in such nutrient-limited conditions. Here, we cover the physiology and regulation of these proteins and their potential role in *Candida* virulence. This review also presents an evolutionary analysis of orthologues of the *Saccharomyces cerevisiae* Jen1 lactate and Ady2 acetate transporters, including a phylogenetic analysis of 101 putative carboxylate transporters in twelve medically relevant *Candida* species. These proteins are assigned to distinct clades according to their amino acid sequence homology and represent the major carboxylic acid uptake systems in yeast. While Jen transporters belong to the sialate:H^+ symporter (SHS) family, the Ady2 homologue members are assigned to the acetate uptake transporter (AceTr) family. Here, we reclassify the later members as ATO (acetate transporter ortholog). The new nomenclature will facilitate the study of these transporters, as well as the analysis of their relevance for *Candida* pathogenesis.

2.1 INTRODUCTION

Transport of carboxylic acids across cell membranes is of critical importance for all living systems, from bacteria to fungi to mammalian cells [1]. At physiological pH, these organic compounds prevail in their anionic form, requiring a transport system to cross the plasma membrane; whereas, at lower pH, the undissociated form of the acid can enter the cell by simple diffusion [1,2]. Integral membrane transporters and channels, the two major classes of transport proteins, are thereby important mediators between the intracellular and extracellular environment by precisely controlling the influx of important nutrients or the efflux of unwanted metabolites [3]. In *Saccharomyces cerevisiae*, Jen1 and Ady2 are the main transport systems responsible for the uptake of monocarboxylates at conditions where these substrates can be used as main carbon sources. The aquaglyceroporin channel Fps1 has also been reported to mediate the import of undissociated acetic acid by facilitated diffusion [4], though this seems to depend on the extracellular environment [5]. Both Jen1 and Ady2 transporters have also been suggested to be involved in the export of monocarboxylates [6,7]; yet, it is unclear how these efflux processes are regulated.

Opportunistic pathogens can acquire the available carboxylic acids present in the human host, either produced by host microbiota or host cells [8]. The uptake of carboxylates, such as lactate and acetate, sustains cell metabolism and growth when other preferable carbon sources are limited. This is particularly relevant for a group of pathogenic *Candida* species, which are well-adapted to different human environmental niches and import these carboxylic acids in order to survive under host conditions that otherwise would be deleterious. These nutrient-restricted environments are predominantly found within the gut and vagina, with the host microbiota having a predominant role in the production of propionate, acetate and lactate [9,10]. The induction of lactate and acetate transporters in *Candida* upon macrophage or neutrophil internalization also supports the idea that these nutrients are readily available inside phagocytic cells [11-16].

The different species comprising the genus *Candida* are spread among distinct phylogenetic clades, which also include other nonpathogenic species (Figure 2.1). This suggests that the ability to infect humans has evolved several times, independently, among this diverse group of yeasts [17]. In this review, we revisit the two major families of carboxylic acid transporters in yeast and explore their contribution for *Candida* pathogenesis. The expansion and functional specialization of some members of these families in pathogenic species, such as in *Candida albicans* and *Candida parapsilosis*, may have emerged as means of either environmental or host adaptation, increasing the ability of these species to thrive within the human host and consequently account for their increased virulence. To give a better overview on the representation of these transporters in *Candida*, we conducted protein BLAST (pBLAST) searches in NCBI (https://blast.ncbi.nlm.nih.gov), and identified all the orthologues of the functionally validated *Saccharomyces cerevisiae* monocarboxylate transporters (Jen1 and Ady2) for a set of medically relevant *Candida* species. In particular, these two transporters were independently used as BLAST queries in searching the proteome of *C. albicans*, *Candida glabrata*, *Candida tropicalis*, *C. parapsilosis*, *Candida orthopsiliosis*, *Candida dubliniensis*, *Candida krusei*, *Candida auris*, *Candida lusitaniae*, *Candida haemulonis*, *Candida guilliermondii*, and *Candida kefyr*. This set includes the most studied and well-characterized *Candida* species but also infrequent species that are emerging as successful pathogens. Finally, we reclassified and renamed some of these homologues based on recently reported structural and functional data. In particular, we propose the exclusive use of ATO (acetate transporter ortholog) for all the yeast Ady2 ortholog members of the acetate uptake transporter (AceTr) family to better describe their function as acetate transporters [18–20].

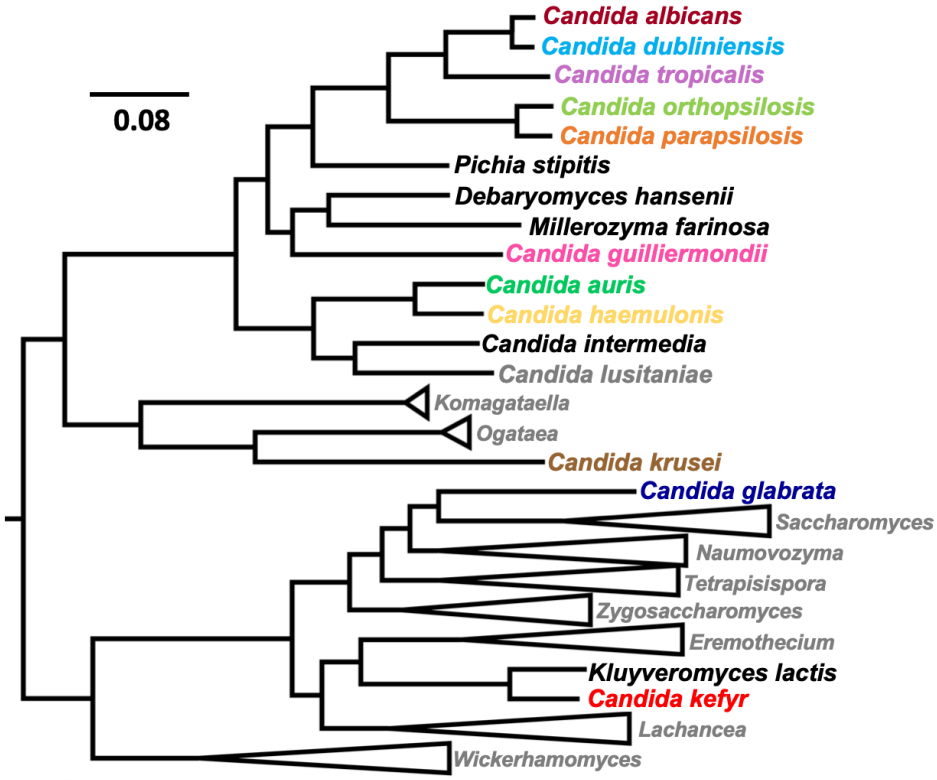

Figure 2.1. Evolutionary relationship between *Candida* species and other yeasts. Phylogenetic reconstruction was performed using maximum-likelihood in IQ-TREE [73], the JTT (Jones-Taylor-Thornton) model of amino-acid evolution, and four gamma-distributed rates. Phylogeny was based on a total of 1567 concatenated proteins within the proteome of the different species. BLAST searches were performed comparing the proteome (obtained in NCBI) of the selected species in order to detect those conserved proteins across a total of 77 fungal species. These proteins are essential proteins beyond the specific biology of the different yeasts offering a clear high-resolution evolutionary view between the different species. All obtained bootstrap values showed 100% in confidence. *Candida* species relevant for this study are highlighted with different colours. Branches that were not relevant were collapsed with the representative genus indicated.

2.2 Phylogenetic evolution of JEN transporters

The lactate transporter Jen1 was the first monocarboxylate transporter identified in fungi [21]. This proton-coupled monocarboxylate transporter is a member of the major facilitator superfamily (MFS; TCDB 2.A.1.12.2) [22], which is responsible for the active transport of lactate, pyruvate, acetate and propionate

[21,23,24], and also selenite [25]. So far, among all *Candida species*, only two *S. cerevisiae* Jen1 (ScJen1) orthologues were functionally characterized in *C. albicans*, one encoding a monocarboxylate transporter (CaJen1) for lactate, pyruvate and propionate [26], and the other encoding a dicarboxylate transporter (CaJen2) for succinate and malate [13]. Both CaJen1 and CaJen2 transporters are tightly regulated by different carbon sources, being repressed by glucose and induced by their specific substrates [13]. This upregulation was also confirmed *in vivo*, in *C. albicans* cells infecting the kidney, in a murine model of systemic candidiasis, and upon phagocytosis by murine macrophages or human neutrophils [13].

The phylogenetic analysis of ScJen1 was performed with the available amino acid sequences for several *Candida* species. The obtained tree displays 36 Jen-like proteins and suggests the existence of two functional clusters, which we designated as clade A and clade B (Figure 2.2A; see also Table S2.1 in the supplemental material). While clade A comprises the functionally characterized CaJen1 monocarboxylate transporter, clade B contains the CaJen2 dicarboxylate transporter (Figure 2.2A). The branching pattern within the two clades is consistent with the species tree topology (see Figure 2.1 for reference tree). With the exception of *C. glabrata*, which does not have any Jen transporter, all *Candida* species analyzed have at least two ScJen1 orthologues. The absence of Jen transporters has already been reported for other *Saccharomycetacea* yeasts that diverged after the whole genome duplication [27]. Curiously, though, lactate assimilation is required for *C. glabrata* survival in the intestine, as mutants in the lactate dehydrogensase Cyb2 are rapidly outcompeted [28]. *C. parapsilosis*, *C. orthopsilosis* and *C. guilliermondii* contain, respectively, twelve, four and three ScJen1 homologues, which are not equally distributed within the two clades (Figure 2.2A). In the case of *C. parapsilosis* and *C. orthopsilosis*, this observation is consistent with the high level of genomic variation displayed by these species, including copy number variations, a phenomenon likely due to selective pressures present in the environment rather than in the human host [29]. This phenomenon was also reported for *Yarrowia lipolytica*, which has 6 ScJen1 homologues. A phylogenetic analysis predicted that 12 duplications and losses occurred during evolution in the *Yarrowia* Jen clade [27]. Moreover, the ScJen1 orthologs found in *C. krusei*, *C. auris*, *C. lusitaniae* and *C. haemulonis* are exclusively clustered in clade B (Figure 2B). While these clades were initially assumed to be two different functional clusters in fungi, with the Jen1 cluster comprising only monocarboxylate transporter proteins and the Jen2 containing dicarboxylate transporters [1,30], recent evidence has shown that members of both clades may have overlapping substrate specificities [31]. The possibility that an ancestral Jen transporter encoded a promiscuous protein with the ability of transporting

both mono- and dicarboxylates is highly plausible, but it still remains unclear [30]. Studies that have attempted to reconstruct the evolutionary origin of the Jen family suggest *JEN2* as the ancestral gene [27,30]. However, due to a dynamic evolutionary history of subsequent duplications and losses, other members of this family, such as JEN1, have merged [27,30].

The predicted three-dimensional structure of ScJen1, consisting in 12 transmembrane segments (TMSs), resembles the common topology of other MFS members. Structure-function studies, benefiting from the solved structure of other MFS members, have identified several conserved amino acids that are essential for the binding and co-translocation of the substrates [32,33]. When analyzing the amino acid sequences, it is possible to observe that most of the functional motifs and amino acids described for ScJen1 are highly conserved across all of the identified orthologues (Figure 2.2B). This observation suggests that these transporters are likely to retain the same function. For instance, the conserved motif NXX[S/T]HX[S/T]QDXXXT, located at the end of the putative seventh TMS, has been reported as part of the translocation pathway [33]. Protein modelling has demonstrated that the conserved amino acids of this motif face an internal pore and potentially interact with the carboxylic substrates, which is consistent with their crucial roles in protein activity, transport ability and specificity, as well as substrate affinity [32,33]. Other polar conserved residues located at different TMSs have also been identified to be part of the pore and play special roles in substrate specificity by allowing the discrimination between mono- and dicarboxylates [32].

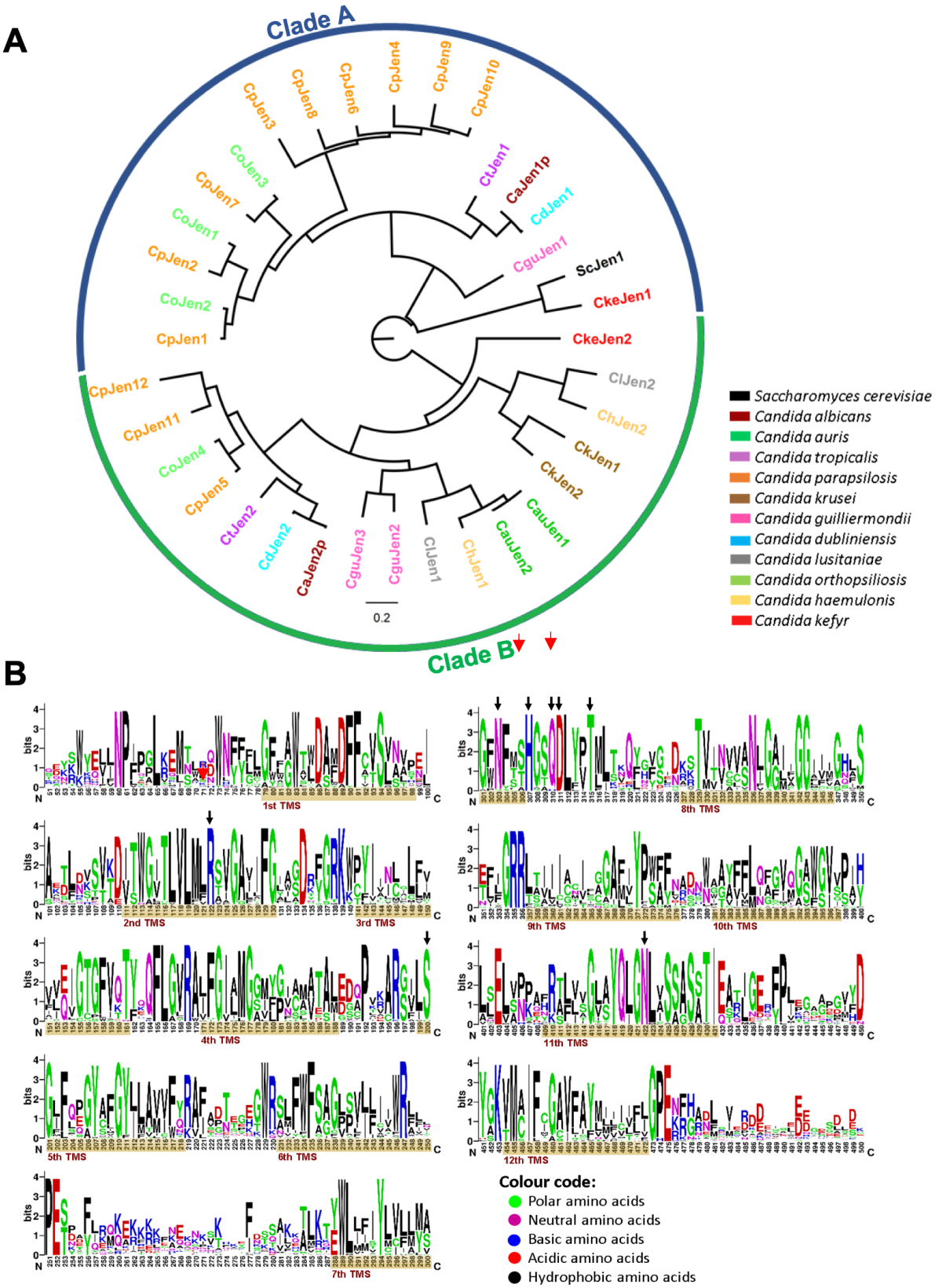

Figure 2.2. Evolutionary analysis of *S. cerevisiae* Jen homologues in *Candida* species. (A) A multiple-alignment with the 36 ScJen1 homologues found in *Candida* species was performed using MAFFT v.7 [74] and checked manually for incongruences. The alignments were then used in the phylogenetic

reconstruction. A maximum-likelihood approach, suitable for deep evolution, was conducted in MEGA7 [75] using the JTT model of amino acid evolution, four gamma-distributed rates, and a site coverage cutoff of 90%. A total of 250 replications were performed for the bootstrap analysis. Names of the homologues are colored according to the species where they were detected. Output trees were edited in Figtree v. v.1.4.4. (http://tree.bio.ed.ac.uk/software). **(B)** Conservation logo of the alignment that displayed residues in 90% of the sequences using WebLogo (https://weblogo.berkeley.edu). Transmembrane segments (TMSs) predicted with TMHMM 2.0 (http://www.cbc.dtu.dk/services/TMHMM/) are highlighted as brown bars in the logo, and black arrows indicate amino acids belonging to previously identified functional domains [32,33].

2.3 Phylogenetic evolution of ATO transporters

The first member of the acetate transporter family to be reported in the literature was the yeast *Yarrowia lipolyptica* Gpr1 protein [34,35], which was later confirmed to be an acetate transporter [18]. Since then, many orthologues have been identified in the three domains of life [18]. Some examples include the *S. cerevisiae* Ady2 (ScAdy2) and the *Aspergillus nidulans* AcpA in eukarya [36,37], AceP in archaea [18,38], and SatP in bacteria [39]. Although well-represented among the different taxonomic groups, these orthologues seem almost ubiquitous in fungi [18]. This observation suggests that acetate transporters play key roles in fungal species, which is in agreement with their involvement in essential physiological processes such as ascus formation in *S. cerevisiae* or germination of conidiophores in *Aspergillus nidulans* [40]. In *S. cerevisiae*, Ady2 has been identified as an acetate permease with the ability to transport other monocarboxylates, such as propionate, formate, and lactate [18,36]. Besides *ADY2* (also known as *ATO1*), the genome of *S. cerevisiae* harbors two additional homologues, *FUN34* (also known as *ATO2*) and *ATO3*. These three transporters are highly induced under carbon-limiting conditions and during the stationary phase of glucose grown cells [41,42]. The deletion of Sc*ADY2* results in the loss of mediated acetate uptake at pH 6.0 [36].

ScAdy2 (named originally for "accumulation of dyads protein 2") was also reported to be expressed during meiosis, which is required for the regulation of meiotic plaque components in sporulation [43]. Mutants in Sc*ADY2* predominantly form dyads and display a decreased spore formation [44]. The standard

formulation for inducing sporulation in yeast contains acetate as primary carbon source, which probably links the molecular function of the Ady2 protein to this phenotype [44,45].

These transporters were reported to be involved in ammonium export, hence the acronym ATO, which stands for "ammonia transport outward" [43] was adopted. In *S. cerevisiae,* this volatile alkaline compound is transmitted between yeast colonies as a signal to inhibit growth of the facing parts of both colonies, a signaling process that requires amino acid uptake [46]. The three Ato transporters were suggested to act as ammonium/H^+ antiporters by extruding ammonium and importing protons and, thus, contributing to the increase of external pH observed during ammonia signaling [47]. The association of the Ato proteins with ammonium transport is genetic, and there is no homology with bona fide ammonium transporters nor any biochemical evidence that they transport ammonia or ammonium.

These transporters were recently reclassified into the acetate uptake transporter (AceTr) family (TCDB 2.A.96) [22] based on the characterization of the abovementioned orthologues, from all domains of life, as acetate transporters [18–20,37,39]. The confusinh nomenclature, often deriving from phenotypes that are indirectly linked to function (ADY, FUN, ATO), represents a barrier to understanding and studying this interesting family. We, therefore, propose redefining the Ady2/Ato proteins as "acetate transport ortholog" instead of the previous designation as "ammonia transport outward" to better reflect and describe their function as acetate transporters, while still maintaining some consistency with the literature (see Table S2.2 in the supplemental material).

The phylogenetic analysis of ScAdy2/Ato orthologues (hereafter referred as ScAto1) in the selected *Candida* species resulted in a phylogenetic tree containing 65 Ato-like proteins organized into two asymmetrical clusters (Figure 2.3A). Cluster A includes most of the *Candida* orthologues, while the cluster B contains only four orthologues and one homologue of ScAto1. All of the selected *Candida* species have at least two orthologues, and more than 50% of the species have five or more orthologues (Figure 2.3A), which is in agreement with the high frequency of these proteins in fungal organisms [18]. In particular, the Ato family in *C. albicans* is greatly expanded when compared with other species, being composed by 10 Ato-like proteins [48]. However, two of these putative acetate transporters (CaAto9 and CaAto10, see Table S2.2) were shorter than the other retrieved sequences. The examination of the BLAST results and the genomic position of each homologue suggests that these were originally the same gene split by a transposable element. The independent alignment of CaAto9 and CaAto10 with the remaining

homologues revealed that they align consecutively to each other. Furthermore, phylogenetic analyses performed individually on each sequence revealed the same evolutionary position for both CaAto9 and CaAto10 (phylogenetically close to CaAto6, followed by CaAto5). Given this, CaAto9 and CaAto10 were excluded, as they are most probably non-functional homologues. Two other sequences, CtAto8 and CguAto3, were relatively shorter than the other sequences in the alignment. Analyses with TMHMM v. 2.0 (http://www.cbs.dtu.dk/services/TMHMM) showed that these proteins only contain 3 and 5 helices, respectively, instead of the expected six detected for this transporter family. The analysis of the genomic sequence following the termination codon of the protein revealed the presence of the homologous absent portion, indicating that the proteins were truncated, likely recently in evolution. As we have no indication if the truncated proteins are fully functional, we excluded these sequences from further analyses.

As mentioned above, hallmarks of this family include six transmembrane domains but also conserved motifs that are involved in the transport mechanism of acetate in Ato members but also succinate in SatPs [18,19]. The Ato1 orthologues in *Escherichia coli* (ecSatP) and *Citrobacter koseri* (ckSatP) are so far the only members of the AceTr family whose structures are available [19,49]. A hexameric UreI-like channel structure was reported for ecSatP [49]; however, more recently, it was suggested that the closed state of the channel represents a relatively high energy barrier, 15 kcal/mol [20]. The signature NPAPLGL(M/S) motif of the AceTr family, located at the beginning of the first TMS (Figure 2.3B), has been reported to be essential for substrate uptake [18,35]. Recent structural analyses with the SatP homolog from *Citrobacter koseri* have demonstrated that these conserved amino acids are in the vicinity of the first and second acetate/succinate-biding sites, allowing the translocation of the substrate [18,19]. The dissection of the molecular mechanism of the acetate transport in several members of the AceTr family suggests that these transporters are energy dependent [18,20,36,39,50]. This functional motif, as well as other amino acids that play important roles in the transport mechanism of Ato transporters, are highly conserved among all the identified *Candida* orthologues, suggesting that *Candida* Atos are likely to retain the same function (Figure 2.3B). However, an extensive phylogentic analysis has recently assigned all of the known members of this family into two distinct clades – the prokaryotic clade, where SatPs are included, and a eukaryotic clade comprising the Ato transporters [18]. This suggests that despite havinf a conserved motif involved in substrate recognition and transport, the members of these two clades may display different specificities, which is in agreement with what is already described for the Jen1 homologs that present a conserved signature motif and different specificities throughout the distinct family members [1,31].

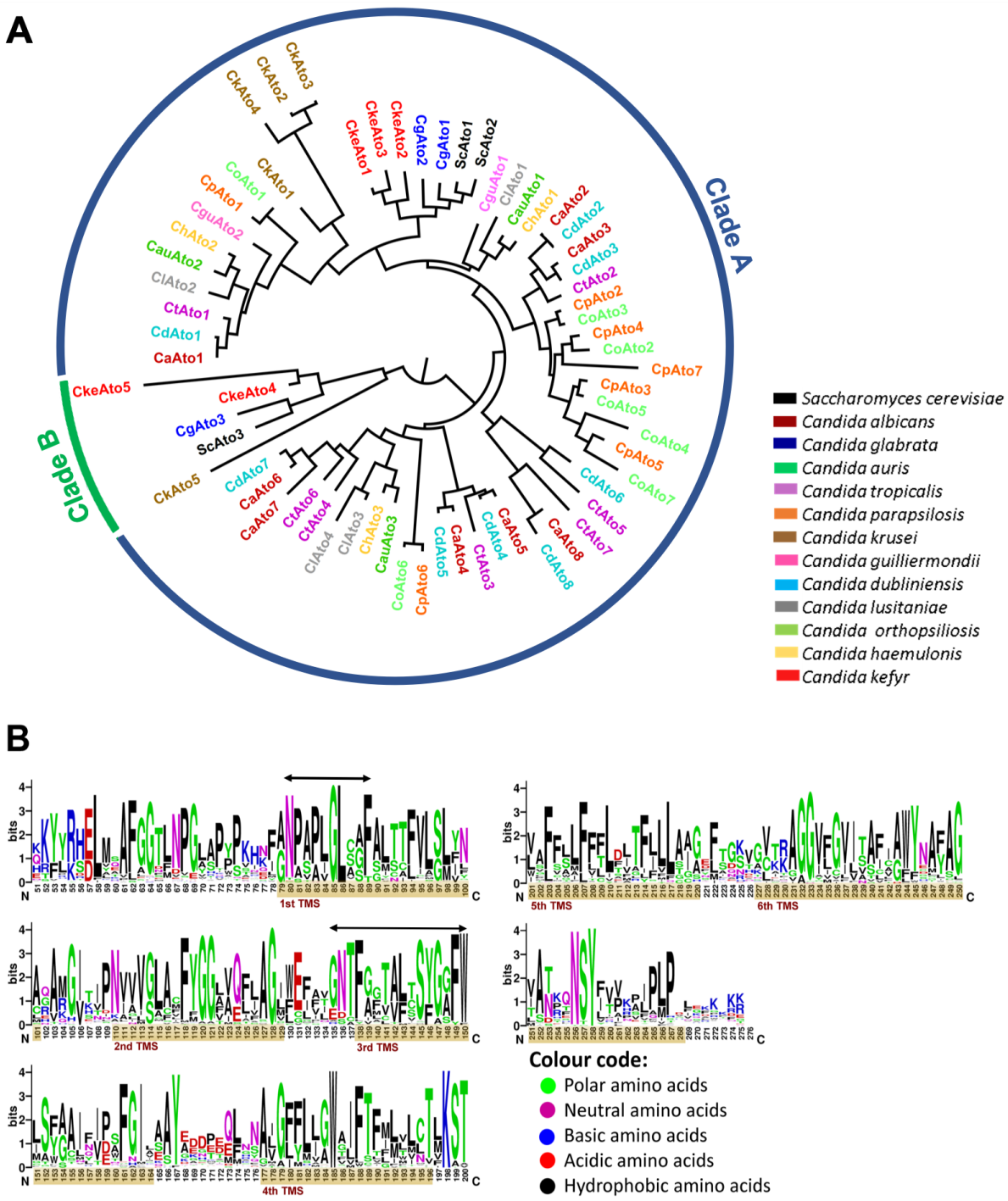

Figure 2.3. Evolutionary analysis of *S. cerevisiae* Ato homologues in *Candida* species. (A) A multiple-alignment with the 65 ScAto1 homologues found in *Candida* species was performed using MAFFT v.7 [74] and checked manually for incongruences. The alignments were then used in the phylogenetic reconstruction. A maximum-likelihood approach, suitable for deep evolution, was conducted in MEGA7 [75] using the JTT model of amino acid evolution, four gamma-distributed rates, and a site coverage cutoff of 90%. 250 replications were performed for the bootstrap analysis. Names of the homologues are colored according to the species where they were detected. Output trees were edited in Figtree v.1.4.4.

(http://tree.bio.ed.ac.uk/software). **(B)** Conservation logo of the alignment that displayed residues in 90% of the sequences, using WebLogo (https://weblogo.berkeley.edu). Transmembrane segments (TMSs) predicted with TMHMM 2.0 (htpp://www.cbs.dtu.dk/services/TMHMM/) are highlighted as brown bars in the logo and arrows indicate amino acids belonging to previously identified functional domains [19] .

2.4 Functional specialization of Jen and Ato transporters in *Candida*

The idea that carboxylates are essential nutrients for the survival of *Candida* species in certain host niches is supported by many studies that have demonstrated that *Candida* cells upregulate several metabolic pathways involved in the utilization of these carbon sources when infecting tissues and organs [12, 51–53]. For instance, several studies in *Candida* have consistently demonstrated that both Jen and Ato transporters are strongly upregulated following phagocytosis, reinforcing the idea that carboxylate assimilation is an integral part of the response to phagocytosis [11, 13-16]. Considering that inside the phagolysosome glucose levels are low, lactate and acetate, along with amino acids, may be the main sources of acetyl-coenzyme A (acetyl-coA) that feed the glyoxylate cycle, allowing *Candida* survival in this environment [11,16, 53]. Indeed, abrogation of both carboxylic acid and amino acid uptake confers additive effects in virulence in macrophage and mouse models [54]. Consistent with this observation, the acetyl-coA synthetases, which convert acetate into acetyl-coA, are upregulated after *C. albicans* phagocytosis by macrophages and neutrophils [12]. *C. glabrata* mutants in Ato1 and Fps1 were reported to be more efficiently internalized and phagocytized by macrophages that wild-type cells in RPMI medium. But the presence of acetic acid rendered the mutant cells more resistant to macrophage killing, showing that this process is dependent on the carbon source [55]. The uptake of carboxylic acids, mediated either by Jen or Ato transporters, results in the alkalization of the extracellular environment in specific growth conditions. The neutralization of the acidic phagolysosome allows *C. albicans* to readily escape from the immune cells by differentiating into filamentous hyphae and inducing macrophage pyroptosis, a programmed cell death pathway [56–60]. Mutations in the *C. albicans ATO1* and *ATO5* impair neutralization, hyphal differentiation, and macrophage killing [48]. This is significant, as *Candida* cells after macrophage killing can continue to successfully thrive in the human host.

Noteworthy, the AceTr family is greatly expanded in *Candida,* especially in *C. albicans*, when compared to other fungi (Figure 2.3A). Gene family expansions in these yeasts occur primarily by gene duplication

and under stressful environmental conditions and are often associated with pathogenicity [61]. Although most of the duplicated genes are often deleted, some may be retained if either gene dosage or functional specialization are advantageous [61-63]. Undoubtedly, an increased number of Ato transporters is expected to endow cells with the advantage of being better adapted for human colonization and infection, which correlates well with pathogenic profile of *C. albicans*. But why would 8 acetate transporter genes be retained in *C. albicans* ? An analogy could be made with the twenty hexose transporter genes of *S. cerevisiae*, where different transporters are tuned to different hexose levels presumably under intense competition [64]. We would have to assume that the Ato proteins perform important functions for growth and survival. Perhaps some of the Atos have evolved to be sensors like glucose sensors Snf3 and Rgt2 in *S. cerevisiae* [64]. Although both Jen and Ato transporters have been mainly associated with nutrient assimilation, they may also play important roles in cellular homeostasis by mediating the export of lactate [7].

Interestingly, lactate appears to be a signal of the host environment, and its presence, even when glucose is abundant, induces multiple physiological changes relevant to pathogenesis, including resistance to certain stresses and antifungal drugs [65, 66]. Some of these changes are mediated via alterations in the cell wall, which then also impacts recognition by phagocytes [67, 68]. This is also true in *C. glabrata* [69]. Lactate and amino acids induce distinct patterns of stress tolerance in *C. albicans*, suggesting that this species has evolved to identify specific nutrients as signals to direct responses to specific host niches [54]. These transporters also have been reported to modulated biofilm formation and resistance tio antifungal drugs in both *C. albicans* and *C. glabrata* [55, 70].

These results taken together suggest that carboxylic acid transporters are important mediators of host-pathogen interactions by allowing rapid adaptation to different environmental conditions and modulating the virulent properties of *Candida* species. Consistent with this idea, dominant mutations have been isolated in the Ato homologues in *S. cerevisiae* and *Y. lipolytica* that render cells hypersensitive to acetic acid [71]. This sensitivity is seen at acidic pH where acetic acid would freely diffuse into the cell and likely would acidify the cytosol without compensatory responses. This suggests the possibility that the Ato proteins are bidirectional transporters and, in some cases, can pump acetate out of the cell [71]. In fact, the only acetate exporter reported in *Candida* species is the *C. glabrata* drug:H^+ antiporter (DHA) CgDtr1, which is responsible for the export of acetate and involved in weak acid stress resistance in RPMI medium at pH 4.5 [72]. In this study, the tested pH was below the pKa of the acid, conditions where the acid

enters the cell mostly by simple diffusion and can impose significant stress in the form of cytosolic acidification. In *Candida* species, no pleiotropic drug resistance (PDR) transporters belonging to the ATP-binding cassette (ABC) superfamily have been so far associated with the export of carboxylates in acid stress conditions. Since weak acid stresses are common in many host niches, the proliferation of the Ato family in pathogenic species may be a response to these stresses.

2.5 CONCLUSIONS

The ability to transport carboxylates inside the cell represents an advantage for *Candida* when these nutrients are the main exogenous carbon sources available. Jen and Ato family members, in certain conditions, seem to play critical roles in *Candida* pathogenesis, as they allow cells to sustain metabolism and survival when thriving in the human host. However, many details are missing regarding the energetics, specificity, and regulation of these transporters. Further research will be needed to determine individual transport properties, potential redundancies, and functional roles of carboxylate transporters in *Candida* virulence and pathogenesis.

2.6 SUPPLEMENTARY MATERIAL

Table S2.1. GenBank accession numbers of ScJen1 homologues present in eleven *Candida* species with the annotated/former designations and the following suggested designation based on ScJen1 gene homology.

ScJen1 homologues by specie	GenBank Ac. no.	Former designation | Alias	Suggested annotation
C. albicans [2]	XP_716108.1	Jen1p [*Candida albicans* SC5314]	CaJen1
	XP_717110.1	Jen2p [*Candida albicans* SC5314]	CaJen2
C. orthopsilosis [4]	XP_003868359.1	hypothetical protein CORT_0C00780 [*Candida orthopsilosis* Co 90-125]	CoJen1
	XP_003868357.1	Jen1 protein [*Candida orthopsilosis* Co 90-125]	CoJen2
	XP_003868365.1	tRNA-Arg [*Candida orthopsilosis* Co 90-125]	CoJen3
	XP_003869929.1	Jen2 protein [*Candida orthopsilosis* Co 90-125]	CoJen4
C. auris [2]	PIS50386.1	hypothetical protein B9J08_004204 [[*Candida*] *auris*]	CauJen1
	PIS50738.1	uncharacterized protein CJI97_004268 [[*Candida*] *auris*]	CauJen2
C. krusei [2]	OUT23441.1	hypothetical protein CAS74_001759 [*Pichia kudriavzevii*]	CkJen1
	OUT23260.1	hypothetical protein CAS74_001578 [*Pichia kudriavzevii*]	CkJen2
C. lusitaniae [2]	XP_002614689.1	hypothetical protein CLUG_05468 [*Clavispora lusitaniae* ATCC 42720]	ClJen1
	XP_002617815.1	hypothetical protein CLUG_01274 [*Clavispora lusitaniae* ATCC 42720]	ClJen2
C. parapsilosis [12]	CCE42292.1	hypothetical protein CPAR2_808410 [*Candida parapsilosis*]	CpJen1
	CCE42290.1	hypothetical protein CPAR2_808390 [*Candida parapsilosis*]	CpJen2
	CCE44929.1	hypothetical protein CPAR2_407310 [*Candida parapsilosis*]	CpJen3
	CCE44923.1	hypothetical protein CPAR2_407250 [*Candida parapsilosis*]	CpJen4
	CCE44403.1	hypothetical protein CPAR2_402040 [*Candida parapsilosis*]	CpJen5
	CCE44586.1	hypothetical protein CPAR2_403890 [*Candida parapsilosis*]	CpJen6
	CCE42284.1	hypothetical protein CPAR2_808330 [*Candida parapsilosis*]	CpJen7
	CCE44209.1	hypothetical protein CPAR2_400100 [*Candida parapsilosis*]	CpJen8
	CCE44928.1	hypothetical protein CPAR2_407300 [*Candida parapsilosis*]	CpJen9
	CCE44927.1	hypothetical protein CPAR2_407290 [*Candida parapsilosis*]	CpJen10
	CCE44404.1	hypothetical protein CPAR2_402050 [*Candida parapsilosis*]	CpJen11
	CCE40688.1	hypothetical protein CPAR2_107230 [*Candida parapsilosis*]	CpJen12
C. dubliniensis [2]	XP_002419556.1	carboxylic acid transporter, putative [*Candida dubliniensis* CD36]	CdJen1

	XP_002420040.1	carboxylic acid transporter protein, putative [*Candida dubliniensis* CD36]	CdJen2
C. tropicalis [2]	XP_002551411.1	hypothetical protein CTRG_05709 [*Candida tropicalis* MYA-3404]	CtJen1
	XP_002545520.1	hypothetical protein CTRG_00301 [*Candida tropicalis* MYA-3404]	CtJen2
C. kefyr [2]	XP_022677158.1	uncharacterized protein KLMA_60073 [*Kluyveromyces marxianus* DMKU3-1042]	CkeJen1
	XP_022674588.1	putative sialic acid transporter [*Kluyveromyces marxianus* DMKU3-1042]	CkeJen2
C. guilliermondii [3]	XP_001484059.1	hypothetical protein PGUG_03440 [*Meyerozyma guilliermondii* ATCC 6260]	CguJen1
	XP_001484060.1	hypothetical protein PGUG_03441 [*Meyerozyma guilliermondii* ATCC 6260]	CguJen2
	XP_001486752.1	hypothetical protein PGUG_00129 [*Meyerozyma guilliermondii* ATCC 6260]	CguJen3
C. haemulonis [2]	XP_025341865.1	hypothetical protein CXQ85_004438 [*Candida haemulonis*]	ChJen1
	XP_025341422.1	*hypothetical protein CXQ85_002273* [*Candida haemulonis*]	ChJen2

Table S2.2. GenBank accession numbers of *Sc*Ady2 homologues present in twelve *Candida* species with the annotated/former designations and the following suggested designation based on ScAdy2 gene homology.

ScAto1 homologues by specie	GenBank Ac. no.	Former designation	Suggested annotation
C. glabrata [3]	XP_449497.1	uncharacterized protein CAGL0M03465g [*Candida glabrata*]	CgAto1
	XP_449115.1	uncharacterized protein CAGL0L07766g [*Candida glabrata*]	CgAto2
	XP_444907.1	uncharacterized protein CAGL0A03212g [*Candida glabrata*]	CgAto3
C. albicans [10]	XP_710295.1	putative ammonium permease [*Candida albicans* SC5314]	CaAto1
	XP_710650.1	Ato1p [*Candida albicans* SC5314]	CaAto2
	XP_718515.2	Ato2p [*Candida albicans* SC5314]	CaAto3
	XP_714701.1	Ato6p [*Candida albicans* SC5314]	CaAto4
	XP_714703.1	Ato5p [*Candida albicans* SC5314]	CaAto5
	XP_716748.1	Frp6p [*Candida albicans* SC5314]	CaAto6
	XP_716747.2	Frp5p [*Candida albicans* SC5314]	CaAto7
	XP_019330752.1	Ato7p [*Candida albicans* SC5314]	CaAto8
	XP_717953.1	Ato10p [*Candida albicans* SC5314]	CaAto9
	XP_717951.1	Ato9p [*Candida albicans* SC5314]	CaAto10
C. auris [3]	XP_028889701.1	uncharacterized protein CJI97_002436 [*Candida auris*]	CauAto1
	XP_028890140.1	uncharacterized protein CJI97_002886 [*Candida auris*]	CauAto2
	XP_028890274.1	uncharacterized protein CJI97_003024 [*Candida auris*]	CauAto3
C. krusei [5]	XP_029319197.1	uncharacterized protein C5L36_0A03220 [*Pichia kudriavzevii*]	CkAto1
	XP_029320118.1	uncharacterized protein C5L36_0A12180 [*Pichia kudriavzevii*]	CkAto2
	XP_029320117.1	uncharacterized protein C5L36_0A12170 [*Pichia kudriavzevii*]	CkAto3
	XP_029320119.1	uncharacterized protein C5L36_0A12190 [*Pichia kudriavzevii*]	CkAto4
	XP_029319710.1	uncharacterized protein C5L36_0A08310 [*Pichia kudriavzevii*]	CkAto5
C. guilliermondii [3]	EDK38382.1	hypothetical protein PGUG_02480 [*Meyerozyma guilliermondii* ATCC 6260]	CguAto1
	EDK40033.2	hypothetical protein PGUG_04131 [*Meyerozyma guilliermondii* ATCC 6260]	CguAto2
	EDK36918.2	hypothetical protein PGUG_01016 [*Meyerozyma guilliermondii* ATCC 6260]	CguAto3
C. lusitaniae [4]	XP_002619494.1	hypothetical protein CLUG_00653 [*Clavispora lusitaniae* ATCC 42720]	ClAto1

	XP_002618592.1	hypothetical protein CLUG_02051 [*Clavispora lusitaniae* ATCC 42720]	ClAto2
	XP_002618879.1	hypothetical protein CLUG_00038 [*Clavispora lusitaniae* ATCC 42720]	ClAto3
	XP_002617751.1	hypothetical protein CLUG_01210 [*Clavispora lusitaniae* ATCC 42720]	ClAto4
C. parapsilosis [7]	CCE40409.1	hypothetical protein CPAR2_104450 [*Candida parapsilosis*]	CpAto1
	CCE44056.1	hypothetical protein CPAR2_502810 [*Candida parapsilosis*]	CpAto2
	CCE44055.1	hypothetical protein CPAR2_502800 [*Candida parapsilosis*]	CpAto3
	CCE44009.1	hypothetical protein CPAR2_502340 [*Candida parapsilosis*]	CpAto4
	CCE45313.1	hypothetical protein CPAR2_703260 [*Candida parapsilosis*]	CpAto5
	CCE39768.1	hypothetical protein CPAR2_601880 [*Candida parapsilosis*]	CpAto6
	CCE44054.1	hypothetical protein CPAR2_502790 [*Candida parapsilosis*]	CpAto7
C. dubliniensis [8]	XP_002418576.1	acetate transporter, putative [*Candida dubliniensis* CD36]	CdAto1
	XP_002419032.1	acetate transporter, putative [*Candida dubliniensis* CD36]	CdAto2
	XP_002419033.1	ammonia export protein, putative [*Candida dubliniensis* CD36]	CdAto3
	XP_002419463.1	acetate transporter, putative [*Candida dubliniensis* CD36]	CdAto4
	XP_002419461.1	acetate transporter, putative [*Candida dubliniensis* CD36]	CdAto5
	XP_002421693.1	acetate transporter, putative [*Candida dubliniensis* CD36]	CdAto6
	XP_002420929.1	ammonia transport protein, putative [*Candida dubliniensis* CD36]	CdAto7
	XP_002418190.1	acetate transporter, putative [*Candida dubliniensis* CD36]	CdAto8
C. tropicalis [8]	XP_002547488.1	protein FUN34 [*Candida tropicalis* MYA-3404]	CtAto1
	XP_002549734.1	protein FUN34 [*Candida tropicalis* MYA-3404]	CtAto2
	XP_002546727.1	hypothetical protein CTRG_06205 [*Candida tropicalis* MYA-3404]	CtAto3
	XP_002548540.1	conserved hypothetical protein [*Candida tropicalis* MYA-3404]	CtAto4
	XP_002546210.1	conserved hypothetical protein [*Candida tropicalis* MYA-3404]	CtAto5
	XP_002548538.1	conserved hypothetical protein [*Candida tropicalis* MYA-3404]	CtAto6
	XP_002547090.1	conserved hypothetical protein [*Candida tropicalis* MYA-3404]	CtAto7
	XP_002546489.1	conserved hypothetical protein [*Candida tropicalis* MYA-3404]	CtAto8
C. kefyr [5]	XP_022674350.1	hypothetical protein KLMA_20009 [*Kluyveromyces marxianus* DMKU3-1042]	CkeAto1
	XP_022674438.1	hypothetical protein KLMA_20099 [*Kluyveromyces marxianus* DMKU3-1042]	CkeAto2

	XP_022678050.1	hypothetical protein KLMA_70455 [*Kluyveromyces marxianus* DMKU3-1042]	CkeAto3
	XP_022674905.1	ammonia transport outward protein 3 [*Kluyveromyces marxianus* DMKU3-1042]	CkeAto4
	XP_022674904.1	hypothetical protein KLMA_20586 [*Kluyveromyces marxianus* DMKU3-1042]	CkeAto5
C. haemulonis [3]	XP_025340936.1	hypothetical protein CXQ85_001773 [[*Candida*] *haemulonis*]	ChAto1
	XP_025341341.1	hypothetical protein CXQ85_002189 [[*Candida*] *haemulonis*]	ChAto2
	XP_025341450.1	hypothetical protein CXQ85_002302 [[*Candida*] *haemulonis*]	ChAto3
C. orthopsiliosis [7]	XP_003867713.1	Frp3 ammonium transporter [*Candida orthopsilosis* Co 90-125]	CoAto1
	XP_003867405.1	hypothetical protein CORT_0B02520 [*Candida orthopsilosis* Co 90-125]	CoAto2
	XP_003867454.1	Ato2 fungal-specific transmembrane protein [*Candida orthopsilosis* Co 90-125]	CoAto3
	XP_003871155.1	Yhr032w protein [*Candida orthopsilosis* Co 90-125]	CoAto4
	XP_003867455.1	Ato1 fungal-specific transmembrane protein [*Candida orthopsilosis* Co 90-125]	CoAto5
	XP_003870637.1	Frp6 protein [*Candida orthopsilosis* Co 90-125]	CoAto6
	XP_003871144.1	hypothetical protein CORT_0G03430 [*Candida orthopsilosis* Co 90-125]	CoAto7

2.7 REFERENCES

1. Casal M, Paiva S, Queirós O, Soares-Silva I. 2008. Transport of carboxylic acids in yeasts. FEMS Microbiol Rev 32:974–994. doi:10.1111/j.1574-6976.2008.00128.x.
2. Casal M, Queirós O, Talaia G, Ribas D, Paiva S. 2016. Carboxylic acids plasma membrane transporters in *Saccharomyces cerevisiae*. Adv Exp Med Biol 892:229–251. doi:10.1007/978-3-319-25304-6_9.
3. Conde A, Diallinas G, Chaumont F, Chaves M, Gerós H. 2010. Transporters, channels, or simple diffusion? Dogmas, atypical roles and complexity in transport systems. Int J Biochem Cell Biol 42:857–868. doi:10.1016/j.biocel.2009.12.012.
4. Mollapour M, Piper PW. 2007. Hog1 mitogen-activated protein kinase phosphorylation targets the yeast Fps1 aquaglyceroporin for endocytosis, thereby rendering cells resistant to acetic acid. Mol Cell Biol 27:6446–6456. doi:10.1128/MCB.02205-06.
5. Lindahl L, Genheden S, Faria-Oliveira F, Allard S, Eriksson LA, Olsson L, Bettiga M. 2017. Alcohols enhance the rate of acetic acid diffusion in *S. cerevisiae*: biophysical mechanisms and implications for acetic acid tolerance. Microb Cell 5:42–55. doi:10.15698/mic2018.01.609.
6. Branduardi P, Sauer M, De Gioia L, Zampella G, Valli M, Mattanovich D, Porro D. 2006. Lactate production yield from engineered yeasts is dependent from the host background, the lactate dehydrogenase source and the lactate export. Microb Cell Fact 5:4. doi:10.1186/1475-2859-5-
7. Pacheco A, Talaia G, Sá-Pessoa J, Bessa D, Gonçalves MJ, Moreira R, Paiva S, Casal M, Queirós O. 2012. Lactic acid production in *Saccharomyces cerevisiae* is modulated by expression of the monocarboxylate transporters Jen1 and Ady2. FEMS Yeast Res 12:375–381. doi:10.1111/j.1567-1364.2012.00790.x.
8. Morrison DJ, Preston T. 2016. Formation of short chain fatty acids by the gut microbiota and their impact on human metabolism. Gut Microbes 7:189–200. doi:10.1080/19490976.2015.1134082.
9. Rowland I, Gibson G, Heinken A, Scott K, Swann J, Thiele I, Tuohy K. 2018. Gut microbiota functions: metabolism of nutrients and other food components. Eur J Nutr 57:1–24. doi:10.1007/s00394-017-1445-8.
10. O'Hanlon DE, Moench TR, Cone RA. 2013. Vaginal pH and microbicidal lactic acid when lactobacilli dominate the microbiota. PLoS One 8:e80074. doi:10.1371/journal.pone.0080074.

11. Lorenz MC, Bender JA, Fink GR. 2004. Transcriptional response of *Candida albicans* upon internalization by macrophages. Eukaryot Cell 3:1076–1087. doi:10.1128/EC.3.5.1076-1087.2004.
12. Fradin C, De Groot P, MacCallum D, Schaller M, Klis F, Odds FC, Hube B. 2005. Granulocytes govern the transcriptional response, morphology and proliferation of *Candida albicans* in human blood. Mol Microbiol 56:397–415. doi:10.1111/j.1365-2958.2005.04557.x.
13. Vieira N, Casal M, Johansson B, MacCallum DM, Brown AJP, Paiva S. 2010. Functional specialization and differential regulation of short-chain carboxylic acid transporters in the pathogen *Candida albicans*. Mol Microbiol 75:1337–1354. doi:10.1111/j.1365-2958.2009.07003.x.
14. Fukuda Y, Tsai HF, Myers TG, Bennett JE. 2013. Transcriptional profiling of *Candida glabrata* during phagocytosis by neutrophils and in the infected mouse spleen. Infect Immun 81:1325–1333. doi:10.1128/IAI.00851-12.
15. Kaur R, Ma B, Cormack B. 2007. A family of glycosylphosphatidylinositol-linked aspartyl proteases is required for virulence of *Candida glabrata*. Proc Natl Acad Sci U S A 104:7628–7633. doi:10.1073/pnas.0611195104.
16. Piekarska K, Mol E, Van Den Berg M, Hardy G, Van Den Burg J, Van Roermund C, MacCallum D, Odds F, Distel B. 2006. Peroxisomal fatty acid β-oxidation is not essential for virulence of *Candida albicans*. Eukaryot Cell 5:1847–1856. doi:10.1128/EC.00093-06.
17. Gabaldón T, Naranjo-Ortíz MA, Marcet-Houben M. 2016. Evolutionary genomics of yeast pathogens in the Saccharomycotina. FEMS Yeast Res 16:fow064. doi:10.1093/femsyr/fow064.
18. Ribas D, Soares-Silva I, Vieira D, Sousa-Silva M, Sá-Pessoa J, Azevedo-Silva J, Viegas SC, Arraiano CM, Diallinas G, Paiva S, Soares P, Casal M. 2019. The acetate uptake transporter family motif "NPAPLGL(M/S)" is essential for substrate uptake. Fungal Genet Biol 122:1–10. doi:10.1016/j.fgb.2018.10.001.
19. Qiu B, Xia B, Zhou Q, Lu Y, He M, Hasegawa K, Ma Z, Zhang F, Gu L, Mao Q, Wang F, Zhao S, Gao Z, Liao J. 2018. Succinate-acetate permease from *Citrobacter koseri* is an anion channel that unidirectionally translocates acetate. Cell Res 28:644–654. doi:10.1038/s41422-018-0032-8.
20. Wu M, Sun L, Zhou Q, Peng Y, Liu Z, Zhao S. 2019. Molecular mechanism of acetate transport through the acetate channel SatP. J Chem Inf Model 59:2374–2382. doi:10.1021/acs.jcim.8b00975.

21. Casal M, Paiva S, Andrade RP, Gancedo C, Leão C. 1999. The lactate-proton symport of *Saccharomyces cerevisiae* is encoded by JEN1. J Bacteriol 181:2620–2623. doi:10.1128/JB.181.8.2620-2623.1999.

22. Saier MH, Reddy VS, Tsu BV, Ahmed MS, Li C, Moreno-Hagelsieb G. 2016. The transporter classification database (TCDB): recent advances. Nucleic Acids Res 44:D372–D379. doi:10.1093/nar/gkv1103.

23. Akita O, Nishimori C, Shimamoto T, Fujii T, Iefuji H. 2000. Transport of pyruvate in *Saccharomyces cerevisiae* and cloning of the gene encoded pyruvate permease. Biosci Biotechnol Biochem 64:980–984. doi:10.1271/bbb.64.980.

24. Soares-Silva I, Schuller D, Andrade RP, Baltazar F, Cássio F, Casal M. 2003. Functional expression of the lactate permease Jen1p of *Saccharomyces cerevisiae* in *Pichia pastoris*. Biochem J 376:781–787. doi:10.1042/BJ20031180.

25. McDermott JR, Rosen BP, Liu Z. 2010. Jen1p: a high affinity selenite transporter in yeast. Mol Biol Cell 21:3934–3941. doi:10.1091/mbc.E10-06-0513.

26. Soares-Silva I, Paiva S, Kötter P, Entian K-D, Casal M. 2004. The disruption of JEN1 from *Candida albicans* impairs the transport of lactate. Mol Membr Biol 21:403–411. doi:10.1080/09687860400011373.

27. Dulermo R, Gamboa-Meléndez H, Michely S, Thevenieau F, Neuvéglise C, Nicaud JM. 2015. The evolution of Jen3 proteins and their role in dicarboxylic acid transport in *Yarrowia*. Microbiologyopen 4:100–120. doi:10.1002/mbo3.225.

28. Ueno K, Matsumoto Y, Uno J, Sasamoto K, Sekimizu K, Kinjo Y, Chibana H. 2011. Intestinal resident yeast *Candida glabrata* requires Cyb2p-mediated lactate assimilation to adapt in mouse intestine. PLoS One 6:e24759. doi:10.1371/journal.pone.0024759.

29. Pryszcz LP, Németh T, Gácser A, Gabaldón T. 2013. Unexpected genomic variability in clinical and environmental strains of the pathogenic yeast *Candida parapsilosis*. Genome Biol Evol 5:2382–2392. doi:10.1093/gbe/evt185.

30. Lodi T, Diffels J, Goffeau A, Baret PV. 2007. Evolution of the carboxylate Jen transporters in fungi. FEMS Yeast Res 7:646–656. doi:10.1111/j.1567-1364.2007.00245.x.

31. Soares-Silva I, Ribas D, Foskolou IP, Barata B, Bessa D, Paiva S, Queirós O, Casal M. 2015. The Debaryomyces hansenii carboxylate transporters Jen1 homologues are functional in *Saccharomyces cerevisiae*. FEMS Yeast Res 15:fov094. doi:10.1093/femsyr/fov094.

32. Soares-Silva I, Sá-Pessoa J, Myrianthopoulos V, Mikros E, Casal M, Diallinas G. 2011. A substrate translocation trajectory in a cytoplasm-facing topological model of the monocarboxylate/H+ symporter Jen1p. Mol Microbiol 81:805–817. doi:10.1111/j.1365-2958.2011.07729.x.

33. Soares-Silva I, Paiva S, Diallinas G, Casal M. 2007. The conserved sequence NXX[S/T]HX[S/T]QDXXXT of the lactate/pyruvate:H+ symporter subfamily defines the function of the substrate translocation pathway. Mol Membr Biol 24:464–474. doi:10.1080/09687680701342669.

34. Tzschoppe K, Augstein A, Bauer R, Kohlwein SD, Barth G. 1999. Trans-dominant mutations in the GPR1 gene cause high sensitivity to acetic acid and ethanol in the yeast *Yarrowia lipolytica*. Yeast 15:1645–1656. doi:10.1002/(SICI)1097-0061(199911)15:15<1645::AID-YEA491>3.0.CO;2-G.

35. Augstein A, Barth K, Gentsch M, Kohlwein SD, Barth G. 2003. Characterization, localization and functional analysis of Gpr1p, a protein affecting sensitivity to acetic acid in the yeast *Yarrowia lipolytica*. Microbiology 149:589–600. doi:10.1099/mic.0.25917-0.

36. Paiva S, Devaux F, Barbosa S, Jacq C, Casal M. 2004. Ady2p is essential for the acetate permease activity in the yeast Saccharomyces cerevisiae. Yeast 21:201–210. doi:10.1002/yea.1056.

37. Robellet X, Flipphi M, Pégot S, MacCabe AP, Vélot C. 2008. AcpA, a member of the GPR1/FUN34/YaaH membrane protein family, is essential for acetate permease activity in the hyphal fungus Aspergillus nidulans. Biochem J 412:485–493. doi:10.1042/BJ20080124.

38. Rohlin L, Gunsalus RP. 2010. Carbon-dependent control of electron transfer and central carbon pathway genes for methane biosynthesis in the Archaean, *Methanosarcina acetivorans* strain C2A. BMC Microbiol 10:62. doi:10.1186/1471-2180-10-62.

39. Sá-Pessoa J, Paiva S, Ribas D, Silva IJ, Viegas SC, Arraiano CM, Casal M. 2013. SATP (YaaH), a succinate-acetate transporter protein in *Escherichia coli*. Biochem J 454:585–595. doi:10.1042/BJ20130412.

40. Sá-Pessoa J, Amillis S, Casal M, Diallinas G. 2015. Expression and specificity profile of the major acetate transporter AcpA in *Aspergillus nidulans*. Fungal Genet Biol 76:93–103. doi:10.1016/j.fgb.2015.02.010.

41. Gasch AP, Spellman PT, Kao CM, Carmel-Harel O, Eisen MB, Storz G, Botstein D, Brown PO. 2000. Genomic expression programs in the response of yeast cells to environmental changes. Mol Biol Cell 11:4241–4257. doi:10.1091/mbc.11.12.4241.

42. Boer VM, De Winde JH, Pronk JT, Piper M. 2003. The genome-wide transcriptional responses of *Saccharomyces cerevisiae* grown on glucose in aerobic chemostat cultures limited for carbon, nitrogen, phosphorus, or sulfur. J Biol Chem 278:3265–3274. doi:10.1074/jbc.M209759200.
43. Taxis C, Keller P, Kavagiou Z, Jensen LJ, Colombelli J, Bork P, Stelzer EHK, Knop M. 2005. Spore number control and breeding in *Saccharomyces cerevisiae*: a key role for a self-organizing system. J Cell Biol 171:627–640. doi:10.1083/jcb.200507168.
44. Rabitsch KP, Tóth A, Gálová M, Schleiffer A, Schaffner G, Aigner E, Rupp C, Penkner AM, Moreno-Borchart AC, Primig M, Esposito RE, Klein F, Knop M, Nasmyth K. 2001. A screen for genes required for meiosis and spore formation based on whole-genome expression. Curr Biol 11:1001–1009. doi:10.1016/s0960-9822(01)00274-3.
45. Jungbluth M, Mösch HU, Taxis C. 2012. Acetate regulation of spore formation is under the control of the Ras/cyclic AMP/protein kinase A pathway and carbon dioxide in *Saccharomyces cerevisiae*. Eukaryot Cell 11:1021–1032. doi:10.1128/EC.05240-11.
46. Palkova Z, Janderova B, Gabriel J, Zikanova B, Pospisek M, Forstova J. 1997. Ammonia mediates communication between yeast colonies. Nature 390:532–536. doi:10.1038/37398.
47. Palková Z, Devaux F, Ř̆ičcová M, Mináriková L, Le Crom S, Jacq C. 2002. Ammonia pulses and metabolic oscillations guide yeast colony development. Mol Biol Cell 13:3901–3914. doi:10.1091/mbc.E01-12-0149.
48. Danhof HA, Lorenz MC. 2015. The *Candida albicans* ATO gene family promotes neutralization of the macrophage phagolysosome. Infect Immun 83:4416–4426. doi:10.1128/IAI.00984-15.
49. Sun P, Li J, Zhang X, Guan Z, Xiao Q, Zhao C, Song M, Zhou Y, Mou L, Ke M, Guo L, Geng J, Deng D. 2018. Crystal structure of the bacterial acetate transporter SatP reveals that it forms a hexameric channel. J Biol Chem 293:19492–19500. doi:10.1074/jbc.RA118.003876.
50. Casal M, Cardoso H, Leão C. 1996. Mechanisms regulating the transport of acetic acid in *Saccharomyces cerevisiae*. Microbiology 142:1385–1390. doi:10.1099/13500872-142-6-1385.
51. Barelle CJ, Priest CL, MacCallum DM, Gow NAR, Odds FC, Brown A. 2006. Niche-specific regulation of central metabolic pathways in a fungal pathogen. Cell Microbiol 8:961–971. doi:10.1111/j.1462-5822.2005.00676.x.
52. Fradin C, Kretschmar M, Nichterlein T, Gaillardin C, d'Enfert C, Hube B. 2003. Stage-specific gene expression of *Candida albicans* in human blood. Mol Microbiol 47:1523–1543. doi:10.1046/j.1365-2958.2003.03396.x.

53. Lorenz MC, Fink GR. 2001. The glyoxylate cycle is required for fungal virulence. Nature 412:83–86. doi:10.1038/35083594.

54. Williams RB, Lorenz MC. 2020. Multiple alternative carbon pathways combine to promote *Candida albicans* stress resistance, immune interactions, and virulence. mBio 11:e03070-19. doi:10.1128/mBio.03070-19.

55. Mota S, Alves R, Carneiro C, Silva S, Brown AJ, Istel F, Kuchler K, Sampaio P, Casal M, Henriques M, Paiva S. 2015. *Candida glabrata* susceptibility to antifungals and phagocytosis is modulated by acetate. Front Microbiol 6:919. doi:10.3389/fmicb.2015.00919.

56. Vylkova S, Lorenz MC. 2014. Modulation of phagosomal pH by *Candida albicans* promotes hyphal morphogenesis and requires Stp2p, a regulator of amino acid transport. PLoS Pathog 10:e1003995. doi:10.1371/journal.ppat.1003995.

57. Vylkova S, Carman AJ, Danhof HA, Collette JR, Zhou H, Lorenz MC. 2011. The fungal pathogen *Candida albicans* autoinduces hyphal morphogenesis by raising extracellular pH. mBio 2:e00055-11. doi:10.1128/mBio.00055-11.

58. Wellington M, Koselny K, Sutterwala FS, Krysan DJ. 2014. *Candida albicans* triggers NLRP3-mediated pyroptosis in macrophages. Eukaryot Cell 13:329–340. doi:10.1128/EC.00336-13.

59. Uwamahoro N, Verma-Gaur J, Shen HH, Qu Y, Lewis R, Lu J, Bambery K, Masters SL, Vince JE, Naderer T, Traven A. 2014. The pathogen *Candida albicans* hijacks pyroptosis for escape from macrophages. mBio 5:e00003-14. doi:10.1128/mBio.00003-14.

60. O'Meara TR, Veri AO, Ketela T, Jiang B, Roemer T, Cowen LE. 2015. Global analysis of fungal morphology exposes mechanisms of host cell escape. Nat Commun 6:6741. doi:10.1038/ncomms7741.

61. Moran GP, Coleman DC, Sullivan DJ. 2011. Comparative genomics and the evolution of pathogenicity in human pathogenic fungi. Eukaryot Cell 10:34–42. doi:10.1128/EC.00242-10.

62. Langkjaer RB, Cliften PF, Johnston M, Piskur J. 2003. Yeast genome duplication was followed by asynchronous differentiation of duplicated genes. Nature 421:848–852. doi:10.1038/nature01419.

63. Naseeb S, Ames RM, Delneri D, Lovell SC. 2017. Rapid functional and evolutionary changes follow gene duplication in yeast. Proc R Soc B 284:20171393. doi:10.1098/rspb.2017.1393.

64. Leandro MJ, Fonseca C, Gonçalves P. 2009. Hexose and pentose transport in ascomycetous yeasts: an overview. FEMS Yeast Res 9:511–525. doi:10.1111/j.1567-1364.2009.00509.x.

65. Ene IV, Heilmann CJ, Sorgo AG, Walker LA, De Koster CG, Munro CA, Klis FM, Brown A. 2012. Carbon source-induced reprogramming of the cell wall proteome and secretome modulates the adherence and drug resistance of the fungal pathogen *Candida albicans*. Proteomics 12:3164–3179. doi:10.1002/pmic.201200228.

66. Ene IV, Adya AK, Wehmeier S, Brand AC, Maccallum DM, Gow NAR, Brown A. 2012. Host carbon sources modulate cell wall architecture, drug resistance and virulence in a fungal pathogen. Cell Microbiol 14:1319–1335. doi:10.1111/j.1462-5822.2012.01813.x.

67. Ene IV, Cheng SC, Netea MG, Brown A. 2013. Growth of *Candida albicans* cells on the physiologically relevant carbon source lactate affects their recognition and phagocytosis by immune cells. Infect Immun 81:238–248. doi:10.1128/IAI.01092-12.

68. Ballou ER, Avelar GM, Childers DS, Mackie J, Bain JM, Wagener J, Kastora SL, Panea MD, Hardison SE, Walker LA, Erwig LP, Munro CA, Gow NAR, Brown GD, MacCallum DM, Brown A. 2016. Lactate signalling regulates fungal β-glucan masking and immune evasion. Nat Microbiol 2:16238. doi:10.1038/nmicrobiol.2016.238.

69. Chew SY, Ho KL, Cheah YK, Sandai D, Brown AJP, Than L. 2019. Physiologically relevant alternative carbon sources modulate biofilm formation, cell wall architecture, and the stress and antifungal resistance of *Candida glabrata*. Int J Mol Sci 20:E3172. doi:10.3390/ijms20133172.

70. Alves R, Mota S, Silva S, Rodrigues CF, Alistair JP, Henriques M, Casal M, Paiva S. 2017. The carboxylic acid transporters Jen1 and Jen2 affect the architecture and fluconazole susceptibility of *Candida albicans* biofilm in the presence of lactate. Biofouling 33:943–912. doi:10.1080/08927014.2017.1392514.

71. Gentsch M, Kuschel M, Schlegel S, Barth G. 2007. Mutations at different sites in members of the Gpr1/Fun34/YaaH protein family cause hypersensitivity to acetic acid in *Saccharomyces cerevisiae* as well as in *Yarrowia lipolytica*. FEMS Yeast Res 7:380–390. doi:10.1111/j.1567-1364.2006.00191.x.

72. Romão D, Cavalheiro M, Mil-Homens D, Santos R, Pais P, Costa C, Takahashi-Nakaguchi A, Fialho AM, Chibana H, Teixeira MC. 2017. A new determinant of *Candida glabrata* virulence: the acetate exporter CgDtr1. Front Cell Infect Microbiol 7:473. doi:10.3389/fcimb.2017.00473.

73. Nguyen LT, Schmidt HA, Von Haeseler A, Minh BQ. 2015. IQ-TREE: a fast and effective stochastic algorithm for estimating maximum-likelihood phylogenies. Mol Biol Evol 32:268–274. doi:10.1093/molbev/msu300.

74. Katoh K, Rozewicki J, Yamada KD. 2019. MAFFT online service: multiple sequence alignment, interactive sequence choice and visualization. Brief Bioinform 20:1160–1166. doi:10.1093/bib/bbx108.

75. Kumar S, Stecher G, Tamura K. 2016. MEGA7: molecular evolutionary genetics analysis version 7.0 for bigger datasets. Mol Biol Evol 33:1870–1874. doi:10.1093/molbev/msw054

CHAPTER 3

THE CARBOXYLIC ACID TRANSPORTERS *JEN1* AND *JEN2* AFFECT THE ARCHITECTURE AND FLUCONAZOLE SUSCEPTIBILITY OF *CANDIDA ALBICANS* BIOFILMS IN THE PRESENCE OF LACTATE

Disclaimer

The work presented in this chapter has been previously published in *Biofouling, The Journal of Bioadhesion and Biofilm Research*.

-

Alves R, Mota S, Silva S, Rodrigues CF, Brown AJP, Henriques M, Casal M, Paiva S (2017) The carboxylic acid transporters Jen1 and Jen2 affect the architecture and fluconazole susceptibility of *Candida albicans* biofilm in the presence of lactate. *Biofouling.* doi: 10.1080/08927014.2017.1392514

-

ABSTRACT

Candida albicans has the ability to adapt to different host niches, often glucose-limited but rich in alternative carbon sources. In these glucose-poor microenvironments, this pathogen expresses *JEN1* and *JEN2* genes, encoding carboxylate transporters, which are important in the early stages of infection. This work investigated how host microenvironments, in particular acidic containing lactic acid, affect *C. albicans* biofilm formation and antifungal drug resistance. Multiple components of the extracellular matrix were also analyzed, including their impact on antifungal drug resistance, and the involvement of both Jen1 and Jen2 in this process. The results show that growth on lactate affects biofilm formation, morphology and susceptibility to fluconazole and that both Jen1 and Jen2 might play a role in these processes. These results support the view that the adaptation of *Candida* cells to the carbon source present in the host niches affects their pathogenicity.

3.1 INTRODUCTION

The human fungal pathogen *C. albicans* is the main etiological agent of candidiasis and one of the most frequent causes of hospital-acquired infections [1,2]. This opportunistic fungus is commonly found as a commensal in the human microbial flora of healthy people. However, in individuals with a weakened immune system, it can overgrow and cause serious or fatal infections. The pathogenicity of *C. albicans* and the high mortality rates associated with these infections are, in part, due to the ability to form biofilms and, consequently, resist against the common classes of antifungals [3,4]. Nevertheless, some fitness attributes, such as the flexibility to utilize multiple nutrients, also play an important role in virulence [5,6].

Inside the human host, *C. albicans* faces different pH environments, from acidic to mildly basic, and the ability to adjust to these fluctuations is essential for its pathogenicity [7–10]. In some glucose-poor niches, like in the colon and in the vagina, this fungus has also to adapt to changes in the availability of carbon sources, assimilating alternative nutrients, such as lactate or acetate [6,11–13]. This adaptation requires a metabolic switch [13–16], as verified, for instance, upon phagocytosis [17]. Microarray data of *C. albicans* cells internalized by macrophages showed the upregulation of *JEN1* [15], encoding a lactate permease [18], and its close homolog *JEN2*, encoding a malate and a succinate permease [16]. Both

Jen1-GFP and Jen2-GFP were expressed inside macrophages and neutrophils, which are rich in alternative carbon sources, but not in the bloodstream where glucose is abundant [16]. These results suggest that lactate inside the phagosome might help to sustain *C. albicans* following phagocytosis.

In addition to the phagosome, lactate is present in ingested foods and in the human body. It is produced at high rates by red blood cells, brain, and muscle, it is present in the urogenital tract and represents almost 2% of all carbon metabolites originating from the gut microbiota [19]. This carbon source is also a component of the lactated Ringer's solutions, Hartmann's solutions, commonly used intravenously after trauma, surgery or burn injury and whose usage increases the risk of systemic candidiasis and the formation of biofilms in catheters [20], representing a severe problem in modern medicine [21]. Growth of *C. albicans* on physiologically relevant concentrations of lactate affects stress adaptation, antifungal drug resistance, the architecture and proteome of the cell wall, immune detection and, in consequence, the virulence of this fungus [13,22,23]. Lactate-grown cells of *C. albicans* are more resistant to amphotericin B and caspofungin, but more sensitive to miconazole [22]. They also exhibit distinct compositions in the cell wall proteome and secretome in comparison with glucose-grown cells [22]. These changes lead to a stronger adherence to plastic surfaces and an increase in biofilm formation on both silicone and plastic surfaces in minimal medium, a condition that generally does not promote the yeast-hyphae transition or classical biofilm formation [22].

In this work, host microenvironments, in particular acidic niches that contain lactic acid, were studied regarding their effect on *C. albicans* biofilm formation and susceptibility to the most commonly used antifungal, fluconazole. Little is known about the effect of alternative carbon sources in *C. albicans* biofilm formation and development as the majority of studies are performed using glucose, as sole carbon source. Here, *C. albicans* cells were grown in RPMI medium containing different substrates, such as glucose and lactate, and then they were characterized with respect to their ability to form biofilms and resist fluconazole. Multiple components of the extracellular matrix were also analyzed, including their impact on drug resistance, and the involvement of both carboxylic acid transporters, Jen1 and Jen2, on these processes. By clarifying the effect of local nutrients on biofilm formation and antifungal resistance in *C. albicans*, new and effective treatment strategies can be developed for both mucosal and systemic infections.

3.2 MATERIAL AND METHODS

3.2.1 Yeast strains and growth conditions

Experiments were performed with *C. albicans* RM1000 (*ura3::imm434/ura3::imm434, his1::hisG/his1::hisG*) [24] and the double *jen1jen2* mutant (*ura3::imm434/ura3::imm434 his1::hisG/his1::hisG jen1::HIS1/jen1::ura3-, jen2::ura3-/jen2::URA3*) [16]. *C. albicans* RM1000 (isogenic to the SC5314 strain) was routinely cultured on YPD (1% yeast extract, 1% peptone, 2% glucose and 2% agar) plates stored at room temperature. *C. albicans jen1jen2* mutant strain was maintained on YNB (yeast nitrogen base 0.67% w v^{-1}) agar plates supplemented with the appropriate requirements for prototrophic growth. Cells were inoculated in YPD broth and incubated for 16-18 h at 37°C under agitation. After incubation, the cells were harvested by centrifugation at 3,000 *g* for 10 min at 4°C and washed twice with phosphate buffered saline (PBS). Pellets were then suspended in PBS and the cellular density adjusted to $1x10^5$ cells mL^{-1} using a Neubauer counting chamber. Biofilm growth was performed using Roswell Park Memorial Institute (RPMI) 1640 medium (Sigma, St. Louis, USA) with or without lactic acid (0.5%, v v^{-1}). The pH for the RPMI medium was always set either to 5 with HCl or to 7 with NaOH.

3.2.2 Minimal inhibitory concentration

The minimal inhibitory concentration (MIC) assays were performed according to the Clinical and Laboratory Standards Institute M27-A3 document [25] with some modifications, using RPMI 1640 broth supplemented with 0.165 M of MOPS at pH 7.0 and with or without adding 0.5% lactic acid at pH 5.0. Different concentrations of fluconazole were used, ranging from 0 to 1,250 μg mL^{-1} [26]. Briefly, a colony of the strain grown in YPD solid medium was resuspended in 5 mL of saline solution (NaCl 0.85%, w v^{-1}) until a cellular density equivalent to 0.5 McFarland standard. The yeast suspensions were diluted (1:100) in saline solution and diluted again (1:20) in RPMI 1640. This suspension in RPMI 1640 was added to the respective well of microtiter plates containing the specific concentration of fluconazole solutions. Controls without antifungal agents were also performed. The microtiter plates were incubated at 37°C during 48 h under aerobic conditions. The MICs of the antifungal agent against each *Candida* strain were determined visually and by total number of colony forming units (CFUs). For this purpose, cells corresponding to each condition were serial diluted in PBS and 10 μL of each one were plated in YPD. Experiments were performed in triplicate, using three independent biological samples.

3.2.3 Biofilm formation

Biofilm formation was performed as previously described [26]. Briefly, 200 µL of $1x10^5$ cells ml^{-1} suspensions in the required medium were placed into 96-wells polystyrene microtiter plates (Orange Scientific, Braine-l'Alleud, Belgium) and incubated at 37°C under aerobic conditions with gentle agitation. At 24 h, the entire volume of medium was removed and 200 µL of fresh medium were added to each well. In order to study the effect of fluconazole on biofilm formation, different concentrations (50, 150, 312.5 and 1,250 µg mL^{-1}) were prepared in RPMI 1640 medium and added to the 24 h formed biofilm. The microtiter plates were then incubated for an additional 24 h, totaling 48 h of biofilm growth.

3.2.4 Biofilm biomass quantification

After biofilm formation for 48 h, the entire volume of medium was aspirated and non-adherent cells removed by washing once with PBS. Biofilm forming ability was assessed through quantification of the total biomass by crystal violet (CV) staining [27]. Thus, after washing, biofilms were fixed with 200 µL of methanol, which were removed after contact for 15 min. The microtiter plates were allowed to dry at room temperature, and 200 µL of CV (1%, v v^{-1}) were added to each well and incubated for 5 min. The wells were then gently washed twice with water and 200 µL of acetic acid (33%, v v^{-1}) were added to release and dissolve the stain. The absorbance of the solution obtained was read in a microtiter plate reader (Bio-Tek Synergy HT, Izasa, Portugal) at 570 nm. The results were presented as absorbance per unit area, Abs (570 nm) cm^{-2}. Experiments were performed in triplicate, using three independent biological samples.

3.2.5 Biofilm viability quantification

The number of cultivable cells in biofilms was determined by the enumeration of CFUs. For that, after biofilm growth for 48 h and the PBS washing step described previously, the biofilms were scraped from wells into 200 µL PBS and the suspensions were vigorously vortexed to disaggregate cells from matrix [28]. Serial 10-fold dilutions in PBS were plated onto YPD plates and incubated for 24 h at 37°C. Complete removal of the biofilm was confirmed by subsequent CV staining and spectrophotometric reading for inspection of the wells. The results were presented as the total of CFUs per unit area (log_{10} CFU cm^{-2}). Experiments were performed in duplicate, using three independent biological samples.

3.2.6 Biofilm structure analysis

Biofilm structure was assessed by Scanning Electron Microscopy (SEM). Biofilms were formed in 24-wells polystyrene microtiter plates (Orange Scientific) with 1 mL of $1x10^5$ cells ml^{-1} suspensions, as described previously. After 48 h incubation the biofilms formed were washed with PBS, dehydrated with alcohol (using 70% ethanol for 10 min, 90% ethanol for 10 min and 100% ethanol for 20 min) and air-dried. Prior to observation, the base of the wells was mounted onto aluminum stubs, sputter coated with a thin film (15nm) of Au-Pd (80-20 weight %) and observed with an ultra-high resolution Field Emission Gun Scanning Electron Microscopy (FEG-SEM; Nova NanoSem 200, FEI Company, OR, USA).

3.2.7 Biofilm matrix extraction

Biofilms were formed in a 24-wells polystyrene microtiter plate (Orange Scientific), for each condition, as described previously. After 48 h, the formed biofilm was washed with PBS, scraped from the wells and resuspended in 5 mL of PBS. The extracted matrices were sonicated (Ultrasonic Processor, Cole-Parmer, IL, USA) for 30 s at 30% amplitude and vortexed for 30 s. 1 mL of the suspension was used for dry biofilm weight determination and the rest was centrifuged at 5,000 rpm for 5 min at 4°C. The supernatant was filtered through a 0.45 µm nitrocellulose filter and stored at -20°C until further analysis. The experiments were performed in triplicate, using two independent biological samples.

3.2.8 Protein determination in the biofilm matrix

The protein quantification was measured using the BCA Protein Assay Kit (Thermo Scientific, MA, USA), using bovine serum albumin as standard and following the manufacturer's instructions. Briefly, 25 µL of each sample were mixed with 200 µL of BCA Working Reagent. After incubation for 30 min at 37°C, the absorbance of the obtained solution was read in a microtiter plate reader (Bio-Tek Synergy HT, Izasa, Portugal) at 562 nm, using PBS as blank. The values were normalized per g of dry weight of biofilm and presented as mg of protein per g of dry weight of biofilm (m g^{-1} biofilm).

3.2.9 Carbohydrate determination in the biofilm matrix

Carbohydrate quantification was assessed by the phenol-sulphuric acid method [29], using glucose as standard. Briefly, 500 µL of each sample were mixed with 500 µL of phenol (50 g L^{-1}) and 2,500 µL of sulphuric acid (90-95%). After incubation for 15 min at room temperature, all polysaccharides and their derivatives were stained orange-yellow and the absorbance of the solution obtained read in a microtiter

plate reader (Bio-Tek Synergy HT, Izasa, Portugal) at 490 nm, using PBS as blank. The values were normalized per g of dry weight of biofilm (mg g^{-1} biofilm).

3.2.10 β-1,3 glucan determination in the biofilm matrix

The matrix β-1,3-glucan content was determined using the Glucatell (1,3)-Beta-D-Glucan detection reagent kit (Associates of Cape Cod, East Falmouth, MA, USA), as per the manufacturer's directions. Briefly, 50 µL of each sample were mixed with 50 µL of Glucatell reagent. After incubation for 40 min at 37°C, the reaction was stopped by adding sequentially 50 µL of sodium nitrite, 50 µL of ammonium sulphamate and then 50 µL of N-(1-napthyl)ethylenediamine dihydrochloride (NEDA). All solutions and glucan standards were supplied with the kit. The obtained solution was read in a microtiter plate reader (Bio-Tek Synergy HT, Izasa, Portugal) at 540 nm, using PBS as blank. The values were normalized per g of dry weight of biofilm and presented as ng of β-1,3-glucans per g of dry weight of biofilm (ng g^{-1} biofilm).

3.2.11 Ergosterol extraction and quantification

For the ergosterol extraction, 2 mL of n-hexan (Thermo Scientific, Waltham, MA, USA) were added to 10 mL of the matrix suspension prepared as previously described. This preparation was then submitted to vortex for 1 min. This procedure was performed three times and the top solution sequestered to a 10 mL amber bottle. After the extraction, the solutions were dried with nitrogen until all the organic solvent has evaporated. The dried extract was resuspended in 2 mL of methanol, filtered with a 0.45 µm filter to an Eppendorf tube and stored at -20°C [30]. For the ergosterol quantification, the high-pressure liquid chromatography (HPLC) method was performed in Varian STAR 9002 (Varian, Walnut Creek, CA, USA) using a C18 column (YMC, Allentown, PA, USA). An isocratic mobile phase of 100% of methanol with a flow of 1 mL min^{-1}, for 20 min, was used for the quantification of each sample. The results were automatically shown by the HPLC detector [30], and then normalized by g of dry weight biofilm and presented as µg of ergosterol per g of dry weight of biofilm (µg g^{-1} biofilm).

3.2.12 Statistical analyses

Data were analyzed using Graph Pad Prism (v.7). Statistical significance was determined by one-way or two-way ANOVA with Tukey's multiple comparison post-test. All tests were performed with a confidence level of 95%.

3.3 RESULTS

3.3.1 Characterization of *C. albicans* biofilms in the presence of lactic acid

Lactic acid, naturally present in several sites of the human body, can be used as an alternative carbon source by *Candida* cells. To determine the influence of lactic acid on the formation and behavior of *C. albicans* biofilms *in vitro*, they were characterized using *C. albicans* RM1000 (wild type) cells in RPMI-containing 0.5% lactic acid medium at pH 5.0, a condition where most of the acid is present in its anionic form and its assimilation depends on a transporter-mediated system [31]. In order to mimic different host microenvironments, and given that glucose is the preferential carbon source for *C. albicans*, assays using RPMI medium containing glucose, and no lactic acid, at both pH 7.0 and pH 5.0 were also carried out. Biofilms were analyzed by total biomass quantification through CV staining and the enumeration of cultivable cells (CFUs) (Figure 3.1A and C). Both quantifications were carried out on biofilms grown for 48 h. The ultrastructure of biofilms was assessed by SEM analysis (Figure 3.1B and D).

The results obtained indicate that *C. albicans* wild type (WT) cells displayed an enhanced biofilm formation in the presence of lactate when compared to biofilms formed in the presence of glucose ($p < 0.001$; Figure 3.1A). It was also observed that, depending on pH and the carbon source, biofilms formed in the presence of lactate developed different structures and the cells exhibited different morphological characteristics. Mature biofilms grown in the presence of glucose at pH 7.0 (RPMI pH7) consisted of a dense network of hyphae without yeast forms, while at pH 5.0 (RPMI pH5) a reduction in filaments was evident (Figure 3.1B). In the presence of lactic acid (RPMI 0.5% lactic acid pH5) most of the cells were in the yeast form (Figure 1B). Both WT and mutant strains displayed an identical growth profile, exhibiting more biofilm biomass in the presence of lactic acid than in glucose ($p < 0.001$ and $p < 0.01$, respectively; Figure 3.1A and C). Regarding the ultrastructural and morphological features, the *jen1jen2* double mutant mainly formed hyphae in the presence of glucose; while in the presence of lactic acid the yeast form was the most predominant with almost no filamentous forms observed (Figure 3.1D). The mutant strain also exhibited a compact biofilm structure with some cracks and less hyphae than the WT (Figure 3.1B and D).

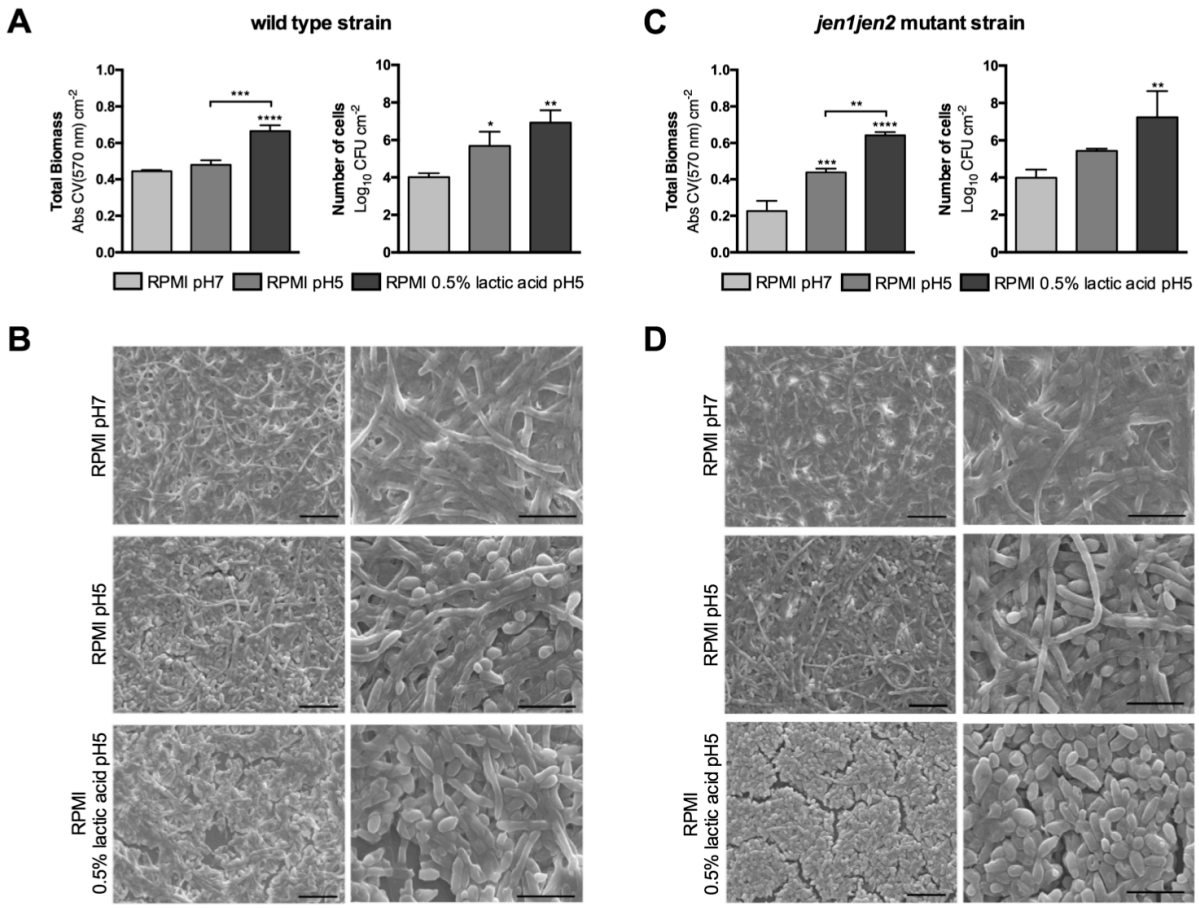

Figure 3.1. Effect of lactic acid on *C. albicans* biofilms (wild type strain *vs* the *jen1jen2* mutant strain). **(A, C)** Total biomass of biofilms and number of cells in biofilms formed after 48 h in different conditions: RPMI pH 7.0, RPMI pH 5.0 and RPMI 0.5% lactic acid pH 5.0. The absorbance value of CV solution (Abs CV) at 570 nm and logarithm of colony forming units (CFU) were normalized by unit of area (Abs CV_{570nm} cm^{-2} and $Log_{10}CFU\ cm^{-2}$, respectively). Error bars represent standard deviations. Statistically significant changes appear above error bars when compared with the control group (RPMI pH 7.0) or above brackets when compared with the second control group (RPMI pH 5.0); $^{**}p < 0.01$, $^{***}p < 0.001$, $^{****}p < 0.001$. **(B, D)** SEM images of mature biofilms. The left and the right images in each panel represent a magnification of 1,000x and 3,000x, respectively. Bars on the images correspond to 20 µm at 1,000x magnification and 10 µm at 3,000x magnification.

3.3.2 Lactic acid increases the susceptibility of *C. albicans* planktonic cells to fluconazole

In an attempt to further explore the role of Jen1 and Jen2 in *C. albicans* resistance to fluconazole, the minimal fungicidal concentration (MFC) and the MIC by CFU counting for WT and *jen1jen2* planktonic cells grown either in lactic acid or glucose were determined (Table 3.1). In RPMI medium, independently of the pH, no differences in MIC values were observed between the tested strains, which displayed equal

growth behavior up to the highest concentration of fluconazole (Table 3.1). In the presence of lactic acid, a MIC value of 150 μg mL^{-1} and a MFC value of 312.5 μg mL^{-1} were obtained for the WT strain, and a lower fluconazole MIC and MFC values (50 and 150 μg mL^{-1}, respectively) were found for the mutant strain (Table 3.1). Therefore, with the addition of fluconazole, all strains became more susceptible in the presence of lactic acid and the double mutant was even more susceptible than the WT. These results suggest that Jen1 and Jen2 play a role in antifungal resistance to fluconazole.

Table 3.1. Effect of fluconazole on *C. albicans* WT and *jen1jen2* planktonic cells using different growth conditions: cells grown in RPMI pH 7.0, RPMI pH 5.0 and RPMI 0.5% lactic acid pH 5.0.

Strain	Condition	MIC (μg mL^{-1})	MFC (μg mL^{-1})
WT	RPMI pH 7.0	≥1,250	>1,250
	RPMI pH 5.0	625	1,250
	RPMI 0.5% lactic acid pH 5.0	150	312.5
JEN1JEN2	RPMI pH 7.0	≥1,250	>1,250
	RPMI pH 5.0	625	1,250
	RPMI 0.5% lactic acid pH 5.0	50	150

Note: MICs were determined visually and MFCs by total number of CFUs, according to the microdilution method [25].

3.3.3 Characterization of fluconazole antifungal activity in *C. albicans* biofilms

The effect of fluconazole was also evaluated for biofilms (Figure 3.2), similar to what was done for planktonic cells. Figure 3.2A shows that in RPMI medium at pH 7.0, the presence of fluconazole did not significantly affect the amount of total biomass. Interestingly, at pH 5.0 and in the presence of lactic acid, the reduction was significant for both strains. While in RPMI lactic acid *jen1jen2* planktonic cells were more susceptible to fluconazole compared to the WT strain (Table 3.1), their biofilm counterparts did not follow the same behavior. In general, a significant reduction in cell viability was only observed at the highest tested concentration of fluconazole (Figure 3.2A). The effect of fluconazole on the biofilm structure was also assessed by SEM analysis (Figure 3.2B). In RPMI medium, the differences were only visible with 1,250 μg mL^{-1} of fluconazole for both strains and conditions. In the case of RPMI lactic acid, significant differences were observed between both strains in the absence of fluconazole (Figure 3.2B). The absence of an antifungal resulted in a dense, compact biofilm with almost no hyphal forms in the mutant strain, in contrast to a hyphae containing biofilm structure in the WT strain. Interestingly, the highest fluconazole concentration led to an increase in hyphae formation for WT and mutant strains (Figure 3.2B).

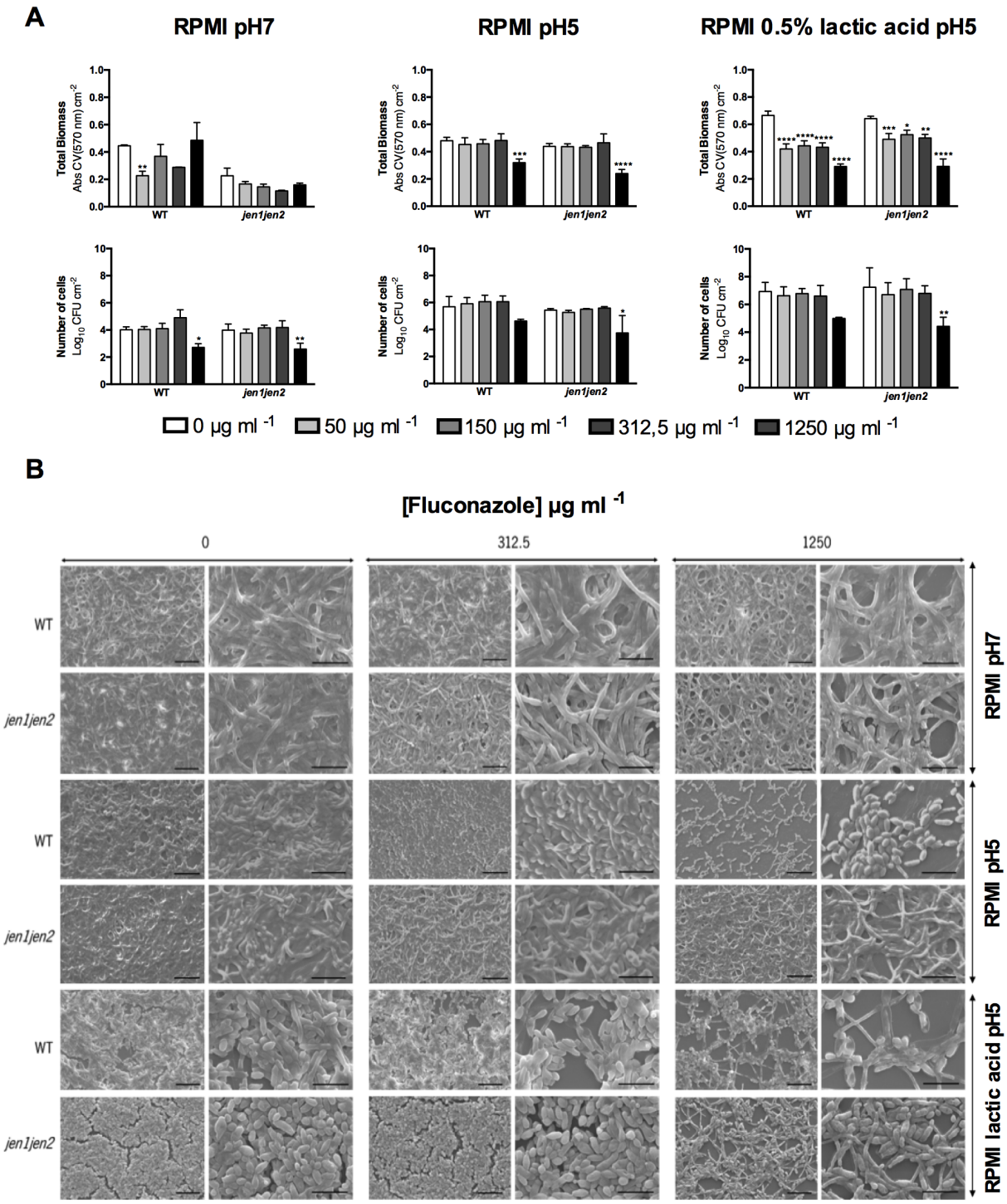

Figure 3.2. Effect of fluconazole on *C. albicans* WT and *jen1jen2* biofilms grown in RPMI pH 7.0, RPMI pH 5.0 and RPMI 0.5% lactic acid pH 5.0. (A) Histograms at the top represent the absorbance values of CV solution at 570 nm normalized by unit of area (Abs CV_{570nm} cm^{-2}) and histograms at the bottom represent the logarithm of CFUs normalized by unit of area (Log_{10} CFU cm^{-2}) of biofilm. The legend displays the different fluconazole concentrations used. Error bars represent standard deviations. *, **, *** and **** mean that results are statistically significant (p <0.05, p< 0.01, p< 0.001 and p< 0.0001, respectively).

(B) SEM images showing the effect of fluconazole on both WT and *jen1jen2* biofilms. The left and the right image in each strain for the respective fluconazole concentration represents a magnification of 1,000x and 3,000x, respectively. Bars in the images correspond to 20 μm at 1,000x magnification and 10 μm at 3,000x magnification.

3.3.4 Impact of carbon sources and fluconazole treatment on the biofilm matrix of *C. albicans*

The matrix of *Candida* has a prominent role in the antifungal drug resistance associated with biofilms [32,33]. The biofilm matrix composition of both strains was analyzed in response to changes in carbon sources and antifungal treatment. Several components that have been involved in the sequestration of antifungals were evaluated, such as polysaccharides (Figure 3.3A), the extracellular carbohydrate β-1,3-glucan (Figure 3.3B), proteins (Figure 3.3C) and ergosterol (Table 3.2).

The content of polysaccharides increased in the presence of fluconazole, particularly in the highest concentration, in all tested conditions (Figure 3.3A). However, in RPMI pH 5.0 medium this increase was lower in both strains. A significant decrease in polysaccharides in the *jen1jen2* mutant strain was observed, when compared with the WT, in the presence of lactate and high concentrations of fluconazole (Figure 3.3A). This result suggests that there may be a greater requirement for Jen1/2-mediated lactate uptake, in these stress conditions.

Inversely, the amount of β-1,3-glucans found in the biofilm matrices did not follow the same pattern in the growth conditions tested, in response to antifungal treatment (Figure 3.3B).

The total protein content, in contrast to what was observed for the polysaccharides, decreased in the presence of fluconazole, in both strains (Figure 3.3C).

In general, the concentration of ergosterol in the matrices increased with the addition of fluconazole up to 312.5 μg mL^{-1} (Table 3.2). However, the addition of 1,250 μg ml^{-1} of fluconazole, inverted this tendency, with the exception of matrices extracted from WT biofilms, grown in the presence of lactic acid. As observed for the polysaccharides, the *jen1jen2* mutant strain displayed a lower amount of ergosterol when compared with WT, in the presence of lactate and 1,250 μg mL^{-1} of fluconazole (Table 3.2).

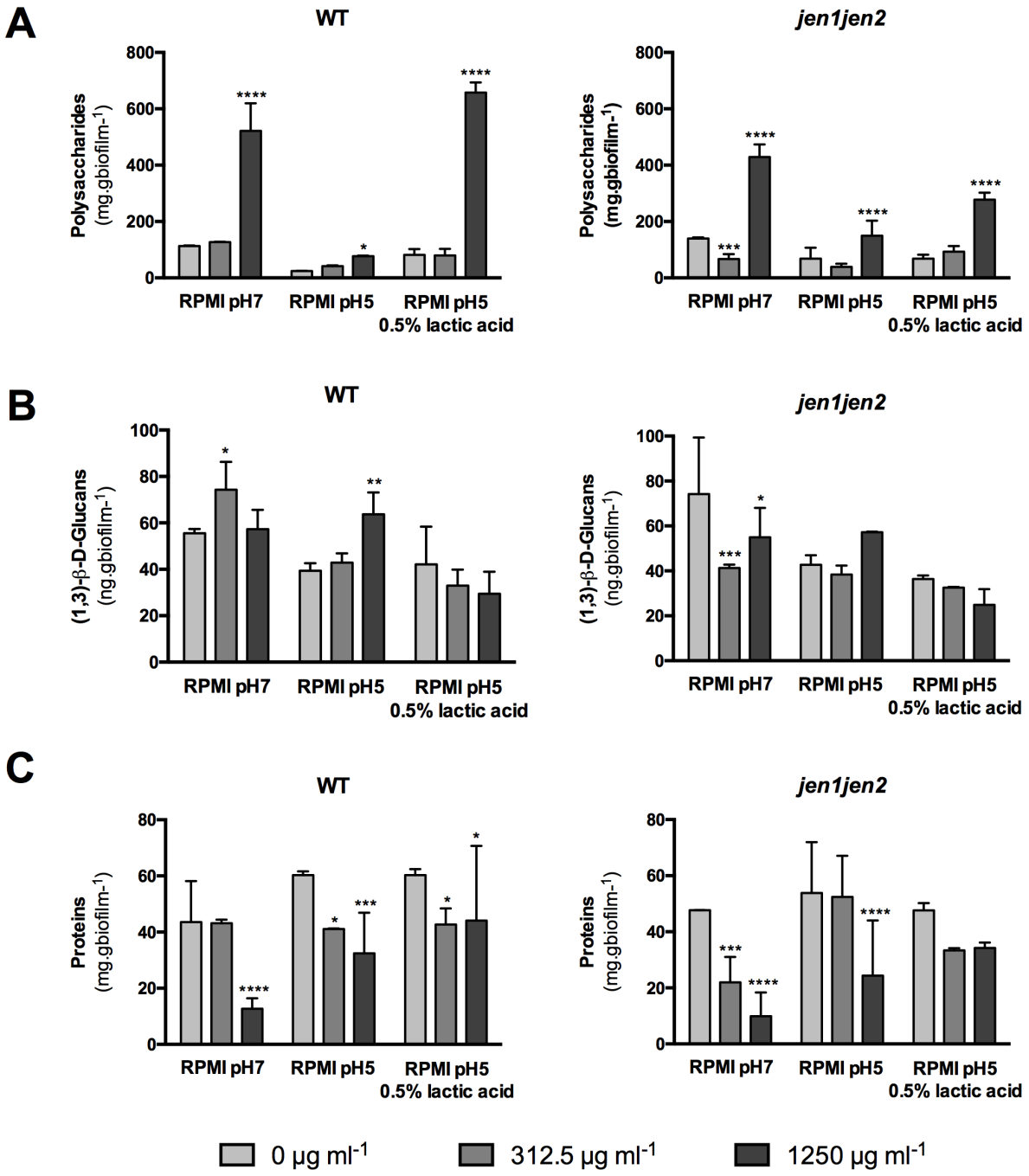

Figure 3.3. Effect of fluconazole on the biofilm matrix composition of *C. albicans* WT and *jen1jen2* strains grown in RPMI pH 7.0, RPMI pH 5.0 and RPMI 0.5% lactic acid pH 5.0. Concentrations are presented in mg for (A) polysaccharides and (C) proteins or ng for (B) 1,3-β-D-glucans per g of 48 h biofilm dry weight (mg g^{-1} biofilm or ng g^{-1} biofilm, respectively). Error bars represent standard deviations. *, **, *** and **** mean that the results are statistically significant ($p < 0.05$, $p < 0.01$, $p < 0.001$ and $p < 0.0001$, respectively).

Table 3.2. Effect of fluconazole on ergosterol production in the biofilm matrices of *C. albicans* WT and the mutant strain *jen1jen2*.

STRAIN	CONDITION	FLUCONAZOLE (μG ML^{-1})	ERGOSTEROL (μG G^{-1} BIOFILM)
WT	RPMI pH 7.0	0	≤14.360
		312.5	≤256.000
		1,250	≤33.750
	RPMI pH 5.0	0	≤17.724
		312.5	≤27.442
		1,250	≤9.333
	RPMI 0.5% lactic acid pH 5.0	0	≤80.350
		312.5	≤105.560
		1,250	≤131.200
JEN1JEN2	RPMI pH 7.0	0	≤30.000
		312.5	≤128.570
		1,250	≤23.680
	RPMI pH 5.0	0	≤31.163
		312.5	≤11.224
		1,250	≤9.063
	RPMI 0.5% lactic acid pH 5.0	0	≤60.000
		312.5	≤68.870
		1,250	≤0.220

Note: The table displays the highest concentrations detected in μg per g of 48 h biofilm dry weight (μg g^{-1} biofilm).

3.4 DISCUSSION

Candida biofilms can occur on most biological and non-biologic substrata, such as catheters, serving as reservoirs or sources for potential infections [4,34,35]. Most studies on *Candida* species, including *Candida* biofilms, have been carried out using glucose as the sole carbon source in the medium. However, the concentration of glucose in some host niches is usually limited and *Candida* depends on alternative substrates for growth and invasion. The physiology of *Candida* is profoundly affected by carbon sources so it is crucial to accurately reflect this variable in experiments in order to understand biofilm formation in these niches. Some studies have shown that lactate-grown cells, in minimal medium, adhere more strongly to plastic surfaces and display increased biofilm formation [13,22]. However, the growth conditions used in this study did not promote the yeast hyphae transitions and classical biofilm formation [22]. In this context, *C. albicans* biofilm formation was studied in media containing both glucose and lactate at different pH values, conditions that mimic host microenvironments where this pathogen can be found.

The presence of lactic acid promoted biofilm formation (Figure 3.1A). Regarding morphology, *C. albicans* biofilms can comprise yeast cells, hyphae and pseudohyphae [36]. It is well established that *C. albicans* changes its morphology according to environmental conditions, which constitutes one of its virulence factors [37]. Nutrient starvation, the presence of serum, an increase in temperature and pH have been reported as hypha-inducing environmental factors [38]. As expected, the present study shows that in RPMI pH 7.0 the hyphal morphology predominated, whereas in RPMI pH 5.0 the yeast form was the most prevalent (Figure 3.1B). However, in the presence of lactate (RPMI 0.5% lactic acid pH 5.0) the yeast form was even more predominant and minimal hypha formation was observed (Figure 3.1B). In addition to pH, the carbon source available is also important in *C. albicans* morphology and ultimately in *C. albicans* biofilm formation.

Regarding the contribution of the carboxylic acid transporters Jen1 and Jen2, the disruption of *JEN1* and *JEN2*, compromises biofilm formation in RPMI containing lactate. These results indicate that the *jen1jen2* mutant is capable of forming biofilm in all the tested conditions and its behavior is similar to that of WT, as both strains have more biofilm biomass in the presence of lactic acid (Figure 3.1A and C). Regarding ultrastructure, the *jen1jen2* mutant presented a compact biofilm structure with some cracks and even less hyphae than the WT in lactate containing media (Figure 3.1D). These differences, observed in the

presence of lactate, point to an involvement of these transporters in biofilm formation, at least in terms of ultrastructure.

Biofilm cells display unique phenotypic characteristics, the most remarkable of which is that they are particularly resistant to both antifungal agents and host immune factors [4,35]. Attempts were also made to elucidate the role of Jen1 and Jen2 in *C. albicans* resistance to the commonly used antifungal drug fluconazole. In a *jen1jen2* double mutant strain, carboxylic acids only enter the cell by simple diffusion of the undissociated form of the acid, a process dependent on extracellular pH. These studies were conducted both in planktonic and biofilm cells. The results indicate that lactate-grown planktonic cells of the mutant strain were more susceptible to fluconazole than the WT cells (Table 3.1), pointing to an involvement of these transporters in antifungal drug resistance. Additionally, the presence of lactic acid in the medium acts synergistically with fluconazole, since WT cells became more susceptible to fluconazole in this condition. These results are in agreement with previous studies, that showed an increase of *C. albicans* susceptibility to miconazole, another azole antifungal drug, in lactic acid-grown cells [22], and to fluconazole in a synthetic vagina-simulative medium in an acidic pH [39]. The analysis of the components of the medium indicated that acetic acid was responsible for the synergistic, fungicidal effect and not lactic acid [39]. Here, the results indicate that lactic acid also triggers this effect and maybe, in this niche, both acids can contribute equally to this phenomenon. These findings support the results from Ene *et al.* (2012) [22] with the demonstration of growth inhibition by a clinically important azole, reinforcing the idea that lactate reduces azole resistance. Regarding biofilms, fluconazole had almost no effect on biofilm reduction (Table 3.1). While in the presence of lactic acid *jen1jen2* planktonic cells were more susceptible to fluconazole comparatively to WT cells, their biofilm counterparts did not follow the same behavior. In general, a significant reduction in cell viability was only observed at the highest tested concentration of fluconazole (Table 3.2). However, these results should be interpreted carefully since in planktonic cells, according with the standard method used [25], the antifungal drug is added at the beginning of the assay, and in biofilms the drug is added after 24 hours. These different procedures, inherent in biofilm growth assays, may be responsible for the observed phenotypes. It was reported that the addition of fluconazole at the initiation of biofilm formation inhibited this process even in *C. albicans* strains known to be resistant to fluconazole [40]. Nevertheless, these results are in accordance with what has been reported in other studies that demonstrated that biofilms need about 100 to 1000 times more of an antifungal drug to be eradicated [41–43].

An interesting phenotype was observed as a result of fluconazole treatment in the RPMI medium containing lactic acid. In this condition both strains showed increased hyphae formation (Figure 3.2B), an important feature of this fungus in pathogenesis. According to previous studies, hypha formation in planktonic cells of *C. albicans* is inhibited in the presence of fluconazole or other azole derivatives [44,45]. However, in the case of biofilms, the cells are immersed in an extracellular matrix that provides better protection against stress factors.

Antifungal resistance in biofilms is complex. It can be inducible in response to a drug, or an irreversible genetic change resulting from a prolonged exposure. The mechanisms utilized by fungi to combat the effects of antifungal drugs comprise modifications or overexpression of target molecules, active extrusion through efflux pumps, limited diffusion, tolerance, and cell density [34,46,47]. Recent studies suggest that the composition of extracellular matrix and its regulation might play a central role in resistance, with the polysaccharide β-1,3-glucan being linked to biofilm protection against antifungal agents [48–50]. Besides conferring significant resistance to antifungal therapy, the composition of extracellular matrix also contributes to defense from the host immune response and maintenance of nutrients [51]. The matrix contains polysaccharides, small amounts of proteins, DNA and can also have several other components [35,51–53]. The results of this study strengthen the role of polysaccharides in antifungal drug resistance. The increase in this component upon fluconazole treatment could reflect a cell mechanism for survival under the presence of the drug. This reinforces the resistance model which suggests that the polysaccharides present in the extracellular matrix cover biofilm cells are capable of sequestering antifungal drugs, acting as a "drug sponge". This has the ability to prevent invading cells from reaching their targets, thus limiting their toxicity to these cells and associated transcriptional responses [48–50]. Additionally, these results also show that in the presence of lactic acid and at high concentrations of fluconazole, the production of general polysaccharides is affected in a *jen1jen2* mutant strain (Figure 3.3A). This suggests that Jen1/2-mediated lactate uptake or Jen1/2-mediated signaling is required in these conditions. However, the amount of β-1,3-glucans found in the biofilm matrices was almost constant in all conditions (Figure 3.3B), suggesting that these molecules only represent a small portion of the total matrix polysaccharides [33]. In contrast with the polysaccharides, the matrices from all strains and conditions exhibited a decrease in the protein content with the antifungal treatment (Figure 3.3C), suggesting a possible compensatory mechanism of the matrix content. Another mechanism of resistance is the overexpression of target molecules. It has been reported that the exposure of biofilms to fluconazole results in overexpression of the genes encoding enzymes involved in ergosterol biosynthesis [55]. An

increase in ergosterol in the extracellular matrix was observed with fluconazole treatment (up to 312.5 μg mL^{-1}) and a decrease in the presence of the highest concentration of the drug (Table 3.2). This may be due to differential regulation of ergosterol genes associated with antifungal treatment.

In summary, this work indicates that the alternative carbon source lactic acid affects the structure and morphology of *C. albicans* biofilms and has an impact in antifungal resistance to fluconazole in both planktonic and biofilm cells. It also suggests that the carboxylic acid transporters Jen1 and Jen2 might play a role in these processes during growth in host microenvironments containing lactate. These findings have an important clinical impact, namely in the treatment of vaginal candidiasis, a host niche with an acidic pH, rich in alternative carbon sources, such as lactate.

3.5 REFERENCES

1. Pfaller MA, Diekema DJ. Epidemiology of invasive candidiasis: a persistent public health problem. Clin Microbiol Rev. 2007;20: 133–163. doi:10.1128/CMR.00029-06
2. Pappas PG, Kauffman CA, Andes D, Benjamin, Jr. DK, Calandra TF, Edwards, Jr. JE, et al. Clinical Practice Guidelines for the Management of Candidiasis: 2009 Update by the Infectious Diseases Society of America. Clin Infect Dis. 2009;48: 503–535. doi:10.1086/596757
3. Ramage G, Martínez JP, López-Ribot JL. *Candida* biofilms on implanted biomaterials: A clinically significant problem. FEMS Yeast Research. 2006. pp. 979–986. doi:10.1111/j.1567-1364.2006.00117.x
4. Ramage G, Mowat E, Jones B, Williams C, Lopez-Ribot J. Our Current Understanding of Fungal Biofilms. Crit Rev Microbiol. 2009;35: 340–355. doi:10.3109/10408410903241436
5. Miramón P, Lorenz MC. A feast for *Candida*: Metabolic plasticity confers an edge for virulence. PLoS Pathogens. 2017. doi:10.1371/journal.ppat.1006144
6. Brown AJP, Brown GD, Netea MG, Gow NAR. Metabolism impacts upon *Candida* immunogenicity and pathogenicity at multiple levels. Trends in Microbiology. 2014. pp. 614–622. doi:10.1016/j.tim.2014.07.001
7. De Bernardis F, Mühlschlegel FA, Cassone A, Fonzi WA. The pH of the host niche controls gene expression in and virulence of *Candida albicans*. Infect Immun. 1998;66: 3317–3325.
8. Vylkova S, Carman AJ, Danhof HA, Collette JR, Zhou H, Lorenz MC. The fungal pathogen *Candida albicans* autoinduces hyphal morphogenesis by raising extracellular pH. MBio. 2011;2. doi:10.1128/mBio.00055-11
9. Vylkova S, Lorenz MC. Modulation of Phagosomal pH by *Candida albicans* Promotes Hyphal Morphogenesis and Requires Stp2p, a Regulator of Amino Acid Transport. PLoS Pathog. 2014;10. doi:10.1371/journal.ppat.1003995
10. Davis DA. How human pathogenic fungi sense and adapt to pH: the link to virulence. Current Opinion in Microbiology. 2009. pp. 365–370. doi:10.1016/j.mib.2009.05.006
11. Staib P, Kretschmar M, Nichterlein T, Kohler G, Michel S, Hof H, et al. Host-induced, stage-specific virulence gene activation in *Candida albicans* during infection. Mol Microbiol. 1999;32: 533–546.
12. Barelle CJ, Priest CL, MacCallum DM, Gow NAR, Odds FC, Brown AJP. Niche-specific regulation of central metabolic pathways in a fungal pathogen. Cell Microbiol. 2006;8: 961–971. doi:10.1111/j.1462-5822.2005.00676.x

13. Ene I V., Cheng SC, Netea MG, Brown AJP. Growth of *Candida albicans* cells on the physiologically relevant carbon source lactate affects their recognition and phagocytosis by immune cells. Infect Immun. 2013;81: 238–248. doi:10.1128/IAI.01092-12

14. Lorenz MC, Fink GR. The glyoxylate cycle is required for fungal virulence. Nature. 2001;412: 83–86. doi:10.1038/35083594

15. Lorenz MC, Bender JA, Fink GR. Transcriptional response of *Candida albicans* upon internalization by macrophages. Eukaryot Cell. 2004;3: 1076–1087. doi:10.1128/EC.3.5.1076-1087.2004

16. Vieira N, Casal M, Johansson B, MacCallum DM, Brown AJP, Paiva S. Functional specialization and differential regulation of short-chain carboxylic acid transporters in the pathogen *Candida albicans.* Mol Microbiol. 2010;75: 1337–1354. doi:10.1111/j.1365-2958.2009.07003.x

17. Miramón P, Dunker C, Windecker H, Bohovych IM, Brown AJP, Kurzai O, et al. Cellular Responses of *Candida albicans* to Phagocytosis and the Extracellular Activities of Neutrophils Are Critical to Counteract Carbohydrate Starvation, Oxidative and Nitrosative Stress. PLoS One. 2012;7. doi:10.1371/journal.pone.0052850

18. Soares-Silva I, Paiva S, Kötter P, Entian K-D, Casal M. The disruption of *JEN1* from *Candida albicans* impairs the transport of lactate. Mol Membr Biol. 2004;21: 403–411. doi:10.1080/09687860400011373

19. Flint HJ, Scott KP, Louis P, Duncan SH. The role of the gut microbiota in nutrition and health. Nat Rev Gastroenterol Hepatol. 2012;9: 577–589. doi:10.1038/nrgastro.2012.156

20. Pfaller MA, Diekema DJ. Epidemiology of Invasive Mycoses in North America. Crit Rev Microbiol. 2010;36: 1–53. doi:10.3109/10408410903241444

21. Donelli G, Vuotto C. Biofilm-based infections in long-term care facilities. Future Microbiol. 2014;9: 175–188. doi:10.2217/fmb.13.149

22. Ene I V., Adya AK, Wehmeier S, Brand AC, Maccallum DM, Gow NAR, et al. Host carbon sources modulate cell wall architecture, drug resistance and virulence in a fungal pathogen. Cell Microbiol. 2012;14: 1319–1335. doi:10.1111/j.1462-5822.2012.01813.x

23. Ballou ER, Avelar GM, Childers DS, Mackie J, Bain JM, Wagener J, et al. Lactate signalling regulates fungal β-glucan masking and immune evasion. Nat Microbiol. 2016;2: 16238. doi:10.1038/nmicrobiol.2016.238

24. Negredo A, Monteoliva L, Gil C, Pla J, Nombela C. Cloning, analysis and one-step disruption of the ARG5,6 gene of *Candida albicans*. Microbiology. 1997;143: 297–302. doi:10.1099/00221287-143-2-297

25. CLSI. Clinical and Laboratory Standards Institute: Reference method for broth dilution antifungal susceptibility testing of yeasts; approved standard-; CLSI document M27-A3. CLSI 2008a. 2008.
26. Mota S, Alves R, Carneiro C, Silva S, Brown AJ, Istel F, et al. *Candida glabrata* susceptibility to antifungals and phagocytosis is modulated by acetate. Front Microbiol. 2015;6. doi:10.3389/fmicb.2015.00919
27. Stepanovic S, Vukovic D, Dakic I, Savic B, Svabic-Vlahovic M. A modified microtiter-plate test for quantification of staphylococcal biofilm formation. J Microbiol Methods. 2000;40: 175–179. doi:10.1016/S0167-7012(00)00122-6
28. Silva S, Henriques M, Martins A, Oliveira R, Williams D, Azeredo J. Biofilms of non-*Candida albicans Candida* species: quantification, structure and matrix composition. Med Mycol. 2009;47: 681–9. doi:10.3109/13693780802549594
29. DuBois M, Gilles KA, Hamilton JK, Rebers PA, Smith F. Colorimetric Method for Determination of Sugars and Related Substances. Anal Chem. 1956;28: 350–356. doi:10.1021/ac60111a017
30. Marín S, Morales H, Ramos AJ, Sanchis V. Evaluation of growth quantification methods for modelling the growth of Penicillium expansum in an apple-based medium. J Sci Food Agric. 2006;86: 1468–1474. doi:10.1002/jsfa.2517
31. Casal M, Paiva S, Queirós O, Soares-Silva I. Transport of carboxylic acids in yeasts. FEMS Microbiol Rev. 2008;32: 974–994. doi:10.1111/j.1574-6976.2008.00128.x
32. Branda SS, Vik Å, Friedman L, Kolter R. Biofilms: The matrix revisited. Trends in Microbiology. 2005. pp. 20–26. doi:10.1016/j.tim.2004.11.006
33. Zarnowski R, Westler WM, Lacmbouh GA de, Marita JM, Bothe JR, Bernhardt J, et al. Novel entries in a fungal biofilm matrix encyclopedia. MBio. 2014;5: e01333–e01314. doi:10.1128/mBio.01333-14
34. Donlan RM, Costerton JW. Biofilms: Survival mechanisms of clinically relevant microorganisms. Clinical Microbiology Reviews. 2002. pp. 167–193. doi:10.1128/CMR.15.2.167-193.2002
35. Douglas LJ. *Candida* biofilms and their role in infection. Trends in Microbiology. 2003. pp. 30–36. doi:10.1016/S0966-842X(02)00002-1
36. Ramage G, Saville SP, Thomas DP, López-Ribot JL. Candida biofilms: An update. Eukaryotic Cell. 2005. pp. 633–638. doi:10.1128/EC.4.4.633-638.2005
37. Calderone R, Fonzi W. Virulence factors of *Candida albicans*. Trends Microbiol. 2001;9: 327–35. doi:10.1016/S0966-842X(01)02094-7

38. Whiteway M, Bachewich C. Morphogenesis in *Candida albicans*. Annu Rev Microbiol. 2007;61: 529–553. doi:10.1146/annurev.micro.61.080706.093341

39. Moosa MYS, Sobel JD, Elhalis H, Du W, Akins RA. Fungicidal Activity of Fluconazole against *Candida albicans* in a Synthetic Vagina-Simulative Medium. Antimicrob Agents Chemother. 2004;48: 161–167. doi:10.1128/AAC.48.1.161-167.2004

40. Bruzual I, Riggle P, Hadley S, Kumamoto CA. Biofilm formation by fluconazole-resistant *Candida albicans* strains is inhibited by fluconazole. J Antimicrob Chemother. 2007;59: 441–450. doi:10.1093/jac/dkl521

41. Baillie GS, Douglas LJ. Iron-limited biofilms of *Candida albicans* and their susceptibility to amphotericin B. Antimicrob Agents Chemother. 1998;42: 2146–2149.

42. Chandra J, Kuhn DM, Mukherjee PK, Hoyer LL, McCormick T, Ghannoum MA. Biofilm formation by the fungal pathogen *Candida albicans*: development, architecture, and drug resistance. J Bacteriol. 2001;183: 5385–94. doi:10.1128/JB.183.18.5385

43. Ramage G, Vandewalle K, Wickes BL, López-Ribot JL. Characteristics of biofilm formation by *Candida albicans*. Rev Iberoam Micol organo la Asoc Esp Espec en Micol. 2001;18: 163–170. doi:200118163 [pii]

44. Odds FC, Kerridge D. Morphogenesis in *Candida albicans*. CRC Crit Rev Microbiol. 1985;12: 45–93. doi:10.3109/10408418509104425

45. Ha KC, White TC. Effects of azole antifungal drugs on the transition from yeast cells to hyphae in susceptible and resistant isolates of the pathogenic yeast *Candida albicans*. Antimicrob Agents Chemother. 1999;43: 763–768.

46. Kumamoto CA. *Candida* biofilms. Current Opinion in Microbiology. 2002. pp. 608–611. doi:10.1016/S1369-5274(02)00371-5

47. Tobudic S, Kratzer C, Presterl E. Azole-resistant *Candida* spp. - Emerging pathogens? Mycoses. 2012;55: 24–32. doi:10.1111/j.1439-0507.2011.02146.x

48. Nett J, Lincoln L, Marchillo K, Andes D. ß-1,3 Glucan As a Test for Central Venous Catheter Biofilm Infection. J Infect Dis. 2007;195: 1705–1712. doi:JID37747 [pii]\r10.1086/517522

49. Nett JE, Sanchez H, Cain MT, Andes DR. Genetic Basis of *Candida* Biofilm Resistance Due to Drug-Sequestering Matrix Glucan. J Infect Dis. 2010;202: 171–175. doi:10.1086/651200

50. Taff HT, Nett JE, Zarnowski R, Ross KM, Sanchez H, Cain MT, et al. A *Candida* Biofilm-Induced Pathway for Matrix Glucan Delivery: Implications for Drug Resistance. PLoS Pathog. 2012;8. doi:10.1371/journal.ppat.1002848

51. Cuellar-Cruz M, Lopez-Romero E, Villagomez-Castro JC, Ruiz-Baca E, Cuellar-Cruz M, Lopez-Romero E, et al. *Candida* species: new insights into biofilm formation. [Review]. Future Microbiol. 2012;7: 755–771.

52. Nett J, Andes D. *Candida* albicans biofilm development, modeling a host-pathogen interaction. Current Opinion in Microbiology. 2006. pp. 340–345. doi:10.1016/j.mib.2006.06.007

53. Martins M, Uppuluri P, Thomas DP, Cleary IA, Henriques M, Lopez-Ribot JL, et al. Presence of extracellular DNA in the candida albicans biofilm matrix and its contribution to biofilms. Mycopathologia. 2010;169: 323–331. doi:10.1007/s11046-009-9264-y

54. Nett J, Lincoln L, Marchillo K, Massey R, Holoyda K, Hoff B, et al. Putative role of β-1,3 glucans in *Candida* albicans biofilm resistance. Antimicrob Agents Chemother. 2007;51: 510–520. doi:10.1128/AAC.01056-06

55. Nailis H, Vandenbosch D, Deforce D, Nelis HJ, Coenye T. Transcriptional response to fluconazole and amphotericin B in *Candida* albicans biofilms. Res Microbiol. 2010;161: 284–292. doi:10.1016/j.resmic.2010.02.004

CHAPTER 4

THE ROLE OF *CANDIDA ALBICANS* TRANSCRIPTION FACTOR *RLM1* IN RESPONSE TO CARBON ADAPTATION

Disclaimer

The work presented in this chapter has been previously published in *Frontiers in Microbiology*.

-

Oliveira-Pacheco J*, Alves R*, Costa-Barbosa A, Cerqueira-Rodrigues B, Pereira-Silva P, Paiva S, Silva S, Henriques M, Pais C and Sampaio P (2018) The Role of *Candida albicans* Transcription Factor *RLM1* in Response to Carbon Adaptation. *Front. Microbiol.* 9:1127. doi: 10.3389/fmicb.2018.01127

*These authors have contributed equally to this work.

-

ABSTRACT

Candida albicans is the main causative agent of candidiasis and one of the most frequent causes of nosocomial infections worldwide. In order to establish an infection, this pathogen supports effective stress responses to counter host defenses and adapt to changes in the availability of important nutrients, such as alternative carbon sources. These stress responses have clear implications on the composition and structure of *Candida* cell wall. Therefore, the impact of a physiologically relevant carbon source, lactate, on the activity of *C. albicans RLM1* transcriptional factor was studied. *RLM1* is involved in the cell wall integrity pathway and plays an important role in regulating the flow of carbohydrates into cell wall biosynthesis pathways. The role of *C. albicans RLM1* in response to lactate adaptation was assessed in respect to several virulence factors, such as the ability to grow under cell wall damaging agents, filament, adhere or form biofilm, as well as to immune recognition. The data showed that growth of *C. albicans* cells in the presence of lactate induces the secretion of tartaric acid, which has the potential to modulate the TCA cycle on both the yeast and the host cells. In addition, the adaptation of *C. albicans* cells to lactate was found to reduce their internalization by immune cells and consequent % of killing, which could be correlated with a lower exposure of the cell wall ß-glucans. In addition, absence of *RLM1* has a minor impact on internalization, compared with the wild-type and complemented strains, but it reduces the higher efficiency of lactate grown cells at damaging phagocytic cells and induces a high amount of IL-10, rendering these cells more tolerable to the immune system. The data suggests that *RLM1* mediates cell wall remodeling during carbon adaptation, impacting *Candida* interaction with immune cells.

4.1 INTRODUCTION

Candida albicans is an opportunistic pathogenic fungus responsible for a wide spectrum of infections in immunocompromised individuals, ranging from superficial mycosis to systemic and disseminated candidiasis [1,2]. These infections are estimated to cause 400,000 deaths each year, remaining by far the most common of all invasive fungal infections [1,3]. This pathogen thrives within distinct niches in the human host, including the skin, the oral cavity, the gut and the genitourinary tract [4]. These niches differ considerably in terms of nutrients, pH and local microbiota and, in order to survive and proliferate, *C. albicans* must adapt to the changing host environment. This extraordinary flexibility to adapt to the

different environmental conditions activates the expression of several virulence factors, affecting the resistance of this fungus to multiple stresses [5–7]. Like most microorganisms, *C. albicans* possesses a dynamic cell wall that responds efficiently to host-imposed stresses, including changes in carbon sources [8–10] or exposure to antifungal drugs [11]. This protection is conferred by a carbohydrate-based matrix containing chitin, β-glucans and mannoproteins, each of which has an important role in innate immune recognition [12]. For instance, the recognition of β-glucans by the receptor dectin-1, which is present at the cell surface of immune cells, promotes phagocytosis and killing by macrophages and neutrophils [13,14]. Consequently, any change in the structure of cell wall will therefore impact innate immune recognition and virulence [7]. Much of what is known about the fungal cell wall integrity (CWI) results from studying the yeast model *Saccharomyces cerevisiae*, where the CWI mitogen-activated protein kinase pathway (also known as the PKC pathway) is the main system responsible to repair the cell wall and maintain the cell integrity [15,16]. The targets of the CWI pathway activation are the Swi4-Swi6 cell cycle box-binding factor (SBF) [17] and the major effector the MADS-box transcription factor *RLM1* [18–20]. Although this pathway is conserved in *C. albicans*, the role of Rlm1 as the main transcriptional regulator of the cell wall stress responses is not conserved in this pathogenic species and other additional transcription factors, such as Cas5, have been proposed as key regulators in this pathway [21–24]. Even so, *C. albicans RLM1* gene has been shown to be required for cell wall integrity, at least under caspofungin, calcofluor white and congo red stresses [22,25]. This gene has also an increased genetic variability that has been associated with strain susceptibility to different stress conditions, with some genetic variations enhancing resistance [26]. Additionally, the absence of *RLM1* alters the cell wall content, specifically the chitin and the mannan layers, increasing cell adhesion *in vitro* and reducing virulence *in vivo* [25]. Some findings also suggested that this gene participates in the cell wall biogenesis, particularly in regulating the flow of carbohydrates into cell wall biosynthesis pathways [25]. Here, the involvement of *C. albicans RLM1* on cell wall biogenesis and virulence during carbon source adaptation is explored. To approach this, *C. albicans* cells were grown in the presence of lactate, a particularly abundant metabolite in several host niches [27,28]. Exposure to the alternative carbon source lactate is particularly relevant as it has been shown to affect the cell wall architecture of *C. albicans* [8–10]. In order to understand whether *RLM1* is involved in this process, two *RLM1* mutant strains adapted to lactate were characterized with respect to several virulence factors, such as the ability to grow under cell wall damaging agents, filament, adhere or form biofilm. The involvement of *RLM1* in host-pathogen interaction was also assessed, providing new insights into the role of *C. albicans RLM1* in cell wall regulatory responses and pathogenicity.

4.2 MATERIAL AND METHODS

4.2.1 Strains and growth conditions

Five *C. albicans* strains were used during this study: the wild type (WT) SC5314 strain [29], two *RLM1* mutant strains (SCRLM1M4A and SCRLM1M4B) and two *RLM1* complemented strains (SCRLM1K2A and SCRLM1K2B) [25]. All strains were stored as frozen stocks with 30% (v v^{-1}) glycerol and routinely cultured on YPD agar plates (1% yeast extract, 2% peptone, 2% dextrose and 2% agar) stored at room temperature. For all experiments, a pre-inoculum was prepared by collecting one colony from the YPD plate and allowing the cells to adapt to minimal medium containing either 2% glucose or 2% lactate, and 0.67% yeast nitrogen base (YNB) without amino acids (pH 5.2 to 5.6) at 30°C, overnight (for glucose) or during 24 h (for lactate). The inoculum was then prepared with adapted cells into new medium, diluting the cells to an optical density (OD 600nm) of 0.1, and allowing the cells to grow.

4.2.2 High-performance liquid chromatography

C. albicans cells were grown in YNB 2% glucose or YNB 2% lactate (30°C, 200 rpm) as previously described and, at different time points, 1 mL of cell cultures were harvested by centrifugation (5 min, 5000 *g*). The supernatants were then prepared and analyzed for the detection of different organic acids, including glucose, glycerol, and ethanol by high-performance liquid chromatography (HPLC). Culture supernatant samples were treated with 10% trichloroacetic acid to remove protein contaminants, centrifuged for 15 min at 14,000 rpm, and then filtered through a 0.22-µm filter before analysis. HPLC analysis was performed in a Rezex 8 µm ROA-organic acid H+ (8%) HPLC column (Phenomenex) with an Elite LaChrom (VWR Hitachi) chromatography system [30]. A total of 2.5 mM H_2SO_4 was used for the mobile phase, the column was maintained at 60°C, and detection was by refractive index measurement with an Elite LaChrom L-2490 RI detector (VWR Hitachi) at 40°C. Samples from at least five independent replicates were analyzed.

4.2.3 Susceptibility assays

Fungal cells were incubated overnight in YNB 2% glucose or YNB 2% lactate (30°C, 200 rpm), diluted to OD(600nm) = 0.05-0.1 and left to grow until OD ≈ 1 with fresh medium. Drop tests were performed by spotting 5 µL of the serially diluted cell suspension onto YNB 2% glucose or 2% lactate agar plates supplemented with the following compounds individually: 200 µg mL^{-1} calcofluor white, 100 µg mL^{-1} congo

red, 90 ng mL^{-1} caspofungin, 10 mM caffeine and 0.035% (w v^{-1}) SDS. Plates were incubated for 48 h at 30°C before observation. A minimum of three independent replicates was performed.

4.2.4 Filamentation tests

All strains were grown overnight in YNB 2% glucose or YNB 2% lactate (30°C, 200 rpm), diluted to OD(600nm) = 0.05-0.1 and left to grow until OD ≈ 1 with fresh medium. Cells were then spin down, rinsed two times with PBS, diluted to the same volume with Dulbecco's modified Eagle's medium (DMEM) and incubated at 37°C and 5% CO_2. In order to observe the filamentation, yeast cells were stained with calcofluor white and monitored by fluorescence microscopy (Leica, DM5000B). Hyphal length was then measured with ImageJ 1.51s (NIH, United States). A minimum of 50 cells from each condition was measured in images taken from three independent replicates.

4.2.5 Adhesion and biofilm formation assays

To determine the impact of different carbon sources on adhesion and biofilm formation ability, 24-well microplates (Orange Scientific, Braine-l'Alleud, Belgium) were filled with *C. albicans* cell suspensions (containing $1x10^5$ cells per mL) grown on each carbon source until reaching stationary phase (20 h for glucose grown cells and 40 h for lactate-grown cells) as described above, and incubated at 37°C, 120 rpm. Adhesion and biofilm formation were assessed through quantification of total biomass by crystal violet (CV) staining [31]. The measurements were performed after 2 h of incubation for adhesion ability and the biofilm formation was assessed after 24 and 48 h. At 24 h, 500 µL of cultured medium was removed and replaced by fresh medium. After the defined times of incubation, the medium was aspirated and non-adherent cells removed by washing the wells with sterile ultra-pure water. For total biomass quantification, cells were fixed with 1 mL of methanol during 15 min. After that, the methanol was removed, the plates were allowed to dry at room temperature and 1 mL of CV (1% v v^{-1}) was added to each well. After 5 min, the wells were gently washed with sterile, ultra-pure water and 1 ml of acetic acid (33% v v^{-1}) was added to release and dissolve the stain. The absorbance of the obtained solution was read in triplicate in a microtiter plate reader (SpectraMax Plus) at 570 nm. Results were presented as absorbance per area of the wells (abs cm^{-2}), from three independent replicates.

4.2.6 Scanning electron microscopy

The biofilm structure was observed by scanning electron microscopy (SEM). For that, biofilms were formed in 24-wells polystyrene microtiter plates (Orange Scientific, Braine-l'Alleud, Belgium) with 1 mL of

$1x10^5$ cells suspensions, as described previously. After 48 h of incubation the formed biofilms were washed with PBS, dehydrated with alcohol (using 70% ethanol for 10 min, 90% ethanol for 10 min and 100% ethanol for 20 min) and air-dried. Prior to observation, the base of the wells were mounted onto aluminum stubs, sputter coated with gold and observed with an Ultra-high resolution Field Emission Gun Scanning Electron Microscopy (FEG-SEM; Nova NanoSem 200, FEI Company, OR, USA).

4.2.7 Quantification of β-glucan exposure

Quantification of β-glucans was performed as described previously [10], with some modifications. Briefly, *C. albicans* cells were grown in YNB 2% glucose or YNB 2% lactate and collected at stationary phase, as described above. A total of $2.5x10^6$ cells were counted with a hemocytometer, and washed with cold FACS buffer (1x PBS, 1% FBS, 0.5 mM EDTA). Cells were then resuspended in 100 µL FACS buffer + 5 ng $µL^{-1}$ anti-β-1,3-glucans (BioSupplies) and incubated in the dark on ice for 1 h. Cells were washed (5,000 rpm, 3 min) twice in FACS buffer, resuspended in 100 µL FACS buffer plus 1:200 anti-mouse IgG conjugated to Alexafluor 647 (Invitrogen) and incubated in the dark on ice for 1 h. Cells were washed as above, fixed in 4% formaldehyde, diluted in FACS buffer, washed again, and analyzed by flow cytometry (BD LSR II, Becton Dickinson) using FACSDiva software. For each experiment, at least 20,000 events were acquired for each sample. As a control, aliquots from all cells to be analyzed were pooled, diluted to $2.5x10^6$ cells and treated as above except that no anti-β-1,3-glucan was added. Median fluorescence intensities (MFIs) were determined using FlowJo software (Tree Star, v 10.2) and reported for each sample. Plots are representative of two independent assays.

4.2.8 Phagocytosis assays

All experiments were conducted with the approval of the Ethical Committee Board of the Portuguese Veterinary Directorate and they all adhered to local and institutional policy requirements. Single-cell suspensions of bone marrow cells were prepared by aseptically removing femurs from C57BL/6J wild-type mice. Bones were cut on both ends and marrow was flushed with ice-cold supplemented RPMI 1640 (10% heat-inactivated FBS, 10 mM HEPES, 1 mM NaPyruvate, 2 mM L-glutamine, 50 mg mL^{-1} streptomycin, and 50 U mL^{-1} penicillin, all from Merck). Bone marrow cells were then resuspended in RPMI 1640 supplemented with M-CSF (20 ng mL^{-1} Peprotech) and seeded in a 24-well plate at $5×10^5$ cells per well. Cells were incubated for 7 days at 37°C with 5% CO_2. After 4 days of incubation, 1 mL of fresh RPMI 1640 supplemented with M-CSF (20 ng mL^{-1}, Peprotech) and seeded in a 24-well plate at $5x10^5$ cells per well. Cells were incubated for 7 days at 37°C with 5% CO_2. After 4 days of incubation, 1

mL of fresh RPMI 1640 supplemented with M-CSF was added. For fluorescence microscopy assays, macrophages were incubated in the presence of sterile glass coverslips (diameter 13 mm). On the day of co-culture, macrophages were washed with sterile PBS and fresh medium was added. *C. albicans* grown in YNB 2% glucose or YNB 2% lactate until stationary phase, as described before, were fixed with formol-ethanol (1:9) for 10 min, washed five times with sterile PBS, and incubated for 10 min with Sytox Green at room temperature in the dark. Yeast cells were then washed with sterile PBS to remove unbound dye and brought to the desired cell density in RPMI 1640. Macrophages were incubated with labeled yeast suspensions at a multiplicity of infection (MOI) of 5Y:1M ratio, for 30 min at 37°C and 5% CO_2. After incubation plates were kept on ice to stop phagocytosis, and wells rinsed twice with PBS to remove unbound yeasts. Macrophages and associated yeasts were then incubated with Propidium Iodide (PI) at a final concentration of 6 µg mL^{-1}, for 5 min at room temperature [32]. Cells were analyzed by flow cytometry (BD LSR II, Becton Dickinson) and by fluorescence microscopy (Leica DM5000B). Cytometry data was analyzed using FlowJo software (Tree Star, v 10.2) and fluorescence microscopy images using ImageJ cell counter software. All experiments were done in duplicate and results were obtained from three independent experimental assays.

4.2.9 Host viability assays

The yeast killing assay was performed as described previously [33]. Macrophages and yeast cells, adapted to each carbon source, were cultured in a 96-well tissue culture plate (SpectraMaxPlus), and incubated for 1 h at a MOI 5Y:1M ratio. After incubation, the 96-well tissue culture plate was centrifuged for 2 min at 750 *g* and 80 µL of supernatant was transferred to a new 96-well microplate and stored at -80°C for further analysis. The final volume was restored by adding 80 µL of 10% saponin followed by gently up and down pipetting in order to lyse macrophages and release the adhered cells. Wells with *Candida* alone and incubated in the same conditions represented 100% viability. Serial 10-fold dilutions were then plated on YPD agar and incubated at 30°C for 24 h. Lactate dehydrogenase (LDH) activity was measured in the supernatant of the yeast killing assay. Each reaction contained 40 µL of extracellular LDH, 250 µl of NADH (0.28 mM) and 10 µL of pyruvate (0.32 mM). Both NADH and pyruvate solutions were prepared in 0.05 M phosphate buffer pH 7.4. NADH conversion to NAD^+ was spectrophotometrically evaluated in a microplate reader (Molecular Devices, SPECTRAmax Plus 384) at 340 nm, every 10 s for 3 min, at 30°C [34]. MTT assay was used to evaluate metabolic activity of 10^5 macrophages per mL (cell line RAW 264.7) supplemented with tartaric acid (0.075 g L^{-1}). Briefly, after tartaric acid incubation, for 24 and 72h, the supernatants were removed and cells were incubated with MTT solution (final

concentration 0.45 mg mL^{-1}) for 2h at 37°C and 5% CO_2. Then, the supernatant was discarded, the formazan crystals resuspended in DMSO-Ethanol 1:1 (v v^{-1}) and final absorbance measured at 570 nm in the SPECTRAmax Plus 384 microplate reader. TNF-α and IL-10 levels were quantified using commercially available sandwich ELISA kits (Quantikine, R&D Systems, Abingdon, United Kingdom and KMC0102, Biosource, Camarillo, CA, United States, respectively) according to manufacturer's instructions. All experiments were carried out in triplicate.

4.2.10 Statistical analyses

Statistical analyses were performed using Graph Pad Prism (v. 7) and significance was determined using two-way ANOVA with Tukey's multiple comparison test. All tests were performed with a confidence level of 95%.

4.3 RESULTS

4.3.1 Characterization of *C. albicans* growth and metabolism on lactate

The major role of *C. albicans RLM1* was proposed to be in the biogenesis of the cell wall, particularly in regulating the flow of carbohydrates into cell wall biosynthesis pathways [25]. However, these conclusions were based in experiments using *C. albicans* cells grown on media containing 2% glucose, leaving the effects of other host carbon sources, such as lactate, largely unexplored. Here, a set of *RLM1* null mutants previously constructed from the prototrophic WT model strain SC5314 [25] was used to evaluate phenotype and impact on immune recognition when cells are exposed to different carbon sources: glucose or lactate.

Slow growth of the mutant strains may lead to differences in phenotypes, thus WT, mutant, and complemented *C. albicans* cells were grown on minimal medium in which the sole carbon sources were glucose or lactate (Figure 4.1). As reported previously [25], the growth rate of the different strains was unaffected in minimal medium with glucose (Figure 4.1). The doubling time of the mutant in glucose was 4.9 h, with no significant difference to the WT strain (4.5 h) or complemented strain (4.5 h). In contrast, growth was significantly slower for all strains, when lactate was the sole carbon source (Figure 4.1). The doubling time of the mutant in lactic acid was 17.7 h, with no significant difference to the WT strain (17.3 h) or complemented strain (16.5 h). Therefore, the loss of *RLM1* did not affect growth rate on any carbon source.

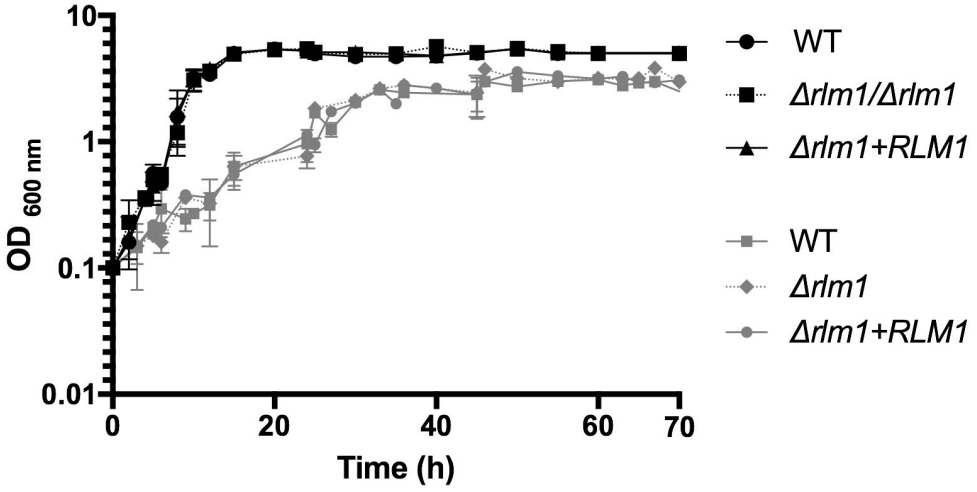

Figure 4.1. Growth of *C. albicans RLM1* wild type (WT), mutant and complemented strains. *C. albicans* WT, homozygous mutants (Δ*rlm1*/Δ*rlm1*) and complemented (Δ*rlm1*+*RLM1*) strains were grown in

minimal YNB medium containing 2% of glucose (black lines) or lactate (gray lines), as the sole carbon source. Growth was monitored by optical density. Presented results are mean values displaying standard deviation ($n \geq 5$).

The production of several metabolites by the different strains during growth either in glucose or lactate was also evaluated (Figure 4.2). After 20 h of growth in the presence of glucose, this carbon source was totally consumed and, as expected, all strains produced mainly glycerol, ethanol and acetic acid (Figure 4.2). In contrast, during growth in lactate, the consumption of this carbon source was slower, stabilized after 45 h of growth and less than 20% of the initial amount was consumed (Figure 4.2). This consumption was significant after 45 h ($p < 0.05$) for the WT and complemented strains but not for the mutant ($p = 0.2056$). During this time, no ethanol, acetic acid, nor glycerol were detected (Figure 4.2), since this is a non-fermentative carbon source. Curiously, the production of a small amount of tartaric acid was observed only with lactate-grown cells (Figure 4.2). However, the loss of *RLM1* did not significantly affect the metabolic usage of each carbon source.

4.3.2 *C. albicans RLM1* hypersensitivity to congo red is rescued by growth on lactate

In order to evaluate the impact of an alternative carbon source on the role of *C. albicans RLM1*, the sensitivity of the WT, Δ*rlm1*/Δ*rlm1* mutant and complemented strains to a range of cell wall-perturbing agents in the presence of glucose or lactate was determined. In glucose medium, WT strains were able to grow well in the presence of all the compounds except in caspofungin, with the homozygous mutants being more sensitive. The mutant strains presented hypersensitivity to congo red when compared with complemented and parental strains (Figure 4.3A), as previously reported [22,25]. In contrast, in the presence of lactate, all strains presented high sensitivity to SDS, caffeine and caspofungin (Figure 4.3B). In the absence of a functional *RLM1*, *C. albicans* cells grown in the presence of lactate showed more sensitivity to caspofungin, when compared to their glucose counterparts. However, the hypersensitivity to congo red observed with these cells grown in glucose diminished greatly. This result indicates that when grown in lactate, cells are more sensitive to cell wall stressing agents but, curiously, the absence of a functional *RLM1* rescues the hypersensitivity to congo red observed in glucose grown cells (Figure 4.3B).

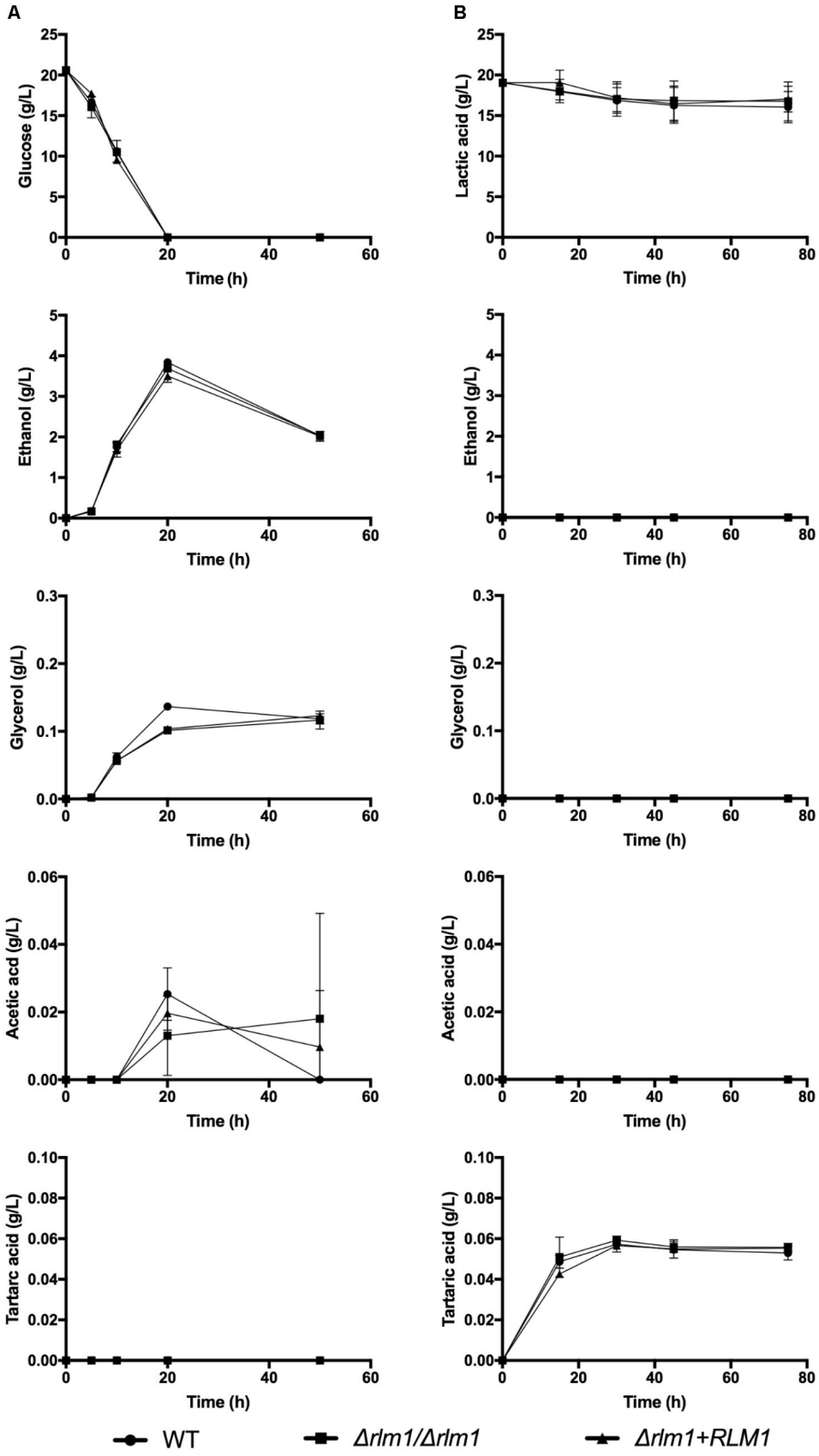

Figure 4.2. Identification of *C. albicans* metabolites during growth on different carbon sources by HPLC.

C. albicans wild type (WT), homozygous mutants (Δ*rlm1*/Δ*rlm1*), and complemented (Δ*rlm1*+*RLM1*)

strains were grown in YNB 2% glucose **(A)** or lactate **(B)**. Glucose and lactate consumption and the variations in glycerol, ethanol, acetic acid and tartaric acid levels were monitored at different time-points by HPLC. Results represent mean values with respective standard deviation (n ≥ 5).

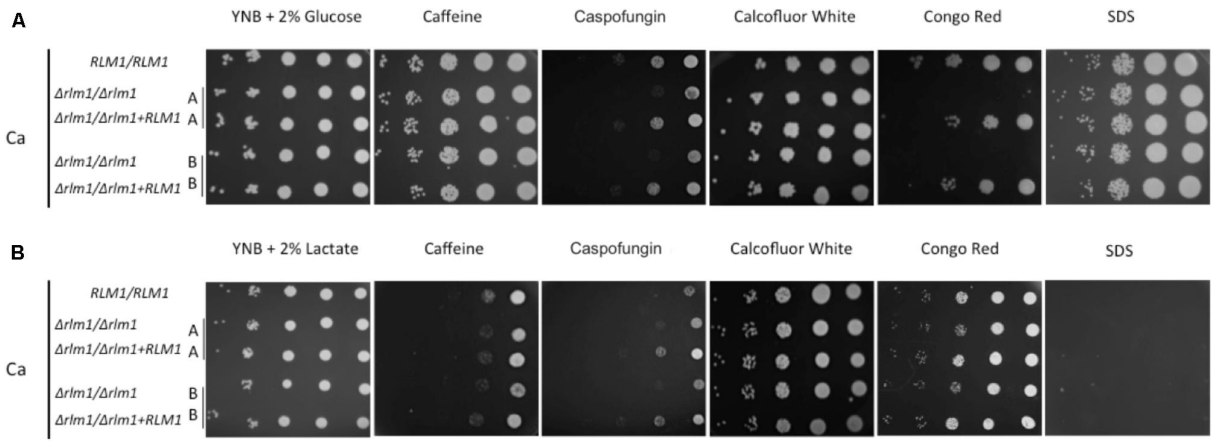

Figure 4.3. Sensitivity of *C. albicans* wild type (WT), mutant (Δ*rlm1*/Δ*rlm1*), and complemented (Δ*rlm1*+*RLM1*) strains to several agents that affect cell integrity. (A) Serial 10-fold dilutions of overnight cultures were spotted on YNB 2% glucose or **(B)** YNB 2% lactate plates with 10 mM caffeine, 90 ng ml^{-1} caspofungin, 200 μg ml^{-1} calcofluor white, 100 μg ml^{-1} congo red, and 0.035% SDS for 2 days at 30°C. Images are representative of three independent experiments.

4.3.3 The transcription factor *RLM1* is important for *C. albicans* filamentation and biofilm formation

Filamentation and biofilm formation represent two of the major virulence factors contributing to *Candida* pathogenesis. A previous work using Δ*rlm1*/Δ*rlm1* mutant strains grown on glucose-containing media has shown a higher upregulation of proteins involved in adhesion and biofilm formation [25]. Additionally, some studies have demonstrated that lactate-grown cells display higher ability to adhere and form biofilm when compared with glucose-grown cells [35,36]. Based on these studies, Δ*rlm1*/Δ*rlm1* mutant strains were tested regarding their ability to filament (Figure 4.4), to adhere to a polystyrene surface (Figure 4.5A), and to form biofilm after 24h (Figure 4.5B) and 48h (Figure 4.5C) of incubation, in the presence of lactate.

For filamentation analysis, glucose- and lactate-grown cells were incubated in induced media for 30, 60, 120 and 240 min, stained with calcofluor white and monitored by fluorescence microscopy. Independently of the condition, all strains were able to filament and hyphae length increased with time.

In glucose-grown cells, filaments were visible right after 30 min of incubation, while in lactate-grown cells only after 60 min (Figure 4.4). Moreover, lactate-grown cells presented shorter hyphae than glucose-grown cells. The lack of a functional *RLM1* affected filamentation of cells adapted to both carbon sources, and although the differences in hyphae length were visible in early time points, only after 240 min of incubation the differences were significant ($p < 0.001$). This difference was more pronounced in cells grown on glucose (Figure 4.4).

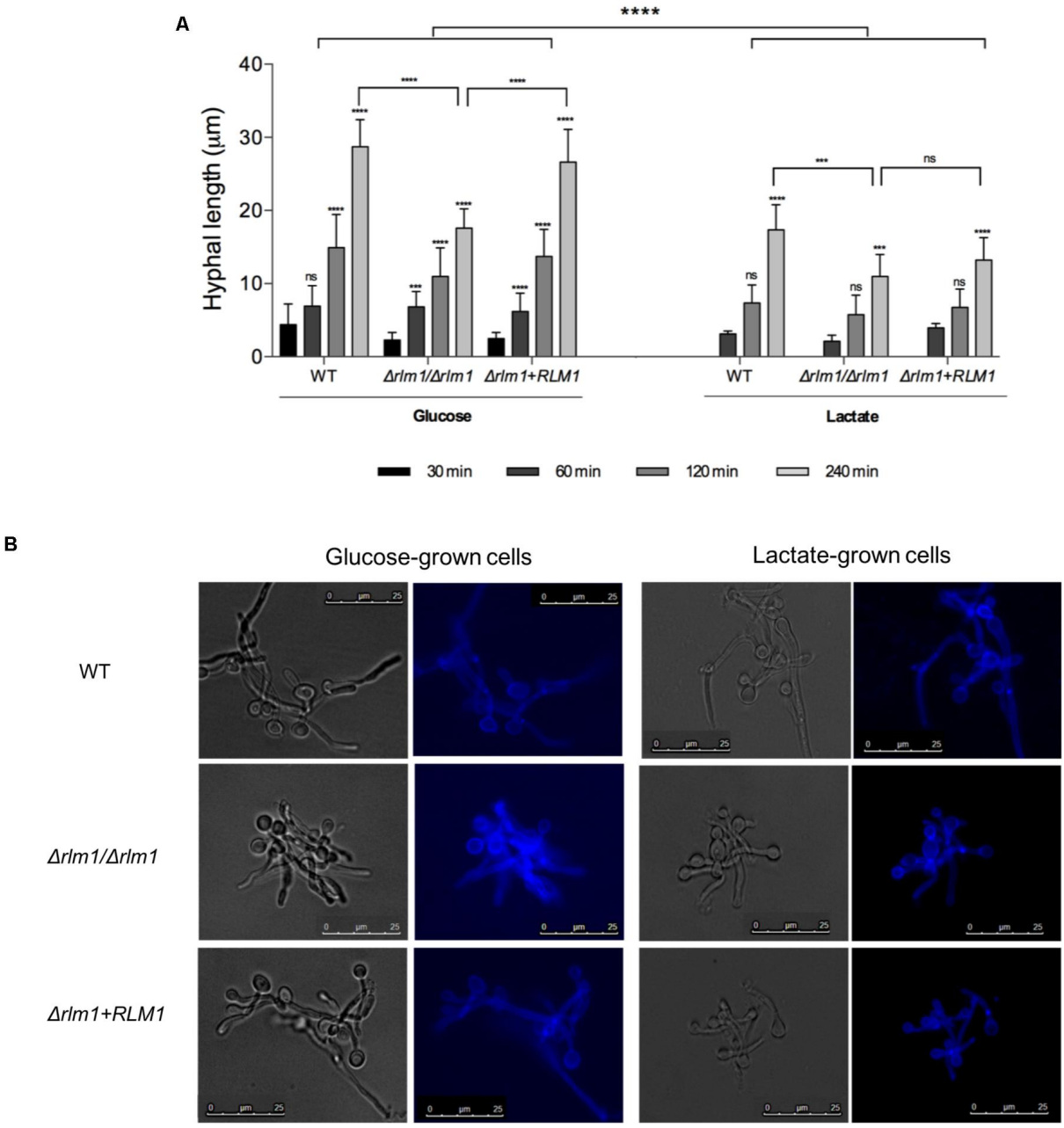

Figure 4.4. Filamentation of *C. albicans* wild type (WT), mutant (*Δrlm1/Δrlm1*) and complemented strains (*Δrlm1+RLM1*). (A) Hyphal length of glucose and lactate-grown cells measured after 30, 60, 120, and 240 min of incubation in DMEM medium supplemented with 10% FEBS at 37°C. Results represent

mean and standard deviation of three independent replicates. *$p < 0.05$, ** $p < 0.01$, ***$p < 0.001$, and ****$p < 0.0001$ indicate statistically significant results; ns indicates not significant. For each strain and condition, *p* values were always calculated in comparison with the previous time point. **(B)** Morphology of glucose and lactate grown cells after 240 min of incubation in DMEM. *Candida* cells were stained with calcofluor white and monitored by fluorescence microscopy. Images are representative of three independent experiments.

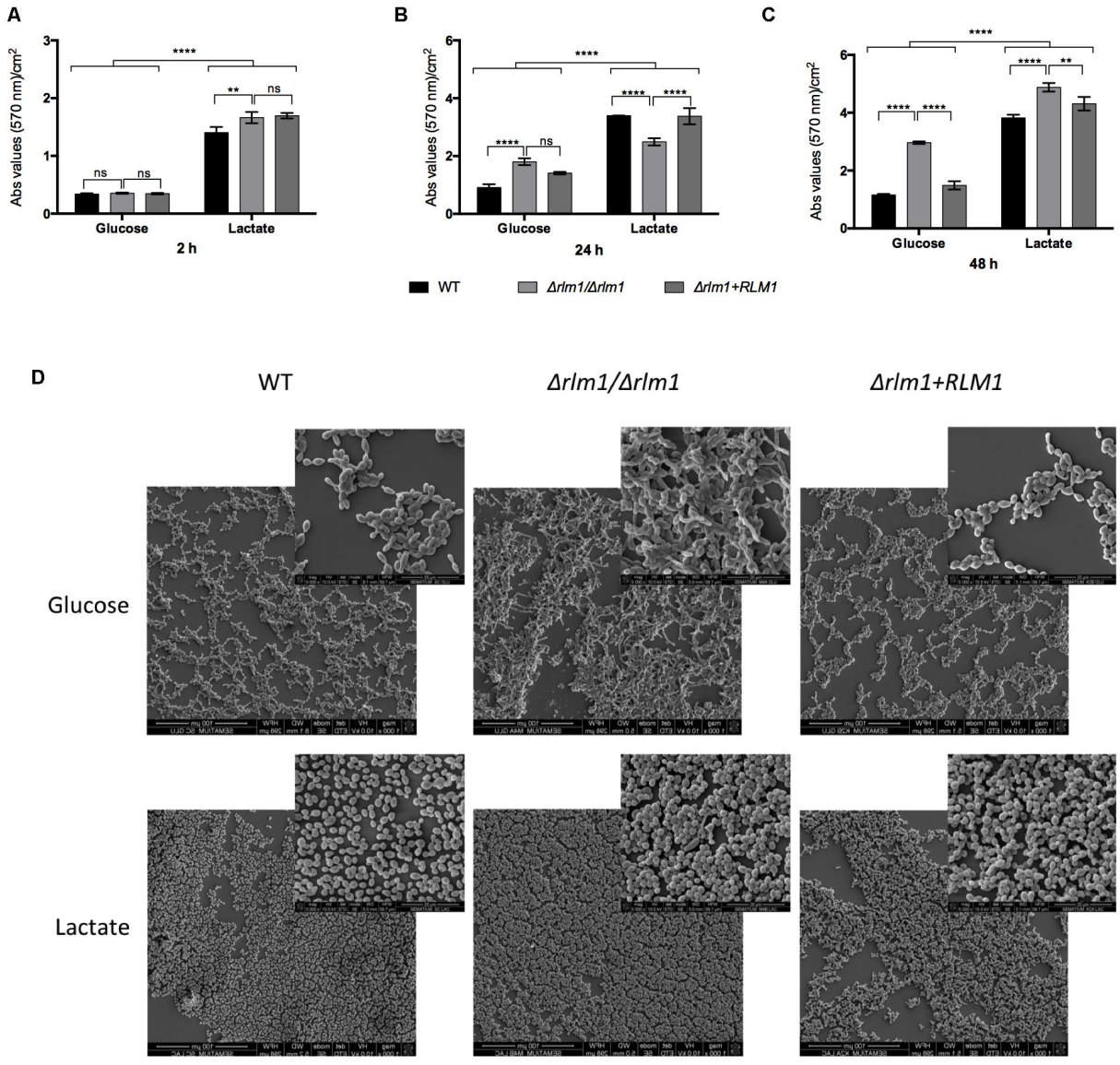

Figure 4.5. ***In vitro*** **adhesion and biofilm formation of** ***C. albicans*** **wild type (WT), mutant (*Δrlm1/Δrlm1*), and complemented strains (*Δrlm1+RLM1*). (A)** WT, *Δrlm1/Δrlm1* and *Δrlm1+RLM1* cells were allowed to adhere 2 h and **(B)** to form biofilm during 24 h and **(C)** 48 h in a polystyrene surface. Results represent mean values and standard deviation of three independent replicates ($n = 3$ per group per experiment).

*$p < 0.05$, ** $p < 0.01$, ***$p < 0.001$, and ****$p < 0.0001$ indicate statistically significant results; ns indicates not significant. **(D)** Representative SEM images of cells after 48 h of incubation.

Then, all strains were evaluated regarding their ability to adhere to a polystyrene surface. After 2h of incubation, lactate-grown cells showed a higher ability to adhere when compared with the glucose-grown cells ($p < 0.0001$), as previously reported [35], and no differences were seen regarding the Δ*rlm1*/Δ*rlm1* mutant strain (Figure 4.5A). Considering biofilm formation, cells grown in lactate were able to form more biofilm than cells grown in glucose. As expected, Δ*rlm1*/Δ*rlm1* mutant formed more biofilm than the WT in presence of glucose at 24 and 48 h of incubation (Figures 4.5B and C). However, in the presence of lactate, at 24 h of incubation the mutant presented lower biofilm formation but at 48 h the amount of biofilm formed was higher than the WT and complemented strains (Figure 4.5B and C). SEM analyses confirmed the differences in biofilm formation after 48 h of incubation (Figure 4.5D). These results showed that lactate-grown cells presented higher biomass than their glucose counterparts and the mutant presented higher biofilm formation in both conditions, after biofilm maturation.

Overall, these results indicate that *RLM1* is important for filamentation, adhesion, and biofilm formation and that these phenotypes were similar for cells adapted to glucose or to lactate, suggesting that they are independent of the carbon source.

4.3.4 *C. albicans RLM1* does not affect immune recognition but is important for immune activation

In order to determine the importance of *C. albicans RLM1* in cell wall remodeling, the growth of the different strains in the presence of the alternative carbon source lactate was tested to check whether it would influence the interaction with phagocytic cells (Figure 4.6). It was previously shown that the absence of *C. albicans RLM1* on glucose grown cells significantly alters the proportions of the major cell wall components, enhancing the chitin content and reducing the glucan and mannan content [25]. However, nothing about the exposure of these components was previously observed. Thus, as the host immune defenses rely on the recognition of conserved molecular patterns in the fungal cell wall, particularly the glucans, the exposure of β-glucans at the cell surface of *C. albicans* cells grown either in the presence of glucose or lactate was analyzed. All cells were stained with anti-β-1,3-glucan and analyzed by flow cytometry. Glucose-grown cells exhibited significantly ($p < 0.0001$) higher levels of β-glucan exposure than lactate-grown cells (Figure 4.6A), consistent with previously published data [10]. Although

the mutant seemed to present a different pattern of β-glucan exposure in both carbon sources, the differences were not significant.

To evaluate the phagocytosis of *C. albicans* cells, a previously described assay [31] was used, which allowed the identification of different macrophage populations by differential staining. In this way, macrophages with only internalized *C. albicans* cells (sytox green-stained) and with both internalized and surface adhered cells (PI and sytox green double stained) were clearly distinguished. As previously described, results indicate that glucose-grown cells are internalized more efficiently by murine bone marrow-derived macrophages (BMDMs) compared to lactate-grown cells (Figure 4.6B) [9]. In contrast, lactate-grown cells displayed higher levels of adhesion than glucose-grown cells (Figure 4.6B). However, no significant changes were observed between the WT and Δ*rlm1*/Δ*rlm1* mutant strains under these conditions (Figure 4.6B). Representative fluorescence microscopy analyses are shown in Figure 4.6C.

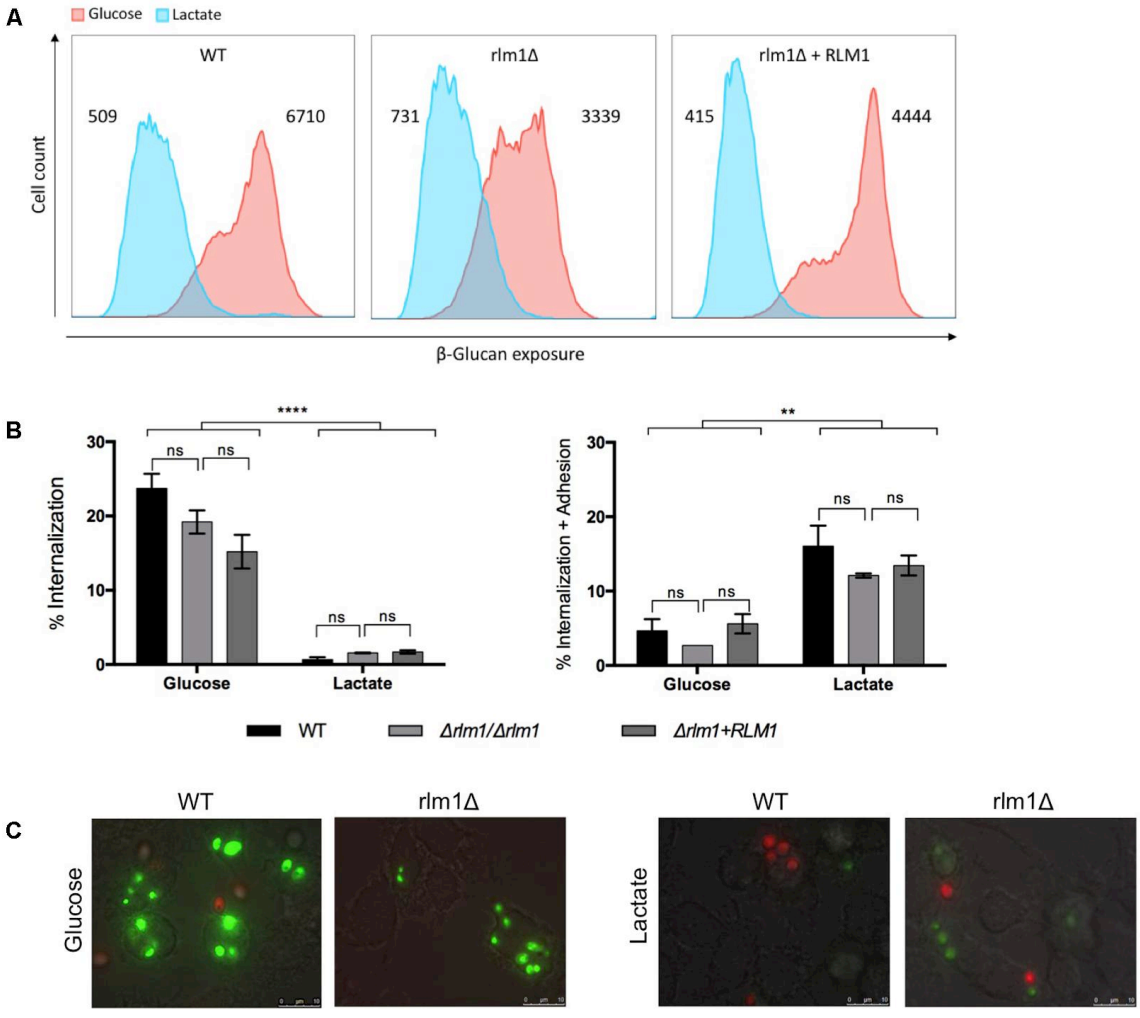

FIGURE 4.6. Immune recognition of *C. albicans* wild type (WT), mutant (Δ*rlm1*/Δ*rlm1*), and complemented strains (Δrlm1+*RLM1*). (A) Flow cytometry analysis of β-glucan exposure for cells grown

either in YNB 2% Glucose (red) or in YNB 2% Lactate (blue). MFIs are indicated at the top of each panel and plots are representative of two independent replicate experiments (n = 3 per group per experiment). **(B)** Flow cytometry analysis of phagocytosis after 30 min of incubation with macrophages. Graphs represent the % of macrophages with internalized yeast cells (left), and the % of macrophages with internalized and adhered yeasts (right). $^{*}p < 0.05$, $^{**}p < 0.01$, $^{***}p < 0.001$, and $^{****}p < 0.0001$ indicate statistically significant results; ns indicates not significant. Plots are representative of three independent replicate experiments (n = 3 per group per experiment). **(C)** Representative micrographs showing macrophages with internalized (green labeled) or adhered (red labeled) yeast cells grown either in YNB 2% glucose or in YNB 2% Lactate.

Additionally, the effect of *RLM1* on phagocyte interaction and activation was assessed. For that, macrophages were infected with *C. albicans* cells, previously grown in glucose or lactate, in a MOI of 5 yeasts to 1 macrophage for 1 h. The uptake of live fungal cells by macrophages was measured by colony-forming units (CFUs) and presented in percentage of yeast killing (Figure 4.7A). Results indicated that WT and complemented lactate-grown cells were less efficiently killed by macrophages than their glucose counterparts (Figure 4.7A), as previously reported [9]. However, no significant differences were observed between the Δ*rlm1*/Δ*rlm1* mutant strain adapted to glucose in comparison to lactate, suggesting that the mutant lost part of its resistance to killing.

The cell damage caused by the different strains was also quantified by measuring the amount of lactate dehydrogenase (LDH) released by murine macrophages after 1 h of incubation with yeast cells (Figure 4.7B). Results showed that the WT and complemented strains adapted to glucose led to a lower production of LDH than their lactate counterparts, resulting in higher percentage of viable macrophages ($p < 0.001$; Figure 7B). In contrast, the Δ*rlm1*/Δ*rlm1* mutant strain was able to cause less damage in the murine macrophages when cells were grown on lactate, in comparison with glucose, indicating that it also lost its ability to kill macrophages when grown in lactate. These results suggest that *RLM1* is involved in cell damage but when cells are grown in lactate.

Cell activation was also evaluated by quantifying IL-10 and TNF-α after 1 h of co-incubation (Figures 4.7C and D). Results showed that glucose-grown cells stimulated less production of TNF-α (Figure 4.7D) and IL-10 (Figure 4.7C), compared to lactate-grown cells, consistent with previously published data [9]. Furthermore, the Δ*rlm1*/Δ*rlm1* mutant strain grown in lactate showed higher levels of IL-10 when

compared with WT ($p < 0.001$) and complemented ($p < 0.001$) strains (Figure 4.7C), while when grown in glucose the results were the opposite. The same results were observed considering TNF-α secretion (Figure 4.7D), confirming that *RLM1* is relevant for immune activation. Overall, these results indicate that *RLM1* does not mediate immune recognition but is important in immune cell resistance and activation, particularly in cells grown in lactate.

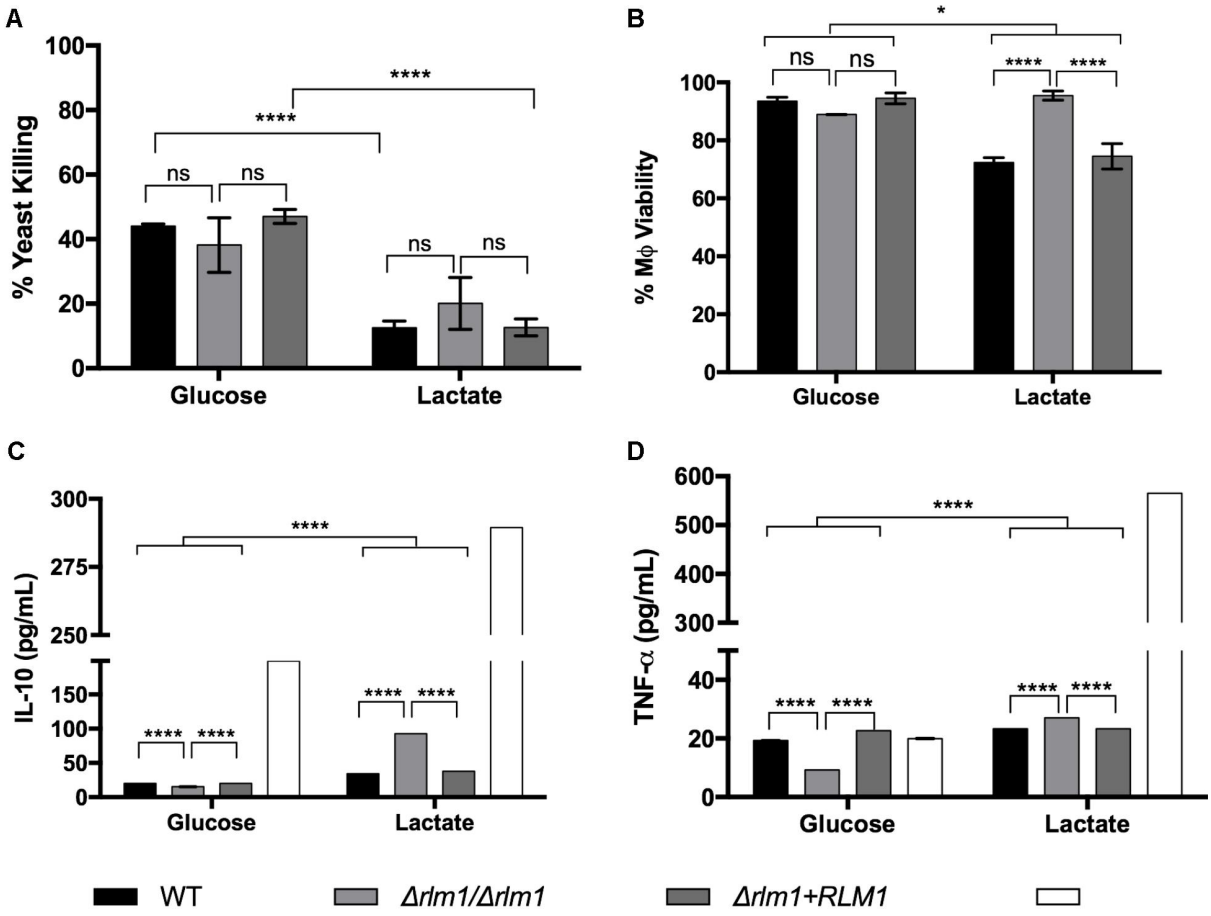

FIGURE 4.7. Host viability and immune response to *C. albicans* wild type (WT), mutant (*Δrlm1/Δrlm1*), and complemented (*Δrlm1+RLM1*) cells grown on glucose or lactate after 1 h of infection. (A) Killing of yeast cells adapted to glucose or lactate and incubated with macrophages at 5:1 ratio. Results are expressed as the percentage of yeast killing. **(B)** Assessment of host viability by measuring LDH released by murine macrophages. Concentrations of IL-10 **(C)** and TNF-α **(D)** detected in culture supernatants of murine macrophages after incubation with the yeast cells. $^{*}p < 0.05$, $^{**}p < 0.01$, $^{***}p < 0.001$, and $^{****}p < 0.0001$ indicate statistically significant results; ns indicates not significant. Plots are representative of three independent replicate experiments ($n = 3$ per group per experiment). Mϕ indicates macrophages alone (near glucose) or incubated with LPS (near lactate).

Finally, in order to evaluate whether tartaric acid could contribute for cellular cytotoxicity, we incubated macrophages with this organic acid and evaluate metabolic activity by MTT assay. Results showed that, after 72 h of incubation, tartaric acid reduces cellular viability by around 35% (Figure 4.8).

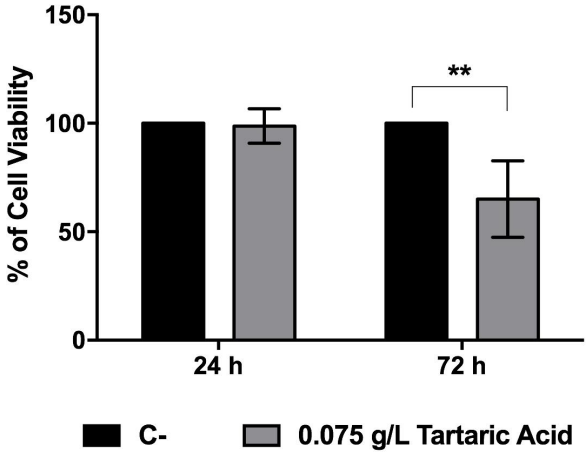

FIGURE 4.8. Host viability after incubation with tartaric acid. Macrophages were incubated with tartaric acid at a final concentration of 0.075 g L^{-1} for 24 and 72 h. Results express the percentage of macrophage viability. $^{*}p < 0.05$, $^{**}p < 0.01$, $^{***}p < 0.001$, and $^{****}p < 0.0001$ indicate statistically significant results; ns indicates not significant. Plots are representative of three independent replicate experiments ($n = 3$ per group per experiment). C– indicates macrophages incubated with DMEM alone.

4.4 DISCUSSION

C. albicans has the ability to survive and proliferate within distinct niches in the human host. This flexibility requires a rapid adaptation to the local conditions, forcing the pathogen to utilize the alternative nutrients that are available. Some of these niches contain glucose, the preferred carbon source of *C. albicans*, while others contain different carboxylic acids such as lactate [27,28]. These fluctuations on carbon sources affect profoundly the physiology of *C. albicans*, including alterations in the cell wall structure that impact immune recognition [8–10]. The transcription factor *RLM1* has been shown to play an important role in the maintenance of the cell wall, affecting the adhesion ability and virulence [22,25]. However, the *in vitro* dissection of these observations has been performed using *C. albicans* cells grown on artificial media containing 2% glucose, a condition that does not accurately reflect the host niches where this fungus can proliferate. Therefore, we studied the role of *C. albicans RLM1* during growth on the physiologically relevant nutrient lactate, using a set of previously constructed Δ*rlm1*Δ/ *rlm1* mutants [25].

Firstly, the growth and metabolism of all strains in glucose or in lactate were characterized (Figures 4.1 and 4.2). As expected, the growth rate of cells grown in glucose was much higher than cells grown in lactate. The absence of a functional *RLM1* did not affect growth rate in both carbon sources. Cells grown in glucose were able to consume the totality of this carbon source within the first 20 h of growth, and produced glycerol, ethanol, and acetic acid, all known fermentative metabolites (Figure 4.2). However, when cells were grown in the presence of lactic acid, they consumed only a small part of the carbon source and none of the above metabolites were observed, but tartaric acid was detected (Figure 4.2). Tartaric acid is an analog of malic acid, which is a key intermediate in the cycle of Krebs. The production of tartaric acid when yeast cells were grown in the presence of lactate may be a way of the yeast to regulate carbon flow through the cycle of Krebs. Moreover, since tartaric acid was excreted, this may affect the Krebs cycle of the host cells, reducing the energy aerobically produced by oxidizing glucose. Instead, the host cells may convert glucose into lactic acid anaerobically, in a positive feedback loop. This overproduction of lactate has a direct toxic effect on muscles, which may explain some symptoms associated with *Candida* overgrow, such as fibromyalgia [37]. Nevertheless, these observations were controversial as no evidence has been found for the production of tartaric acid as a metabolic end-product by *Candida* [38]. Here, production of tartaric acid by *C. albicans* is detected when cells grow in the presence of lactate. This metabolite is shown to reduce cell viability at the same concentration identified in these experiments (Figure 4.8). This is particularly interesting as lactate is present in several niches

within the host, including within the gastrointestinal tract and vagina [27,28], suggesting that when cells grow in these niches, the production of tartaric acid may explain some symptoms associated with *Candida* infections.

The typical cell wall phenotypes described for glucose-grown *C. albicans* Δ*rlm1*/Δ*rlm1* mutant cells were compared by performing the tests in parallel with the control strains grown in the presence of lactate (Figure 4.3). Lactate-grown cells, independently of the mutation, presented hypersensitivity to different stresses that affected the cell wall, such as caffeine, caspofungin, and SDS (Figure 4.3B). The cell wall of *C. albicans* lactate-grown cells is described as being thinner, presenting less β-glucans and mannans, and is more porous than their glucose counterparts [8,35]. The differences observed between the two conditions reflect the alterations in the cell wall composition due to the carbon source, and the porosity may explain the complete absence of growth of lactate adapted cells on SDS. Since these phenotypes were similar for all strains, it is probable that similar cell wall alterations that were observed previously [8,35] may also occur in the mutant strain. Moreover, in lactate grown cells, the absence of a functional *RLM1* reverted the hypersensitivity to congo red observed when cells were grown in glucose (Figures 4.3A and B). It has been described that congo red interacts with cell wall polysaccharides, exhibiting a particularly high affinity for chitin and β-glucans [39]. Thus, the fact that in lactate-grown cells β-glucans are masked may reduce the availability of congo red to β-glucans, rendering the mutant more resistant.

C. albicans has evolved multiple strategies, including the expression of several virulence factors, to overcome the different environmental conditions imposed by the host [40,41]. As many of these factors rely on morphology changes, the *RLM1* was also tested to check whether it could be involved in some virulence mechanisms such as hyphal growth, adhesion and biofilm formation during carbon adaptation. Under these growth conditions, the Δ*rlm1*/Δ*rlm1* strain presented shorter hypha than the WT or complemented strains, when grown in glucose as well as in lactate, indicating that *RLM1* is involved in *C. albicans* filamentation, independently of the carbon source (Figure 4.4) As reported previously [25], the Δ*rlm1*/Δ*rlm1* strain showed a reduction in the cell wall mannans, which was associated with impaired hyphal growth [33]. Thus, the defect in filamentation observed could be correlated with the cell wall composition.

Additionally, *C. albicans RLM1* has been described as a negative regulator of *in vitro* biofilm formation, as the Δ*rlm1*/Δ*rlm1* mutant strain forms more biofilm than the WT in the presence of glucose [25]. This

gene also seems to regulate negatively some of the same targets of *BCR1*, a well-known transcription factor that governs biofilm formation [42]. In the presence of lactate, all strains produced more biofilm, but as previously reported, the Δ*rlm1*/Δ*rlm1* strain formed even more biofilm, than in the presence of glucose (Figure 4.5). This enhanced biofilm formation in lactate may be directly correlated with the higher ability (approximately three times more) of the lactate grown cells to adhere. These results indicate that the role of *RLM1* as a negative regulator of *in vitro* biofilm formation is independent of the carbon source.

Finally, we studied the involvement of *RLM1* in host-pathogen recognition. The cell wall of microbial pathogens is the first point of contact with the host defenses. Then, any modification on the cell surface, especially on the pathogen-associated molecular patterns (PAMPs), such as β-glucans, α–, and β-mannans, phosphomannans and chitin, impacts the immune detection. The host metabolite lactate has been shown to modulate the exposure of some PAMPs in *C. albicans*, affecting the recognition of the fungus by the host phagocytes [6,8–10]. Importantly, during growth in lactate, β-glucans are actively masked by the outer mannans layer [10].

RLM1 does not seem to be involved in β-glucans masking (Figure 4.6A), which is consistent with the phagocytosis results, since no significant differences were observed between the WT and the Δ*rlm1*/Δ*rlm1* mutant in both carbon sources (Figures 4.6B and C). Moreover, these studies confirmed that cells grown in lactate were less internalized when compared with their glucose counterparts (Figure 4.6) [10], but remained attached to the macrophages (Figure 4.6B). Once more *RLM1* does not seem to be involved in this mechanism.

Although no significance differences were observed in the presence of yeast killing between Δ*rlm1*/Δ*rlm1* and their counterpart strains, within each condition (carbon source), the obtained results confirmed previous data that lactate grown cells are more resistant to phagocyte killing [9]. However, it is curious to observe that when the mutant was grown in lactate, the resistance to yeast killing was lower and not statistically different when grown in glucose, indicating that without *RLM1 C. albicans* loses its resistance acquired when cells grow in lactate (Figure 4.7A). Since previous results indicate that *RLM1* is involved in cell wall architecture, when cells were grown in glucose, this loss of resistance to killing could also be due to changes in cell wall structure and composition, and account for its lower virulence in the disseminated mouse model of infection [25]. The levels of LDH released by macrophages, an indicator of cell damage, were increased for the cells grown in the presence of lactate, indicating that these cells

although being taking up by the macrophages less efficiently, are more prone to kill these phagocytic cells (Figure 4.7D). Interestingly, this is not verified for the Δ*rlm1*/Δ*rlm1* mutant. As seen previously (Figure 4.7A), the mutant is more susceptible to macrophage killing which explains the lower ability to escape from macrophages by damaging the phagocyte. Previous data demonstrated that hyphal extension is a key factor promoting fungal escape from phagocytes, therefore the fact that Δ*rlm1*/Δ*rlm1* mutant produces shorter hyphae might also contribute to the lower capacity to damage macrophages.

The amount of IL-10 and TNF-α was also quantified in order to evaluate the ability of the fungus to induce anti- and pro-inflammatory responses, respectively (Figures 4.7C and D). As expected, the cytokines profile of the *C. albicans* lactate grown cells points to an anti-inflammatory response, given the increased levels of IL-10 in these conditions. However, the levels of IL-10 induced by the Δ*rlm1*/Δ*rlm1* mutant were even higher. The masking of β-glucans on the surface of lactate grown cells reduces not only the phagocytosis, which is stimulated via dectin-1, but also the secretion of cytokines, which is under the control of the transduction pathways upon activation of dectin-1 [43]. Here, the levels of TNF-α were lower in the mutant, when compared with the WT and complemented strains, in glucose-grown cells, but slightly higher in lactate-grown cells. This would suggest that β-glucans in the mutant strain grown in glucose would be less exposed than their counterparts, while in lactate-grown cells it would be the opposite. Regarding IL-10, the higher concentration observed when macrophages were incubated with the mutant cells grown in lactate, could also be explained by the fact that the β-glucans' masking of the mutant was much lower than in the WT and complemented strains. However, and once more, the differences were not significant. The fact that interpreting relative MFI for individual runs across strains is sensitive to growth rate, growth phase, staining uptake, and cell size distribution could contribute to not reach statistical significance. These slight differences in β-glucan exposure would not influence phagocytosis but could account for the differences in host cell activation.

Taken together, these results confirmed that *C. albicans* cells grown in the presence of lactate were less internalized and killed by macrophages and suggest that *RLM1*, although not being involved in yeast cells internalization, seems to be involved in the killing by macrophages and inflicting damage to host cells, what could be related to the lower capacity of the mutant to filament. This interaction mediates cytokine levels, rendering the lactate-grown cells less visible to the phagocytic cells, as previously reported [9]. However, although the Δ*rlm1*/Δ*rlm1* induced a higher anti-inflammatory response, the modifications in the cell wall rendered the mutant less resistant to the action of the immune system.

4.5 References

1. Brown GD, Denning DW, Gow NAR, Levitz SM, Netea MG, White TC. Hidden Killers: Human Fungal Infections. Sci Transl Med. 2012;4: 165rv13-165rv13. doi:10.1126/scitranslmed.3004404
2. Pfaller MA, Diekema DJ. Epidemiology of invasive candidiasis: a persistent public health problem. Clin Microbiol Rev. 2007;20: 133–163. doi:10.1128/CMR.00029-06
3. Campion EW, Kullberg BJ, Arendrup MC. Invasive Candidiasis. N Engl J Med. 2015;373: 1445–1456. doi:10.1056/NEJMra1315399
4. Southern P, Horbul J, Maher D, Davis DA. *C. albicans* colonization of human mucosal surfaces. PLoS One. 2008;3. doi:10.1371/journal.pone.0002067
5. Miramón P, Lorenz MC. A feast for *Candida*: Metabolic plasticity confers an edge for virulence. PLoS Pathogens. 2017. doi:10.1371/journal.ppat.1006144
6. Brown AJP, Brown GD, Netea MG, Gow NAR. Metabolism impacts upon *Candida* immunogenicity and pathogenicity at multiple levels. Trends in Microbiology. 2014. pp. 614–622. doi:10.1016/j.tim.2014.07.001
7. Hall RA. Adapting to change : interactions of *Candida albicans* with its environment. Future Microbiol. 2017;12: 931–934. doi:10.2217/fmb-2017-0130
8. Ene I V., Adya AK, Wehmeier S, Brand AC, Maccallum DM, Gow NAR, et al. Host carbon sources modulate cell wall architecture, drug resistance and virulence in a fungal pathogen. Cell Microbiol. 2012;14: 1319–1335. doi:10.1111/j.1462-5822.2012.01813.x
9. Ene I V., Cheng SC, Netea MG, Brown AJP. Growth of *Candida albicans* cells on the physiologically relevant carbon source lactate affects their recognition and phagocytosis by immune cells. Infect Immun. 2013;81: 238–248. doi:10.1128/IAI.01092-12
10. Ballou ER, Avelar GM, Childers DS, Mackie J, Bain JM, Wagener J, et al. Lactate signalling regulates fungal β-glucan masking and immune evasion. Nat Microbiol. 2016;2: 16238. doi:10.1038/nmicrobiol.2016.238
11. Wheeler RT, Kombe D, Agarwala SD, Fink GR. Dynamic, morphotype-specific *Candida albicans* beta-glucan exposure during infection and drug treatment. PLoS Pathog. 2008;4. doi:10.1371/journal.ppat.1000227
12. Netea MG, Brown GD, Kullberg BJ, Gow NAR. An integrated model of the recognition of *Candida albicans* by the innate immune system. Nat Rev Microbiol. 2008;6: 67–78. doi:10.1038/nrmicro1815

13. Brown GD, Gordon S. Immune recognition. A new receptor for beta-glucans. Nature. 2001;413: 36–37. doi:10.1038/35092620

14. Hardison SE, Brown GD. C-type lectin receptors orchestrate antifungal immunity. Nat Immunol. 2012;13: 817–822. doi:10.1038/ni.2369

15. Levin DE. Regulation of cell wall biogenesis in *Saccharomyces cerevisiae*: The cell wall integrity signaling pathway. Genetics. 2011;189: 1145–1175. doi:10.1534/genetics.111.128264

16. Lipke PN, Ovalle R. Cell wall architecture in yeast: New structure and new challenges. Journal of Bacteriology. 1998. pp. 3735–3740.

17. Baetz K, Moffat J, Haynes J, Chang M, Andrews B. Transcriptional Coregulation by the Cell Integrity Mitogen- Activated Protein Kinase Slt2 and the Cell Cycle Regulator Swi4. Mol Cell Biol. 2001;21: 6515–28. doi:10.1128/MCB.21.19.6515-6528.2001

18. Dodou E, Treisman R. The *Saccharomyces cerevisiae* MADS-box transcription factor Rlm1 is a target for the Mpk1 mitogen-activated protein kinase pathway. Mol Cell Biol. 1997;17: 1848–1859.

19. Jung US, Sobering AK, Romeo MJ, Levin DE. Regulation of the yeast Rlm1 transcription factor by the Mpk1 cell wall integrity MAP kinase. Mol Microbiol. 2002;46: 781–789. doi:10.1046/j.1365-2958.2002.03198.x

20. Watanabe Y, Takaesu G, Hagiwara M, Irie K, Matsumoto K. Characterization of a serum response factor-like protein in *Saccharomyces cerevisiae*, Rlm1, which has transcriptional activity regulated by the Mpk1 (Slt2) mitogen-activated protein kinase pathway. Mol Cell Biol. 1997;17: 2615–23. doi:10.1128/MCB.17.5.2615

21. Blankenship JR, Fanning S, Hamaker JJ, Mitchell AP. An extensive circuitry for cell wall regulation in *Candida albicans*. PLoS Pathog. 2010;6. doi:10.1371/journal.ppat.1000752

22. Bruno VM, Kalachikov S, Subaran R, Nobile CJ, Kyratsous C, Mitchell AP. Control of the *C. albicans* cell wall damage response by transcriptional regulator Cas5. PLoS Pathog. 2006;2: 0204–0210. doi:10.1371/journal.ppat.0020021

23. Xie JL, Qin L, Miao Z, Grys BT, Diaz JDLC, Ting K, et al. The *Candida albicans* transcription factor Cas5 couples stress responses, drug resistance and cell cycle regulation. Nat Commun. 2017;8: 499. doi:10.1038/s41467-017-00547-y

24. Rauceo JM, Blankenship JR, Fanning S, Hamaker JJ, Deneault J-S, Smith FJ, et al. Regulation of the *Candida albicans* cell wall damage response by transcription factor Sko1 and PAS kinase Psk1. Mol Biol Cell. 2008;19: 2741–51. doi:10.1091/mbc.E08-02-0191

25. Delgado-Silva Y, Vaz C, Carvalho-Pereira J, Carneiro C, Nogueira E, Correia A, et al. Participation of *Candida albicans* transcription factor RLM1 in cell wall biogenesis and virulence. PLoS One. 2014;9. doi:10.1371/journal.pone.0086270

26. Sampaio P, Nogueira E, Loureiro AS, Delgado-Silva Y, Correia A, Pais C. Increased number of glutamine repeats in the C-terminal of *Candida albicans* Rlm1p enhances the resistance to stress agents. Antonie van Leeuwenhoek, Int J Gen Mol Microbiol. 2009;96: 395–404. doi:10.1007/s10482-009-9352-5

27. Barelle CJ, Priest CL, MacCallum DM, Gow NAR, Odds FC, Brown AJP. Niche-specific regulation of central metabolic pathways in a fungal pathogen. Cell Microbiol. 2006;8: 961–971. doi:10.1111/j.1462-5822.2005.00676.x

28. Owen DH, Katz DF. A vaginal fluid simulant. Contraception. 1999;59: 91–95. doi:10.1016/S0010-7824(99)00010-4

29. Gillum AM, Tsay EYH, Kirsch DR. Isolation of the *Candida albicans* gene for orotidine-5′-phosphate decarboxylase by complementation of *S. cerevisiae ura3* and *E. coli* pyrF mutations. MGG Mol Gen Genet. 1984;198: 179–182. doi:10.1007/BF00328721

30. Collins T, Barroca M, Branca F, Padrão J, Machado R, Casal M. High level biosynthesis of a silk-elastin-like protein in *E. Coli*. Biomacromolecules. 2014; 15: 2701-2708. doi:10.1021/bm5005564

31. Stepanovic S, Vukovic D, Dakic I, Savic B, Svabic-Vlahovic M. A modified microtiter-plate test for quantification of staphylococcal biofilm formation. J Microbiol Methods. 2000;40: 175–179. doi:10.1016/S0167-7012(00)00122-6

32. Carneiro C, Vaz C, Carvalho-Pereira J, Pais C, Sampaio P. A new method for yeast phagocytosis analysis by flow cytometry. J Microbiol Methods. 2014;101: 56–62. doi:10.1016/j.mimet.2014.03.013

33. McKenzie CGJ, Koser U, Lewis LE, Bain JM, Mora-Montes HM, Barker RN, et al. Contribution of Candida albicans cell wall components to recognition by and escape from murine macrophages. Infect Immun. 2010;78: 1650–1658. doi:10.1128/IAI.00001-10

34. Korzeniewski C, Callewaert DM. An enzyme-release assay for natural cytotoxicity. J Immunol Methods. 1983;64: 313–320. doi:10.1016/0022-1759(83)90438-6

35. Ene I V., Heilmann CJ, Sorgo AG, Walker LA, De Koster CG, Munro CA, et al. Carbon source-induced reprogramming of the cell wall proteome and secretome modulates the adherence and drug resistance of the fungal pathogen *Candida albicans*. Proteomics. 2012;12: 3164–3179. doi:10.1002/pmic.201200228

36. Alves R, Mota S, Silva S, Rodrigues CF, Alistair JP, Henriques M, et al. The carboxylic acid transporters Jen1 and Jen2 affect the architecture and fluconazole susceptibility of *Candida albicans* biofilm in the presence of lactate. Biofouling. 2017;7014: 1–12. doi:10.1080/08927014.2017.1392514

37. Garrison RL, Breeding PC. A metabolic basis for fibromyalgia and its related disorders: The possible role of resistance to thyroid hormone. Medical Hypotheses. 2003. pp. 182–189. doi:10.1016/S0306-9877(02)00294-3

38. Lord RS, Burdette CK, Bralley JA. Significance of urinary tartaric acid [1]. Clinical Chemistry. 2005. pp. 672–673. doi:10.1373/clinchem.2004.036368

39. Klis FM, Mol P, Hellingwerf K, Brul S. Dynamics of cell wall structure in *Saccharomyces cerevisiae*. FEMS Microbiol. Rev. 2002. 26: 239-259. doi:10.1111/j.1574-6976.2002.tb00613.x

40. Mayer FL, Wilson D, Hube B. *Candida albicans* pathogenicity mechanisms. Virulence. 2013;4: 119–28. doi:10.4161/viru.22913

41. Calderone R, Fonzi W. Virulence factors of *Candida albicans*. Trends Microbiol. 2001;9: 327–35. doi:10.1016/S0966-842X(01)02094-7

42. Nobile CJ, Andes DR, Nett JE, Smith FJ, Yue F, Phan QT, et al. Critical role of Bcr1-dependent adhesins in *C. albicans* biofilm formation *in vitro* and *in vivo*. PLoS Pathog. 2006;2: 0636–0649. doi:10.1371/journal.ppat.0020063

43. Steele C, Marrero L, Swain S, Harmsen AG, Zheng M, Brown GD, et al. Alveolar macrophage-mediated killing of *Pneumocystis carinii* f. sp. *muris* involves molecular recognition by the Dectin-1 beta-glucan receptor. J. Exp. Med. 2003. 198: 1677-1688. doi:10.1084/jem.20030932

CHAPTER 5

TRANSCRIPTIONAL RESPONSES OF *CANDIDA GLABRATA* BIOFILM CELLS TO FLUCONAZOLE ARE MODULATED BY THE CARBON SOURCE

Disclaimer

The work presented in this chapter has been previously published in *npj Biofilms and Microbiomes*.

-

Alves R, Kastora SL, Gonçalves A, Azevedo N, Rodrigues CF, Silva S, Demuyser L, Van Dijck P, Casal M, Brown AJP, Henriques M and Paiva S (2020) Transcriptional responses of Candida glabrata biofilm cells to fluconazole are modulated by the carbon source. *npj* Biofilms and Microbiomes. DOI: 10.1038/s41522-020-0114-5

-

ABSTRACT

Candida glabrata is an important human fungal pathogen known to trigger serious infections in immune-compromised individuals. Its ability to form biofilms, which exhibit high tolerance to antifungal treatments, has been considered as an important virulence factor. However, the mechanisms involving antifungal resistance in biofilms and the impact of host environments on these processes are still poorly defined. A whole-transcriptome analysis of *C. glabrata* biofilm cells exposed to different environmental conditions and constraints was performed in order to identify the molecular pathways involved in fluconazole resistance and understand how acidic pH niches, associated with the presence of acetic acid, are able to modulate these responses. Fluconazole treatment induces gene expression reprogramming in a carbon source and pH-dependent manner. This is particularly relevant for a set of genes involved in DNA replication, ergosterol and ubiquinone biosynthesis. Additional evidence that the loss of mitochondrial function is associated with fluconazole resistance, independently of the growth condition, is also provided. Lastly, *C. glabrata* Mge1, a cochaperone involved in iron metabolism and protein import into the mitochondria, is proposed as a key regulator of fluconazole susceptibility during carbon and pH adaptation, by reducing the metabolic flux towards toxic sterol formation. These new findings suggest that different host microenvironments influence directly the physiology of *C. glabrata*, with implications on how this pathogen responds to antifungal treatment. These analyses identify several pathways that can be targeted and will potentially prove to be useful for developing new antifungals to treat biofilm-based infections.

5.1 INTRODUCTION

Candida spp. are important fungal pathogens known to trigger serious infections in immune-compromised individuals, affecting billions of people every year [1]. While *C. albicans* has been predominantly identified as the most common cause of candidiasis, infections caused by non-*albicans Candida* strains such as *C. glabrata* have been increasing worldwide [2,3]. This trend has coincided with the prophylactic use of antifungals, which has resulted in increased drug resistance [4]. Moreover, *C. glabrata* has the ability to adhere and to form biofilms on both biotic and abiotic surfaces, such as host tissues and implanted

medical devices [5–8]. This ability makes these infections a clinical challenge, as the cells in biofilms are also intrinsically resistant to conventional antifungal treatments [9].

In order to survive and successfully proliferate in the different host niches, *C. glabrata* must rapidly adapt to a diverse range of environmental stresses, such as temperature, pH fluctuations and nutrient availability. Some of these niches are complex, dynamic and frequently limited in the content of carbon sources available. To survive in such environments, these pathogens have to control the expression of key metabolic functions [10–12]. For instance, during gastrointestinal and vaginal colonization, where glucose concentration is low, alternative carbon sources such as acetate or lactate are particularly abundant [13,14] and may support the growth and the proliferation of *C. glabrata* cells. Interestingly, low glucose environments were found to induce the formation of *C. glabrata* biofilms and confer resistance to antifungal treatment [15]. This behavior suggests that this pathogen has the capacity to adjust its lifestyle in accordance to nutrient availability and determine the outcome of the next phase: either to continue as part of a biofilm population or disperse to find new colonization sites. However, little is known about the physiological effect of acidic environments, containing alternative non-fermentable carbon sources such as acetate, on the antifungal treatment of *C. glabrata* biofilms.

Our group has previously demonstrated that *C. glabrata* cells were more susceptible to fluconazole and better phagocytosed and killed by macrophages, when exposed to both glucose and to physiological concentrations of acetate [16]. Growth in the presence of this substrate also affected the ability of these cells to form biofilms [16]. Although several putative acetate transporters and channels were identified to be involved in the response to acetate and fluconazole, in both planktonic and biofilm cells, the exact molecular mechanisms underlying fluconazole resistance in biofilms under acidic conditions are still unclear. In this work, the specific transcriptomic responses of *C. glabrata* biofilm cells to fluconazole, when grown in the presence of glucose or glucose and acetate, were evaluated by RNA-sequencing. This allowed us to decipher the differentially expressed genes and potential mechanisms developed by biofilms to adapt to these different physiological environments. Our data represent a global view of transcriptomic regulation in *C. glabrata* biofilms in response to carbon adaptation and fluconazole resistance. Considering the urgent need to find adequate and more effective therapeutic approaches to treat *Candida* infections, further understanding of the molecular mechanisms underlying biofilm formation and antifungal resistance could lead to the development of novel inhibitors to control the dissemination of these pathogens.

5.2 MATERIAL AND METHODS

5.2.1 Media, strains and growth conditions

Biofilm experiments were done using *Candida glabrata* ATCC 2001. This strain was subcultured on Sabouraud dextrose agar (SDA, Difco, Le Pont de Claix, France) medium at 37°C for 24 h and then inoculated in Sabouraud dextrose broth (SDB; Difco) medium at 37°C for 20–24 h while shaking at 120 rpm. Yeast cells were harvested by centrifugation after the incubation period (6500 *g*, for 10 min at 4°C), washed twice in phosphate buffered saline (PBS; pH 7.0, 0.1 M), and the cellular concentration was adjusted to 1×10^7 cells/mL using an improved Neubauer chamber. All experimental assays were carried out in filter-sterilized RPMI 1640 medium with L-glutamine (Sigma, R6504) and buffered with 0.165 M morpholinepropanesulfonic acid at pH 7.0 or 5.0. Fluconazole (Sigma; F8929), doxycycline (Sigma, D9891) and acetic acid (Sigma, A6283) were added to the medium at concentrations of 8 or 24 µg/mL, 100 µg/mL and 0.5% (v/v), respectively (unless otherwise stated). Depending on the assay, autoclave-sterilized and precooled agar was added to the medium. Cell cultures containing fluconazole or doxycycline were always kept in the dark. Detailed information about MGE1-overexpressing strain and respective wild-type control can be found in Demuyser et al. [65].

5.2.2 Biofilm development

Candida biofilms were developed on 24-well polystyrene plates (Orange Scientific, Braine-l'Alleud, Belgium; 12 wells for each condition) containing 1 mL of *C. glabrata* cell suspension (1×10^7 cells/mL in RPMI 1640) per well. The plates were then incubated at 37°C under agitation at 120 rpm. After 24 h, 500 µL of media in each well was removed and an equal volume of fresh media was added according to each condition (RPMI at pH 5.0 supplemented with 0.5 % (v/v) acetic acid; RPMI at pH 5.0 supplemented with 0.5% (v/v) acetic acid and 1250 µg/mL fluconazole; RPMI at pH 7.0; and RPMI at pH 7.0 supplemented with 1250 µg/mL fluconazole). The concentration of fluconazole was selected according to previous studies with *C. glabrata* biofilms [16]. Plates were then incubated for additional 24 h at 37°C under agitation at 120 rpm.

5.2.3 RNA isolation

Following *Candida* biofilm development, each well was gently washed with 1 mL of PBS to remove non-adherent cells. Then biofilms were scraped from the plates with 500 µL of PBS per well, sonicated for 30 s at 30% amplitude (Ultrasonic Processor, Cole-Parmer, IL, USA) in order to separate cells from matrix

[74] and then harvested by centrifugation at 8,000 *g* for 10 min at 4°C. Cells drops were flash frozen in liquid nitrogen and total RNA was isolated from frozen cell pellets using the RiboPure Yeast kit (Ambion, Life Technologies, USA), according to manufacturer's instructions. All samples were treated with Turbo DNAse (Ambion) to remove residual DNA, according to manufacturer's instructions. Total RNA yield was quantified using the Nanodrop 1000 (Thermo Scientific) and RNA quality (RNA Integrity Number (RIN) values ≥ 7.0) assessed on a Bioanalyzer 2100 (Agilent Technologies).

5.2.4 RNA sequencing

Library preparation and RNA sequencing were performed at Edinburgh Genomics (Scotland, UK). All samples were prepared in biological triplicates and subject to removal of ribosomal RNA before complementary DNA (cDNA) library generation. From these libraries, 50 base-paired-end sequence reads were produced with Illumina Hiseq 2000. The raw sequence data in fastq format as well as the processed data have been deposited in NCBI's Gene Expression Omnibus [75] and are accessible through GEO Series accession number GSE121074.

5.2.5 Data analysis

Raw fastq files were successively processed in the following order through Fastqc (v. 10.1), Trimgalore (v. 3.1), Samtools (v. 1.19), Bowtie2 (v. 2.1) and Htseq (v. 5.4). Genome alignment was conducted against the C_glabrata_CBS138_version_s02-m04-r05_chromosomes.fasta file provided by *Candida* Genome Database [76]. Aligned data were quality-controlled via the Partek Genomics Suite software (v. 6.6), according to the manufacturer's instructions. Gene expression analysis was performed using Partek Genomics Suite software using a $\log_2$ data transformation as the Partek recommended default. Gene Ontology (GO) term analysis was performed in parallel through the *Candida* Genome Database GO Term Finder and the Cytoscape (v. 3) Clue GO plugin [77]. GO enriched pathways display downregulated (decrease of twofold or lower) and upregulated (greater than twofold) genes ($p < 0.05$). Network construction was performed with Cytoscape V.3 freeware [78], venn diagrams through Venny online freeware (v. 2.0.2) and heatmaps with TM4 MultiExperiment Viewer (MeV, v. 4.9). A statistical comparison among GO term enrichment percentages was performed with GraphPad Prism (v. 6) using the Student's t-test for two-tailed data. Data represent three independent biological replicates for each condition.

5.2.6 Quantitative Real-Time PCR

Real-Time quantitative PCR of cDNA samples was carried out in a CF X96 Real-Time PCR System from Bio-Rad Laboratories using Power SYBR® Green PCR Master Mix (Applied Biosystems, CA, USA), according to manufacturer's instructions. The High-Capacity cDNA Reverse Transcription Kit (Invitrogen, CA, USA) was used to synthesize the cDNA in a 20 µL reaction containing 1 µg of total RNA, according to the manufacturer's instructions. The primers used to amplify the selected genes and the thermocycling conditions are described in Table 5.1. The reaction mixture was set up in a total volume of 20 µL using 10 µL of SYBR Green PCR Master Mix, 0.3 µM of each primer and 4 µL of each synthesized cDNA sample (diluted 1:20) and nuclease-free water. A negative control without template was conducted for each gene in each PCR run, and a control for DNA contamination was implemented by using the purified RNA samples as templates. The housekeeping gene, *PGK1* [79] was used to normalize the gene expression. Experiments were performed in triplicate for three independent biological samples. Statistical analysis were performed using two-way ANOVA with Bonferroni correction.

Table 5.1. Real-Time PCR conditions

Gene	Primer	Sequence	Product size (bp)	Tm (°C)
CAT5	Forward	TATCCGTGTCGACCAAGC	192	54
	Reverse	AAGGGGGTCAGCAATGAT		
COQ6	Forward	CCACCAGAGCATTTCACC	169	55
	Reverse	GCTTTTCCAAATCGAGCA		
ERG9	Forward	TCCTCGGCGTAGTCTCTGAT	150	56
	Reverse	ATTGTCCTTGCAGGTTTTGG		
ERG11	Forward	CACCGGTTACACCGTCTTCT	145	55
	Reverse	CAGGACCTTGTCGTTACCGT		
FTR1	Forward	TCGCACTCGGGTTCTTTA	163	58
	Reverse	CGCAACATTGGAATACCC		
ATX1	Forward	AGAGGCGCTCGAAGGTGTGA	173	54
	Reverse	ACCCACGACATAGCGCAGGA		
CDR1	Forward	TTGTTGGTGTTCCTGGTGAA	142	58
	Reverse	ATGGACCATGCTGTTTGTGA		
SNQ2	Forward	CGATGCACCAACCAAGTATG	130	58
	Reverse	ACCACCGACAGTCATCAACA		
PDR1	Forward	CGGTGAGTTGGCCCTTACAA	171	58
	Reverse	TTTAATGTCGGCGGTTTCGC		
MGE1	Forward	GACGTTGAGAAGGCCAAGAG	80	58
	Reverse	CGCATGTCCAAAGTTATCCA		
PGK1	Forward	CAAACGGTGAAAGAAACGAGAA	100	58
	Reverse	CCGACACAGTCGTTCAAGAAAG		

5.2.7 Sterol measurement

Sterols were extracted according to the method described in Morio et al. [24] with a few adaptations. In summary, cells were grown for 24 h in RPMI medium, with or without 24 μg/mL fluconazole. The cells were collected, resuspended in saponification medium, and subjected to vortex mixing. The samples were incubated for 1 h at 80°C, after which 1 mL of water and 4 mL of hexane were added. After mixing, the two layers were allowed to separate. For spectrophotometrical analysis, UV-transmittable 96-well microtiter plates (Costar Corning) were used to allow measurement of the OD_{281} and OD_{230}. A formula from Arthington-Skaggs et al. [67] was used to measure the percentages of ergosterol (corrected for cellular wet weight and resuspension volume). For GC-MS analysis, the sterols were extracted twice with hexane, which was then evaporated by vacuum centrifugation. The sterols were resuspended in 100 μL silylating mixture (Sigma) and incubated at room temperature for 30 min. Finally, a corrected cellular wet weight resuspension volume of hexane was added and the samples were immediately stored at −20°C for later analysis by GC-MS. One microliter of the sample was injected into a gas chromatograph-mass spectrometer (Shimadzu QP2010 Ultra Plus) equipped with an HP-5ms nonpolar column (Agilent) (30 m in length, 0.25-mm inner diameter [id.]; 0.25-μm thin layer). Helium was used as carrier gas with a flow rate of 1.4 mL/min. Injection was carried out at 250°C in split mode after 1 min and with a ratio of 1:10. The temperature was first held at 50°C for 1 min and then allowed to rise to 260°C at a rate of 50°C/min, followed by a second ramp of 2°C/min until 325°C was reached; that temperature was maintained for 3 min. The mass detector was operated in scan mode (50 to 600 atomic mass units [amu]), using electron impact ionization (70 eV). The temperatures of the interface and detector were 290 and 250°C, respectively. A mix of linear *n*-alkanes (from C_8 to C_{40}) was injected to serve as external retention index markers. Sterols were identified by their retention time relative to the internal standard (cholestane) and specific mass spectrometric patterns using AMDIS version 2.71. The deconvoluted spectra were matched to GC-MS libraries described in Müller et al. [81] and NIST/EPA/NIH version 2011. Analysis was performed by integration over the base ion of each sterol, and abundance was calculated relative to the internal standard, comparing the relative peak areas of the compounds across treatments using two-way ANOVA with Bonferroni correction.

5.3 RESULTS

5.3.1 Transcriptional responses of C. glabrata biofilm cells to fluconazole are modulated by the presence of acetate

C. glabrata biofilms are frequently grown on artificial media conditions that do not mimic physiological environments, leaving the effects of important alternative metabolites largely unexplored. In order to understand the impact of both acidic and acetate-enriched environments in response to fluconazole treatment, we evaluated the whole transcriptome of *C. glabrata* biofilm cells by RNA-sequencing.

Biofilms were developed for 48 hours in RPMI media (with low glucose concentration, 0.2%), either supplemented or not with 0.5% acetate, and in the presence and absence of fluconazole. This resulted in a total of four different conditions. The total RNA was extracted for twelve independent samples, corresponding to four conditions and three biological replicates. Illumina whole transcriptome sequencing produced around 1.6×10^7 ($\pm 1.4 \times 10^6$) reads per sample, which resulted approximately in 98% overall alignment rate. We then performed pair-wise comparisons between conditions to investigate transcriptional responses to fluconazole treatment, either when biofilms were grown in the presence of acetate (RPMI + acetate) or only in glucose (RPMI).

Figure 5.1A shows a heatmap depicting the gene regulation of *C. glabrata* biofilms in response to both conditions. The adaptation of biofilm cells to the shift from RPMI to RPMI supplemented with acetate, when treated with fluconazole, was accompanied by extensive changes in gene expression. The data show that the transcriptional response of *C. glabrata* biofilm cells to fluconazole is clearly modulated by the presence of acetate (Figure 5.1).

For both comparisons, we obtained lists of genes significantly up- and downregulated and analyzed those displaying at least twofold regulation (Figure 5.1B). We also performed a global functional analysis on the identified genes in order to find significantly enriched GO biological process terms and better understand the biological mechanisms associated with them.

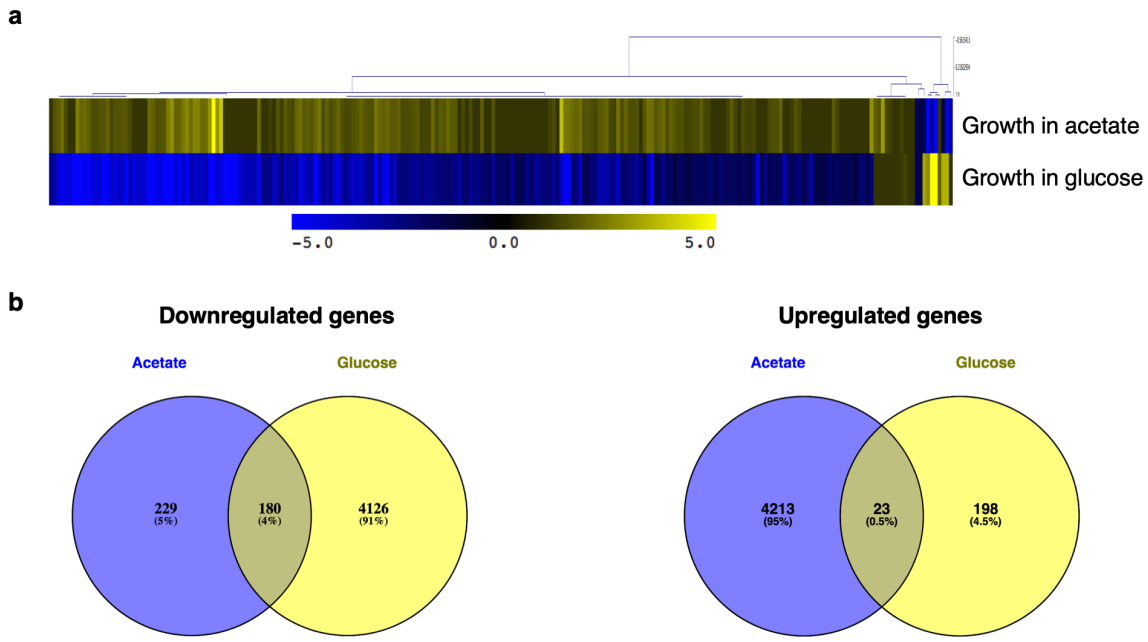

Figure 5.1. Global transcriptional response of *C. glabrata* biofilm cells to fluconazole treatment when grown in the presence of glucose (RPMI + fluconazole *versus* RPMI) or in the presence of both glucose and acetate (RPMI + acetate + fluconazole *versus* RPMI + acetate). a) Heat map of all genes differentially expressed genes ($p < 0.005$) in the presence versus the absence of fluconazole in both growth conditions. **b)** Venn diagrams of all downregulated and upregulated genes ($p < 0.5$) in *C. glabrata* biofilm cells due to fluconazole treatment in both growth conditions.

5.3.2 The transcription of genes involved in DNA replication, ergosterol and ubiquinone biosynthesis is modulated by the presence of acetate in response to fluconazole treatment

In order to characterize the transcriptional responses to fluconazole of *C. glabrata* biofilms grown in the presence of acetate, we compared the transcript profiles of samples grown in RPMI media supplemented with acetate and fluconazole, with those grown just in RPMI supplemented with acetate. Upregulated genes were significantly enriched in biological categories such as "DNA replication initiation" (*CgMCM6* and *CgMCM7*), "ergosterol biosynthetic process" (*CgERG9* and *CgERG11*) and "ubiquinone biosynthetic process" (*CgCAT5*, *CgCOQ6* and *CgCOQ9*; Figure 5.2). The overexpression of both Mcm6p and Mcm7p, which are associated with the MCM complex that initiates and regulates DNA replication [17], may be indicative of increased cell proliferation that ultimately may lead to chromosomal instability. This hypothesis is in agreement with previous observations correlating chromosomal abnormalities in several

Candida spp. with exposure to fluconazole [18]. However, this response has never been associated with the presence of acetate or other non-fermentable carbon sources during *C. glabrata* biofilm growth.

Considering the overexpression of ergosterol biosynthetic genes, this is one of the most common mechanisms of resistance in response to fluconazole treatment in *Candida spp.* [18]. The mechanism of action of fluconazole involves the inhibition of cytochrome P450 enzyme lanosterol demethylase, encoded by *ERG11* [19]. This reaction occurs due to the binding of a free nitrogen atom of the azole ring to an iron atom within the heme group of the enzyme. This binding prevents oxygen activation and consequently demethylation of lanosterol, resulting in the inhibition of ergosterol biosynthesis. Moreover, Erg9p is also involved in ergosterol biosynthesis but functions upstream of lanosterol demethylase in the biosynthetic pathway [20]. As ergosterol is an important component of fungal cell membranes, any impairment in the ergosterol biosynthetic pathway results in increased cellular permeability leading to the disruption of cell membranes. Thus, ergosterol overexpression confers protection against fluconazole treatment by maintaining sterol homeostasis.

Lastly, the three genes encoding proteins involved in the ubiquinone biosynthesis, Coq6p, Cat5p and Coq9p, are part of a multi-subunit complex of nine proteins required for ubiquinone biosynthesis [21–24]. Ubiquinone, also known as Coenzyme Q, is an essential component of the electron transport chain, carrying electrons from Complexes I and II to Complex III in mitochondria. These proteins are required for respiratory growth and gluconeogenic gene activation [21–23]. Indeed, during growth on non-fermentable carbon sources, such as acetate, *Candida* cells induce gluconeogenesis in order to obtain sugar phosphates for the synthesis of essential cellular components [25].

Collectively, these data suggest that fluconazole increases chromosome instability, ergosterol biosynthesis and endogenous respiration in *C. glabrata* biofilm cells grown in the presence of acetate (Figure 5.2). When grown in the presence of glucose as sole carbon source, all of these genes were found to be downregulated (Figure 5.3), suggesting that these pathways are regulated in a carbon source-dependent manner.

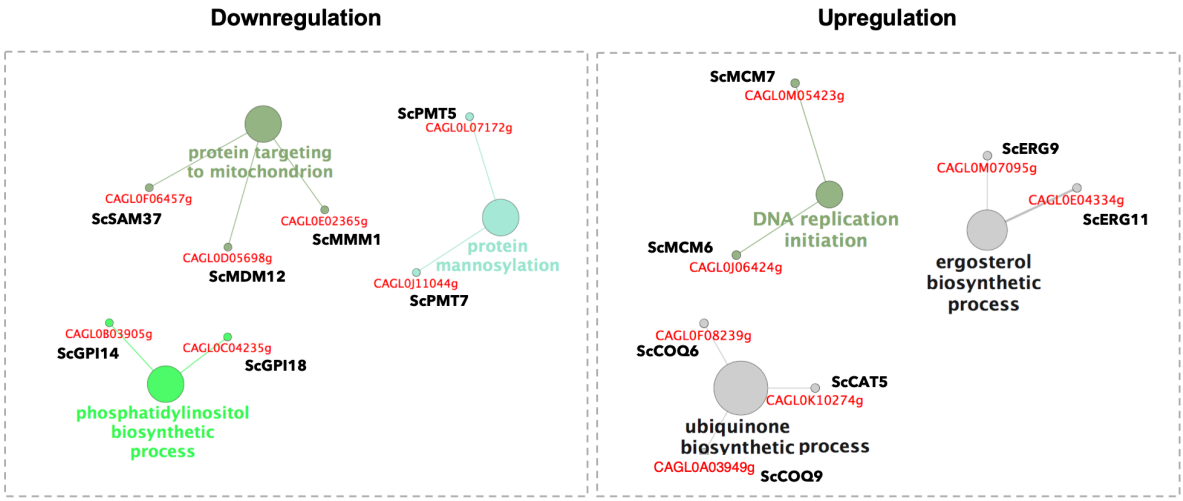

Figure 5.2. Transcriptional response of *C. glabrata* biofilm cells to fluconazole when grown in the presence of acetate. Network visualization of enriched pathways with the systematic names of *C. glabrata* (downregulated, left panel; and upregulated, right panel) when grown in the presence of acetate and fluconazole was performed by ClueGO analysis. The size of the nodes represents the statistical significance of the terms. The systematic names of *C. glabrata* genes and respective orthologs in *S. cerevisiae* associated with each biological process are shown in red and black, respectively.

5.3.3 Reduction of mitochondrial activity appears to be induced in response to fluconazole treatment in a manner independent of carbon source

On the other hand, downregulated genes were significantly enriched in biological processes related to alterations in mitochondrial biogenesis and cell wall organization, as a response to fluconazole treatment. Genes involved in "protein targeting to mitochondrion" (*CgSAM37*, *CgMDM12* and *CgMMM1*) codify a set of translocases that are part of a Sorting Assembly Machinery (SAM) complex that mediates the insertion of beta-barrel proteins into the mitochondrial outer membrane [26–28]. The core of this complex is composed of Sam50p, Sam37p and Sam35p [29–32], but other proteins such as Mdm12p and Mmm1p are required to successfully complete this process [33]. This transcriptional response is in accordance with previous transcriptomics and metabolomics analysis in *C. albicans* that suggest a downregulation of mitochondrial activity as a result of biofilm maturation [34–37]. Other studies have also suggested that the reduction of mitochondrial activity might be beneficial for biofilm growth, conferring protection against oxidative damage and promoting prolonged survival of biofilm cells [38,39]. The downregulation of these genes provides additional evidence that the loss of mitochondrial functions is associated with fluconazole resistance in *C. glabrata*.

Other biological categories also found to be downregulated due to fluconazole treatment include "protein mannosylation" (*CgPMT5* and *CgPMT7*) and "phosphatidylinositol biosynthetic process" (*CgGPI14* and *CgGPI18;* Figure 5.2). The cell wall glycoproteins of *Candida spp.* are modified by *N*- and *O*-linked glycosylation and are attached to the polysaccharides at the cell wall by either covalent links or glycosylphosphatidylinositol (GPI) anchors [40]. The Protein O-MannosylTransferases (PMTs) are an evolutionarily conserved, essential family of proteins that mannosylate distinct targets in the endoplasmic reticulum [41]. In *C. albicans*, where these proteins have been well studied, this posttranslational modification was shown to be involved in morphogenesis, adhesion and antifungal resistance, suggesting that PMTs can be studied as potential antifungal targets [42–44]. Both Gpi14p and Gpi18p are also mannosyltransferases but specifically responsible for adding α-1,4-linked and α-1,6-linked mannoses to GPI, respectively [45–47]. As in fungi all of these genes have several subfamily members that are highly redundant, the effect of their downregulation is unclear.

Interestingly, our data show that upon fluconazole treatment, biofilm cells grown only in the presence of glucose exhibit the same transcriptional pattern of regulation for all categories mentioned above (Figures 5.2 and 5.3). We conclude that these transcriptional responses to fluconazole are independent of the carbon source.

5.3.4 In glucose-grown biofilm cells, fluconazole treatment induces the overexpression of genes involved in metabolism, protein folding and adhesion

To characterize the transcriptional response of glucose-grown biofilm cells to fluconazole, we compared the transcript profile of samples grown in RPMI and fluconazole with those grown in RPMI. Upregulated genes due to fluconazole treatment were significantly enriched in processes related to "primary metabolic process" (*CgAPJ1* and *CgHSP104*) and aggregation (*CgFLO1,* also known as *CgEPA1*) (Figure 3).

Apj1p is a J protein cochaperone of the HSP40 family while Hsp104p is a general anti-stress chaperone that in conjunction with other proteins helps to disassemble protein aggregates accumulated due to stress [48,49]. Heat-shock proteins (HSPs) are induced by several types of stress and have broadly protective functions [50]. Their expression has been associated with biofilm formation and drug resistance in *Candida spp.*, reinforcing their potential as antifungal targets [48,50,51]. Some links between azole resistance and protein folding functions have also been reported in *C. albicans* [52,53]. *CgEPA1* is a GPI-anchored cell wall protein that participates in cell-cell interactions, allowing adherence to host epithelial

tissues [54]. In *C. glabrata*, Epa1p is the major adhesin mediating adhesion and its overexpression is associated with resistance to fluconazole [55].

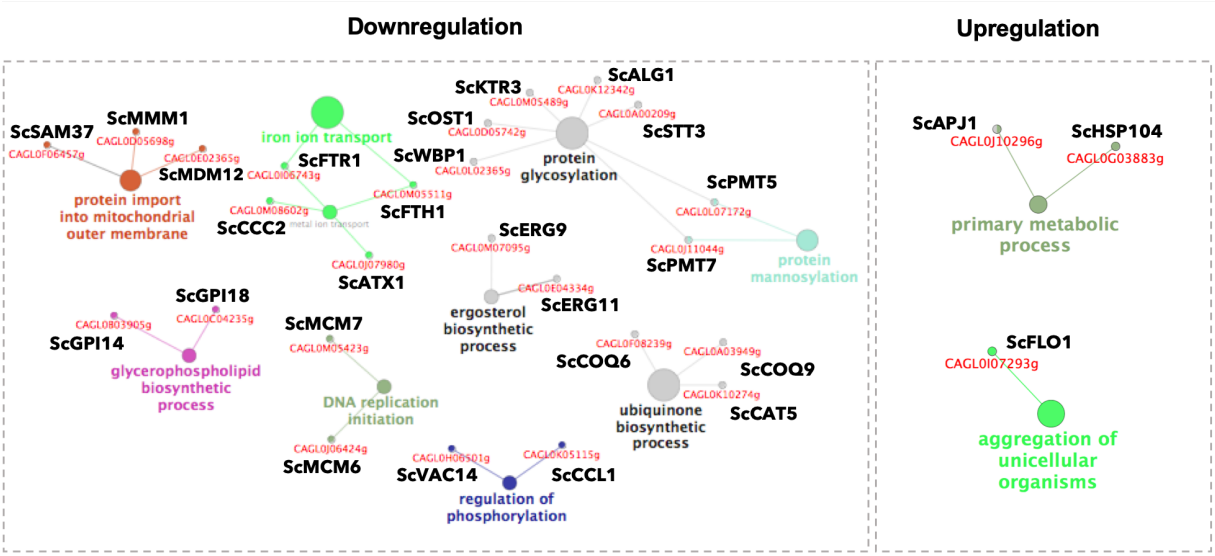

Figure 5.3. Transcriptional response of *C. glabrata* biofilm cells to fluconazole, grown in the presence of glucose, as sole carbon source. Network visualization of enriched pathways with the systematic names of *C. glabrata* (downregulated, left panel; and upregulated, right panel) when grown in the presence of glucose and fluconazole was performed by ClueGO analysis. The size of the nodes represents the statistical significance of the terms. The systematic names of *C. glabrata* genes and respective orthologs in *S. cerevisiae* associated with each biological process are shown in red and black, respectively.

5.3.5 Iron acquisition and glycosylation appear to be attenuated by fluconazole treatment when glucose is present, as sole carbon source

The transcriptional responses to fluconazole when *C. glabrata* biofilm cells were grown in the presence of glucose are associated with a higher number of differentially regulated genes when compared with the acetate-dependent responses described above. Downregulated genes were significantly enriched in several processes (Figure 5.3), including "iron ion transport" (*CgFTR1*, *CgFTH1*, *CgCCC2* and *CgATX1*). Since Ftr1p, Fth1p and Ccc2p are part of the high-affinity iron uptake system in *C. glabrata*, and Atx1p is also involved in iron absorption, downregulation of these genes may result in perturbed iron homeostasis [56]. Given that iron acts as a cofactor for numerous metalloproteins involved in several fundamental cellular processes, such as oxygen transport, respiration, energy metabolism and DNA synthesis and repair, perturbations in iron homeostasis also have a direct impact on these processes. This is consistent

with some of the downregulated categories found under the same conditions, namely, ergosterol biosynthesis.

Additionally, genes involved in "protein glycosylation" (*CgWBP1*, *CgOST1*, *CgKTR3*, *CgALG1* and *CgSTT3*) were also found to be downregulated in response to fluconazole (Figure 5.2). The cell wall glycoproteins in *Candida spp.* can be *N*- or *O*-glycosylated. The *N*-linked glycosylation pathway requires the action of different glycosyltransferases and comprises two sequential stages [40,57]. The first stage involves the synthesis of a dolichol-linked glycan precursor and its transfer to a nascent protein in the rough endoplasmic reticulum. Alg1p is involved in the synthesis process and Wbp1p, Stt3p and Ost1p are transmembrane subunits of the Oligosaccharyl Transferase Complex (OST) that mediate the transference [57]. The second stage includes the *N*-linked glycan processing and maturation in the rough endoplasmic reticulum and Golgi. *CgKTR3*, a member of the *KRE2/MNT1* gene family, may be involved in this last stage but also in *O*-linked protein glycosylation [58]. A reduction in the levels of glycosylation will impact the composition of the cell wall and thus the interaction between the biofilm cells. This is consistent with data from *C. albicans* showing that changes in carbon source affect cell wall architecture, the cell wall proteome and cell wall organization [59–61].

Besides glycosylation, some proteins involved in the "regulation of phosphorylation" (*CgCCL1* and *CgVAC14*) also appear to be downregulated in response to fluconazole treatment (Figure 5.3). *CgCCL1* positively regulates transcription by Polymerase II by stimulating phosphorylation of RNA polymerase II C-terminal domain, with mutants showing increased competitive fitness in *Saccharomyces cerevisiae* [62]. Vac14p controls the synthesis of phosphatidylinositol-3,5-biphosphates, impacting several mechanisms such as organelle morphology, membrane recycling, and ion transport [63].

Altogether, these biological categories represent a deregulation in mitochondrion function, cell cycle, cell wall composition, iron transport and post-translation modifications, such as mannosylation, glycosylation and phosphorylation.

5.3.6 Validation of RNA-seq results with quantitative real-time PCR (qRT-PCR)

In order to validate the RNA-seq findings, qRT-PCR was performed on all conditions for six genes that are key members of the most significant differentially expressed categories found by GO analysis: *CAT5*, *COQ6*, *ERG9*, *ERG11*, *FTR1* and *ATX1* (Figure 5.4).

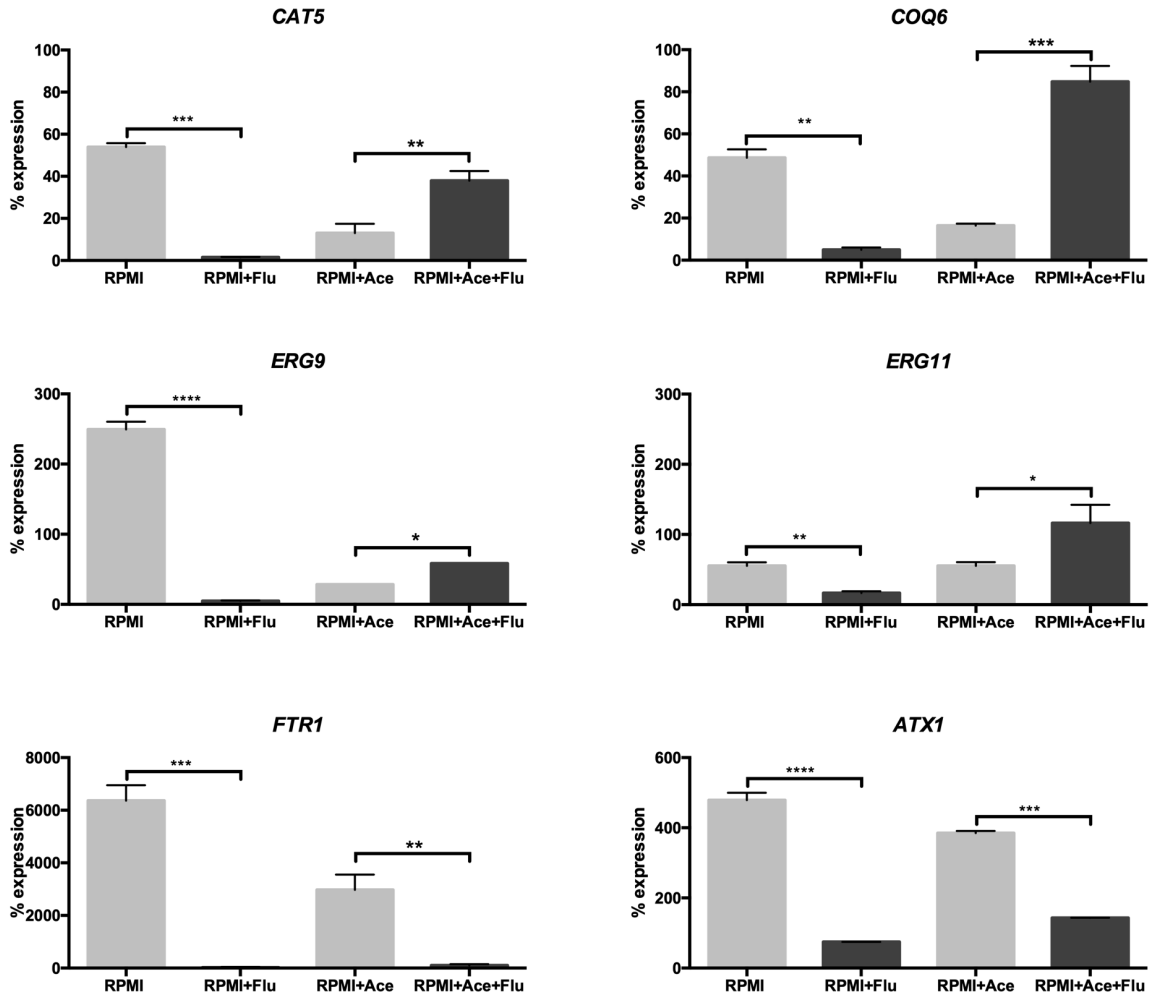

Figure 5.4. Validation by qRT-PCR of genes that were differentially expressed (*CAT5*, *COQ6*, *ERG9*, *ERG11*, *FTR1* and *ATX1*) in response to fluconazole in *C. glabrata* biofilm cells grown with glucose as sole carbon source (RPMI; pH 7.0) or supplemented with acetate (RPMI + Ace; pH 5.0). Graphs show percentage expression of each gene compared to a housekeeping gene, *PGK1*. The error bars show standard deviation. * $p < 0.05$, ** $p < 0.01$, *** $p < 0.001$, **** $p < 0.0001$ were considered statistically significant relative to untreated *C. glabrata* biofilm cells.

All of these genes were also tested when *C. glabrata* biofilm cells were grown in the presence of fluconazole, and when using glucose as sole carbon source at pH 5.0, to check whether the pH influenced the changes in gene expression (Figure 5.5). Significantly, the changes in expression observed by RNA-seq were confirmed by qRT-PCR for all the tested genes. Furthermore, the changes in expression observed between growth conditions were independent of the pH (Figures 5.4 and 5.5).

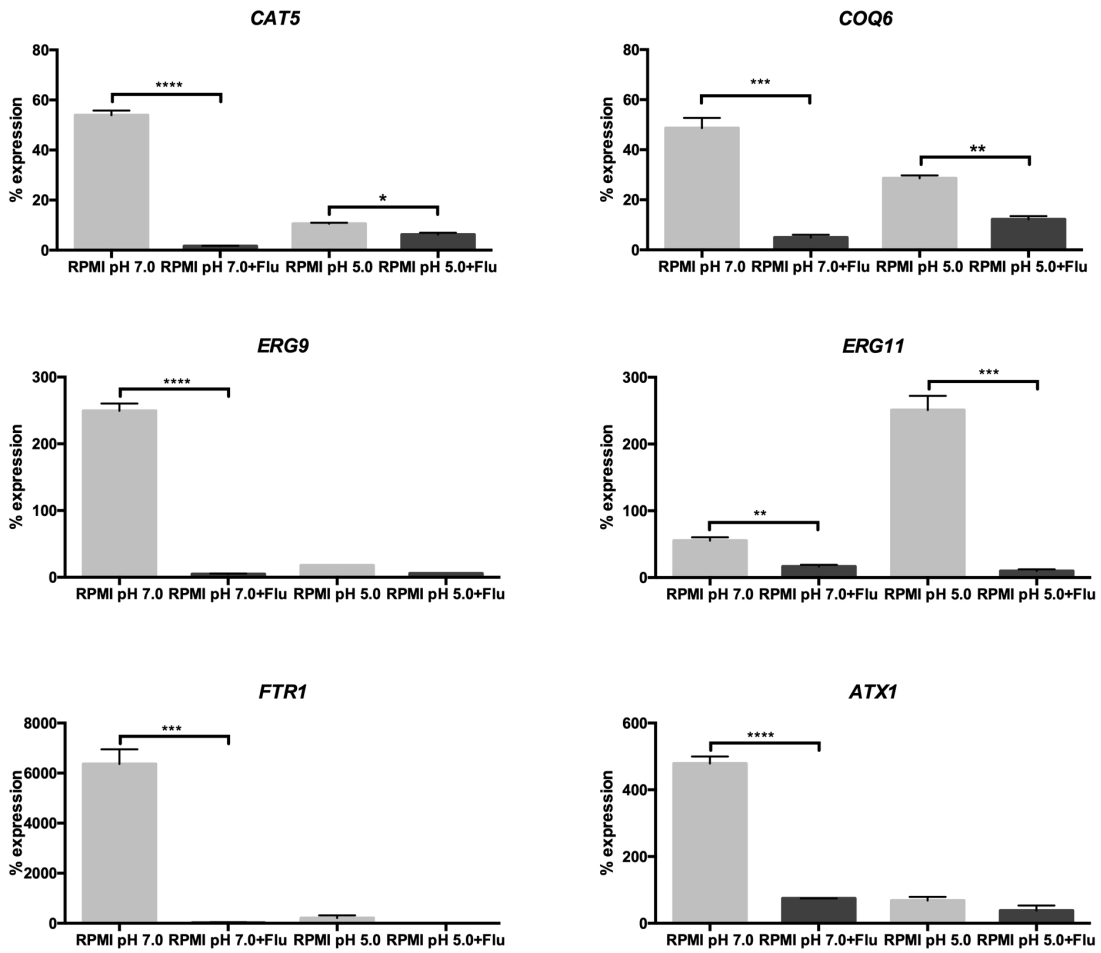

Figure 5.5. Expression of *CAT5*, *COQ6*, *ERG9*, *ERG11*, *FTR1* and *ATX1* assessed by qRT-PCR in response to fluconazole in *C. glabrata* biofilm cells grown using glucose as sole carbon source (RPMI pH 7.0 vs RPMI pH 5.0). Graphs show percentage expression of each gene compared to a housekeeping gene, *PGK1*. Error bars show standard deviation. * $p < 0.05$, ** $p < 0.01$, *** $p < 0.001$, **** $p < 0.0001$ were considered statically significant relative to untreated *C. glabrata* biofilm cells.

5.3.7 CgMge1 drives fluconazole resistance in acidic and acetate-enriched environments

C. glabrata is able to colonize and infect acidic and acetate-enriched anatomical sites, including the gastro-intestinal tract and vagina. We identified a set of genes that are differently regulated due to fluconazole treatment, when cells are growing in conditions mimicking those acidic environments. Considering the overexpression of both *CgERG9* and *CgERG11* in response to fluconazole, when *Candida* biofilm cells are growing in the presence of acetate (Figure 5.2), we postulated that *C. glabrata* would display increased resistance to fluconazole under those conditions. To physiologically validate our transcriptional data, *C. glabrata* cells were grown in the presence of fluconazole and/or doxycycline, an iron chelator reported to have a synergistic effect with fluconazole [64,65,66]. As a control strain, we used an overexpression

mutant for *MGE1* driven by the *CgTDH3* promoter in the 2001HTL strain (Figure 5.6) [65]. This gene encodes a putative mitochondrial matrix cochaperone, which is a known suppressor of fluconazole susceptibility in both *C. albicans* and *C. glabrata* [65]. Since *CgMGE1* is upregulated when cells are treated with fluconazole, under acidic environments (Figure 5A), we hypothesized that WT cells would display the same phenotype as *MGE1*-overexpressing cells, when grown under similar conditions. We tested this, and all experiments were performed in triplicate, showing consistent results among all the independent assays. Growth conditions were maintained by supplementing RPMI medium containing 0.2% glucose with the respective stressor and adjusting the pH to 7.0 or 5.0. This enabled us to compare our physiological data with the transcriptional outputs.

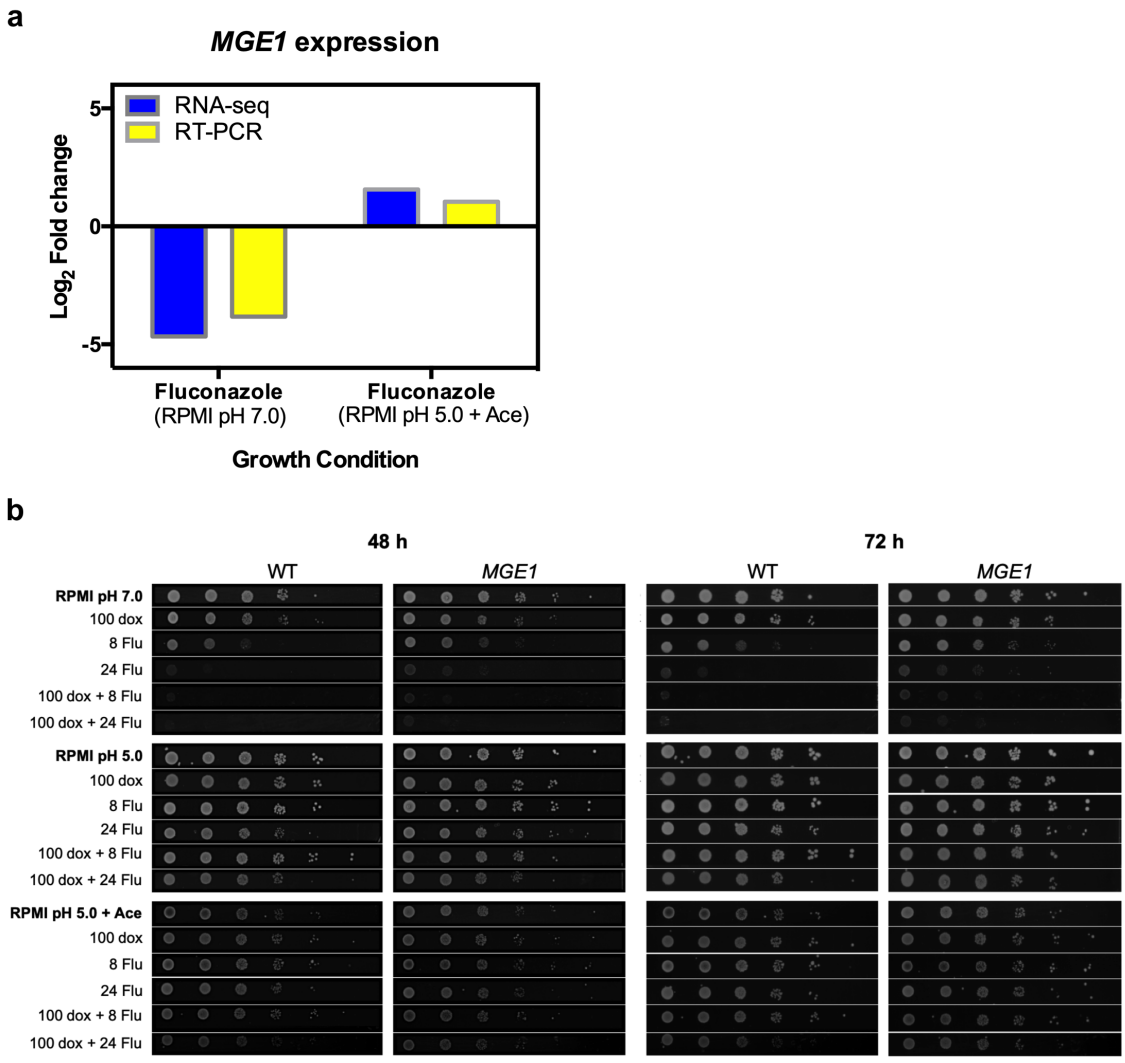

Figure 5.6 Fluconazole susceptibility is modulated by pH, carbon source and *MGE1* expression in *C. glabrata*. (a) Log_2 fold change comparison of RNA-seq (blue bars) and quantitative RT-PCR (yellow bars) for *MGE1* expression in response to fluconazole treatment when *C. glabrata* cells are growing either using

glucose as sole carbon source (RPMI pH 7.0) or in the presence of acetate (RPMI pH 5.0 + Ace). **(b)**. Serial dilutions of *wild-type* strain (WT; 2001HTL strain transformed with the empty plasmid as a control) and overexpression strain (*MGE1*; 2001HTL strain transformed with a plasmid expressing *CgMGE1* ORF, together with its terminator, from the *CgTDH3* promoter [65]) were spotted on RPMI medium containing 0.2% glucose at pH 7.0 or pH 5.0, and/or containing acetate (ace; 0.5% v/v), and/or fluconazole (flu; 8 or 24 µg/mL) and/or doxycycline (dox; 100 µg/mL). Pictures were taken after 48h and 72h of incubation at 37 °C.

Phenotypes from control conditions (RPMI pH 7.0) for the *MGE1*-overexpressing strain were in agreement with previously published data, where *CgMGE1* overexpression was shown to play a role in regulating susceptibility to fluconazole (Figure 5.6B) [65]. As expected, cells grown under acidic conditions, such as RPMI at pH 5.0 and RPMI at pH 5.0 supplemented with 0.5% acetate, were more resistant to fluconazole and doxycycline than those grown only in RPMI at pH 7.0 (Figure 5.6B). Interestingly, the synergistic effect of doxycycline was strongly modulated by pH and the carbon source, since this effect was abolished under acidic pH, and moderately restored for the highest concentration of fluconazole in the presence of acetate (Figure 5.6B). As predicted, both WT and *MGE1*-overexpressing cells displayed the same phenotype under acidic conditions (Figure 5.6B). We can conclude from these data that overexpression of *MGE1* under acidic conditions (confirmed both by RNA-seq and RT-PCR; Figure 5.6A) causes a decrease in the susceptibility of *C. glabrata* to fluconazole (Figure 5.6B). These data also highlight the importance of mimicking distinct environmental niches as local inputs significantly affect the responses of *Candida* cells to antifungal treatment.

5.3.8 Overexpression of CgMGE1 reduces toxic sterol formation

Ergosterol biosynthesis is inhibited in the presence of fluconazole, favoring the formation of toxic sterols due to the accumulation of lanosterol (Figure 5.7A). Previous work has demonstrated that the overexpression of *CgMGE1* reduces the metabolic flux to toxic sterol formation [65]. Therefore, gas chromatography-mass spectrometry (GC-MS) analysis was performed to investigate the possible role of sterols in mediating fluconazole resistance, which is higher when *C. glabrata* cells grow in acidic environments and when *MGE1* is upregulated. Sterols were isolated from both WT and *MGE1*-overexpressing cells grown in RPMI at pH 7.0, RPMI at pH 5.0 and RPMI at pH 5.0 + 0.5% acetate, in the presence and absence of fluconazole (Figure 5.7B).

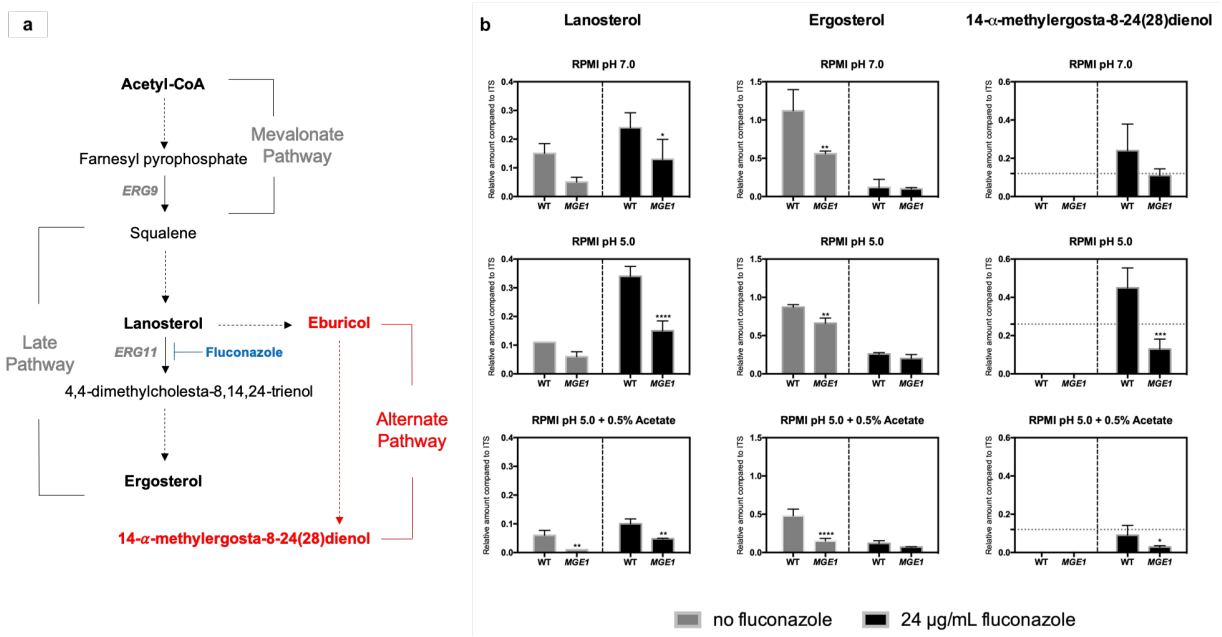

Figure 5.7. ***MGE1*** **overexpression modulates the aberrant flux of sterols following fluconazole treatment.** **(a)** Schematic representation of sterol biosynthetic pathways. Erg11 is the primary target of fluconazole. Red names represent toxic fungistatic sterols. **(b)** *CgMGE1* overexpression reduces toxic sterol formation. Cells were grown in RPMI medium containing 0.2% glucose at pH 7.0, or pH 5.0, and/or containing 0.5% acetate, in the presence or absence of fluconazole for 24 h. Sterol levels were determined by GC-MS and are displayed for lanosterol, ergosterol, and 14-methylergosta-8,24(28)-dien-3β,6α-diol. The values were calculated relative to the internal standard (ITS; cholestane). The error bars show standard error of the mean. * $p < 0.05$, ** $p < 0.01$, *** $p < 0.001$, **** $p < 0.0001$ were considered statistically significant relative to *C. glabrata* WT cells. Gray dotted grid lines in each condition represent the mean obtained for ergosterol content for the same *MGE1* overexpressing cells.

In addition to sterols such as ergosterol and lanosterol, we detected other sterols that were less abundant or could not be identified. This approach was validated by using an alternative sterol quantitation method (data not shown) [67].

As can be seen from Figure 5.7B, fluconazole treatment leads to lanosterol accumulation and ergosterol depletion under all the growth conditions examined. This accumulation favors the formation of toxic sterols such as 14-methylergosta-8,24(28)-dien-3β,6α-diol. Remarkably, *MGE1*-overexpressing cells displayed reduced levels of this toxic sterol (Figure 5.7B). This reduction is statistically significant only for cells grown under acidic conditions ($p < 0.001$ and $p < 0.05$ for RPMI pH 5.0 and RPMI pH 5.0 + 0.5% acetate, respectively). Additionally, the balance between ergosterol and 14-methylergosta-8,24(28)-dien-

3β,6α-diol in these cells is higher for RPMI at pH 5.0 and RPMI at pH 5.0 + 0.5% acetate (Figure 5.7B). By reducing the metabolic flux towards 14-methylergosta-8,24(28)-dien-3β,6α-diol, other sterol intermediates can migrate to plasma membrane and replace the essential ergosterol functions. Considering that under these conditions, *C. glabrata* cells present higher fluconazole resistance (Figure 5.6B), these data present additional evidence for the role of *MGE1* in reducing the levels of toxic sterols and, consequently, decreasing susceptibility to fluconazole.

5.4 DISCUSSION

Natural niches of *C. glabrata* include the human gastrointestinal and vaginal tracts [68], environments particularly rich in alternative carbon sources and often limited in the amount of glucose [11]. In order to thrive in these changing nutrient environments, *C. glabrata* has evolved sophisticated regulatory mechanisms, including major metabolic changes that have been associated with virulence and, in particular, biofilm formation [15,16,69]. Once established, *Candida* biofilms are very difficult to eradicate due to their intrinsic tolerance to antifungals. In fact, azole resistance among *Candida* species, especially *C. glabrata*, is currently one of the greatest clinical challenges [2,4,7]. Here, we investigated the effect of different carbon sources on fluconazole-treated *C. glabrata* biofilms by using a RNA-seq approach. For that, biofilms were grown in the presence of low glucose or low glucose plus acetate, a non-fermentable carbon source frequently found in several host niches [14,70]. The differentially regulated genes identified in both growth conditions allowed us to decipher the potential molecular mechanisms associated with carbon adaptation and fluconazole resistance. Indeed, since most of the genes are still uncharacterized in *C. glabrata*, their function was predicted based on their orthologs in the phylogenetically closely related yeast *S. cerevisiae*.

Depending on the growth condition, some genes were found to be differently regulated in response to fluconazole. These included genes encoding proteins involved in DNA replication, mitochondrial function and ergosterol biosynthesis (Figures 5.2 and 5.3). While this observation could be anticipated for the genes involved in DNA replication and mitochondrial function, as metabolism is finely coordinated with cell growth, chromosome replication and cell division, it was quite surprising to find that the carbon source affects the degree to which fluconazole induces ergosterol-related genes. As sterol biosynthesis requires heme, we hypothesize that the expression of these genes is also dependent on the status of iron acquisition in the cells. Indeed, the expression profile of iron-related genes is finely tuned with those involved in the expression of ergosterol (Figures 5.2, 5.3 and 5.4). Curiously, even with all of these impairments, *C. glabrata* cells from biofilms still survive under high concentrations of fluconazole [16]. In fact, it was already shown that deprivation of iron does not seem to affect the ability of cells to form biofilms in *C. albicans* [71]. Moreover, the lack of iron enhances membrane fluidity and drug diffusion in *C. glabrata* planktonic cells [66], consistent with the impairment in ergosterol biosynthesis. On the other hand, our analyses provided additional evidence that the loss of mitochondrial function is associated with fluconazole resistance, independently of the growth condition. Additionally, while physiologically validating

our transcriptional outputs, we realized that *C. glabrata* Mge1, a cochaperone involved in iron metabolism and protein import into the mitochondria, might influence fluconazole susceptibility during carbon and pH adaptation. We confirmed this experimentally (Figure 5.6), thereby reinforcing the role of *CgMGE1* in mediating fluconazole resistance by reducing toxic sterol formation [65].

In this study we did not observe statistically significant deregulations regarding several well-known genes involved in fluconazole resistance in planktonic *C. glabrata* cells. These include the induction of efflux pumps, encoded by the *ABC*-transporter genes such as *CgCDR1*, Cg*CDR2* (also known as *CgPDH1*) and *CgSNQ2*, which are regulated mainly by the transcription factor *CgPDR1* [2]. Our data suggest that their expression levels differ markedly between biofilms and planktonic cells (data not shown). This observation is consistent with previous work done in *C. albicans* [72]. Mutants knocked out in these genes were hypersusceptible to fluconazole when growing as planktonic cells, but not when growing as biofilms [72]. This may reflect altered responses due to the characteristics intrinsically related with the biofilm lifestyle, such as growth on a surface, the presence of a protective extracellular matrix, differences in nutrient requirements and metabolism, and/or quorum-sensing mechanisms [73].

Based on the data presented here, we propose a model in which resistance to fluconazole in *C. glabrata* biofilms is modulated by the available carbon source and pH (Figure 5.8). This is particularly relevant for a set of genes involved in DNA replication, ergosterol and ubiquinone biosynthesis. When grown in the presence of glucose, responses to fluconazole treatment are extensive and involve the deregulation of several cellular functions (Figure 5.8B). On the other hand, when acetate is present in the growth media, fluconazole treatment impacts mainly chromosome instability, cell wall integrity and mitochondrial function (Figure 5.8A).

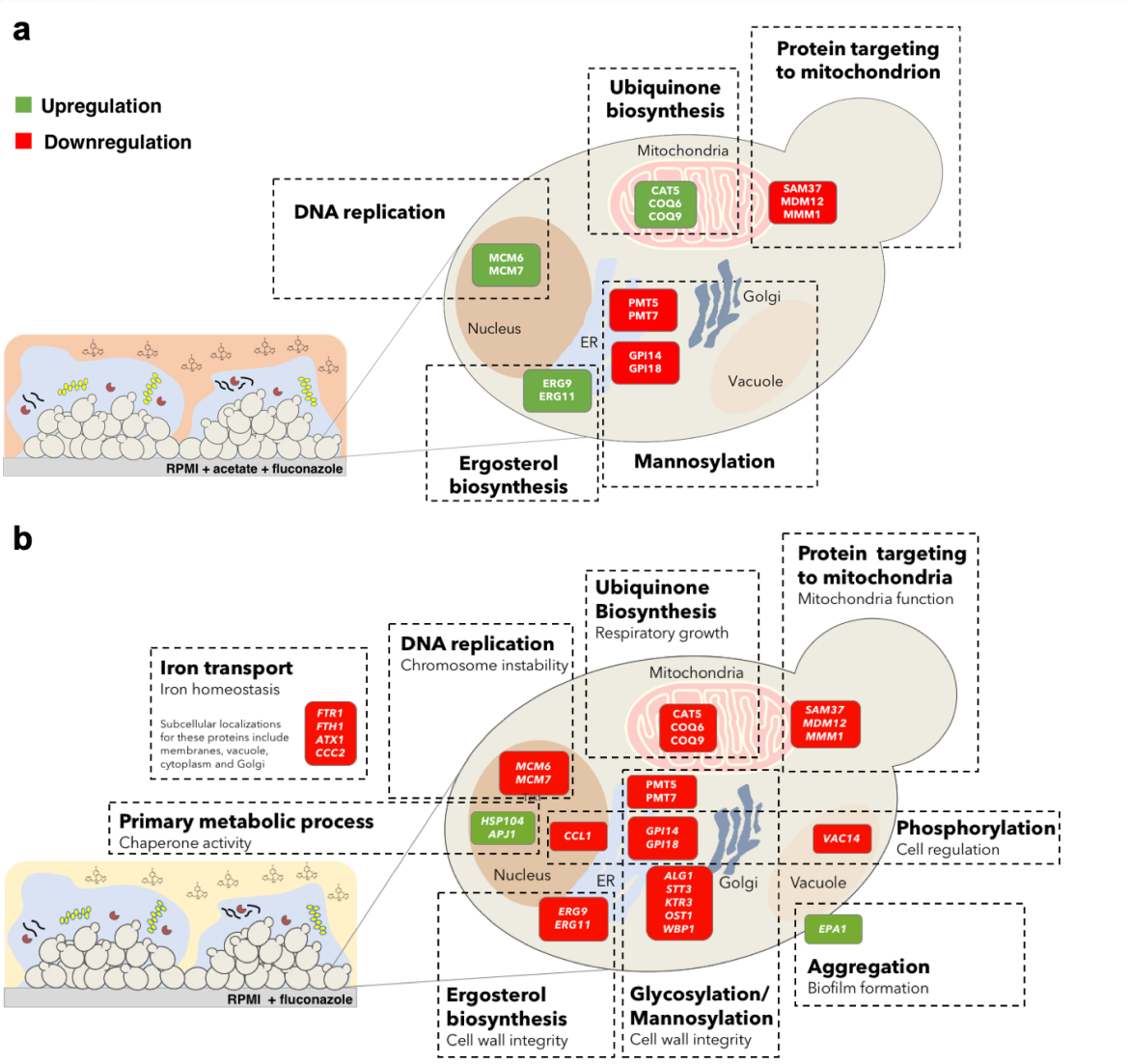

Figure 5.8. Schematic overview of the transcriptional responses of *C. glabrata* biofilms to fluconazole. Differentially expressed genes upon fluconazole treatment when cells are grown in the presence of **(a)** glucose and acetate or **(b)** glucose.

These analyses provide a global overview of the genetic and regulatory mechanisms developed by this fungus in response to antifungal treatment and highlights the impact of acidic environments on these processes. These alterations at transcriptional level following fluconazole treatment, either in the presence of glucose or acetate, enhance the robustness of *C. glabrata* biofilms to tolerate this antifungal. Our data reveal new roles of uncharacterized *C. glabrata* genes and provide more knowledge towards the identification of new potential antifungal targets. Understanding the mechanisms behind fluconazole resistance may improve and facilitate the development of new antifungal compounds to treat *Candida* infections.

5.5 REFERENCES

1. Jermy, A. Stop neglecting fungi. *Nature Microbiology* 2, (2017).
2. Rodrigues, C., Rodrigues, M., Silva, S. & Henriques, M. *Candida glabrata* Biofilms: How Far Have We Come? *J. Fungi* 3, 11 (2017).
3. Khatib, R., Johnson, L. B., Fakih, M. G., Riederer, K. & Briski, L. Current trends in candidemia and species distribution among adults: *Candida glabrata* surpasses *C. albicans* in diabetic patients and abdominal sources. *Mycoses* 59, 781–786 (2016).
4. Perlin, D. S., Rautemaa-Richardson, R. & Alastruey-Izquierdo, A. The global problem of antifungal resistance: prevalence, mechanisms, and management. *The Lancet Infectious Diseases* 17, e383–e392 (2017).
5. Silva, S. *et al.* Adherence and biofilm formation of non-*Candida albicans Candida* species. *Trends in Microbiology* 19, 241–247 (2011).
6. Cuellar-Cruz, M. *et al. Candida* species: new insights into biofilm formation. [Review]. *Future Microbiol.* 7, 755–771 (2012).
7. Cavalheiro, M. & Teixeira, M. C. *Candida Biofilms*: Threats, Challenges, and Promising Strategies. *Front. Med.* 5, (2018).
8. Kucharíková, S. *et al.* In vivo *Candida glabrata* biofilm development on foreign bodies in a rat subcutaneous model. *J. Antimicrob. Chemother.* (2015). doi:10.1093/jac/dku447
9. Rodrigues, C. F., Rodrigues, M. E. & Henriques, M. Susceptibility of *Candida glabrata* biofilms to echinocandins: alterations in the matrix composition. *Biofouling* 1–10 (2018). doi:10.1080/08927014.2018.1472244
10. Barelle, C. J. *et al.* Niche-specific regulation of central metabolic pathways in a fungal pathogen. *Cell. Microbiol.* 8, 961–971 (2006).
11. Miramón, P. & Lorenz, M. C. A feast for *Candida*: Metabolic plasticity confers an edge for virulence. *PLoS Pathogens* 13, (2017).
12. Lorenz, M. C. & Fink, G. R. The glyoxylate cycle is required for fungal virulence. *Nature* 412, 83–86 (2001).
13. Osset, J., García, E., Bartolomé, R. M. & Andreu, A. [Role of Lactobacillus as protector against vaginal candidiasis]. *Med. clínica* 117, 285–8 (2001).
14. Owen, D. H. & Katz, D. F. A vaginal fluid simulant. *Contraception* 59, 91–95 (1999).

15. Ng, T. S., Desa, M. N. M., Sandai, D., Chong, P. P. & Than, L. T. L. Growth, biofilm formation, antifungal susceptibility and oxidative stress resistance of *Candida glabrata* are affected by different glucose concentrations. *Infect. Genet. Evol.* 40, 331–338 (2016).
16. Mota, S. *et al. Candida glabrata* susceptibility to antifungals and phagocytosis is modulated by acetate. *Front. Microbiol.* 6, (2015).
17. Ma, X., Stead, B. E., Rezvanpour, A. & Davey, M. J. The effects of oligomerization on *Saccharomyces cerevisiae* Mcm4/6/7 function. *BMC Biochem.* 11, (2010).
18. Berkow, E. L. & Lockhart, S. R. Fluconazole resistance in *Candida* species: A current perspective. *Infection and Drug Resistance* 10, 237–245 (2017).
19. Vanden Bossche, H. Biochemical targets for antifungal azole derivatives: hypothesis on the mode of action. *Curr Top Med Mycol* 1, 313–351 (1985).
20. Nakayama, H., Izuta, M., Nakayama, N., Arisawa, M. & Aoki, Y. Depletion of the squalene synthase (ERG9) gene does not impair growth of *Candida glabrata* in mice. *Antimicrob. Agents Chemother.* 44, 2411–2418 (2000).
21. Jonassen, T. *et al.* Yeast clk-1 homologue (Coq7/Cat5) is a mitochondrial protein in coenzyme Q synthesis. *J. Biol. Chem.* 273, 3351–3357 (1998).
22. Ozeir, M. *et al.* Coq6 is responsible for the C4-deamination reaction in coenzyme Q biosynthesis in *Saccharomyces cerevisiae*. *J. Biol. Chem.* 290, 24140–24151 (2015).
23. Johnson, A. *et al.* COQ9, a new gene required for the biosynthesis of coenzyme Q in *Saccharomyces cerevisiae*. *J. Biol. Chem.* 280, 31397–31404 (2005).
24. Turunen, M., Olsson, J. & Dallner, G. Metabolism and function of coenzyme Q. *Biochim. Biophys. Acta - Biomembr.* 1660, 171–199 (2004).
25. Eschrich, D., Kötter, P. & Entian, K. D. Gluconeogenesis in *Candida albicans*. *FEMS Yeast Res.* 2, 315–325 (2002).
26. Pfanner, N., Wiedemann, N., Meisinger, C. & Lithgow, T. Assembling the mitochondrial outer membrane. *Nat. Struct. Mol. Biol.* 11, 1044–1048 (2004).
27. Paschen, S. a, Neupert, W. & Rapaport, D. Biogenesis of beta-barrel membrane proteins of mitochondria. *Trends Biochem. Sci.* 30, 575–82 (2005).
28. Kutik, S. *et al.* Dissecting membrane insertion of mitochondrial beta-barrel proteins. *Cell* 132, 1011–1024 (2008).
29. Wiedemann, N. *et al.* Machinery for protein sorting and assembly in the mitochondrial outer membrane. *Nature* 424, 565–571 (2003).

30. Kozjak, V. *et al.* An essential role of Sam50 in the protein sorting and assembly machinery of the mitochondrial outer membrane. *J. Biol. Chem.* 278, 48520–48523 (2003).
31. Milenkovic, D. *et al.* Sam35 of the mitochondrial protein sorting and assembly machinery is a peripheral outer membrane protein essential for cell viability. *J. Biol. Chem.* 279, 22781–22785 (2004).
32. Ishikawa, D., Yamamoto, H., Tamura, Y., Moritoh, K. & Endo, T. Two novel proteins in the mitochondrial outer membrane mediate beta-barrel protein assembly. *J. Cell Biol.* 166, 621–7 (2004).
33. Meisinger, C. *et al.* The morphology proteins Mdm12/Mmm1 function in the major β-barrel assembly pathway of mitochondria. *EMBO J.* 26, 2229–2239 (2007).
34. Fox, E. P. *et al.* Anaerobic bacteria grow within *Candida albicans* biofilms and induce biofilm formation in suspension cultures. *Curr. Biol.* 24, 2411–2416 (2014).
35. Nobile, C. J. *et al.* A recently evolved transcriptional network controls biofilm development in *Candida albicans*. *Cell* 148, 126–138 (2012).
36. Holland, L. M. *et al.* Comparative Phenotypic Analysis of the Major Fungal Pathogens *Candida parapsilosis* and *Candida albicans*. *PLoS Pathog.* 10, (2014).
37. Zhu, Z. *et al.* Time course analysis of *Candida albicans* metabolites during biofilm development. *J. Proteome Res.* 12, 2375–2385 (2013).
38. Verma-Gaur, J. *et al.* Integration of Posttranscriptional Gene Networks into Metabolic Adaptation and Biofilm Maturation in *Candida albicans*. *PLoS Genet.* 11, (2015).
39. Calderone, R., Li, D. & Traven, A. System-level impact of mitochondria on fungal virulence: To metabolism and beyond. *FEMS Yeast Research* 15, (2015).
40. Mora-Montes, H. M. *et al.* Protein glycosylation in *Candida*. *Future Microbiology* 4, 1167–1183 (2009).
41. Gentzsch, M. & Tanner, W. Protein-O-glycosylation in yeast: Protein-specific mannosyltransferases. *Glycobiology* 7, 481–486 (1997).
42. Timpel, C., Zink, S., Strahl-Bolsinger, S., Schröppel, K. & Ernst, J. Morphogenesis, adhesive properties, and antifungal resistance depend on the Pmt6 protein mannosyltransferase in the fungal pathogen *Candida albicans*. *J. Bacteriol.* 182, 3063–3071 (2000).
43. Ernst, J. F. & Prill, S. K. O-glycosylation. *Med. Mycol.* 39 Suppl 1, 67–74 (2001).
44. Prill, S. K. H. *et al.* PMT family of *Candida albicans:* Five protein mannosyltransferase isoforms affect growth, morphogenesis and antifungal resistance. *Mol. Microbiol.* 55, 546–560 (2005).

45. Maeda, Y. *et al.* PIG-M transfers the first mannose to glycosylphosphatidylinositol on the lumenal side of the ER. *EMBO J.* 20, 250–261 (2001).

46. Fabre, A. L., Orlean, P. & Taron, C. H. *Saccharomyces cerevisiae* Ybr004c and its human homologue are required for addition of the second mannose during glycosylphosphatidylinositol precursor assembly. *FEBS J.* 272, 1160–1168 (2005).

47. Kang, J. Y. *et al.* PIG-V involved in transferring the second mannose in glycosylphosphatidylinositol. *J. Biol. Chem.* 280, 9489–9497 (2005).

48. Fiori, A. *et al.* The heat-induced molecular disaggregase Hsp104 of *Candida albicans* plays a role in biofilm formation and pathogenicity in a worm infection model. *Eukaryot. Cell* 11, 1012–1020 (2012).

49. Gillies, A. T., Taylor, R. & Gestwicki, J. E. Synthetic lethal interactions in yeast reveal functional roles of J protein co-chaperones. *Mol. Biosyst.* 8, 2901–2908 (2012).

50. Gong, Y., Li, T., Yu, C. & Sun, S. *Candida albicans* Heat Shock Proteins and Hsps-Associated Signaling Pathways as Potential Antifungal Targets. *Front. Cell. Infect. Microbiol.* 7, (2017).

51. Yoo, J. Il *et al.* Proteomic analysis of cellular and membrane proteins in fluconazole-resistant candida glabrata. *Osong Public Heal. Res. Perspect.* 3, 74–78 (2012).

52. Cowen, L. E. & Lindquist, S. Hsp90 potentiates the rapid evolution of new traits: Drug resistance in diverse fungi. *Science (80-.).* 309, 2185–2189 (2005).

53. Cowen, L. E., Carpenter, A. E., Matangkasombut, O., Fink, G. R. & Lindquist, S. Genetic architecture of Hsp90-dependent drug resistance. *Eukaryot. Cell* 5, 2184–2188 (2006).

54. Cormack, B. P., Ghori, N. & Falkow, S. An adhesin of the yeast pathogen *Candida glabrata* mediating adherence to human epithelial cells. *Science* 285, 578–582 (1999).

55. Vale-Silva, L. A. *et al.* Upregulation of the Adhesin Gene EPA1 Mediated by PDR1 in *Candida glabrata* Leads to Enhanced Host Colonization. *mSphere* 1, 1–16 (2016).

56. Srivastava, V. K., Suneetha, K. J. & Kaur, R. A systematic analysis reveals an essential role for high-affinity iron uptake system, haemolysin and CFEM domain-containing protein in iron homoeostasis and virulence in *Candida glabrata*. *Biochem. J.* 463, 103–114 (2014).

57. Martínez-Duncker, I., Díaz-Jímenez, D. F. & Mora-Montes, H. M. Comparative analysis of protein glycosylation pathways in humans and the fungal pathogen candida albicans. *International Journal of Microbiology* 2014, (2014).

58. Lussier, M., Sdicu, A. M., Bussereau, F., Jacquet, M. & Bussey, H. The Ktr1p, Ktr3p, and Kre2p/Mnt1p mannosyltransferases participate in the elaboration of yeast O- and N-linked

carbohydrate chains. *J. Biol. Chem.* 272, 15527–15531 (1997).

59. Ene, I. V. *et al.* Host carbon sources modulate cell wall architecture, drug resistance and virulence in a fungal pathogen. *Cell. Microbiol.* 14, 1319–1335 (2012).

60. Ene, I. V. *et al.* Carbon source-induced reprogramming of the cell wall proteome and secretome modulates the adherence and drug resistance of the fungal pathogen *Candida albicans*. *Proteomics* 12, 3164–3179 (2012).

61. Ballou, E. R. *et al.* Lactate signalling regulates fungal β-glucan masking and immune evasion. *Nat. Microbiol.* 2, 16238 (2016).

62. Rodriguez, C. R. *et al.* Kin28, the TFIIH-Associated Carboxy-Terminal Domain Kinase, Facilitates the Recruitment of mRNA Processing Machinery to RNA Polymerase II. *Mol. Cell. Biol.* 20, 104–112 (2000).

63. Alghamdi, T. A. *et al.* Vac14 protein multimerization is a prerequisite step for Fab1 protein complex assembly and function. *J. Biol. Chem.* 288, 9363–9372 (2013).

64. Fiori, A. & Van Dijck, P. Potent synergistic effect of doxycycline with fluconazole against *Candida albicans* is mediated by interference with iron homeostasis. *Antimicrob. Agents Chemother.* (2012). doi:10.1128/AAC.06017-11

65. Demuyser, L. *et al.* Mitochondrial cochaperone Mge1 is involved in regulating susceptibility to fluconazole in *Saccharomyces cerevisiae* and *Candida* species. *MBio* 8, (2017).

66. Prasad, T., Chandra, A., Mukhopadhyay, C. K. & Prasad, R. Unexpected link between iron and drug resistance of *Candida spp.*: Iron depletion enhances membrane fluidity and drug diffusion, leading to drug-susceptible cells. *Antimicrob. Agents Chemother.* 50, 3597–3606 (2006).

67. Arthington-Skaggs, B. A., Jradi, H., Desai, T. & Morrison, C. J. Quantitation of ergosterol content: Novel method for determination of fluconazole susceptibility of *Candida albicans*. *J. Clin. Microbiol.* (1999).

68. Rodrigues, C. F., Silva, S. & Henriques, M. *Candida glabrata*: a review of its features and resistance. *Eur. J. Clin. Microbiol. Infect. Dis.* 33, 673–88 (2014).

69. Brown, A. J. P., Brown, G. D., Netea, M. G. & Gow, N. A. R. Metabolism impacts upon *Candida* immunogenicity and pathogenicity at multiple levels. *Trends in Microbiology* 22, 614–622 (2014).

70. Mortensen, P. B. & Clausen, M. R. Short-chain fatty acids in the human colon: relation to gastrointestinal health and disease. *Scand. J. Gastroenterol. Suppl.* 216, 132–148 (1996).

71. Hameed, S. *et al.* Iron deprivation induces EFG1-mediated hyphal development in *Candida albicans* without affecting biofilm formation. *FEMS Yeast Res.* 8, 744–755 (2008).

72. Ramage, G. Investigation of multidrug efflux pumps in relation to fluconazole resistance in *Candida albicans* biofilms. *J. Antimicrob. Chemother.* (2002). doi:10.1093/jac/dkf049

73. Mathé, L. & Van Dijck, P. Recent insights into *Candida albicans* biofilm resistance mechanisms. *Curr. Genet.* (2013). doi:10.1007/s00294-013-0400-3

74. Fonseca, E. *et al.* Effects of fluconazole on *Candida glabrata* biofilms and its relationship with ABC transporter gene expression. *Biofouling* 30, 447–57 (2014).

75. Edgar, R., Domrachev, M. & Lash, A. Gene Expression Omnibus: NCBI gene expression and hybridization array data repository. *Nucleic Acids Res.* 30, 207–210 (2002).

76. Inglis, D. O. *et al.* The *Candida* genome database incorporates multiple *Candida* species: Multispecies search and analysis tools with curated gene and protein information for *Candida albicans* and *Candida glabrata*. *Nucleic Acids Res.* 40, (2012).

77. Bindea, G. *et al.* ClueGO: A Cytoscape plug-in to decipher functionally grouped gene ontology and pathway annotation networks. *Bioinformatics* 25, 1091–1093 (2009).

78. Shannon, P. *et al.* Cytoscape: A Software Environment for Integrated Models of Biomolecular Interaction Networks. *Genome Res. 13(11), 2498–2504.* 13, 2498–2504 (2003).

79. Li, Q. Q., Skinner, J. & Bennett, J. E. Evaluation of reference genes for real-time quantitative PCR studies in *Candida glabrata* following azole treatment. *BMC Mol. Biol.* 13, (2012).

80. Morio, F., Pagniez, F., Lacroix, C., Miegeville, M. & Le pape, P. Amino acid substitutions in the *Candida albicans* sterol δ5,6-desaturase (Erg3p) confer azole resistance: Characterization of two novel mutants with impaired virulence. *J. Antimicrob. Chemother.* (2012)

81. Müller, C., Binder, U., Bracher, F. & Giera, M. Antifungal drug testing by combining minimal inhibitory concentration testing with target identification by gas chromatography-mass spectrometry. *Nat. Protoc.* (2017).

CHAPTER 6

ACETATE ASSIMILATION IS AN INTEGRAL PART OF *CANDIDA GLABRATA* PERSISTENCE WITHIN THE HUMAN HOST

Disclaimer

The work presented in this chapter is in preparation for publication.

-

Alves R, Duarte C, Timmermans B, Van Ende M, Rogiers O, Mota S, Brunke S, Casal M, Van Dijck P, Paiva S. Acetate assimilation is an integral part of *Candida glabrata* persistence within the human host.

-

ABSTRACT

The pathogenic yeast *Candida* glabrata has evolved distinct strategies to survive and proliferate within the human host. These strategies include sophisticated mechanisms to rapidly adapt to a diverse range of environmental stresses and assimilate the available nutrients. During gastrointestinal and vaginal colonization, or inside immune effector cells, nonfermentable carbon sources, including acetate, are particularly abundant and may support the growth and the proliferation of these pathogens. Our studies have previously demonstrated that the presence of acetate influences biofilm formation and antifungal drug resistance, and modulates immune recognition, suggesting that acetate transporters and channels have an important impact on these processes.

Here, we provide a functional characterization and a detailed view on the role of *C. glabrata* acetate transporters and channels during host colonization. We confirmed by heterologous expression that these proteins restore the growth in acetic acid, in a strain deleted in acetate transporters. We also addressed their physiological role within human monocyte-derived macrophages. Studies regarding the involvement of these transporters and channels in biofilm formation and antifungal resistance are also being performed in a murine subcutaneous biofilm model. Our data support the view that these transporters are required for *Candida* adaptation to the human host and, in particular, for *Candida* survival and persistence inside phagocytes.

6.1 INTRODUCTION

The pathogenic yeast *Candida glabrata* has evolved distinct strategies to survive and proliferate within the human host, including sophisticated mechanisms to rapidly adapt to a diverse range of environmental stresses [1]. During gastrointestinal and vaginal colonization, glucose is scarce and alternative, nonfermentable carbon sources, mostly acetate and lactate, may support growth, proliferation and survival of *Candida* [2–5]. Adaptation to these environments requires dramatic transcriptional and metabolic changes, including a switch to a respiratory metabolism [6] and the overexpression of carboxylate transporters to assimilate these nonfermentable carbon sources [4,5]. Some components of these metabolic pathways are required for full virulence in animal models of candidiasis [6–9], highlighting the importance of nutrient assimilation for the success of these yeasts as human pathogens.

Phagocytosed *Candida* cells display similar transcriptional and metabolic responses, suggesting that carboxylic acids are readily available and sustain the persistence of these pathogens within phagocytic cells via glyoxylate cycle and gluconeogenesis [10–15]. This is particularly relevant for *C. glabrata* [11,12,15], which is able to survive and replicate for extended periods of time inside macrophages [16,17], while triggering a very low cytokine response [18].

Current hypothesis point to the involvement of some members of the Acetate Uptake Transporter Family (AceTr; TCDB 2.A.96.1.4) for the fitness of *Candida* species during host colonization. In particular, interaction studies with *C. glabrata* and immune cells have consistently demonstrated the upregulation of Cg*ATO1* (CAGL0M03465g) during phagocytosis either by macrophages [11] or neutrophils [15], as well as its implication in the phagocytic process [5]. In *C. albicans*, this family is greatly expanded relative to other fungi, with eight potentially functional orthologs whereas both *Saccharomyces cerevisiae* and *C. glabrata* only have three. Many of these orthologs, but not all, are also upregulated in phagocytosed cells and contribute to the alkalization of the phagosome [19,20]. The environmental modulation of the extracellular pH stimulates morphogenesis, allowing *C. albicans* to escape from macrophages either by rupturing the immune cell [19,21] or by inducing macrophage pyroptosis [22]. The contribution of these AceTr family members (also known as ATOs) to the extracellular alkalization was reported to occur via the export of ammonia, and potentially, via other carboxylic acids [19,20]. However, biochemical and structural data from phylogenetically distant members of this family, including from eukarya [23], bacteria [24] or archaea [25,26], support their function mainly as acetate transporters [26–28]. Yet, the *Candida* AceTr family members remain fully uncharacterized. Therefore, we reasoned that *C. glabrata* Ato transporters might play a significant role in the uptake of acetate. We confirmed this by showing that each *C. glabrata* Ato protein restores the ability to complement the loss of ScAto function. In parallel, we also functionally characterized two *C. glabrata* aqua(glycerol)porins, CgFps1 and CgFps2, since ScFps1 has been previously reported to be involved in acetic acid uptake [29]. Both genes in *C. glabrata* are also upregulated in the presence of acetic acid [5]. In fact, aqua(glycerol)porins have been shown to transport carboxylic acids, including lactate and acetate, in several organisms [29–32]. Given the importance of acetate as a nonfermentable carbon source in some host niches, we studied the role of these transporters and channels in some disease models. In particular, we addressed the importance of acetate assimilation for *C. glabrata* persistence within human monocyte-derived macrophages. We are also evaluating whether biofilm formation and antifungal drug resistance are affected when acetate uptake is blocked in *C. glabrata*, by using a murine subcutaneous biofilm model.

6.2 MATERIAL AND METHODS

6.2.1 Yeast strains and growth conditions

The *C. glabrata* reference strain used in this study (ΔHTL) was derived from ATC2001 strain with deletions in the histidine (*HIS3*), tryptophan (*TRP1*) and leucine (*LEU2*) loci [33]. All *C. glabrata* mutant strains were generated from ΔHTL and are listed in Table 6.1.

Table 6.1 *C. glabrata* strains used and generated in this study.

Name	Relevant genotype	Parental strain	Origin
ΔHTL	ATCC 2001 *his3*Δ::FRT *leu2*Δ::FRT *trp1*Δ::FRT	ATCC 2001	[33]
CGRA01	ATCC 2001 *his3*Δ::FRT *leu2*Δ::FRT *trp1*Δ::FRT *ato1*Δ::natNT2	ΔHTL	This study
CGRA04	ATCC 2001 *his3*Δ::FRT *leu2*Δ::FRT *trp1*Δ::FRT ***ato1*Δ::FRT**	CGRA01	This study
CGRA07	ATCC 2001 *his3*Δ::FRT *leu2*Δ::FRT *trp1*Δ::FRT *ato2*Δ::natNT2	ΔHTL	This study
CGRA10	ATCC 2001 *his3*Δ::FRT *leu2*Δ::FRT *trp1*Δ::FRT ***ato2*Δ::FRT**	CGRA07	This study
CGRA13	ATCC 2001 *his3*Δ::FRT *leu2*Δ::FRT *trp1*Δ::FRT *ato3*Δ::natNT2	ΔHTL	This study
CGRA16	ATCC 2001 *his3*Δ::FRT *leu2*Δ::FRT *trp1*Δ::FRT ***ato3*Δ::FRT**	CGRA13	This study
CGRA19	ATCC 2001 *his3*Δ::FRT *leu2*Δ::FRT *trp1*Δ::FRT *fps1*Δ::natNT2	ΔHTL	This study
CGRA22	ATCC 2001 *his3*Δ::FRT *leu2*Δ::FRT *trp1*Δ::FRT ***fps1*Δ::FRT**	CGRA19	This study
CGRA25	ATCC 2001 *his3*Δ::FRT *leu2*Δ::FRT *trp1*Δ::FRT *fps2*Δ::natNT2	ΔHTL	This study
CGRA28	ATCC 2001 *his3*Δ::FRT *leu2*Δ::FRT *trp1*Δ::FRT ***fps2*Δ::FRT**	CGRA25	This study
CGRA31	ATCC 2001 *his3*Δ::FRT *leu2*Δ::FRT *trp1*Δ::FRT *fps1*Δ::FRT *fps2*Δ::natNT2	CGRA22	This study
CGRA34	ATCC 2001 *his3*Δ::FRT *leu2*Δ::FRT *trp1*Δ::FRT ***fps1*Δ::FRT *fps2*Δ::FRT**	CGRA31	This study
CGRA37	ATCC 2001 *his3*Δ::FRT *leu2*Δ::FRT *trp1*Δ::FRT *ato1*Δ::FRT *ato2*Δ::natNT2	CGRA04	This study
CGRA40	ATCC 2001 *his3*Δ::FRT *leu2*Δ::FRT *trp1*Δ::FRT ***ato1*Δ::FRT *ato2*Δ::FRT**	CGRA37	This study
CGRA43	ATCC 2001 *his3*Δ::FRT *leu2*Δ::FRT *trp1*Δ::FRT *ato1*Δ::FRT *ato2*Δ::FRT *ato3*Δ::natNT2	CGRA40	This study
CGRA46	ATCC 2001 *his3*Δ::FRT *leu2*Δ::FRT *trp1*Δ::FRT ***ato1*Δ::FRT *ato2*Δ::FRT *ato3*Δ::FRT**	CGRA43	This study
CGRA49	ATCC 2001 *his3*Δ::FRT *leu2*Δ::FRT *trp1*Δ::FRT *ato1*Δ::FRT *ato2*Δ::FRT *ato3*Δ::FRT *fps1*Δ::natNT2	CGRA46	This study
CGRA52	ATCC 2001 *his3*Δ::FRT *leu2*Δ::FRT *trp1*Δ::FRT ***ato1*Δ::FRT *ato2*Δ::FRT *atot3*Δ::FRT *fps1*Δ::FRT**	CGRA49	This study
CGRA55	ATCC 2001 *his3*Δ::FRT *leu2*Δ::FRT *trp1*Δ::FRT *atot1*Δ::FRT *ato2*Δ::FRT *ato3*Δ::FRT *fps1*Δ::FRT *fps2*Δ::natNT2	CGRA52	This study
CGRA58	ATCC 2001 *his3*Δ::FRT *leu2*Δ::FRT *trp1*Δ::FRT ***ato1*Δ::FRT *ato2*Δ::FRT *ato3*Δ::FRT *fps1*Δ::FRT *fps2*Δ::FRT**	CGRA55	This study
CGRA61	ΔHTL + pBC6-mcherry-Cg*ATO1*	ΔHTL	This study
CGRA63	ΔHTL + pBC6-mcherry-Cg*ATO2*	ΔHTL	This study
CGRA66	ΔHTL + pBC6-mcherry-Cg*ATO3*	ΔHTL	This study
CGRA69	ΔHTL + pBC6-mcherry-Cg*FPS1*	ΔHTL	This study
CGRA72	ΔHTL + pBC6-mcherry-Cg*FPS2*	ΔHTL	This study

The *S. cerevisiae* host strain used in this study, for heterologous expression, was IMX1000, deleted in 25 transporter genes in a CEN.PK113-7D background [34]. All *S. cerevisiae* strains generated during this work are listed in Table 6.2. Cultures were routinely grown either in YPD (1% yeast extract, 2% peptone and 2% glucose), synthetic complete (SC) medium (0.67% yeast nitrogen base with ammonium sulfate, 2% glucose or 0.5% acetic acid, supplemented with a complete amino acid mixture; CSM from Formedium) or synthetic defined (SD) medium (0.67% yeast nitrogen base with ammonium sulfate, 2% glucose or 0.5% acetic acid, supplemented with the appropriate mixture of amino acids) at 30°C for *S. cerevisiae* and at 37°C for *C. glabrata*. Both SC and SD media were buffered either at pH 5.0 or 6.0, as specified for each experiment. For solid YPD, SC or SD media, 1.5% agar was added.

Table 6.2 *S. cerevisiae* strains used in this study.

Name	Relevant genotype	Parental strain	Origin
IMX1000	*MATa ura3-52 trp1-289 leu2-3112 his3*Δ can1::cas9-natNT2 *mch1*Δ *mch2*Δ *mch5*Δ *aqy1*Δ *itr1*Δ *pdr12*Δ *mch3*Δ *mch4*Δ *yil166c*Δ *hxt1*Δ *jen1*Δ *ady2*Δ *aqr1*Δ *thi73*Δ *fps1*Δ *aqy2*Δ *yll053c*Δ *ato2*Δ *ato3*Δ *aqy3*Δ *tpo2*Δ *yro2*Δ *azr1*Δ *yhl008c*Δ *tpo3*Δ	CEN.PK113-7D	[34]
SCRA01	IMX1000 + p416-Cg*ATO1*	IMX1000	This study
SCRA04	IMX1000 + p416-Cg*ATO2*	IMX1000	This study
SCRA07	IMX1000 + p416-Cg*ATO3*	IMX1000	This study
SCRA10	IMX1000 + p416-Cg*FPS1*	IMX1000	This study
SCRA13	IMX1000 + p416-Cg*FPS2*	IMX1000	This study

6.2.2 Construction of *C. glabrata* mutant strains

Gene deletions were performed in the ΔHTL strain by homologous recombination, using the *SAT1* flipping method, resulting in several *C. glabrata* mutants (Table 6.1) [35]. Briefly, a cassette containing the *C. albicans NAT1* (Ca*NAT1*) gene, which confers nourseothricin resistance, flanked by FLP recombinase recognition target (FRT) sites, was amplified by PCR from the pYC44 plasmid (Table 6.3) [36], using forward and reverse primers that included 100 nucleotides upstream and downstream the noncoding sequence of each selected gene, respectively (Table 6.4). The PCR reaction was performed using Ex Taq DNA Polymerase according to manufacturer's protocol (Takara). The thermocycler setting consisted of one cycle of 98°C for 30 sec, 30 cycles of 98°C for 30 sec, 60°C for 30 sec and 72°C for 2 min, and one cycle of 72°C for 10 min. The correct size of each fragment was confirmed by electrophoresis. Cells from a YPD preculture were diluted in 50 mL fresh YPD medium to an optical density at 600 nm (OD_{600nm}) of approximately 0.2 and grown at 37°C for 3-4 h to an OD_{600nm} of approximately 1.5. Cells were then collected by centrifugation at 3000 *g* for 5 min, washed two times with 50 mL of sterile water and finally resuspended in 8 mL of sterile water. After addition of 1 mL of 10x TE (100 mM Tris-HCl, 10 mM EDTA,

pH 7.5) and 1 mL of 1M lithium acetate (pH 7.5), the suspension was incubated in a rotary shaker at 200 rpm for 30 min at 37°C. Then, 250 µL of 1M dithiothreitol were added to the cell culture and incubated for 1 h at 37°C with shaking. After addition of 40 mL of sterile water the cells were centrifuged at 3000 *g* for 5 min, and kept on ice until the electroporation step. Cells were washed sequentially two times in 25 mL ice-cold water and one time in 5 mL of ice-cold 1M sorbitol. Cells were resuspended in 500 µL of ice-cold 1M sorbitol. For each transformation, 45 µL of electrocompetent cells and approximately 1 µg of the amplified NAT cassette (5 µL) were mixed and electroporated at 1.5 kV; 200 Ω; 25 µF. Recovery was carried out by adding 2 mL of YPD and incubation at 37°C for 4 h with shaking. After that, cells were harvested at 3000 *g* for 5 min, resuspended in 100 µL of sterile water and plated on YPD containing 200 µg.mL^{-1} of nourseothricin (clonNAT; Jena Bioscience GmbH, Germany). Resistant colonies were picked after 1-2 days of growth and confirmed by colony PCR analysis, using X-upstream-fw and NAT-rv primers (Table 6.4). The PCR reaction was performed using a homemade Taq DNA Polymerase. The thermocycler setting consisted of one cycle of 98°C for 10 min, 30 cycles of 98°C for 30 sec, 60°C for 30 sec and 72°C for 1 min, and one cycle of 72°C for 10 min. Positive confirmed transformants were streaked on YPD plates containing 200 µg.mL^{-1} of clonNAT for further use. To create the multiple mutants, the *NAT* cassette was removed by transforming the clonNAT resistant mutants with a vector expressing the FLP1 recombinase (pLS10; Table 6.3). Flp1-induced recombination at the FRT sites was selected on YPD plates containing 300 µg.mL^{-1} of hygromycin B (HYG; Invitrogen, CA, USA). Resistant colonies were picked up after 2 days of growth and confirmed by colony PCR analysis using primers X-upstream-fw and X-downstream-rv (Table 6.4), as previously described. Positive confirmed transformants were streaked on YPD plates, resulting in the restoration of both clonNAT and HYG sensitivities and allowing the generation of a second deletion by the same method.

Table 6.3 Plasmids used and generated in this study.

Name	Description	Origin
pYC44	Plasmid containing CaNAT1 flanked by FRT sites	[36]
pLS10	Plasmid expressing FLP1 recombinase (HYG^R)	Van Dijck Lab
p416-GPD	Yeast expression vector containing GPD promoter	[37]
pBC6	Yeast expression vector containing TEF promoter	Van Dijck Lab
pYC42	Recipient mCherry replicative vector	[36]
pYC55	Recipient YFP replicative vector	[36]
p416-CgATO1	Plasmid expressing Cg-*ATO1* from GPD promoter	This study
p416-CgATO2	Plasmid expressing Cg-*ATO2* from GPD promoter	This study
p416-CgATO3	Plasmid expressing Cg-*ATO3* from GPD promoter	This study
p416-CgFPS1	Plasmid expressing Cg-*FPS1* from GPD promoter	This study
p416-CgFPS2	Plasmid expressing Cg-*FPS2* from GPD promoter	This study

pBC6-mcherry-CgATO1	Plasmid expressing N-tagged Cg*ATO1* with mCherry	This study
pBC6-YFP-CgATO1	Plasmid expressing N-tagged Cg*ATO1* with YFP	This study
pBC6-mcherry-CgATO2	Plasmid expressing N-tagged Cg*ATO2* with mCherry	This study
pBC6-YFP-CgATO2	Plasmid expressing N-tagged Cg*ATO2* with YFP	This study
pBC6-mcherry-CgATO3	Plasmid expressing N-tagged Cg*ATO3* with mCherry	This study
pBC6-YFP-CgATO3	Plasmid expressing N-tagged Cg*ATO3* with YFP	This study
pBC6-mcherry-CgFPS1	Plasmid expressing N-tagged Cg*FPS1* with mCherry	This study
pBC6-YFP-CgFPS1	Plasmid expressing N-tagged Cg*FPS1* with YFP	This study
pBC6-mcherry-CgFPS2	Plasmid expressing N-tagged Cg*FPS2* with mCherry	This study
pBC6-YFP-CgFPS2	Plasmid expressing N-tagged Cg*FPS2* with YFP	This study

Table 6.4 Oligonucleotides used in this study.

Oligonucleotide name	Sequence
ato1-pYC44-fw	TTACTAGATATAAAAAAAAAAAGTTACCTTTTTTTTTTTATTGAACGTACACTGCACATAATTAAA TTGTTTCAAAATTAAGTTCCTACACAAATTTCAGgctctagaactagtggatcc
ato1-pYC44-rv	GACTAGCACGACATTTGTTATTATTATTGTTAGTGTTTTGTTTTATGGTTTAAATTGAAATTAAAA CCGTAAGATTTGAAATTGCAGAAGTTCAAAAAAAagggaacaaaagctggtacc
ato2-pYC44-fw	GACTTGATGTGGTTTCGATTGAAATTTACTTGTAGAACAGGTATAGATATTTGCTGGATAGGTAA TATACCAGTTGAATAATCAAAGAAACATAAAAAAAgctctagaactagtggatcc
ato2-pYC44-rv	AATTTCAGGAAAATTTAAATTGTTGCATACAGTAAAGTAGCGATTTATTTTTTTTCATTATGTGCA TTTCTTAAGCTCTGCATCAGTTATTGTTAATATTagggaacaaaagctggtacc
ato3-pYC44-fw	AATTCCCTTGTGCACTCGTAAATTCAGTGTAGAACTCGTAAAAAATTGTGTACAATATTACCGAT AAGCCACAAACACAATAACTAATCATATAAGTCACgctctagaactagtggatcc
ato3-pYC44-rv	CGTGAAGTAAAAATTATGCTATCTTGATGAGCGCAGAGTCTGGAGATGTGTAGATTTTCGGAATA TAATTAAAAGGGACGAGATGAAGTTAGTTTTGGATagggaacaaaagctggtacc
fps1-pYC44-fw	CCGTCTAGCATTTTCTGGATATACATTATAAAAATACAATCAAAAATCAATAAAAAACAATCTAGA CTGATACTATTCTGATACTAAAGTATAACAAAAAgctctagaactagtggatcc
fps1-pYC44-rv	AATAATGCTAGAAAATGGGACGTGCTCTATCTCTTCCTTCCTGGGAACAGAAGCACATTGAGGT ATACTATCCATGGGCATGACGATTCGTTCCGTTTATagggaacaaaagctggtacc
fps2-pYC44-fw	GACTATCTCAAAACAATACTAAAACAACTCGACAATCTACATTTTACTACTTTTCTTTGAAGAATA ATATACTACACTTTGAGACTCCAGCTTGACAAAGgctctagaactagtggatcc
fps2-pYC44-rv	GAATCATCAAATATTGCGTAAGTTATAAATATAACCTGGCGTTATGAGTGGAGTGGTAACAATTCA TGTAAACTCACATTTACTTTATGAGTAAGAGACCagggaacaaaagctggtacc
ato1-upstream-fw	GCTGTCTTTCGAATATCAACAACAC
ato1-dowstream-rv	GCTCTGTTTCAATTGTAGATCAATAGG
ato2-upstream-fw	GGTATTGAGTTCATCTCCGGTATAA
ato2-dowstream-rv	GTTACTGTGAGCGAAATATGAAGTAGTA
ato3-upstream-fw	CGATGCACAGAACGGATAAATTAAG
ato3-dowstream-rv	CTCGATGAACCCAGTGATGTC
fps1-upstream-fw	GTATATCGGATTACTTGTGCGCT
fps1-dowstream-rv	CTACTTGACGCTCGGACTG
fps2-upstream-fw	GTCCACGGACTTACCTATTCTG
fps2-dowstream-rv	CCTTGATGGACATAATAAGCTTCCT
NAT-rv	CGTCAAGACTGTCAAGGAGGG
p416-GPD-ATO1-fw	CTAGAACTAGTGGATCCCCCGGGCTGCAGGATGTCTGACAAAGATCAAGG
p416-GPD-ATO1-rv	TCGACGGTATCGATAAGCTTGATATCGAATTTAGTATAGGGTCTTTTCGTTT
p416-GPD-ATO2-fw	CTAGAACTAGTGGATCCCCCGGGCTGCAGGATGGTTTCTATTAGCTCCAG
p416-GPD-ATO2-rv	TCGACGGTATCGATAAGCTTGATATCGAATTCTAAAAAAACACCTTCTCGTTA
p416-GPD-ATO3-fw	CTAGAACTAGTGGATCCCCCGGGCTGCAGGATGAGCTCATCATCCTCACA
p416-GPD-ATO3-rv	TCGACGGTATCGATAAGCTTGATATCGAATTTTAGTTTGGCATCATGATGG
p416-GPD-FPS1-fw	CTAGAACTAGTGGATCCCCCGGGCTGCAGGATGTCTCATCAGCAAGGG

p416-GPD-FPS1-rv	TCGACGGTATCGATAAGCTTGATATCGAATTTCAGTTACTGTTCTTGGAAC
p416-GPD-FPS2-fw	CTAGAACTAGTGGATCCCCCGGGCTGCAGGATGGAATCTATTCATGATGCTATG
p416-GPD-FPS2-rv	TCGACGGTATCGATAAGCTTGATATCGAATTCTAATATGACACCTTCTCATCA
pBC6-BamHI-CgATO1-fw	TTTCTAGAACTAGTGGATCCACAATGTCTGACAAAGATCAA
pBC6-CgATO1-linker-rv	CCCGCCTCCAGATCCTCCGCCAGAGCCTCCCCCGTATAGGGTCTTTTCGTTTG
pBC6-BamHI-CgATO2-fw	TTTCTAGAACTAGTGGATCCACAATGAGCTCATCATCC
pBC6-CgATO2-linker-rv	CCCGCCTCCAGATCCTCCGCCAGAGCCTCCCCCAAAAAACACCTTCTCGTTAG
pBC6-BamHI-CgATO3-fw	TTTCTAGAACTAGTGGATCCACAATGAGCTCATCATCCTCACAG
pBC6-CgATO3-linker-rv	CCCGCCTCCAGATCCTCCGCCAGAGCCTCCCCCGTTTGGCATCATGATGGCTC
pBC6-BamHI-CgFPS1-fw	TTTCTAGAACTAGTGGATCCACAATGTCTCATCAGCAAGGG
pBC6-CgFPS1-linker-rv	CCCGCCTCCAGATCCTCCGCCAGAGCCTCCCCCGTTACTGTTCTTGGAACTGT
pBC6-BamHI-CgFPS2-fw	TTTCTAGAACTAGTGGATCCACAATGGAATCTATTCATGAT
pBC6-CgFPS2-linker-rv	CCCGCCTCCAGATCCTCCGCCAGAGCCTCCCCCATATGACACCTTCTCATCAG
D12-linker-mCherry-fw	GGAGGATCTGGAGGCGGGAGCGGCGGAGGTTCTATGGTGAGCAAGGGCGA
D13-mCherry-SacII-rv	AAACCCCGGGGCGGCCGCGGCTACTTGTACAGCTCGTCC
D14-linker-YFP-fw	GGAGGATCTGGAGGCGGGAGCGGCGGAGGTTCTatgAGTAAAGGAGAAGAAC
D15-YFP-SacII-rv	AAACCCCGGGGCGGCCGCGGCTATTTGTATAGTTCATCC

6.2.3 Heterologous expression of *C. glabrata* transporters and channels in *S. cerevisiae*

C. glabrata ATO1 (CAGL0M03465g), *ATO2* (CAGL0L07766g), *ATO3* (CAGL0A03212g), *FPS1* (CAGL0C03267g) and *FPS2* (CAGL0E03894g) were cloned into the p416-GPD vector [37] by homologous recombination using the *Escherichia coli* strain DH5α [38]. Each gene was amplified by PCR from about 50 ng of genomic DNA from the *C. glabrata* ΔHTL strain per 50 µL reaction volume. Yeast specific primers were designed based on the available *C. glabrata* genome at CGD [39] and are listed in Table 6.4 (p416-GPD-X-fw and p416-GPD-X-rv, where X represents the target gene). PCRs were carried out using Phusion High-Fidelity DNA Polymerase (Thermo Fisher Scientific, Massachusetts, USA), following manufacturer's instructions. The thermocycler setting consisted of one cycle of 98°C for 30 sec, 30 cycles of 98°C for 30 sec, 56°C for 30 sec and 72°C for 1 min, and one cycle of 72°C for 10 min. The p416-GPD vector was digested with FastDigest *EcoRI* (Thermo Fisher Scientific, Massachusetts, USA) for 1 h in the respective buffer, following manufacturer's instructions. Competent *E. coli* cells were transformed by the heat shock method [40]. Briefly, each PCR fragment was mixed with the linear vector in a 10 µL volume of pure water. Then this volume was transferred into a microcentrifuge tube containing 50 µL of thawed competent cells and the mixture was incubated for 20 min on ice. Heat shock was carried out by placing the tubes in a water bath for 45 s at 42°C. Readily after the heat shock, cells were placed on ice for 5 min. Then 240 µL of the LB medium were added on the thermal-shocked cells, which were left to recover at 37°C for 1 h. After that time, cells were plated on solid LB medium containing ampicillin as selective antibiotic. Cells grew overnight at 37°C. To test for positive clones, cells from 8

randomly chosen colonies were tested by Colony PCR, as previously described, using p416-GPD-X-fw and p416-GPD-X-rv (Table 6.4). Plasmid DNA was purified from selected positive clones to confirm the correct insertion of the fragment into the vector by sequencing (Eurofins Genomics, Germany GmbH).

6.2.4 Spot assays

C. glabrata cells were incubated overnight as previously described, washed two times in sterile water and diluted to OD_{600nm} = 1 with sterile water. Drop tests were performed by spotting 3 µL of the serially diluted cell suspensions onto SC or SD plates supplemented with: glucose (2% w v^{-1}, pH 5.0); acetate (0.5% v v^{-1}, pH 5.0 or pH 6.0); lactate (0.5% w v^{-1}, pH 5.0); glycerol (1% v v^{-1}, pH 5.0); pyruvate (0.5% w v^{-1}, pH 5.0); succinate (0.5% w v^{-1}, pH 5.0); malate (0.5% w v^{-1}, pH 5.0), citrate (0.5% w v^{-1}, pH 5.0), propionate (0.5% v v^{-1}) or butyrate (0.5% v v^{-1}). Pictures were taken after 2 days of incubation at 37°C or 9 days of incubation at 18°C. Experiments were performed in triplicate.

6.2.5 Construction of plasmids containing the fluorescent-tagged *C. glabrata* transporters

C. glabrata transporter genes were fused with fluorescent tags at the 3'end using the vector pBC6 (Table 6.3) by Gibson Assembly (New England Biolabs) of three gel purified DNA fragments that have at least 20 bp overlap. Each transporter was PCR amplified from about 50 ng of genomic DNA from the *C. glabrata* ΔHTL strain with pBC6-BamHI-X-fw and pBC6-X-linker-rv primers, where X represents the target gene (Table 6.4). Each forward primer has an extended 5'end containing an overlap with the pBC6 plasmid. Each reverse primer has an extended 5' end corresponding to the linker present in the amplified fluorescent tag. The mcherry tag was amplified using D12 and D13 primers, while YFP was amplified using D14 and D15 primers (Table 6.4). D12 and D14 primers have an extended 5'end corresponding to the linker, while D13 and D15 primers have an extended 5'end containing an overlap with the pBC6 plasmid. PCRs were carried out using Phusion High-Fidelity DNA Polymerase (Thermo Fisher Scientific, Massachusetts, USA), following manufacturer's instructions. The thermocycler setting consisted of one cycle of 98°C for 30 sec, 30 cycles of 98°C for 30 sec, 60°C for 30 sec and 72°C for 1 min, and one cycle of 72°C for 10 min. The purified PCR fragments were Gibson assembled with *Bam*HI and *Sac*I digested pBC6 plasmid and transformed into *E. coli* as described before [38]. The resulting plasmids were named pBC6-mcherry-X or pBC6-YFP-X, where X represents the transporter gene, and are listed in Table 6.3. All plasmids were confirmed by restriction analysis and sequencing (Eurofins Genomics, Germany GmbH).

6.2.6 Fluorescent microscopy

C. glabrata cells for fluorescent microscopy were grown overnight using SD-glucose medium (-trp) as described above. A volume of 1 mL of each cell culture was harvested, concentrated and manually immobilized on slides. Cells were immediately visualized under a Zeiss LSM 780 inverted confocal microscope using a 63x oil immersion objective and the 488 nm argon laser. Images were processed using the Zeiss ZEN 2010 software (Carl Zeiss, Jena, Germany).

6.2.7 Transport assays

Measurement of transport activity in *C. glabrata* strains was performed as previously described [24]. Briefly, *C. glabrata* cells were incubated in 50 mL of SC medium supplemented with 2% glucose (pH 5.0) at 37°C, 200 rpm, until OD600nm ≈ 0.5. Then cells were harvested by centrifugation, washed twice in sterile water, resuspended in SC medium supplemented with 0.5% acetic acid, pH 5.0, and incubated again for 6 hours. Cells were then washed with sterile water and resuspended in 0.1 M potassium phosphate buffer, pH 5.0, to a final concentration of about 5–15 mg of dry weight/mL. Then, 30 µL of each yeast cell suspension were added to 60 µL of phosphate buffer in a microtube and after 2 min of incubation at 27°C, the reaction was started by the addition of 10 µL of an aqueous solution of [1-^{14}C]acetate, sodium salt (10 mM, pH 6.0; specific activity of 2000 d.p.m./nmol) purchased from Perkin Elmer. The reaction was stopped by the addition of ice-cold 100 mM non-labelled acid at pH 6.0 after 15 s. The reaction mixtures were centrifuged at 4°C for 5 min at 16,000 g, the pellet was resuspended by vertexing in 1 mL of ice-cold water, centrifuged again and finally resuspended in 1 mL of scintillation liquid (Opti-Phase HiSafe II; LKB FSA Laboratory Supplies). Radioactivity was measured in a Packard Tri-Carb 2200CA liquid scintillation spectrophotometer with d.p.m. correction. The data shown are mean values of triplicates of at least three independent experiments. Statistical analyses were performed using Graph Pad Prism (v. 7) and significance was determined using two-way ANOVA with Tukey's multiple comparison test. All tests were performed with a confidence level of 95%.

6.2.8 *Ex vivo* models of *C. glabrata* phagocytosis using human monocyte-derived macrophages

Phagocytosis assays were performed with human monocyte derived macrophages (MDMs) isolated from buffy coats and differentiated for 7 days to macrophages. *C. glabrata* cells (ΔHTL) were grown in YPD until log-phase and washed twice with sterile water. Experiments were performed in 6 well-plates at a MOI 20Y:1M. After 3 h of incubation, media was removed and macrophages were washed twice with PBS. After 24 h of interaction, 0.5 mL of fresh media were added to each well. From day 2 till day 6, 0.5 mL

of media were removed from the top of each well and replaced by fresh media daily. Media was supplemented with caspofungin after 6 h of incubation. *C. glabrata* cells were retrieved from macrophages after 6, 24 (1 day), 48 (2 days), 96 (4 days) and 168 h (7 days) of incubation. Isolation and amplification of fungal RNA for microarray analysis was performed as previously described [41].

6.2.9 In vivo *C. glabrata* biofilm formation in a murine subcutaneous biofilm model

All animal experiments were performed in accordance with the KU Leuven animal care guidelines and were approved by the ethical committee of KU Leuven (PDO-ECD project from 01-03-2019 till 01-06-2020). All animals were given a standard *ad libitum* diet and housed at random with 4 animals in filter-top cages in a dedicated animal room where temperature, light, and humidity were regulated. This model was adapted from a rat subcutaneous biofilm model [42] to specific-pathogen-free immunocompetent BALB/c mice (6 to 8 weeks old, 20 g). C. glabrata (1×10^6 cells mL^{-1}) attached onto the surface of serum-coated polyurethane catheter pieces during *in vitro* adhesion (90 min, 37°C) followed by a washing step with PBS. Mice were anesthetized as previously described [42]. In order to compare biofilm formation from the WT control strain and mutant strain in a single animal two small incisions were made, one on the left and one on the right side of the back of a mouse, as previously reported [43]. For catheter explant, animals were sacrificed by cervical dislocation. Catheter fragments were removed, washed twice with PBS, and placed in microcentrifuge tubes containing PBS. Devices were sonicated, vigorously vortexed, and plated to enumerate the number of CFUs. The dissemination of *C. glabrata* cells from biofilms into the kidneys, liver, spleen, and the tissue surrounding the catheter pieces was examined after 48 and 144 h of biofilm formation.

6.3 RESULTS

6.3.1 Construction of *C. glabrata* mutants on putative acetate transporters and channels

C. glabrata ATO1 (CAGL0M03465g), *ATO2* (CAGL0L07766g) and *ATO3* (CAGL0A03212g) loci were annotated as putative acetate plasma membrane transporters based on the sequence similarities of their encoded proteins (protein BLAST identities of 74.30%, 73.66% and 31.07%, respectively) to the *S. cerevisiae* acetate transporter Ato1 (YCR010C) [23,26]. *C. glabrata FPS1* (CAGL0C03267g) and *FPS2* (CAGL0E03894g) were annotated as putative acetate channels based on the sequence similarities of their encoded proteins (protein BLAST identities of 53.79% and 46.94%, respectively) to the *S. cerevisiae* aqua(glycerol)protein Fps1 (YLL043W), involved in acetic acid uptake [29]. In *C. glabrata*, these proteins are upregulated in the presence of acetic acid at pH 5.0 [5], supporting their role as potential acetate transporters or channels.

To determine the physiological function of these proteins, each gene was successively deleted in the *C. glabrata* ΔHTL strain by using the *SAT1* flipping method (Figure 6.1A). Two rounds of integration/excision generated deletion strains that differ from the wild type parental strain only by the absence of the target gene and the presence of a single FRT site. The integration of each nourseothricin cassette and subsequent excision was confirmed by colony PCR, using primers that bind either upstream and inside the cassette (X-upstream-fw and NAT-rv, where X represents the target gene; Figure 6.1C; Table 6.4) or upstream and downstream the deleted open reading frames (X-upstream-fw and X-dowstream-fw; Figure 6.1D; Table 6.4). As a control, the same PCR reactions were performed with genomic DNA from the parental strain (Figure 6.1B), where all five target genes were intact, according to the published *C. glabrata* genome at CGD [39]. Gene deletion experiments resulted in five different single mutants (*ato1*Δ, *ato2*Δ, *ato3*Δ, *fps1*Δ and *fps2*Δ), two double (*ato1*Δ*ato2*Δ and *fps1*Δ*fps2*Δ), one triple (*ato1*Δ*ato2*Δ*ato3*Δ) and one quintuple (*ato1*Δ*ato2*Δ*ato3*Δ*fps1*Δ*fps2*Δ) mutants (Table 6.1).

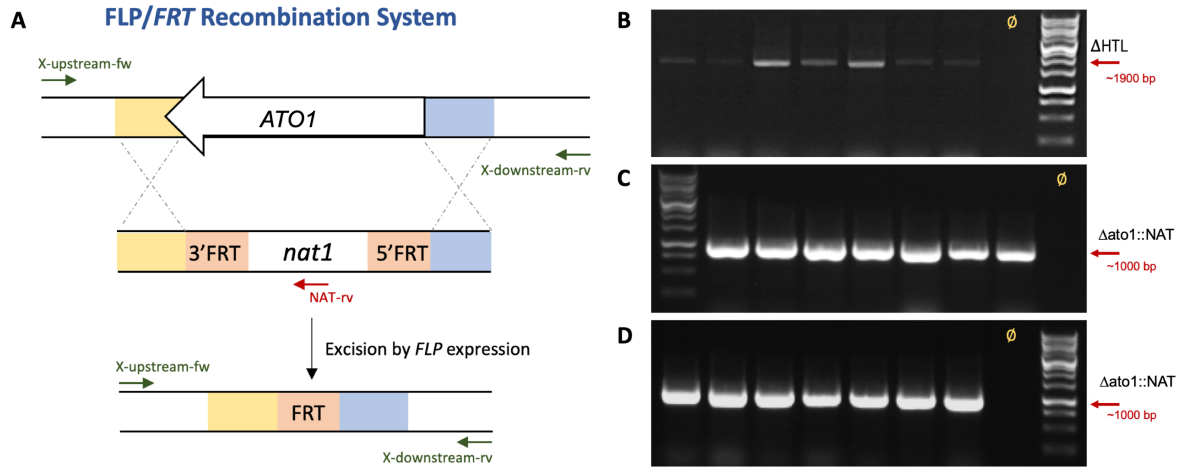

Figure 6.1. Schematic representation of *SAT1* flipping method and diagnostic tests for the verification of correct cassette integration and deletion. A. Integration of nourseothricin (*nat1*) cassette by homologous recombination (homology arms are approximately 100 bp long) and subsequent excision induced by the expression of *FLP1*. **B.** Colony PCR reactions were performed on the genomic DNA of the parental strain as a control using X-upstream-fw and X-downstream-rv primers, where X represents the target gene (Table 6.4). Each primer binds approximately 500 bp upstream or downstream the target gene. **C.** Colony PCR reactions were performed on seven *nat1*-resistant colonies obtained after transformation with *nat1* cassette, using X-upstream-fw and NAT-rv primers (Table 6.4). NAT-rv primer binds approximately 500 bp downstream the start of the cassette. **D.** Colony PCR reactions were performed on seven hygromycin-resistant colonies obtained after transformation with *FLP1* expression plasmid to confirm gene deletion, by using X-upstream-fw and X-downstream-rv primers.

6.3.2 Growth phenotypes of *C. glabrata* mutant strains

The phenotypes of the mutant strains were analyzed by growth assays in liquid and solid medium. All strains were grown at 37°C for 24 h in Synthetic Complete (SC) medium, adjusted to an initial pH value of 5.0, in the presence of 2% glucose (Figure 6.2 A). Results indicate that all strains grew well in the presence of glucose, with no significant changes detected in the growth rates between the different strains.

We also collected samples to measure the pH values over time. When cells grown in glucose, as sole carbon source, there is an acidification of the external medium (Figure 6.2B). This is expected due to the excretion of metabolites resulting from glucose metabolism, which was confirmed by HPLC (data not shown).

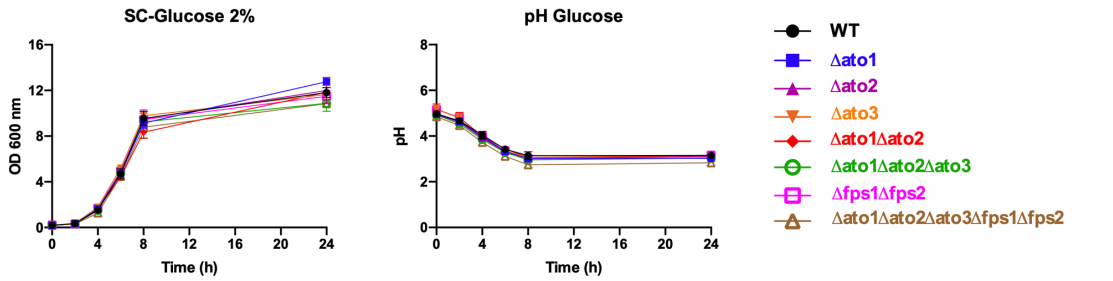

Figure 6.2. Growth and pH curves of *C. glabrata* wild type (WT) and mutant strains in the presence of glucose. A. *C. glabrata* strains were grown at 37°C for 24 h in Synthetic Complete (SC) medium, adjusted to an initial pH of 5.0, supplemented with 2% glucose. Cell growth was monitored by optical density at 600 nm (OD 600nm). **B**. The pH was recorded over time using a pH probe. Error bars show standard deviations. Experiments were done in triplicate.

Growth of wild type and mutant strains was also evaluated on solid media, with plates being incubated either at 37°C for 48 h or 18°C for 216 h (Figure 6.4). At 37°C, no differences in growth were observed between the wild-type and mutant strains in all tested conditions (Figure 6.3), except in propionate and butyrate containing media (data not shown), where no growth was observed. In an attempt to decrease the diffusion rate of the undissociated form of the acids across the plasma membrane, which usually allows a better phenotype discrimination, the growth for all strains was also evaluated at 18°C (Figure 6.4).

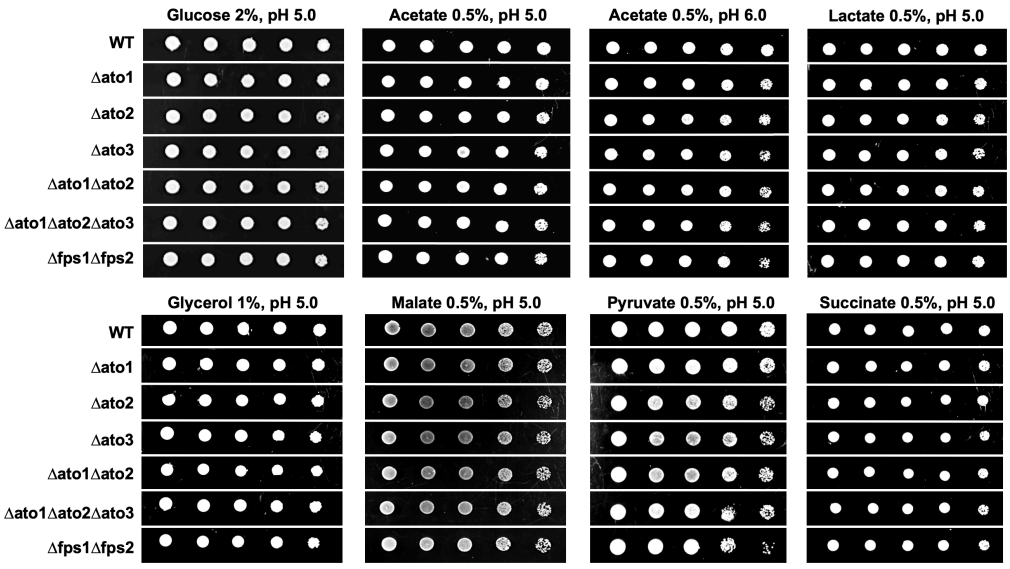

Figure 6.3. Growth phenotypes of *Candida glabrata* wild type (WT; ΔHTL) and knock-out strains. Serial dilutions were spotted on Synthetic Complete (SC) solid medium containing different carbon sources:

glucose (2% w v^{-1}, pH 5.0); acetate (0.5% v v^{-1}, pH 5.0 and 6.0); lactate (0.5% w v^{-1}, pH 5.0); glycerol (1% v v^{-1}, pH 5.0); malate (0.5% w v^{-1}, pH 5.0); pyruvate (0.5% w v^{-1}, pH 5.0) and succinate (0.5% w v^{-1}, pH 5.0). Cell growth was not detected (data not shown) in the presence of propionate (0.5% v v^{-1}) or butyrate (0.5% v v^{-1}). Pictures were taken after 48 h of incubation at 37°C. Experiments were performed in triplicate, showing consistent results among all the independent assays.

After 9 days of incubation (216 h) at 18 °C, all strains displayed a similar growth as the wild type in the presence of glucose (Figure 6.4). However, some differences were observed between the wild type and the mutant strains for other growth conditions. In particular, the double and triple Ato mutants, as well as the quintuple, display a small growth defect in the presence of acetate and lactate, when compared with the wild type strain (Figure 6.4). This observation suggests that Ato transporters may mediate the uptake of these substrates. In the presence of glycerol, as expected [29], the *C. glabrata* strains deleted in both *FPS1* and *FPS2* channels (Δ*fps1*Δ*fps2* and Δ*ato1*Δ*ato2*Δ*ato3*Δ*fps1*Δ*fps2*) display an evident growth defect (Figure 6.4). Interestingly, the wild type strain is not able to grow at 18 °C in the presence of pyruvate, succinate or malate, but the mutant strains seem to revert this phenotype (Figure 6.4). Deletion of any of the Ato transporters or Fps channels seems to slightly improve growth under these conditions, yet the growth is still poor. No differences were observed among the different strains in the presence of citrate (Figure 6.4).

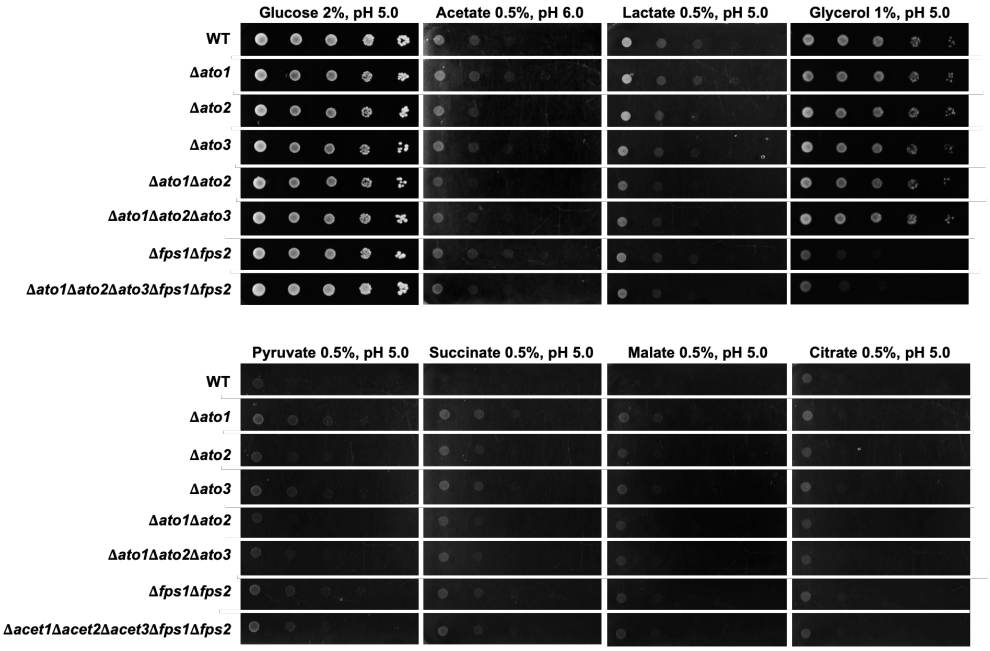

Figure 6.4. Growth phenotypes of *Candida glabrata* wild type (WT; ΔHTL) and knock-out strains. Serial dilutions were spotted on Synthetic Complete (SC) solid medium containing different carbon sources:

glucose (2% w v^{-1}, pH 5.0); acetate (0.5% v v^{-1}, pH 6.0); lactate (0.5% w v^{-1}, pH 5.0); glycerol (1% v v^{-1}, pH 5.0); pyruvate (0.5% w v^{-1}, pH 5.0); succinate (0.5% w v^{-1}, pH 5.0); malate (0.5% w v^{-1}, pH 5.0) and citrate (0.5% w v^{-1}, pH 5.0). Cell growth was not detected (data not shown) in the presence of propionate (0.5% v v^{-1}) or butyrate (0.5% v v^{-1}). Pictures were taken after 9 days of incubation at 18°C. Experiments were performed in triplicate, showing consistent results among all the independent assays.

6.3.3 Heterologous expression of *C. glabrata* acetate transporters and channels in *S. cerevisiae*

To further determine if the function of the Ato proteins is conserved in *S. cerevisiae*, we examined the ability of Cg*ATO1*, Cg*ATO2*, Cg*ATO3*, Cg*FPS1* and Cg*FPS2* to rescue the *S. cerevisiae* IMX1000 growth defect on acetic acid. This strain is deleted in 25 membrane-protein-encoding genes, including all the transporters known to mediate acetic acid uptake, namely Sc*ATO1*, Sc*ATO2*, Sc*ATO3* and Sc*FPS1* [34]. As a control we used the well-characterized acetate transporter Sc*ATO1* [23]. Each gene was independently expressed in the IMX1000 strain in Synthetic Defined (SD) medium supplemented with 0.5% acetic acid. The pH of the media was adjusted to 6.0, in order to guarantee that a high percentage of dissociated acid (acetic acid pKa=4.76) is present and enters the cell by a mediated transport mechanism. The obtained results show that the expression of each gene was sufficient to restore acetate growth, suggesting that they play a role in acetate uptake (Figure 6.5).

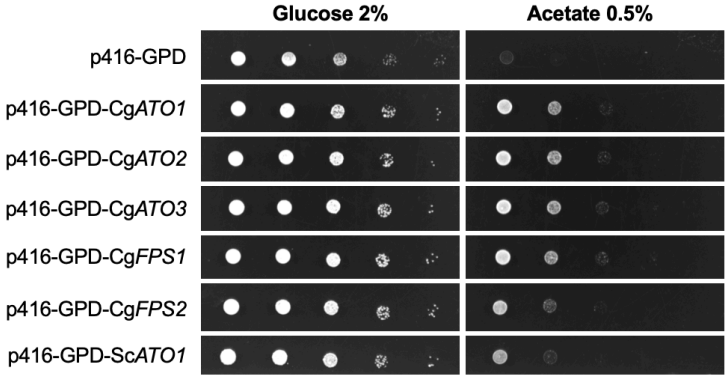

Figure 6.5. Growth phenotypes of *S. cerevisae* IMX1000 heterologously expressing *C. glabrata* Ato transporters and Fps channels. Cg*ATO1*, Cg*ATO2*, Cg*ATO3*, Cg*FPS1* and Cg*FPS2* were independently cloned into the p416-GPD expression vector (Table 6.3) and transformed into the IMX1000 strain. Serial dilutions were spotted on Synthetic Defined (SD) solid medium containing either glucose (2% w v^{-1}, pH 6.0) or acetate (0.5% v v^{-1}, pH 6.0) and supplemented with the required amino acids for auxotrophic growth. Pictures were taken after 9 days of incubation at 18°C. Experiments were performed in triplicate, showing consistent results among all the independent assays.

To study the expression and subcellular localization of these proteins, we also used *S. cerevisiae* IMX1000 cells transformed with plasmids harboring genetic fusions of the transporters encoding genes with fluorescent tags. The coding sequence of the fluorescent mCherry tag was cloned at the 3'end of each gene and introduced into the pBC6 expression vector, containing a constitutive and strong TEF promoter (Table 6.3). We could only test two transporters, CgAto1 and CgFps1, due to technical issues. Confocal microscopy revealed that both CgAto1-mCherry and CgFps1-mCherry localize to the plasma membrane (Figure 6.6). Although the mCherry signal is predominantly at the cell surface (Figure 6.6), some fluorescence is also associated with intracellular structures in both cases. These structures resemble the endoplasmic reticulum, suggesting that the overexpression of these proteins, driven by the *TEF* strong promoter, may result in some ER retention. In contrast to CgAto1-mCherry, the CgFps1-mCherry signal was not uniformly distributed over the cell surface but rather appeared in patches, as previously reported for Sc*FPS1* (Figure 6.6) [45].

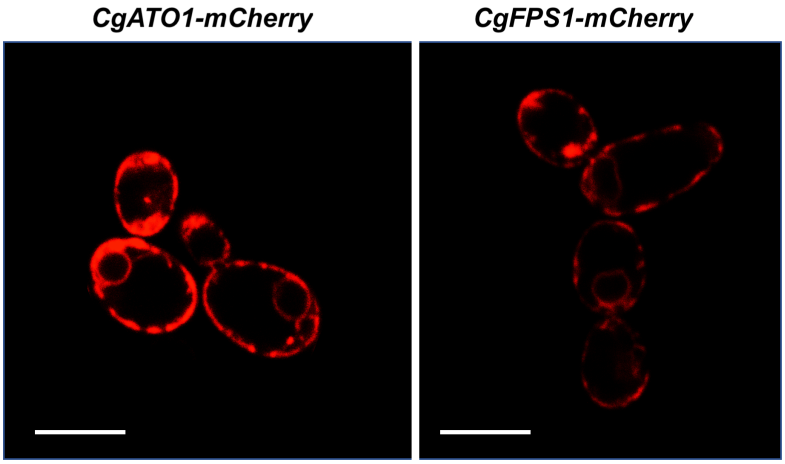

Figure 6.6. *C. glabrata* Ato1 transporter and Fps1 channel localize to the plasma membrane. *S. cerevisiae* IMX1000 strain was transformed with pBC6 plasmids containing Cg*ATO1* (left) and Cg*FPS1* (right) both tagged at their 3'end with the fluorescent tag mCherry (Table 6.3). Representative images were captured using a Zeiss LSM 780 confocal microscope equipped with a 63 x NA1.4 oil immersion lens. Scale bars, 5 μm.

6.3.4 Uptake assays with radiolabeled acetic acid support *C. glabrata* Ato function

C. glabrata mutant cells were also tested regarding their ability to transport radiolabeled acetic acid (Figure 6.7). Data show that a single deletion of any of the tested proteins is sufficient to reduce the ability of the cells to transport acetate (not statistically significant only for Δ*fps1* strain; Figure 6.7). This data

provides additional evidence about the function of these transporters and channels as putative plasma membrane proteins that mediate the transport of acetic acid.

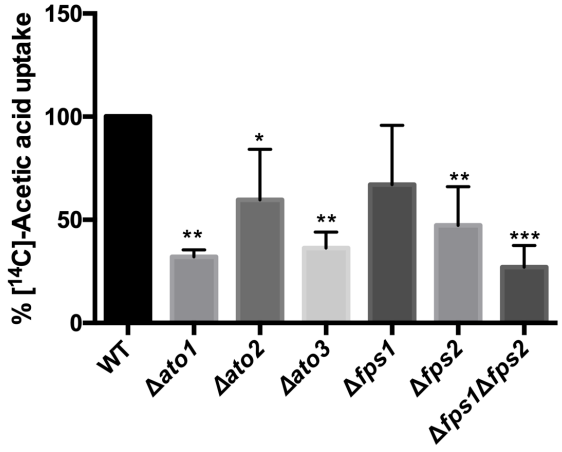

Figure 6.7. Transport assays support Ato function. Percentage of 1mM ^{14}C-acetic acid uptake, at pH 5.0, considering the velocity of transport found for *C. glabrata* ΔHTL as 100%. Cells were cultivated in Synthetic Complete (SC) medium 2% glucose until mid-exponential growth phase, washed and transferred during 6 h to SC supplemented with 0.5% acetic acid, pH 5.0. Error bars show standard deviations. Experiments were done in triplicate. *$p < 0.05$, ** $p < 0.01$ and ***$p < 0.001$ indicate statistically significant results.

6.3.5 Acetate transporters contribute to *C. glabrata* persistence within macrophages

C. glabrata is particularly well-adapted to the intracellular environment of phagocytes [11,12,15], being able to survive and replicate for extended periods of time within these cells [16,17]. The upregulation of Cg*ATO1* following phagocytosis has been supported by independent studies either in macrophages [11] or neutrophils [15]. This transporter has been also implicated in the phagocytic process [5]. We investigated the expression profile of *C. glabrata ATO1*, *ATO2*, *ATO3*, *FPS1* and *FPS2* during phagocytosis by human monocyte-derived macrophages. *C. glabrata* cells were challenged with these phagocytes and retrieved at several time points, over a period of seven days (Figure 6.8). As a control, we used a log-phase YPD culture. Early after engulfment (6 h), we observed an upregulation of all genes, with the exception of *CgATO3* (Figure 6.8). In particular, the expression of Cg*ATO2* was induced about 8-fold, being maintained over time (Figure 6.8). Cg*ATO1* was the most upregulated gene over time (Figure 6.8), supporting previously reported data [11,15]. On the other hand, the expression of Cg*FPS2* decreased over time, being about 16-fold downregulated at days 4 and 7 (Figure 6.8). Interestingly, the expression profile of the cells following phagocytosis was very similar with the one observed in cells growing in a

long-term, stationary YPD culture (right stars Figure 6.8), but totally different from the one found when cells are growing in a log-phase YPD culture (left triangles, Figure 6.8). This suggests that *C. glabrata* cells within macrophages might be starving just like those experiencing a long stationary phase.

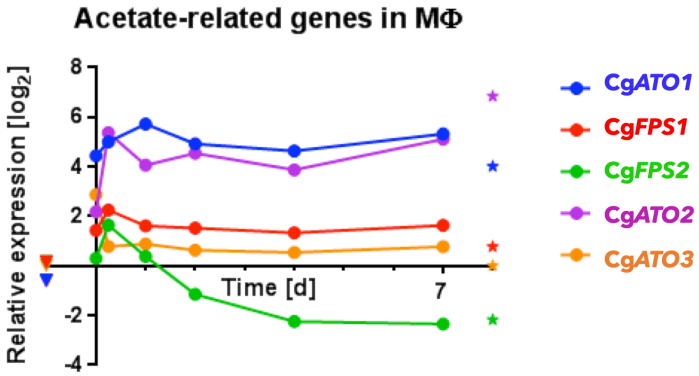

Figure 6.8. Relative expression of *C. glabrata* acetate transporters and channels during phagocytosis by human monocyte-derived macrophages. Relative expression of Cg*ATO1*, Cg*ATO2*, Cg*ATO3*, Cg*FPS1* and Cg*FPS2* in response to phagocytosis by macrophages after 0, 6, 24 (1 day), 48 (2 days), 96 (4 days) and 168 h (7 days) based on microarray data. The baseline is a log-phase YPD culture. Triangles and stars indicate the expression of genes in *C. glabrata* cells when growing in log-phase YPD (left side) and long-term YPD (right side), respectively.

6.3.6 Impact of carboxylate transporters on *C. glabrata* biofilm formation and fluconazole activity *in vivo*

Acetate transporters have been implicated in *in vitro C. glabrata* biofilm formation and susceptibility to fluconazole [5]. In order to assess whether full disruption of Ato transporters and Fps channels would interfere with both *C. glabrata* biofilm formation and fluconazole activity *in vivo*, we are using a validated subcutaneous mouse model [46]. Experiments are being conducted in immunocompetent mice as no differences have been found regarding *C. glabrata* biofilm formation and dissemination into surrounding tissues when using immunosuppressed mice [46]. For each *C. glabrata* strain (WT, triple and quintuple mutants), three catheter fragments are infected with $1x10^6$ cells each and subcutaneously implanted either on the left or on the right side of the lower back of the mice. At every time point (48 h and 144 h), three mice are sacrificed and the catheters explanted for *ex vivo* quantification by CFU counts. Biofilm development is also being assessed in the absence and presence of fluconazole (125 mg per kg of body weight per day) in order to confirm previously *in vitro* data [5]. The experiments are still ongoing and therefore the impact of mutant strains on both biofilm formation and antifungal resistance is still unknown.

6.4 DISCUSSION

In this work we carried out a functional characterization of a set of *C. glabrata* transporters and channels, and studied the role of acetate assimilation in *C. glabrata* during host colonization. Firstly, based on sequence homology with previously well-known and characterized acetate transporters and channels in *S. cerevisiae*, we identified five proteins as the main potential mediators for the uptake of acetate in *C. glabrata*. These proteins include the three AceTr family members, CgAto1, CgAto2 and CgAto3, and the two FPS channels, CgFps1 and CgFps2. One of the main outputs of this work was the generation of single and multiple mutants on the genes encoding these transporters.

The preliminary phenotypic analysis of these mutant strains revealed that growth in a solid medium, containing acetic acid as a sole carbon source, was compromised when the *ATO* genes were disrupted. We also tested the growth in a liquid culture using minimal media with glucose 2%, pH 5.0. No differences were observed between the wild type and mutant strains. In addition, several assays are underway using rich or minimal medium with acetic acid 0.5% at pH 5.0 or 6.0. We expect that this experiments will confirm the growth defects observed in the solid culture. The multiple Ato mutants also displayed a small growth defect in the presence of lactate, suggesting that Ato transporters may also mediate the uptake of this substrate. Additional studies to test this hypothesis are currently being carried out.

These genes were also heterologously expressed in the *S. cerevisiae* IMX1000 strain. The three *C. glabrata* Ato transporters were able to restore the growth defect in acetic acid, as sole carbon source. This confirms that these proteins have an important role in the uptake of acetate. The localization of the *C. glabrata* transporters in *S. cerevisiae* has shown that both CgAto1-mCherry and CgFps1-mcherry localize mainly to the plasma membrane, but, some fluorescence signal was also associated with intracellular structures. Those structures are likely to represent the ER, suggesting that the overexpression of these proteins, driven by the strong *TEF* promoter, may be associated with some cortical ER retention. We will test if these proteins are exclusively expressed at the plasma membrane in the host strain *C. glabrata*. If not, we will change the promoter to confirm whether the strong promoter is associated with the ER retention and eventually traffic jam to the plasma membrane.

The function of *C. glabrata* Ato transporters and Fps channels as uptake mediators of acetate was also confirmed by testing the ability of the mutant strains to transport radiolabeled acetic acid (Figure 6.7).

Although these are still preliminary experiments, the function of these transporters was reinforced. We are currently characterizing the transport kinetics of both wild type and mutant strains to get more insights into the specificity of this mediated process.

Finally, we addressed the physiological role of these transporters and channels for *C. glabrata* by using two different *in vivo* models of infection, namely human monocyte-derived macrophages and a murine subcutaneous biofilm model. Although macrophages are important for the elimination of these pathogens in the human host, *C. glabrata* is able to subvert their function by using them as "safe houses". Adaptation to the intracellular environment of these phagocytes offers the pathogen the opportunity to continue to replicate and thrive inside the human host, while triggering surprisingly low damage and release of cytokines. Our studies have demonstrated that the transcriptional response observed in *C. glabrata* following phagocytosis resembles that from cells within a long-term stationary phase, suggesting that these cells are likely starving. Our hypothesis is that the upregulation of Ato transporters, which was also supported by previous studies [11,18], allows cells to import acetate and use it as an alternative carbon source to fuel the respiratory metabolism. This is significant as several studies have been demonstrating the importance of the glyoxylate cycle in the virulence of *C. glabrata* [11,15].

Ongoing experiments are relying on the *C. glabrata* mutant strains, valuable molecular tools generated during this study, to test whether disruption of acetate uptake correlates with a decreased level of *C. glabrata* persistence within phagocytes.

6.5 REFERENCES

1. Miramón P, Lorenz MC. A feast for Candida: Metabolic plasticity confers an edge for virulence. PLoS Pathogens. 2017. doi:10.1371/journal.ppat.1006144
2. Ene I V., Brunke S, Brown AJP, Hube B. Metabolism in fungal pathogenesis. Cold Spring Harb Perspect Med. 2014. doi:10.1101/cshperspect.a019695
3. Ueno K, Matsumoto Y, Uno J, Sasamoto K, Sekimizu K, Kinjo Y, et al. Intestinal resident yeast *Candida glabrata* requires Cyb2p-Mediated lactate assimilation to adapt in mouse intestine. PLoS One. 2011. doi:10.1371/journal.pone.0024759
4. Vieira N, Casal M, Johansson B, MacCallum DM, Brown AJP, Paiva S. Functional specialization and differential regulation of short-chain carboxylic acid transporters in the pathogen *Candida albicans*. Mol Microbiol. 2010;75: 1337–1354. doi:10.1111/j.1365-2958.2009.07003.x
5. Mota S, Alves R, Carneiro C, Silva S, Brown AJ, Istel F, et al. *Candida glabrata* susceptibility to antifungals and phagocytosis is modulated by acetate. Front Microbiol. 2015;6. doi:10.3389/fmicb.2015.00919
6. Barelle CJ, Priest CL, MacCallum DM, Gow NAR, Odds FC, Brown AJP. Niche-specific regulation of central metabolic pathways in a fungal pathogen. Cell Microbiol. 2006;8: 961–971. doi:10.1111/j.1462-5822.2005.00676.x
7. Lorenz MC, Fink GR. The glyoxylate cycle is required for fungal virulence. Nature. 2001;412: 83–86. doi:10.1038/35083594
8. Ramírez MA, Lorenz MC. Mutations in alternative carbon utilization pathways in *Candida albicans* attenuate virulence and confer pleiotropic phenotypes. Eukaryot Cell. 2007. doi:10.1128/EC.00372-06
9. Chew SY, Ho KL, Cheah YK, Ng TS, Sandai D, Brown AJP, et al. Glyoxylate cycle gene ICL1 is essential for the metabolic flexibility and virulence of *Candida glabrata*. Sci Rep. 2019. doi:10.1038/s41598-019-39117-1
10. Lorenz MC, Bender JA, Fink GR. Transcriptional response of *Candida albicans* upon internalization by macrophages. Eukaryot Cell. 2004;3: 1076–1087. doi:10.1128/EC.3.5.1076-1087.2004
11. Kaur R, Ma B, Cormack BP. A family of glycosylphosphatidylinositol-linked aspartyl proteases is required for virulence of *Candida glabrata*. Proc Natl Acad Sci U S A. 2007. doi:10.1073/pnas.0611195104

12. Rai MN, Balusu S, Gorityala N, Dandu L, Kaur R. Functional Genomic Analysis of *Candida glabrata*-Macrophage Interaction: Role of Chromatin Remodeling in Virulence. PLoS Pathog. 2012. doi:10.1371/journal.ppat.1002863
13. Roetzer A, Gratz N, Kovarik P, Schüller C. Autophagy supports *Candida glabrata* survival during phagocytosis. Cell Microbiol. 2010. doi:10.1111/j.1462-5822.2009.01391.x
14. Lorenz MC, Fink GR. Life and death in a macrophage: Role of the glyoxylate cycle in virulence. Eukaryotic Cell. 2002. doi:10.1128/EC.1.5.657-662.2002
15. Fukuda Y, Tsai HF, Myers TG, Bennett JE. Transcriptional profiling of *Candida glabrata* during phagocytosis by neutrophils and in the infected mouse spleen. Infect Immun. 2013. doi:10.1128/IAI.00851-12
16. Seider K, Gerwien F, Kasper L, Allert S, Brunke S, Jablonowski N, et al. Immune evasion, stress resistance, and efficient nutrient acquisition are crucial for intracellular survival of *Candida glabrata* within macrophages. Eukaryot Cell. 2014. doi:10.1128/EC.00262-13
17. Duggan S, Essig F, Hünniger K, Mokhtari Z, Bauer L, Lehnert T, et al. Neutrophil activation by *Candida glabrata* but not *Candida albicans* promotes fungal uptake by monocytes. Cell Microbiol. 2015. doi:10.1111/cmi.12443
18. Seider K, Brunke S, Schild L, Jablonowski N, Wilson D, Majer O, et al. The Facultative Intracellular Pathogen *Candida glabrata* Subverts Macrophage Cytokine Production and Phagolysosome Maturation . J Immunol. 2011. doi:10.4049/jimmunol.1003730
19. Vylkova S, Carman AJ, Danhof HA, Collette JR, Zhou H, Lorenz MC. The fungal pathogen candida albicans autoinduces hyphal morphogenesis by raising extracellular pH. MBio. 2011;2. doi:10.1128/mBio.00055-11
20. Danhof HA, Lorenz MC. The *Candida albicans* ATO Gene Family Promotes Neutralization of the Macrophage Phagolysosome. Infect Immun. 2015. doi:10.1128/iai.00984-15
21. Vylkova S, Lorenz MC. Modulation of Phagosomal pH by *Candida albicans* Promotes Hyphal Morphogenesis and Requires Stp2p, a Regulator of Amino Acid Transport. PLoS Pathog. 2014;10. doi:10.1371/journal.ppat.1003995
22. Vylkova S, Lorenz MC. Phagosomal neutralization by the fungal pathogen *Candida albicans* induces macrophage pyroptosis. Infect Immun. 2017. doi:10.1128/IAI.00832-16
23. Paiva S, Devaux F, Barbosa S, Jacq C, Casal M. Ady2p is essential for the acetate permease activity in the yeast Saccharomyces cerevisiae. Yeast. 2004;21: 201–10. doi:10.1002/yea.1056

24. Sá-Pessoa J, Paiva S, Ribas D, Silva IJ, Viegas SC, Arraiano CM, et al. SATP (YaaH), a succinate-acetate transporter protein in *Escherichia coli*. Biochem J. 2013. doi:10.1042/BJ20130412

25. Rohlin L, Gunsalus RP. Carbon-dependent control of electron transfer and central carbon pathway genes for methane biosynthesis in the Archaean, *Methanosarcina acetivorans* strain C2A. BMC Microbiol. 2010. doi:10.1186/1471-2180-10-62

26. Ribas D, Soares-Silva I, Vieira D, Sousa-Silva M, Sá-Pessoa J, Azevedo-Silva J, et al. The acetate uptake transporter family motif "NPAPLGL(M/S)" is essential for substrate uptake. Fungal Genet Biol. 2019. doi:10.1016/j.fgb.2018.10.001

27. Qiu B, Xia B, Zhou Q, Lu Y, He M, Hasegawa K, et al. Succinate-acetate permease from *Citrobacter koseri* is an anion channel that unidirectionally translocates acetate. Cell Res. 2018. doi:10.1038/s41422-018-0032-8

28. Kim H, Wu X, Lee J. SLC31 (CTR) family of copper transporters in health and disease. Mol Aspects Med. 2013;34: 561–70. doi:10.1016/j.mam.2012.07.011

29. Mollapour M, Piper PW. Hog1 Mitogen-Activated Protein Kinase Phosphorylation Targets the Yeast Fps1 Aquaglyceroporin for Endocytosis, Thereby Rendering Cells Resistant to Acetic Acid. Mol Cell Biol. 2007. doi:10.1128/mcb.02205-06

30. Tsukaguchi H, Shayakul C, Berger U V., Mackenzie B, Devidas S, Guggino WB, et al. Molecular characterization of a broad selectivity neutral solute channel. J Biol Chem. 1998. doi:10.1074/jbc.273.38.24737

31. Choi WG, Roberts DM. Arabidopsis NIP2;1, a major intrinsic protein transporter of lactic acid induced by anoxic stress. J Biol Chem. 2007. doi:10.1074/jbc.M700982200

32. Bienert GP, Desguin B, Chaumont F, Hols P. Channel-mediated lactic acid transport: A novel function for aquaglyceroporins in bacteria. Biochem J. 2013. doi:10.1042/BJ20130388

33. Jacobsen ID, Brunke S, Seider K, Schwarzmüller T, Firon A, D'Enfért C, et al. *Candida glabrata* persistence in mice does not depend on host immunosuppression and is unaffected by fungal amino acid auxotrophy. Infect Immun. 2010. doi:10.1128/IAI.01244-09

34. Mans R, Hassing EJ, Wijsman M, Giezekamp A, Pronk JT, Daran JM, et al. A CRISPR/Cas9-based exploration into the elusive mechanism for lactate export in *Saccharomyces cerevisiae*. FEMS Yeast Res. 2017. doi:10.1093/femsyr/fox085

35. Shen J, Guo W, Köhler JR. CaNAT1, a heterologous dominant selectable marker for transformation of *Candida albicans* and other pathogenic *Candida species*. Infect Immun. 2005. doi:10.1128/IAI.73.2.1239-1242.2005

36. Yáñez-Carrillo P, Orta-Zavalza E, Gutiérrez-Escobedo G, Patrón-Soberano A, De Las Peñas A, Castaño I. Expression vectors for C-terminal fusions with fluorescent proteins and epitope tags in Candida glabrata. Fungal Genet Biol. 2015. doi:10.1016/j.fgb.2015.04.020
37. Mumberg D, Müller R, Funk M. Yeast vectors for the controlled expression of heterologous proteins in different genetic backgrounds. Gene. 1995. doi:10.1016/0378-1119(95)00037-7
38. Jacobus AP, Gross J. Optimal cloning of PCR fragments by homologous recombination in *Escherichia coli*. PLoS One. 2015. doi:10.1371/journal.pone.0119221
39. Skrzypek MS, Binkley J, Binkley G, Miyasato SR, Simison M, Sherlock G. The *Candida* Genome Database (CGD): Incorporation of Assembly 22, systematic identifiers and visualization of high throughput sequencing data. Nucleic Acids Res. 2017. doi:10.1093/nar/gkw924
40. Maniatis T, Fritsch EF, Sambrook J. Molecular Cloning : a laboratory manual. 2nd edition. Cold Spring Harb ,New York. 1988.
41. Lüttich A, Brunke S, Hube B. Isolation and amplification of fungal RNA for microarray analysis from host samples. Methods Mol Biol. 2012. doi:10.1007/978-1-61779-539-8_28
42. Kucharíková S, Neirinck B, Sharma N, Vleugels J, Lagrou K, Van Dijck P. In vivo *Candida glabrata* biofilm development on foreign bodies in a rat subcutaneous model. J Antimicrob Chemother. 2015. doi:10.1093/jac/dku447
43. Kucharíková S, Vande Velde G, Himmelreich U, Van Dijck P. *Candida albicans* biofilm development on medically-relevant foreign bodies in a mouse subcutaneous model followed by bioluminescence imaging. J Vis Exp. 2015. doi:10.3791/52239
44. Danhof HA, Vylkova S, Vesely EM, Ford AE, Gonzalez-Garay M, Lorenz MC. Robust Extracellular pH Modulation by *Candida albicans* during Growth in Carboxylic Acids . MBio. 2016. doi:10.1128/mbio.01646-16
45. Tamás MJ, Luyten K, Sutherland FCW, Hernandez A, Albertyn J, Valadi H, et al. Fps1p controls the accumulation and release of the compatible solute glycerol in yeast osmoregulation. Mol Microbiol. 1999. doi:10.1046/j.1365-2958.1999.01248.x
46. Persyn A, Rogiers O, Brock M, Velde G Vande, Lamkanfi M, Jacobsen ID, et al. Monitoring of fluconazole and caspofungin activity against *in vivo Candida glabrata* biofilms by bioluminescence imaging. Antimicrob Agents Chemother. 2019. doi:10.1128/AAC.01555-18

CHAPTER 7

CONCLUSIONS AND FUTURE PERSPECTIVES

7.1 CONCLUSIONS AND FUTURE PERSPECTIVES

Candida species are leading fungal pathogens that can cause both mucosal and invasive infections. Although remarkable progress has been made, in the last few decades, regarding our understanding of the impact of host-derived constraints on *Candida* physiology and pathogenicity, many details remain unclear. Importantly, most of the studies involving *Candida* species rely on artificial laboratory conditions, using glucose as the main carbon source. The extent to which other alternative physiologically relevant nutrients, such as carboxylic acids, impact innate immune responses, antifungal drug resistance or biofilm formation is still far from being uncovered.

Our group has been studying, for several years, plasma membrane carboxylate transporters in different yeast species [1–5]. We have identified Jen1 and Ato1 (previously known as Ady2) in *S. cerevisiae* [1,2], and have been characterizing these permeases homologues at different levels in *Candida* species [3,4,6]. We propose these transporters to be major mediators of *Candida* adaptation to different host microenvironments, where carboxylic acids are the main carbon and energy sources.

7.1.1 JEN transporters in *Candida albicans*

In *C. albicans*, we have shown that Jen1 and Jen2 are tightly regulated by different carbon sources, being repressed by glucose, and induced by their specific substrates, including lactate and pyruvate [3]. These transporters were also found strongly induced during phagocytosis, suggesting that glucose is absent and these carboxylic acids are readily available in the microenvironment of the phagosome [3,7]. The transport of these nonfermentable substrates across the plasma membrane by Jen proteins is therefore essential to feed the glyoxylate cycle, contributing to the survival of this pathogen. Supporting this idea, Jen proteins appear highly distributed among the most medically relevant *Candida* species, reinforcing their key role for the overall *Candida* metabolism and physiology (Chapter 2). Moreover, in this thesis, we have shown that Jen1 and Jen2 are involved in the resistance to antifungal therapy, both in planktonic and in biofilm cells [5] (Chapter 3).

Given the importance of Jen transporters and the fact that changes in carbon sources trigger their reorganization at the plasma membrane, in the future, we intend to study their regulation, at transcriptional and post-transcriptional levels, to identify the mechanisms by which these transporters are expressed and degraded. Until recently, it was thought that *C. albicans* displayed the same regulatory mechanisms as *S. cerevisiae*, however, it has been shown that there is a significant dislocation between the proteome and transcriptome in *C. albicans* [8]. For instance, in *C. albicans*, the addition of glucose rapidly represses genes involved in alternative carbon sources metabolism, but their protein products are stable and apparently active for many hours, contrary to what happens in *S. cerevisiae* [8–10]. Interestingly, posttranslational modifications, such as ubiquitylation, are triggered by specific environment stimuli and the cellular processes they regulate contribute to fungal pathogenicity [11].

In the past, as mentioned above, we have demonstrated that CaJen1 and CaJen2 are sensitive to glucose [3]. Following the addition of this sugar, at concentrations ≥0.1 % (w/v), to cells grown in lactate, both Jen1-GFP and Jen2-GFP are rapidly internalized [3]. We aim at identifying some of the actors involved in CaJen1 and CaJen2 endocytic downregulation and to characterize the mechanisms underlying this process. Hypotheses and concepts stemming from research on Jen1 in *S. cerevisiae* [9,10] will also be applied and tested in the study of these carboxylic acids transporters in *C. albicans*. Some constructs, such as CaJen1-GFP and CaJen2-GFP, are already available to determine if these transporters undergo Rsp5p-dependent ubiquitylation and to test the involvement of arrestin proteins in this process. Specific attention will be also paid to the type of ubiquitylation that these transporters undergo. Additionally, like in *S. cerevisiae,* we will check if phosphorylation is a signal prior to ubiquitylation and if there are experimental conditions where these transporters are synthesized and directly targeted for vacuolar degradation without undergoing plasma membrane targeting. If so, we will determine whether the targeting from Golgi to vacuolar lumen is Rsp5p or ubiquitin dependent.

7.1.2 ATO transporters in *Candida glabrata*

In *C. glabrata*, there are no homologues of *JEN1*, however, there are several homologues of *ATO1*, namely Cg*ATO1*, Cg*ATO2* and Cg*ATO3* (Chapter 2). We have previously shown that these transporters are more expressed in the presence of acetic acid than in glucose, in both planktonic and biofilm cells, suggesting that they may be involved in the uptake of this substrate [4].

In this thesis, we provided additional evidence that, like in *S. cerevisae*, Ato transporters mediate the uptake of acetate and, potentially, lactate (Chapter 6). Ongoing studies are being conducted in order to validate these results. Moreover, we have also shown the importance of this family for the survival and persistence of *C. glabrata* within the human host, especially inside phagocytes (Chapter 6). Ongoing experiments include *in vitro* and *in vivo* immunological assays with dendritic cells, macrophages and neutrophils. We will use *C. glabrata* single and multiple mutants, generated in this work, to validate the outputs of our microarrays. Considering our preliminary studies, we expect that these deletions affect the survival capacity of these pathogens within the different types of immune cells.

We have also previously demonstrated that these transporters are likely to be involved in biofilm formation and antifungal resistance [4]. In particular, the expression levels of all *C. glabrata* Ato transporters vary according to the concentration of fluconazole, one of the most common antifungal drugs used in clinical environments. This has an important clinical impact, namely in the treatment of vaginal candidiasis, since this niche has an acidic pH and it is rich in alternative carbon sources, such as lactate and acetate. We are currently testing whether these *in vitro* findings are translated in an *in vivo* murine subcutaneous biofilm model (Chapter 6). With this, we expect to demonstrate the relevance of acetate assimilation for *C. glabrata* persistence within the human host.

7.1.3 The unprecedent emergence of multidrug resistant species

The number of compounds in clinical use for the treatment of fungal infections is relatively small when compared to the much larger number of drugs to fight bacterial infections [12]. This limitation is mainly due to the similar biology of the eukaryotic host with the fungal pathogen, limiting the number of targets available to develop efficient drugs with lower levels of toxicity. On top of this limitation, fungal cells have developed various mechanisms to tolerate and resist against the widely used antifungal drugs, including fluconazole or the echinocandins [13]. With the unprecedented emergence of multidrug resistant species, such as *C. auris*, there is an urgent need to develop new effective antifungals.

The integration of 'omics data with *in vivo* models, that mimic more closely host conditions, is now a powerful strategy to unravel molecular processes underlying adaptive phenotypes. These platforms have already produced novel lines of research and improved the identification of new potential therapeutic

targets for vaccine and antifungal drug development, enhancing our ability to develop novel strategies to fight *Candida* infections.

7.1.4 The oversimplification of biological reality

During an infection, *Candida* cells are exposed to multiple environmental constraints, sometimes imposed consecutively, and at other times imposed simultaneously. Yet, *in vitro* experiments are predominantly designed to study individual environmental signals, often at single time points, rather than combinatorial stresses over time. Progress has been made using the first approach but, while this has given us valuable insights, it rather oversimplifies biological reality.

The analysis of combinatorial stresses, and of the dynamism of these inputs, would mimic host conditions more closely and reveal more detailed views of which stress, or stresses, prevail and dictate the outcome of different types of infection. The same principle applies to infection and biofilm models, where usually interactions between only a few different microbial populations have generally been examined. Most knowledge in the field has resulted from studies of either *C. albicans* or *C. glabrata.* Yet, the regulatory circuits required to effectively respond to each constraint, including antifungal treatments, differ considerably between the different *Candida* species, illustrating how heterogenous these pathogens are.

7.1.5 Auxotrophic strains versus clinical isolates

Candida auxotrophic strains are routinely used in the field. Several physiological studies rely on the assumption that a metabolic biosynthesis pathway, of either amino acids or nucleobases, can be perturbed as long as the product in question is provided extracellularly. Single and multiple deletions on such pathways have been established in a large number of *Candida* strains, as efficient selection markers for genetic experiments. While some studies claim that deletion of such pathways impacts virulence at many levels [14,15], others have shown that those strains are unaffected by auxotrophic markers, being phenotypically identical to the respective parental strain [16].

A thorough study in *S. cerevisiae* has demonstrated that a single deletion is able to strongly affect gene expression, having impacts on the overall transcriptome, proteome and metabolome [17]. While these strains are still convenient for many applications, including heterologous gene expression, they should be avoided in functional genomic, physiology or metabolic engineering research [18]. In our lab, we are currently considering the reintegration of the respective genetic markers on our auxotrophic strains and the use of clinical isolates, which mimic more closely biological reality. With the recent advances on genetic engineering, especially on CRISPR editing tools, the benefits of such strains may be surpassed.

7.1.6 *CRISPR-systems* in the frontline of molecular biology research

Genetic manipulations in *Candida* are still a big challenge as the efficiency of homologous recombination is low in these species, especially in *C. glabrata*. This is quite surprising, as this yeast is phylogenetically close to *S. cerevisiae*, where genetic modifications are easy to carry out. Deletions in *C. albicans* are also complicated, given that both chromosomes need to be targeted. The CRISPR-Cas9 system has been changing the method of genome editing, being an attractive tool to manipulate the genome of many organisms, without the introduction of any marker or scar sequence.

We have attempted to use this system to generate our mutants strains, by following a previously published approach [19], but this revealed to be a difficult task. Instead, we used the conventional FLP-FRT system. However, this approach results in the insertion of a selection marker at the *locus* of interest, or a small exogenous sequence, when the marker is flipped out. Consequently, the use of this approach for the generation of multiple mutants results in a very laborious task, requiring two rounds of insertion/excision to recycle the selection marker. Moreover, a frustratingly high number of colonies per round to be checked are required, since the occurrence of false positives is quite common. In the meantime, new versions of CRISPR-systems have emerged [20,21], representing an important advance to accelerate *Candida* research. Still, we managed to generated 10 different single and multiple mutants on the selected genes, which will be valuable molecular tools for further studies.

7.2 FINAL REMARKS

Candida species are the most frequent opportunistic fungal pathogens in humans and a common cause of life-threatening infections. Although *C. albicans* remains the most prevalent pathogen, *C. glabrata* has emerged as the second most frequent, being increasingly associated with high antifungal resistance. The ability of these species to cause infection is dependent on their capacity to adapt and grow within different host niches, including the assimilation of the available carbon sources.

In this thesis, we have shown that in order to thrive and persist in the different human microenvironments, both *C. albicans* and *C. glabrata* regulate specific sets of genes involved in an array of stress and metabolic pathways. In addition to conferring metabolic flexibility and stress resistance, this physiological re-programming has been associated with enhanced virulence through either impaired immune recognition, increased biofilm formation and/or acquired antifungal tolerance and resistance (Figure 7.1).

Our studies have demonstrated that carboxylic acid transporters play an important role during host adaptation by regulating the uptake of different substrates, such as lactate or acetate. These nutrients, under certain host microenvironments, are the main exogenous energy and carbon sources available that sustain cell metabolism, and therefore, survival and persistence. We revisited the two major fungal families of carboxylate transporters – the Jen and Ato families - and present a set of studies that demonstrates their importance for *Candida* persistence in the human host.

In particular, we provide additional evidence for the role of both *C. albicans* Jen1 and Jen2 transporters, by showing that they affect biofilm architecture and fluconazole susceptibility in the presence of lactate. We show that in the presence of this nonfermentable carbon source, *C. albicans* secretes tartaric acid, which has the potential to modulate the TCA cycle on the host cells and reduce cellular viability. Moreover, we have identified novel carboxylate transporters in *C. glabrata*, namely Ato1, Ato2 and Ato3, and we propose them as acetate transporters. We have also demonstrated that the AceTr family in *C. glabrata* contributes to the extraordinary ability of this pathogen to survive and replicate within phagocytes.

In addition to the study of carboxylate transporters, we identified regulators with an important impact in *Candida* pathogenesis. In *C. albicans*, the transcription factor Rlm1 is proved to impact immune

recognition by mediating cell wall remodeling during carbon adaption. On the other hand, the cochaperone Mge1 is proposed to be a key regulator of fluconazole susceptibility in *C. glabrata*, by reducing the formation of toxic sterols during carbon and pH adaptation.

By identifying and characterizing some of the molecular players behind metabolic and stress pathways, involved in *Candida* adaptation to the human host, we may discover potential targets for the development of better diagnostics and new antifungal compounds to treat *Candida* infections.

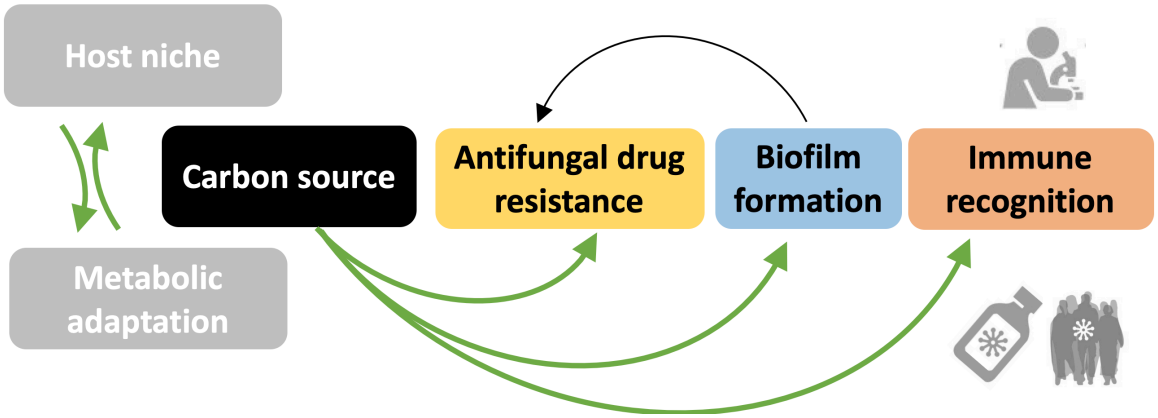

Figure 7.1. Take home message. Adaptation of *Candida* species to the different carbon sources available in host niches is achieved by regulating specific sets of genes involved in several stress and metabolic pathways. In addition to conferring metabolic flexibility and stress resistance, such physiological re-programming has been associated with enhanced virulence through either impaired immune recognition, increased biofilm formation and/or acquired antifungal tolerance and resistance.

7.3 REFERENCES

1. Casal M, Paiva S, Andrade RP, Gancedo C, Leão C. The lactate-proton symport of *Saccharomyces cerevisiae* is encoded by JEN1. J Bacteriol. 1999;181: 2620–2623.
2. Paiva S, Devaux F, Barbosa S, Jacq C, Casal M. Ady2p is essential for the acetate permease activity in the yeast *Saccharomyces cerevisiae*. Yeast. 2004;21: 201–10. doi:10.1002/yea.1056
3. Vieira N, Casal M, Johansson B, MacCallum DM, Brown AJP, Paiva S. Functional specialization and differential regulation of short-chain carboxylic acid transporters in the pathogen C*andida albicans.* Mol Microbiol. 2010;75: 1337–1354. doi:10.1111/j.1365-2958.2009.07003.x
4. Mota S, Alves R, Carneiro C, Silva S, Brown AJ, Istel F, et al. *Candida glabrata* susceptibility to antifungals and phagocytosis is modulated by acetate. Front Microbiol. 2015;6. doi:10.3389/fmicb.2015.00919
5. Alves R, Mota S, Silva S, Rodrigues CF, Alistair JP, Henriques M, et al. The carboxylic acid transporters Jen1 and Jen2 affect the architecture and fluconazole susceptibility of *Candida albicans* biofilm in the presence of lactate. Biofouling. 2017;7014: 1–12. doi:10.1080/08927014.2017.1392514
6. Alves R, Mota S, Silva S, F. Rodrigues C, Alistair AJ, Henriques M, et al. The carboxylic acid transporters Jen1 and Jen2 affect the architecture and fluconazole susceptibility of *Candida albicans* biofilm in the presence of lactate. Biofouling. 2017;33: 943–954. doi:10.1080/08927014.2017.1392514
7. Piekarska K, Mol E, Van Den Berg M, Hardy G, Van Den Burg J, Van Roermund C, et al. Peroxisomal fatty acid β-oxidation is not essential for virulence of *Candida albicans*. Eukaryot Cell. 2006. doi:10.1128/EC.00093-06
8. Sandai D, Yin Z, Selway L, Stead D, Walker J, Leach MD, et al. The evolutionary rewiring of ubiquitination targets has reprogrammed the regulation of carbon assimilation in the pathogenic yeast *Candida albicans*. MBio. 2012. doi:10.1128/mBio.00495-12
9. Becuwe M, Vieira N, Lara D, Gomes-Rezende J, Soares-Cunha C, Casal M, et al. A molecular switch on an arrestin-like protein relays glucose signaling to transporter endocytosis. J Cell Biol. 2012;196: 247–259. doi:10.1083/jcb.201109113

10. Paiva S, Vieira N, Nondier I, Haguenauer-Tsapis R, Casal M, Urban-Grimal D. Glucose-induced ubiquitylation and endocytosis of the yeast Jen1 transporter. Role of lysine 63-linked ubiquitin chains. J Biol Chem. 2009. doi:10.1074/jbc.M109.008318
11. Leach MD, Brown AJP. Posttranslational modifications of proteins in the pathobiology of medically relevant fungi. Eukaryot Cell. 2012. doi:10.1128/EC.05238-11
12. Goffeau A. The fight against fungi. Nature. 2008. doi:10.1038/452541a
13. Santos GC d. O, Vasconcelos CC, Lopes AJO, Cartágenes M do S d. S, Filho AKDB, do Nascimento FRF, et al. *Candida* infections and therapeutic strategies: Mechanisms of action for traditional and alternative agents. Frontiers in Microbiology. 2018. doi:10.3389/fmicb.2018.01351
14. Kirsch DR, Whitney RR. Pathogenicity of *Candida albicans* auxotrophic mutants in experimental infections. Infect Immun. 1991.
15. Roth-Ben AZ, Altboum Z, Shadkchan Y, Segal E. Loss and regain of virulence of a *Candida albicans* mutant as assessed in systemic murine candidiasis. J Mycol Med. 2001.
16. Jacobsen ID, Brunke S, Seider K, Schwarzmüller T, Firon A, D'Enfért C, et al. *Candida glabrata* persistence in mice does not depend on host immunosuppression and is unaffected by fungal amino acid auxotrophy. Infect Immun. 2010. doi:10.1128/IAI.01244-09
17. Alam MT, Zelezniak A, Mülleder M, Shliaha P, Schwarz R, Capuano F, et al. The metabolic background is a global player in *Saccharomyces* gene expression epistasis. Nat Microbiol. 2016. doi:10.1038/nmicrobiol.2015.30
18. Pronk JT. Auxotrophic yeast strains in fundamental and applied research. Applied and Environmental Microbiology. 2002. doi:10.1128/AEM.68.5.2095-2100.2002
19. Cen Y, Timmermans B, Souffriau B, Thevelein JM, Van Dijck P. Comparison of genome engineering using the CRISPR-Cas9 system in *C. glabrata* wild-type and lig4 strains. Fungal Genet Biol. 2017;107: 44–50. doi:10.1016/j.fgb.2017.08.004
20. Enkler L, Richer D, Marchand AL, Ferrandon D, Jossinet F. Genome engineering in the yeast pathogen *Candida glabrata* using the CRISPR-Cas9 system. Sci Rep. 2016;6: 1–12. doi:10.1038/srep35766
21. Ng H, Dean N. Dramatic Improvement of CRISPR/Cas9 Editing in *Candida albicans* by Increased Single Guide RNA Expression. mSphere. 2017;2: 1–17. doi.org/10.1128/mSphere.00385-16.